Pacific Northwest National Laboratory
Operated by Battelle for the
U.S. Department of Energy

Science to Support DOE Site Cleanup: The Pacific Northwest National Laboratory Environmental Management Science Program Awards -- Fiscal Year 2002 Mid-Year Progress Report

June 2002

DISCLAIMER

This report was prepared as an account of work sponsored by an agency of the United States Government. Neither the United States Government nor any agency thereof, nor Battelle Memorial Institute, nor any of their employees, makes **any warranty, express or implied, or assumes any legal liability or responsibility for the accuracy, completeness, or usefulness of any information, apparatus, product, or process disclosed, or represents that its use would not infringe privately owned rights**. Reference herein to any specific commercial product, process, or service by trade name, trademark, manufacturer, or otherwise does not necessarily constitute or imply its endorsement, recommendation, or favoring by the United States Government or any agency thereof, or Battelle Memorial Institute. The views and opinions of authors expressed herein do not necessarily state or reflect those of the United States Government or any agency thereof.

This document was printed on recycled paper.
(9/2003)

Science to Support DOE Site Cleanup: The Pacific Northwest National Laboratory Environmental Management Science Program Awards

Fiscal Year 2002 Mid-Year Progress Report

P. R. Bredt, Program Manager

C. C. Ainsworth	S. V. Mattigod
F. J. Brockman	B. P. McGrail
D. M. Camaion	P. D. Meyer
O. B. Egorov	C. J. Murray
A. R. Felmy	P. D. Panetta
Y. A. Gorby	D. M. Pfund
J. W. Grate	D. Rai
M. S. Greenwood	Y. Su
B. P. Hay	S. K. Sundaram
N. J. Hess	W. J. Weber
T. L. Hubler	J. M. Zachara
J. P. Icenhower	

June 2002

Overview

Pacific Northwest National Laboratory (PNNL) has been awarded a total of 80 Environmental Management Science Program (EMSP) research grants since the inception of the program in 1996. In addition, the Laboratory has collaborated on 14 other EMSP awards with funding received through other institutions. All of the projects awarded at PNNL in fiscal years 1996 and 1997 have published final reports. The projects awarded in 1998 have been completed or are nearing completion. Final reports for these projects will be published this year, so their annual updates are not included in this document.

This section summarizes how each of the projects awarded in 1999, 2000, and 2001 address significant U.S. Department of Energy (DOE) cleanup issues, including those at the Hanford Site. The technical progress made to date in each of these research projects is addressed in more detail in the individual progress reports contained in this document.

The EMSP projects awarded in 1999, 2000, and 2001 EMSP at PNNL are addressing issues in three areas—Tank Waste Remediation, Decontamination and Decommissioning, and Soil and Groundwater Cleanup.

Tank Waste Remediation

One of the main problems confronting DOE is the 350,000 cubic meters (92 million gallons) of mixed chemical and radioactive waste stored in more than 300 underground storage tanks at the Hanford Site (Washington), Oak Ridge Reservation (Tennessee), Savannah River Site (South Carolina), Idaho National Engineering and Environmental Laboratory (Idaho), and West Valley Site (New York). These tanks contain about 70% (720 million curies) of the man-made radioactivity existing in the DOE complex. This waste is a mixture of liquids, sludges, saltcake, and, at Idaho, calcined solids. Remediation of this tank waste is one of the most technically complex, scientifically challenging, and potentially expensive problems with which DOE is faced.

Hanford has 60% of the waste volume and 30% of the radioactivity for all DOE high-level waste tanks. At Hanford, 177 underground storage tanks contain 210,000 cubic meters (54 million gallons) of high-level waste. While DOE is actively pursuing faster and less expensive alternatives, the current baseline approach to remediating this tank waste is to retrieve the waste and then separate the solids from the liquids. Once cesium, strontium, and other radionuclides are removed from the liquid, it will become a relatively low-activity stream that can be immobilized as low-level radioactive and chemical waste. The solid, high-activity stream will be pretreated to

reduce its volume (mainly through the removal of nonradioactive inorganic components such as chromium, phosphorous, and aluminum) and then immobilized as high-level radioactive waste.

Safe Storage

Even safe storage of the waste in the tanks gives rise to technical issues. Chemical reactions in the tanks, including those caused by radiation and the slow corrosion of the steel tank walls, produce gases such as hydrogen, nitrogen, nitrous oxide, ammonia, and methane. Many of these gases are flammable, toxic, or both. In addition to generating gases, the reactions degrade organic compounds in the waste, change organic fuel and oxidant concentrations, and alter the surface chemistry of insoluble colloids, influencing sedimentation and gas/solid interactions. *Mechanisms and Kinetics of Organic Aging and Characterization of Intermediates in High-Level Waste* is focused on understanding the radiolytic processes in these mixed-phase systems. The goals of the project are to determine and understand the radiation-induced physical and chemical changes in the wastes and the rates at which they occur.

Characterization

Characterizing the complex and heterogeneous wastes is difficult and expensive. Yet, an adequate characterization is vital to making decisions about each treatment and storage step. At the Hanford Site, waste delivered to the pretreatment system must be demonstrated to be within certain specifications on composition, solids content, and other important characteristics. *Radioanalytical Chemistry for Automated Nuclear Waste Process Monitoring* is developing rapid, sensitive, and selective techniques for determining low-energy beta- and alpha-emitting radionuclides such as ^{99}Tc, ^{90}Sr, and transuranium elements in waste-processing streams. Nuclear waste process streams are particularly challenging due to the complex and high ionic-strength caustic brine sample matrix, the presence of interfering radionuclides, and the variable and uncertain speciation of the radionuclides to be analyzed. Under this project, scientists are conducting fundamental research in matrix modification, speciation control, and separation chemistries required for the development of automated process analyzers.

Retrieval and Waste Transfer

The wastes are complex and highly alkaline mixtures of many species, with sodium, nitrate, and hydroxide predominant. Some of the most interesting thermodynamics in the waste involve aluminum phases that can precipitate or dissolve during waste processing, depending on the pH of the waste and the concentrations of certain ions. Changes in pH or waste composition during waste retrieval, transfer, and processing must be made thoughtfully to prevent unwanted precipitation or scale formation. Of all the constituents of tank waste, aluminum species have the greatest potential for clogging pipes and transfer lines, fouling highly radioactive components

such as ion exchangers, and shutting down processing operations. The primary focus of *Precipitation and Deposition of Aluminum-Containing Species in Tank Wastes* (renewal of a 1998 award, *Dissolution, Precipitation, and Deposition of Aluminum-Containing Phases in Tank Wastes*) is to understand the major factors controlling precipitation, scale formation, and cementation of existing insoluble particles by aluminum-containing phases so that fouling and clogging can be avoided.

Transferring and processing these highly radioactive, abrasive, and corrosive slurries will require a new set of on-line monitors that can operate under these extreme conditions. Three projects are seeking to develop technologies that will allow process engineering to monitor key physical and rheological properties. *Non-Invasive Diagnostics to Measure Physical Properties in High-Level Wastes,* which PNNL co-leads with the University of California, Davis, is a renewal of a 1996 project, *On-Line Slurry Viscosity and Concentration Measurement as a Real-Time Waste Stream Characterization Tool.* This project is investigating the use of nuclear magnetic resonance imaging and acoustic velocimetry to determine rheological properties, solids loading, and mass flow of tank wastes under processing conditions to permit the monitoring and control of slurries during transport. *Investigating Ultrasonic Diffraction Grating Spectroscopy and Reflection Techniques for Characterizing Slurry Properties* is developing a technique involving ultrasonic diffraction grating spectroscopy to measure particle size and viscosity. The proposed ultrasonic technique, in which the measurement sensors are placed on the outside of the waste-transfer pipeline wall, could result in an instrument that would be simple, rugged, and very small, allowing it to be implemented at facilities across the DOE complex. A complementary project, co-led by PNNL and the University of Washington, *Physical Characterization of Solid-Liquid Slurries at High Weight Fractions Utilizing Optical and Ultrasonic Methods*, is investigating a combination of optical low-coherence reflectometry and ultrasonic backscatter with diffuse field techniques. This combined approach enables researchers to characterize high-level waste over ranges of concentration and particle size wider than can be achieved with current technology.

Pretreatment

Several projects are investigating innovative approaches to separation processes. Radionuclides must be removed to prepare the liquid waste stream for immobilization as low-level waste, while nonradioactive species must be extracted from the high-activity waste stream to minimize its volume. Both aspects present a series of technical challenges.

Current strategies for reducing the volume of the solid, high-activity waste stream involve developing methods to selectively dissolve and remove nonradioactive elements such as aluminum, phosphorus, and chromium while retaining the radioactive elements in the sludges. *Speciation, Dissolution, and Redox Reactions of Chromium Relevant to Pretreatment and*

Separation of High-Level Tank Wastes, renewal of a 1998 project of the same title, looks specifically at chromium. Chromium is not removed effectively by current sludge-washing techniques and is difficult to incorporate into glass. The project seeks to determine and characterize the speciation, dissolution, and redox reactions of chromium under conditions relevant to high-level waste, i.e., multicomponent, highly nonideal electrolyte systems. The project will provide critical data to support the development of pretreatment processes for chromium removal and thereby help to achieve major cost savings in high-level waste disposal.

Turning to the low-level waste stream, the removal of cesium appears to be straightforward, with ion-exchange technologies capable of meeting the performance criteria. In conventional ion-exchange processes, the cesium-bearing liquid passes through a reactor packed with an organic resin or other ion-exchange material. The cesium binds to the resin but not permanently. Once the resin has reached its cesium capacity, the cesium is flushed from the resin with acid and reused. However, this creates a second liquid waste stream that must be processed further (e.g., by incorporating into borosilicate glass) for long-term storage or disposal.

New Metal Niobate and Silicotitanate Ion Exchangers: Development and Characterization is a renewal of our 1997 award, *New Silicotitanate Waste Forms: Development and Characterization*. Crystalline silicotitanate (CST) is the most promising commercially available candidate for removal of cesium and strontium from tank wastes; however, it has been identified as a risk to vitrification due to its high level of titanium dioxide. Our 1997 project developed strategies for disposing of CST ion exchangers by in situ heat treatment with minimal or no additives to produce an alternative waste form. Building on the results obtained from this previous project, the renewal focuses on current needs in the separation of cesium and strontium. The approach could significantly reduce the volume and costs associated with waste disposal, minimize the risk of environmental contamination during processing, eliminate problems associated with radiolytic hydrogen generation during short-term storage, and provide DOE with technical alternatives for waste disposal. As a result of this work and that of other EM-50-funded projects, CSTs were considered as one of three cesium-removal technologies at the Savannah River Site. They remain an important option to the current preferred alternative, caustic side solvent extraction.

In some tanks, there may be a need to remove the lanthanides and actinides (because of their long half-lives of 10^2 to 10^6 years) and/or strontium, which has been complexed by organic chelating agents present in the waste. Partitioning during the separation process is complicated by the presence of organic chelating agents, which bind up both radionuclides and non-radioactive metals. During pretreatment, the radionuclides must be displaced from the chelating agents by manipulating the hydroxide concentration of other metals. To minimize the high-level waste volume, however, this displacement must be selective. Designing a selective separation process for the highly complex waste without resorting to an ad hoc approach requires a

fundamental understanding of what controls the conformation of the chelating agents and their interactions with metals and other ions. ***Development of Fundamental Data on Chemical Speciation and Solubility for Strontium and Americium in High Level Waste: Predictive Modeling of Phase Partitioning During Tank Processing***, renewal of a 1996 project, ***Chemical Speciation of Strontium, Americium, and Curium in High Level Waste: Predictive Modeling of Phase Partitioning During Tank Processing***, addresses the problem of trivalent actinide (americium/cesium) and strontium speciation and solubility in tank liquids. The resulting data will be used to develop thermodynamic models to predict changes in chemical speciation and solubility as a result of changes in tank processing conditions. The resulting models will help in optimizing existing processes and in developing new ones.

Computational Design of Metal Ion Sequestering Agents, renewal of a 1996 project, ***Architectural Design Criteria for f-Block Metal Sequestering Agents***, uses computational and experimental methods to optimize ligand architecture for metal sequestrations, including actinides and lanthanides. Development of an accurate set of criteria for ligand architecture design makes it possible to target ligand structure for synthesis, dramatically reducing the time and cost associated with metal-specific ligand development. This provides cleanup projects with more cost-effective and efficient separations agents that can reduce schedules and save money, especially the costs associated with the regeneration of separations materials and/or the disposal of spent separations materials.

Technetium is a radionuclide that causes significant environmental and regulatory concerns. Due to its moderate half-life, it soon could become a dominant source of radioactivity in tank residuals, plumes, and immobilized low-activity waste. Technetium complexation with organic compounds plays a significant role in the redox chemistry of technetium and the partitioning of technetium between the supernatant and sludge. These processes need to be understood to enable effective removal of technetium from high-level nuclear waste and researcher evaluation of the long-term consequences of technetium in tank residuals. ***Technetium Chemistry in HLW: Role of Organic Complexants*** is studying the thermodynamics of technetium organic complexation. The project is working to develop predictive models of technetium speciation and behavior during waste pretreatment processing and in waste tank residuals.

Technetium is also a relatively volatile material that is difficult to incorporate into glass under the high temperatures used in standard vitrification. Given concerns regarding activity and environmental mobility, removing technetium would make the low-level waste form more benign. However, technetium removal is complicated by its speciation in tank waste, one form of which is pertechnetate anion, TcO_4^-. Although traditional ion exchange processes are quite effective on cations such as cesium and strontium, they are much less effective on anions. ***Electroactive Materials for Anion Separation - Technetium from Nitrate*** is investigating how to use electroactive materials to sorb technetium without also extracting nitrate anions, which are

present in very high concentration. This new process expels (elutes) the technetium electro-chemically rather than using a chemical eluant, reducing the amount of chemicals added and thereby minimizing waste. The research focuses on manipulating specific properties of redox polymers to control their reversibility, selectivity, stability, rates of intercalation/de-intercalation, and capacity.

Immobilization

After the high-activity stream has been reduced in volume, the remaining waste, with its concentrated radionuclides, will be immobilized. The approach DOE has chosen for most of its sites is to vitrify the waste—to incorporate it into glass. With DOE funding, large electrically heated melters have been developed for waste processing. To support this work, PNNL is co-leading *Millimeter-Wave Measurements of High-Level and Low-Level Activity Glass Melts* with the Massachusetts Institute of Technology and the Savannah River Technology Center. The objective of this research is to develop new real-time sensors for characterizing glass melts, which will enable researchers to understand the scientific basis and bridge the gap between glass melt model data and melter performance. Millimeter-wave technology is being developed and applied to the simultaneous measurement of temperature, conductivity, and viscosity. The resulting sensors will decrease the uncertainty in current process control models and will permit increases in waste loading.

Storage and Disposal

Once immobilized, the low-activity waste will be disposed on-site, while the high-activity waste is to be disposed at the federal geologic repository. However, interactions between alkali ions (such as sodium) and radionuclides in the immobilized waste that could affect their release rate are not well understood. The impact of internal radiation on the long-term performance of these immobilized forms also is unclear. And, given the time frames involved (circa 10,000 years), the data will not be gathered from simple experimentation. *Radiation Effects in Nuclear Waste Materials* is a renewal of a 1996 award of the same title. This project is focused on developing a fundamental understanding of radiation effects in glass and ceramic waste forms. The understanding and associated data from this project has shown that the baseline formulation for low-level waste glass would not meet regulatory leaching requirements for long-term disposal. This data has been used to reformulate the low-level waste glass to provide a final product that will retain the radionuclides of interest within the regulatory limits. It is important to note that these studies also will benefit the assessment of waste forms proposed for the immobilization and disposal of plutonium residues and scrap and excess weapons plutonium.

Decontamination and Decommissioning

DOE built thousands of facilities to generate and process nuclear weapons material. Part of the cleanup agenda involves closing the buildings themselves (e.g., nuclear reactors, chemical processing facilities, and reactor fuel pools) after characterizing, dismantling, and cleaning out facilities within them (e.g., glove boxes and hot cells). Radioactive contamination often must be cleaned from surfaces in these facilities to close (i.e., decommission) them. Contamination may be removed physically by wiping, scraping, or scabbling, or it may be washed off using special cleaning agents. Virtually every DOE site has facilities awaiting or undergoing decontamination and decommissioning, and the major sites may have hundreds.

Three PNNL EMSP projects are focused on understanding and improving the methods used for cleaning surfaces. *Microbially Promoted Solubilization of Steel Corrosion Products and Fate of Associated Actinides* probes some of the fundamental scientific issues regarding a microbial process with potential for decontaminating corroding metal surfaces. Certain iron-reducing bacteria can dissolve the rust and oxide layers on steel and thereby release radionuclide contaminants attached to those surfaces. The actinides are sorbed by cell surfaces or precipitated within biofilms that can be removed and recovered by an enzymatic digestion of the microbes. This environmentally benign enzymatic process avoids the use of hazardous or toxic chemicals and minimizes the volume and toxicity of secondary wastes. Similarly, *Contaminant-Organic Complexes: Their Structure and Energetics in Surface Decontaminant Processes*, a renewal of a 1998 award of the same title, investigates the use of powerful, microbially produced chelates (called siderophores) as decontamination and sequestering agents. Studies of these compounds demonstrate that their binding affinity for iron and actinides with a (IV) valence state is as much as 20 orders of magnitude higher than other chelating agents (i.e., EDTA). The third award in this area, *Development of Biodegradable Isosaccharinate-Containing Foams for Decontamination of Actinides: Thermodynamic and Kinetic Reactions between Isosaccharinate and Actinides on Metal and Concrete Surfaces,* seeks fundamental thermodymanic and kinetics information that will lead to the development of a new and more environmentally acceptable technology for decontamination of plutonium. This project is working with isosaccharinate, a degradation product of cellulose that is biodegradable and binds strongly with plutonium. The goal is to incorporate the isosaccharinate into a foam to produce a non-hazardous agent for decontamination of plutonium from steel and concrete surfaces.

Soil and Groundwater Cleanup

Contaminant plumes, contaminated soils, and landfills account for some 4,800 waste sites on DOE property in 31 states. Approximately 35 million cubic meters of soil are contaminated with low-level and mixed low-level waste. Another 1.2 million cubic meters of soil are contaminated with transuranic and mixed transuranic waste. Landfills of buried waste are estimated to contain

3 million cubic meters of low-level waste. This includes 105,000 cubic meters of retrievably stored transuranic waste. Several hundred square miles of groundwater are contaminated with a variety of radionuclides and hazardous chemicals in concentrations above drinking water standards and DOE's concentration guidelines. At the Hanford Site alone, there are nearly 150 square miles of groundwater contamination. The radioactive and hazardous wastes are dispersed through large volumes of soil and groundwater, making potential treatment by conventional soil excavation and groundwater cleanup technologies ineffective and costly. In addition, some 650,000 metric tons of solid waste is buried at Hanford.

In 1997, part of the call was designed to help the project fill many of the gaps in knowledge through the EMSP. The baseline approach for treating contaminated groundwaters was to pump out the groundwater, treat it ex situ, and return it to the subsurface ("pump and treat"). For contaminated soils, the plan is simple: dig it up and dispose of it in a controlled disposal unit. At Hanford, that unit is the Environmental Restoration Disposal Facility (ERDF).

Centrally located on the 200 Area plateau, the ERDF is receiving contaminated soils and solid waste from the 100 Area. As of last year, two cells were operating with a capacity of approximately 1.2 million cubic yards each. The potential exists for eight new cells, depending upon future needs. These cells, classified as Resource Conservation and Recovery Act landfills, have a design life of approximately 20 to 30 years, which may be extended through the use of caps, engineered barriers, or both caps and barriers.

While ex situ options may be available and effective over the short term, they are more expensive and labor-intensive, and have a greater potential for worker and environmental risk, than in situ methods. Consequently, there are many drivers for the development of in situ treatment, monitoring, and characterization solutions.

One area in which there was an identified knowledge gap at Hanford was the rate of migration of radioactive cesium and other contaminants in the subsurface from tank leakage or waste cribs. Although it is strongly sorbed by the micaceous fraction of the soil, cesium appears to be moving faster toward the groundwater and, ultimately, the Columbia River than previously thought possible. *Fixation Mechanisms and Desorption Rates of Sorbed Cs in High-Level Waste Contaminated Subsurface Sediments: Implications to Future Behavior and In-Ground Stability* is a renewal of our 1997 project, *Mineral Surface Processes Responsible for the Decreased Retardation (or Enhanced Mobilization) of ^{137}Cs from High-Level Waste Tank Discharges*. This project is investigating the geochemistry of cesium ion adsorption under conditions appropriate to high-level waste tank releases. The original work showed that high sodium concentrations in tank waste suppress all but the most selective cesium sorption sites on the frayed edges of micaceous particles and that the cesium migration depth is strongly controlled by the sodium concentration. The hydroxide and aluminate compounds in high-level

waste may alter these sites chemically, leading to faster transport through the soil. The renewal will expand our understanding of this cesium mobility.

Contaminant release and migration models that are used to study a broad range of geochemical and environmental science problems of commonly employ Transition-State Theory (TST) to regulate the dissolution kinetics of waste forms and minerals. Unfortunately, TST arguments are inaccurate when modeling solutions that contain high concentrations of dissolved components. A project awarded in 2001, ***Origins of Deviations from Transition-State Theory: Formulating a New Kinetic Rate Law for Dissolution of Silicates,*** is working to develop and validate a new rate law that more accurately predicts dissolution kinetics in realistic solution compositions. From these data, researchers will be able to identify the reactive precursor species that are the key to unraveling rate mechanisms. The resulting model will have widespread applications to contaminant migration, whether originating from future waste disposal sites or existing plumes.

After remediation and closure of the high-level waste tanks, residual radionuclide-bearing solids may remain in the tanks adhering to the inner surfaces. Radionuclide release from these residuals represents a potentially significant source of contaminants migrating in the sediments underlying the tanks. A recent analysis for the Hanford Site has shown the radionuclide source term from the residual solids may be one of the most significant long-term dose contributors on-site. However, this analysis was based on a highly conservative release model. Awarded in 2001, ***Physicochemical Processes Controlling the Source Term from Tank Residuals*** is working to improve the fundamental scientific basis for estimating the release rate of ^{99}Tc, the principal long-term dose contributor from these tank residuals. This study will provide a sound technical basis for DOE and local stakeholders to make more informed cost/benefit/risk decisions regarding closure of high-level waste tanks.

In fiscal year 1998, the Groundwater Vadose Zone (GW/VZ) integrated project was initiated to bring under one program all of the issues affecting contamination of the soils and groundwater at the Hanford Site. To begin the process, a roadmap was developed to determine the underlying gaps in the knowledge needed to solve the problems associated with the contamination. As a result of this roadmapping effort, the EMSP agreed to allow the GW/VZ project to assist in preparing the call for proposals in 1999, focusing the call on the problems identified with the roadmap. The EMSP projects awarded fell into three categories: 1) waste/sediment interactions and process modeling, 2) vadose zone field studies, advanced monitoring, and transport modeling, and 3) dense nonaqueous phase liquid (DNAPL) monitoring and remediation.

In the first category, waste/sediment interactions and process modeling, the goal of the research is to determine how the waste interacts with the soils, resulting in models to predict the holdup and release of contaminants. The surfaces of the minerals will interact with the contaminants, depending on the nature of the surfaces. ***Technetium Attenuation in the Vadose Zone: Role of***

Mineral Interactions is looking at the role of divalent iron-containing minerals in the reduction/precipitation of technetium in the environment. In addition to the initial reactions, the project will determine the stability of the precipitates to find out if natural attenuation in the soils will decrease the mobility of technetium, resulting in potential savings in the cleanup. Another project looking into the reactions of surfaces is *The Influence of Calcium Carbonate Grain Coatings on Contaminant Reactivity in Vadose Zone Sediments.* This project is examining into how calcium carbonate on the surface of minerals will affect the interactions between soil particles and the contaminants. Carbonates will enhance the sorption of some contaminants (e.g., ^{90}Sr and ^{60}Co) but may interfere with the interaction between the minerals and the species that will undergo reduction reactions (e.g., chromate and pertechnetate). Because many of the minerals in the soil are silicates, one of the concerns is how silicates dissolved by the leaking of the basic tank wastes into the subsurface will interact with some of the radionulides, potentially complexing them and increasing their mobility. *The Aqueous Thermodynamics and Complexation Reactions of Anionic Silica Species to High Concentration: Effects on Neutralization of Leaked Tank Wastes and Migration of Radionuclides in the Subsurface* is examining the effect these dissolved silicates have on contaminant mobility.

The second category of projects supporting the GW/VZ effort includes the vadose zone field studies, advanced monitoring, and transport modeling. This work is focused mainly on examining transport phenomena in actual field settings and delineating the contamination within the vadose zone. At the Hanford Site, there are numerous natural formations within the sediments that may restrict the transport of contaminants or may provide preferential pathways that enhance contaminant movement. *Influence of Clastic Dikes on Vertical Migration of Contaminants in the Vadose Zone at Hanford* is investigating the effect of naturally occurring clastic dikes in the vadose zone on flow to better understand the fate and transport of contaminants at the 200 West Hanford tank farms. In a more general treatment of the transport of contaminants, *Quantifying Vadose Zone Flow and Transport Uncertainties Using a Unified, Hierarchical Approach* is developing and demonstrating parameterized models of flow and transport in the heterogeneous vadose zone. This project will enable the elucidation of relationships between the quantity and spatial extent of characterization data and the accuracy and uncertainty of flow and transport predictions. Another important aspect in understanding the flow and transport of contaminants in the subsurface is the ability to delineate the contaminant plumes and identify the specific contaminants. At the Hanford Site, the species of most concern are radionuclides. *Radionuclide Sensors for Water Monitoring* is looking at chemistries for selective preconcentration/separation directly on or within the area of a radioactivity detector. The work involves assessing new materials and processes that can be incorporated into field-deployable sensors.

The final area of study in the GW/VZ project includes monitoring and remediation of DNAPLs, which are still a major problem for many private industries and government agencies, including

DOE. Among the planned remediation technologies for these organic materials, in situ bioremediation offers advantages over physical treatments (e.g., pump and treat systems) due to the potential reduction in schedule, cost, public acceptance, and the final achievable cleanup levels. However, this approach still has many uncertainties, such as the feasibility of this process on recalcitrant contaminants in deep vadose zones where microbial populations are low and discontinuous and how hydrologic features of the vadose zone control microbial processes. *Integrated Field, Laboratory, and Modeling Studies to Determine the Effects of Linked Microbial and Physical Spatial Heterogeneity on Engineered Vadose Zone Bioremediation* will provide an increased understanding of the effect of interacting hydrologic and microbiological processes that control the feasibility of engineered bioremediation of chlorinated compounds in the vadose zone.

For more information, contact

Dr. John P. LaFemina
Manager, Environmental Management Subsector
Environmental Technology Division
Pacific Northwest National Laboratory
509-375-6806

or

Dr. Paul R. Bredt
Senior Research Scientist
Environmental Technology Division
Pacific Northwest National Laboratory
509-376-3777

Contents

1.0 Tank Waste Remediation

2.0 Decontamination and Decommissioning

3.0 Soil and Groundwater Cleanup

1.0 Tank Waste Remediation

Mechanisms and Kinetics of Organic Aging and Characterization of Intermediates in High-Level Waste

(Project Number: 81883)

Principal Investigator

Donald M. Camaioni
Pacific Northwest National Laboratory
P.O. Box 999, MSIN K2-57
Richland, WA 99352
509-375-2739 (phone)
509-375-6660 (fax)
donald.camaioni@pnl.gov

Co-Investigators

S. Tom Autrey
Pacific Northwest National Laboratory
P.O. Box 999, MSIN K2-57
Richland, WA 99352
509-375-3792 (phone)
509-375-6660 (fax)
tom.autrey@pnl.gov

Michel Dupuis
Pacific Northwest National Laboratory
P.O. Box 999, MSIN K8-91
Richland, WA 99352
509-376-4921 (phone)
509-376-0420 (fax)
michel.dupuis@pnl.gov

Wendy Shaw
Pacific Northwest National Laboratory
P.O. Box 999, MSIN K2-57
Richland, WA 99352
509-375-5922 (phone)
509-375-6660 (fax)
wendy.shaw@pnl.gov

Research Objective

The objective of this project is to characterize significant chemical degradation pathways of organic chemicals in nuclear waste storage and treatment streams. The effort at Pacific Northwest National Laboratory (PNNL) is closely coordinated with a Notre Dame Radiation Laboratory project (EMSP No. 73832, "The NOx System in Nuclear Waste," D. Meisel, Principal Investigator) that focuses on radiolytically induced degradation of organic complexants. An understanding of the chemistry of the organic chemicals present in tank wastes is needed to manage the wastes and related site cleanup activities. The underlying chemistries of high-level waste are 1) the chemistry initiated by radioactive decay and the reactions initiated by heat from radioactive decay and 2) the chemistry resulting from waste management activities (waste transfers between tanks, concentration through evaporators, caustic and other chemical additions). Recognizing that experiments cannot reproduce every conceivable scenario, the PNNL and Notre Dame projects work to develop predictive computational models of these chemistries. Participants in both projects combine experimental observations, electronic structure computations, and theoretical methods developed to achieve this goal. The resulting model will provide an accurate evaluation of the hazardous material generated, including flammable gases, and will support decision-making processes regarding safety, retrieval, and treatment issues. The utility of developing an understanding of tank chemistry has been demonstrated in earlier work. None of the Hanford tanks is currently on a watch list, partially due to predictive understanding of organic aging and flammable gas generation that resulted from previous research. Furthermore, concerns that arise from pretreatment and tank closure issues (e.g., Tc speciation) may be rationalized with the mechanistic knowledge provided by these projects.

Research Progress and Implications

At this stage of the project, which is in its fourth year after being renewed in 2001, we are obtaining data on the thermochemical properties and chemical kinetics of reaction intermediates for mechanism verification, structure/reactivity correlation, and reaction-rate prediction. Specifically, the project is 1) developing and applying photoacoustic calorimetry (PAC) for measuring aqueous thermochemistry and reaction kinetics of transient intermediates and 2) improving solvation models for use in computing the thermochemical properties of radicals and ions in aqueous solutions.

Thermodynamics and Kinetics of Aqueous Intermediates

Complexants with hydroxyl groups are thermally the most reactive constituents in Hanford wastes. Nitrite ions also are required, and aluminate ions act as catalysts. The role of Al(III) may be to bind glycolate and nitrite anions, thereby lowering the coulombic contribution to the

reaction barrier. In this way, Al serves as a bridge for electron transfer. Alternatively, or in addition, Al binding of the organic complexant may activate glycolate ions to undergo an H-atom transfer to nitrite. Suggested mechanisms for this reaction are shown in Figure 1. To assess these possibilities, the investigators are using PAC to measure the thermochemical and kinetic properties of the glycolate ion and its metal ion complexes in aqueous solutions. The PAC technique is based on the phenomenon that chemical reactions induced by absorption of a light pulse produce a measurable sound pulse that is relatable to the heats, reaction volumes, and rates of the induced reactions. The investigators have developed methods for recording the signals and for resolving their time-dependent components so that reaction kinetics, reaction heats, and reaction volumes can be obtained. We are adapting the technique to use hydrogen peroxide as the photo precursor, andsome benchmark experiments have been performed. Example determinations of the O-O bond dissociation energy of H_2O_2, and the rate constants for reaction of OH with H_2O_2 and with sodium glycolate are shown in Figures 2 through 4. The adapted technique provides an alternative to optical kinetic methods for measuring equilibrium constants and potentially could provide both enthalpy and free energies of proton transfer and electron transfer equilibria, and ultimately, solvation energies.
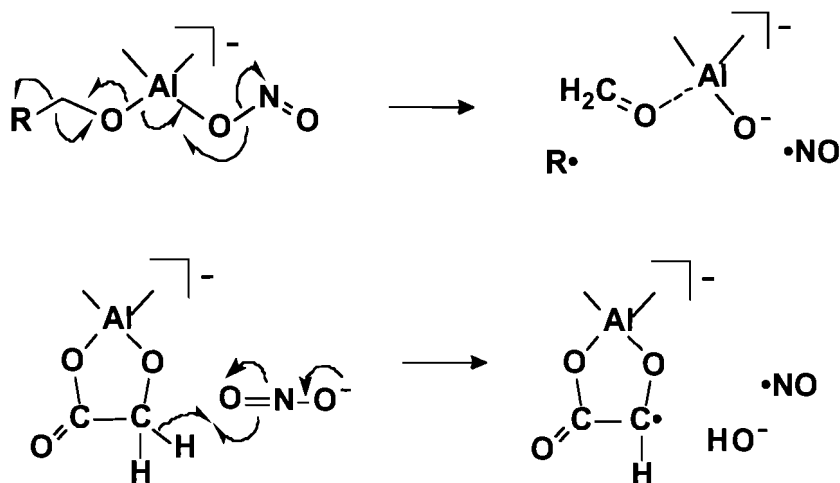
Figure 1. Suggested mechanism for Al(III)-catalyzed oxidation of glycolate (R = CO_2^-), HEDTA (R = $CH_2N(CH_2CO_2^-)CH_2$-$CH_2N(CH_2CO_2^-)_2$), and related structures by nitrite ion. The reactions are being studied to understand flammable gas generation and evolution of organic compounds over time. Aldehydes produced in these reactions degrade in caustic solutions to formate and oxalate ions and H_2 gas and condense with enolizable compounds to make larger adducts. Nitroso compounds from combination of R and NO radicals decompose to ammonia and N_2O gases.
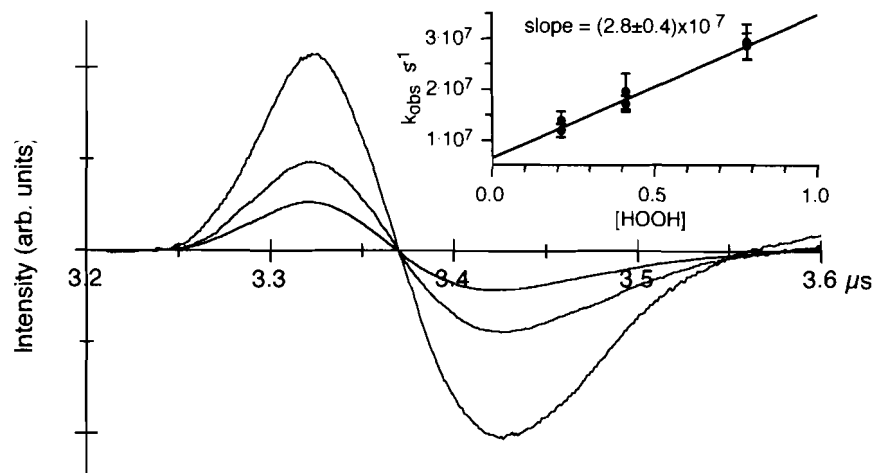
Figure 2. Acoustic signal from 308-nm pulsed laser light absorbed by aqueous H_2O_2 (— 0.2 M, — 0.4 M, — 0.8 M). The signal increases with concentration of H_2O_2 and shifts to longer time due to the exothermic reaction reaction $HO + H_2O_2 \rightarrow H_2O + O_2 + H^+$. The inset shows observed psuedo first-order rate constant extracted from the traces plotted against concentration of peroxide. The slope of the line yields the second-order reaction rate constant.
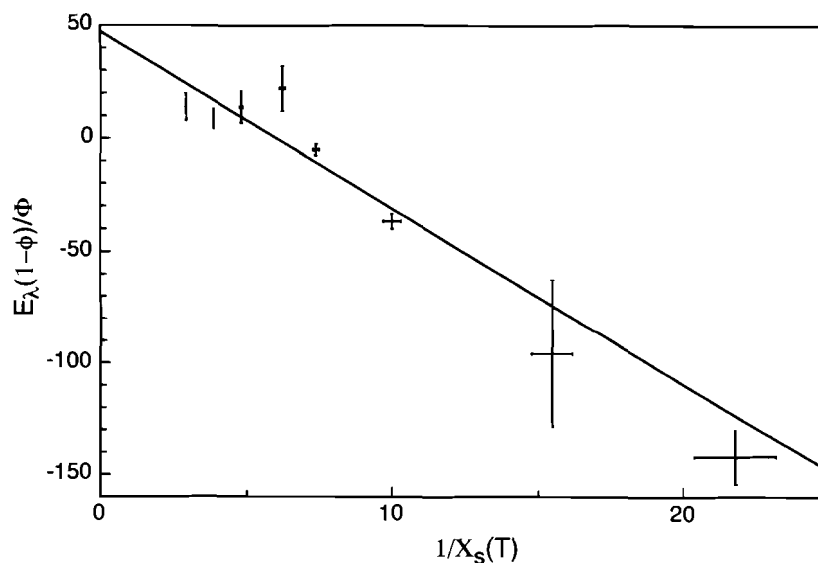
Figure 3. Photoacoustic signals, such as in Figure 2, are related to the changes in heat and volume associated with chemical reactions that occur within the time constant of the piezoelectric detector. The contributions add according to the equation, $E_\lambda(1-\phi)/\Phi = DH^\circ(aq) - \Delta V_r/\chi_s(T)$, where $E_\lambda(1-\phi)/\Phi$ is the apparent heat released to the'solution by photodissociation of H_2O_2, DH° is the bond dissociation energy of H_2O_2, ΔV_r is the solution volume change for H_2O_2 dissociation, and $\chi_s(T)$ is a function of the thermoelastic properties of water. The plot shows a least square fit to the E vs $\chi_s(T)$ for data obtained over a temperature range of 8–35°C yielding $DH^\circ(aq) = 47\pm5$ kcal/mol and $\Delta V_r = 7.8 \pm 0.6$ ml/mol.

1.4
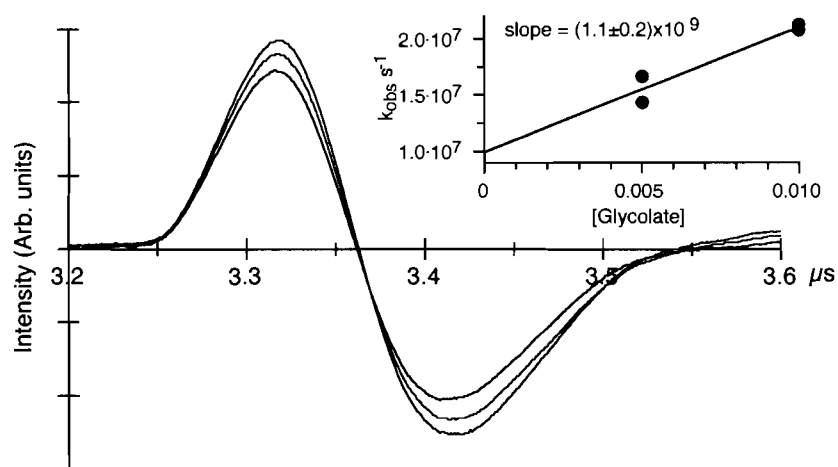
Figure 4. Photoacoustic signals from 0.2-M H_2O_2 solutions containing 0 (—), 5 (—), and 10 (—) mM sodium glycolate. Deconvolution of the time dependence of the signal gives the psuedo-first order rate constant for reactions of HO radical. The inset shows a plot and least squares fit of the observed first-order rate constant vs. glycolate concentration. The slope equals the second-order rate constant for reaction with glycolate and the intercept equals the reaction with H_2O_2 plus other background reactions. Rate constants agree with values found in the literature.

Theoretical Characterization of Intermediates in Aqueous Solution

Mathematical models of solvation based on a dielectric continuum representation of the solvent combined with Molecular Orbital and Density Functional electronic structure theories are available. These models can be used to calculate free energies of solvation for solutes in various solvents so that thermochemical properties, such as acidity (K_a), redox potentials $(E°)$, and reaction energies (ΔH and ΔG) can be determined. These methods are useful because they provide structural and energetics data that aid in verification of a reaction mechanism. Furthermore, the accuracy of computational methods is approaching that of experimental methods so a computational approach may be used when experimental data are either not available or are too difficult and expensive to obtain. A survey of various methods that can be used for computing aqueous solvation energies of molecules and ions and benchmark calculations using the methods were performed. These studies were necessary because few radical and zwitterion radical species usually are included in the evaluation sets used in the development of the methods. The work uses solvation models based on a continuum dielectric representation of the solvent with the solute molecule located within a molecule-shaped cavity embedded in the continuum. In these models, the interaction of the solute with the solvent is simulated by means of effective charges induced by the solute electron density at the cavity boundary. Thus, the shape and size of the cavity determines the strength of the interaction and, consequently, the magnitude of the solvation energy. The results of our benchmark comparisons of experimental and calculated data indicate that anions are not well represented by most

1.5

standard dielectric continuum models. Therefore, a powerful semi-empirical protocol that allows computational results to be directly equated with experimental measurements and a correlation of cavity shape with quantum mechanical descriptors was developed. The resulting methodology generates cavity shapes that capture the physics of anion-water interactions and reproduce anion hydration energies better than other methods [e.g., the United Atom Hartree Fock (UAHF) method (see Figure 5)]. Unlike the UAHF and other methods, our approach does not require knowledge of empirical parameters, such as the Van der Waals radii, or the hybridization of atoms.
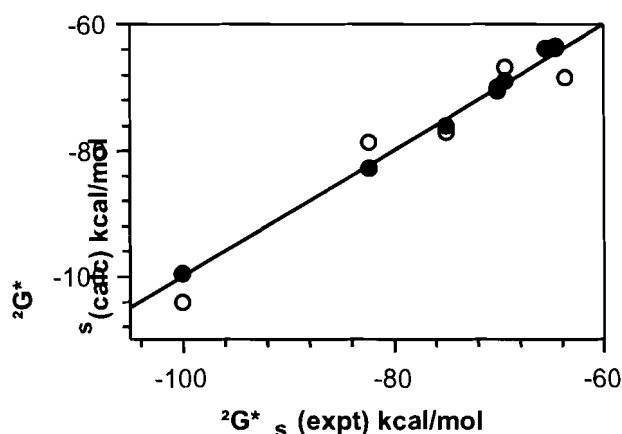
Figure 5. Predicted Gibbs Hydration Free Energies for the Ions in Table 1 Plotted Against the Experimental Values: Open Circles - UAHF Radii Solid Circles - Radii Predicted by Quantum Descriptors, X-O Bond Distance and Potential-Deriven Atomic (CHELPG) charges.

Table 1. Gibb's Free Energies of Hydration and Quantum Descriptors (Cavity Radii, Bond Distance, and Atomic Charges) That Reproduce the Energies Using the Gaussian 98 COSMO-Polarizable Continuum Model of Solvation

Species	$-\Delta G^*_s$ kcal/mol	R_O Å	$D_{X-O}^{(a)}$ Å	R_X Å	$Q_X^{(a)}$
O^-	100	1.46			
O_2^-	82	1.56			
O_3^-	70	1.59	1.352	2.12	0.076
NO_2^-	69	1.6	1.264	2.04	-0.087
$HCO_2^{-(b)}$	75	1.47	1.252	2.19	0.860
NO_3^-	65	1.53	1.260	2.42	1.180
ClO_2^-	64	1.53	1.634	2.71	0.432

(a) B3LYP/6-311+G** CHELPG charges.
(b) X = C-H group.

Planned Activities

Our development and benchmarking of experimental and theoretical methods will continue. The experimental effort on applying the PAC technique in aqueous solution will focus on increasing the accuracy of heat measurements and on titrating the pK_a of OOH and glycolate radicals to determine the potential for measuring ΔH and ΔG for proton transfer. We then will initiate efforts to obtain results for Al complexes of glycolate. In our computational effort, we will develop quantum-descriptors for radii of hydroxyl and alkyl groups in oxoanions and for multiply charged oxyanions. Also, the solvation model will be used to characterize properties of species outside the training set as well as ones of interest to project objectives. Three manuscripts will be prepared and submitted.

Information Access

Camaioni D, M Dupuis, and J Watts. 2001. Characterization of Intermediates in High Level Waste. Sci-Mixer poster representing Nuclear Chemistry Division Symposium on Environmental Management Science Program, Annual Meeting, 222nd American Chemical Society National Meeting, August 29, 2001, Chicago, Illinois.

Carmichael I, GL Hug, D Meisel, DM Camaioni. 2001. NO_x Ions and Radicals in Homogeneous and Heterogeneous Nuclear Waste. Presentation to Nuclear Chemistry Division Symposium on Environmental Management Science Program, 222nd American Chemical Society National Meeting, August 29, 2001, Chicago, Illinois.

Camaioni DM, D Meisel, and T Orlando. 2001. Radiation Chemistry and Stored Defense Nuclear Waste. Presentation to Chemical Education Division Symposium on Radiation Research: From the Science Laboratory to the Real World, American Chemical Society National Meeting, August 30, 2001, Chicago, Illinois.

Camaioni DM, T Autrey, M Dupuis, and WJ Shaw. 2001. Mechanisms and Kinetics of Organic Aging and Characterization of Intermediates in High Level Waste. Kickoff Workshop on New HLW Tasks November 7-8, 2001, Richland, Washington. <http://emsp.em.doe.gov/HLWCD2001/files/breakout/81883.pdf>

Bentley J, I Carmichael, DM Chipman, G Hug, D Meisel, DM Camaioni, and M Dupuis. 2002. Radiolysis Effects in Waste Simulants: Modeling the Chemistry in Waste Tanks. Presentation to session on Science to Applications - DOEs Experience: Success Stories From the Environmental Management Science Program, Spectrum 2002, 9th Biennial International Conference on Nuclear and Hazardous Waste Management, August 4-8, 2002, Reno, Nevada.

Dupuis M, DM Camaioni, D Chipman, and J Bentley. 2002. Towards Ab Initio Cavities for Dielectric Continuum Solvation Models. Invited presentation to Symposium on Classical and Quantum Statistical Mechanics Studies of Solvation, 224th American Chemical Society National Meeting, August 18-22, 2002, Boston, Massachusetts.

Radioanalytical Chemistry for Automated Nuclear Waste Process Monitoring

(Project Number: 81923)

Principal Investigator

Oleg B. Egorov
Pacific Northwest National Laboratory
P.O. Box 999, MSIN P7-22
Richland, WA 99352
509-376-3485 (phone)
509-372-2156 (fax)
oleg.egorov@pnl.gov

Co-Investigator

Jay W. Grate
Pacific Northwest National Laboratory
P.O. Box 999, MSIN K8-93
Richland, WA 99352
509-376-4242 (phone)
509-376-5106 (fax)
jwgrate@pnl.gov

Co-Principal Investigator

Timothy A. DeVol
Environmental Engineering & Science
Clemson University
Clemson, SC 29634-0919
864-656-1014 (phone)
tim.devol@ces.clemson.edu

Graduate Students Actively Involved in the Project: 3
Undergraduate Students Involved (Part-Time) in the Project: 3

Research Objective

This research is directed toward rapid, sensitive, and selective determination of beta- and alpha-emitting radionuclides such as ^{99}Tc, ^{90}Sr, and transuranium (TRU) elements in low-activity waste (LAW) processing streams. The overall technical approach is based on automated radiochemical measurement principles. Nuclear waste process streams are particularly challenging due to the complex, high-ionic-strength, caustic brine sample matrix, the presence of interfering radionuclides, and the sometimes variable and uncertain speciation of the radionuclides to be analyzed. As a result, matrix modification, speciation control, and separation chemistries are required for use in automated process analyzers. Significant knowledge gaps exist relative to designing chemistries for such analyzers so that radionuclides can be quantitatively and rapidly separated and analyzed in high ionic strength solutions derived from low-activity waste processing operations. This research is addressing these knowledge gaps and automated microscale fluid handling techniques will be used to integrate sample modification, chemical separation chemistries, and radiometric detection steps within a single functional process analytical instrument.

The outcome of these investigations will be the knowledge necessary to choose appropriate chemistries for sample matrix modification and analyte speciation control and chemistries for rapid and selective separation and preconcentration of target radionuclides from complex sample matrices. In addition, new approaches for quantification of alpha emitters in solution using solid-state diode detectors, as well as improved instrumentation and signal processing techniques for use with solid-state and scintillation detectors, will be developed. New knowledge of the performance of separation materials, matrix modification and speciation control chemistries, instrument configurations, and quantitative analytical approaches will provide the basis for designing effective instrumentation for radioanalytical process monitoring. Specific analytical targets include ^{99}Tc, ^{90}Sr, and TRU actinides.

Research Progress and Implications

This report summarizes work as of 8 months into a 3-year program. Because of the immediate relevance to our applied effort in the development of the on-line ^{99}Tc process monitor for the Waste Treatment Plant at Hanford, our initial research effort has been directed at 1) chemistry for rapid, automated ^{99}Tc speciation control; 2) ^{99}Tc separation chemistry; and 3) radioanalytical chemistry of the Hanford waste. In the area of radiation detection, our effort to date has been targeted toward the investigation of state-of-the-art photo detectors and procurement of instrumentation needed for the project.

In order to enable *total* ^{99}Tc analysis in process solutions, oxidation chemistries and automated procedures must be developed that convert all of the Tc species to pertechnetate. For the implementation in a process-monitor instrument, oxidation procedures must be rapid, reliable, and quantitative. In addition, oxidizing reagents must be stable over long periods of time. To enable rapid and reliable oxidation of the non-pertechnetate species to pertechnetate, we selected oxidation chemistry based on peroxidisulfate. Peroxidisulfate chemistry was selected and evaluated in detail using actual high-organic Hanford wastes with up to 70% content of the non-pertechnetate fraction. The oxidation chemistry was studied using an automated microwave-assisted reaction module. Our studies with actual waste indicated that sample acidification is necessary prior to oxidation of non-pertechnetate to remove copious quantities of nitrite that interferes with oxidation. Furthermore, we established that acidification and microwave heat treatment alone were not sufficient to enable rapid and quantitative oxidation. However, rapid and reliable oxidation of Tc was possible using peroxidisulfate reagent. Using microwave sample treatment, the oxidation was complete within 20 seconds. No catalyst was necessary to enable rapid and reliable oxidation. In addition, it is significant that complete destruction of the organic matter was determined to be unnecessary for the quantitative oxidation of non-pertechnetate species to pertechnetate. Consequently significant excess of the oxidant is not required for quantitative oxidation of non-pertechnetate. We evaluated the decomposition rate of peroxidisulfate reagent. Results indicate a reliable shelf life of 2 months in de-ionized water is feasible. Slower rates of decomposition and improved shelf life were obtained in slightly alkaline solutions (pH 9). Our results to date indicate that peroxidisulfate oxidation chemistry represents the chemistry of choice for rapid and reliable Tc speciation control in aged waste samples; the chemistry enables rapid and reliable oxidation of non-pertechnetate.

We continue detailed development and investigation of the column separation chemistries for separating ^{99}Tc(VII) from radioactive interferences in aged waste. The separation format selected for detailed investigation is based on the use of strongly basic anion exchange sorbent material. Our results to date indicate that rapid and selective separation of ^{99}Tc from major radioactive interferents and stable matrix is possible. Nevertheless, a sequence of column wash steps is required to ensure adequate removal of the interfering species required for accurate ^{99}Tc determination in the aged waste. Using anion exchange chromatographic material, separation from major radioactive species (e.g., ^{90}Sr/^{90}Y, ^{137}Cs) is straightforward. However, this format is more challenging for separating Tc from other anionic species. Experiments with actual Hanford wastes indicated that Tc separation from Sn, Sb, Ru, and Rh is required to enable accurate analysis of ^{99}Tc under process-monitoring conditions. Work in progress is directed at the development of elution sequences to address these separation requirements.

We continue to investigate the trade-offs of the various photodetectors. We have purchased an avalanche photodiode detector package for evaluation relative to the photomultiplier tube (PMT). Initial results indicate that for high-level waste process-monitoring applications, the PMT may be

1.11

the best suited, as compact size and signal-to-noise ratio are not the major considerations. Digital signal processing of the electronic pulses from a radiation detector is becoming mainstream. We learned of the power and limitations associated with the use of a software-based digital signal processing system under another EMSP project (No. 70179). The primary limitation imposed by a software-based approach is the maximum count rate, which is considerably more limiting for the quantification of high-level waste process streams than for environmental radiation measurements. After considerable investigation, a Digital Gamma Finder - 4C (DGF-4C, X-ray Instrumentation Associates) was purchased for the project. The DGF-4C offers the possibility of hardware-implemented real-time digital signal processing. The negative output pulses from the photodetectors will be digitized at a rate of 40 MHz with 12-bit precision using the XIA's DGF-4C digital spectrometer and waveform digitizer. All four channels of the DGF-4C will be used to digitize anode and dynode pulses from two photodetectors. The DGF-4C module was housed in a low-noise CAMAC crate. Communication to the DGF-4C module is through a Jorway 73A SCSI crate controller to a personal computer.

Standard DGF-4C control software, developed at XIA, will be used initially to collect and analyze the data. As needed, the data can be saved as list mode to the personal computer hard disk and analyzed off-line with the DGF Viewer. The DGF Viewer runs under an interactive programming and data analysis environment IGOR Pro (Wavemetrics, Inc.) whose programming language and graphics were used to analyze the data offline. This gives us the flexibility to optimize the data acquisition algorithms before they are programmed into the field-programmable gate arrays of the DGF-4C. The DGF-4C, CAMAC crate, Jorway 73A Fast CAMAC controller and SCSI card for the PC were received by April 2002. We are in the early stages of the instrument development and software evaluation.

Planned Activities

During the remainder of the first year, we will continue investigation, developing, testing of the ^{99}Tc separation chemistries for rapid, automated radiochemical analysis of ^{99}Tc in Hanford waste-processing streams. We have held discussions with Savannah River Site personnel on the needs of Sr and TRU monitoring for the Salt Processing Facility. Savannah River Site needs are being used to direct our research plans for the second and third years of this project, which will be directed at automated monitoring of ^{90}Sr and TRU in aged nuclear waste streams.

Information Access

Egorov O, MO'Hara, and J Grate. 2002. Automation of the radiochemical analysis: From groundwater monitoring to nuclear waste analysis. Abstracts of Papers, 223rd ACS National Meeting, April 7-11, 2002, Orlando, Florida.

Egorov O, M O'Hara, and J Grate. 2002. "Automated radiochemical analysis of total Tc-99 in nuclear waste processing streams." Abstracts of Papers, 223rd ACS National Meeting, April 7-11, 2002, Orlando, Florida.

Egorov O, T DeVol, and J Grate. 2001. "Advances in automated radioanalytical chemistry: From groundwater monitoring to nuclear waste analysis." Abstracts of Papers, 222nd ACS National Meeting, August 26-30, 2001, Chicago, Illinois.

Precipitation and Deposition of Aluminum-Containing Species in Tank Wastes

(Project Number: 81887)

Principal Investigator

Shas V. Mattigod
Pacific Northwest National Laboratory
P.O. Box 999, MSIN K6-81
Richland, WA 99352
509-376-4311 (phone)
509-376-5368 (fax)
shas.mattigod@pnl.gov

Co-Investigators

David T. Hobbs
Westinghouse Savannah River Company
Savannah River technology Center,
Building 773-A
Aiken, SC 29808
803-725-2838 (phone)
803-725-4704 (fax)
david.hobbs@srs.gov

Li-Qiong Wang
Pacific Northwest National Laboratory
P.O. Box 999, MSIN K2-44
509-376-2078 (phone)
509-376-2186 (fax)
liquong.wong@pnl.gov

Daniel M. Dabbs
Princeton Materials Institute
Princeton University
70 Prospect Avenue
Princeton, NJ 08580-5211
609-258-1572 (phone)
609-258-6878 (fax)
ddabbs@princeton.edu

Ilhan A. Aksay
Princeton Materials Institute
Princeton University
70 Prospect Avenue
Princeton, NJ 08580-5211
609-258-4580 (phone)
609-258-6878 (fax)
iaksay@princeton.edu

Research Objectives

Aluminum-containing phases represent the most prevalent solids that can appear or disappear during the processing of radioactive tank wastes. Processes such as sludge washing and leaching are designed to dissolve Al-containing phases and thereby minimize the volume of high-level waste glass required to encapsulate radioactive sludges. Unfortunately, waste-processing steps that include evaporation can involve solutions that are supersaturated with respect to cementitious aluminosilicates that result in unwanted precipitation and scale formation. Of all the constituents of tank waste, limited solubility cementitious aluminosilicates have the greatest potential for clogging pipes and transfer lines, fouling highly radioactive components such as ion exchangers, and completely shutting down processing operations. For instance, deposit buildup and clogged drain lines experienced during the tank waste volume-reduction process at the Savannah River Site (SRS) required an evaporator to be shut down in October 1999. The Waste Processing Technology Section of Westinghouse Savannah River Company at SRS now is collaborating with team members from Pacific Northwest National Laboratory (PNNL) to verify the thermodynamic stability of aluminosilicate compounds under waste tank conditions in an attempt to solve the deposition and clogging problems. The primary objectives of this study are 1) to understand the major factors controlling precipitation, heterogeneous nucleation, and growth phenomena of relatively insoluble aluminosilicates; 2) to determine the role of organics for inhibiting aluminosilicate formation, and 3) to develop a predictive tool to control precipitation, scale formation, and cementation under tank waste processing conditions. The results of this work will provide crucial information for 1) avoiding problematical sludge processing steps and 2) identifying and developing effective technologies to process retrieved sludges and supernatants before ultimate vitrification of wastes.

Research Progress and Implications

This report summarizes work completed after 1 year of a 3-year project. Studies conducted so far have focused on identifying the insoluble aluminosilicate phase(s) and characterizing their chemistry and microstructure by determining the kinetics of the phase formation and transformation of such aluminosilicate phases under hydrothermal conditions.

The data we obtained from tests conducted at 40°C showed that formation and persistence of crystalline phases were dependent on the initial hydroxide concentrations. The formation and persistence of a zeolitic phase (zeolite A) occurred only at lower hydroxide concentrations, whereas increasing hydroxide concentrations appeared to promote the formation of sodium aluminosilicate phases such as sodalite and cancrinite. The results showed that although zeolite A forms during the initial period of reaction, it converts to more stable crystalline phases such as sodalite and cancrinite because of its metastability. We also observed that the rate of transformation of zeolite A increased with increasing hydroxide concentration. The data from

tests conducted at 80°C revealed relatively rapid formation of sodalite and cancrinite. Although minor amounts of zeolite A were detected initially in some cases, the higher reaction temperatures seemed to promote very rapid transformation of this phase into more stable phases. Also, the higher temperature and hydroxide concentrations appeared to initiate kinetically fast crystallization of sodalite and cancrinite. Figures 1 and 2 illustrate our findings.
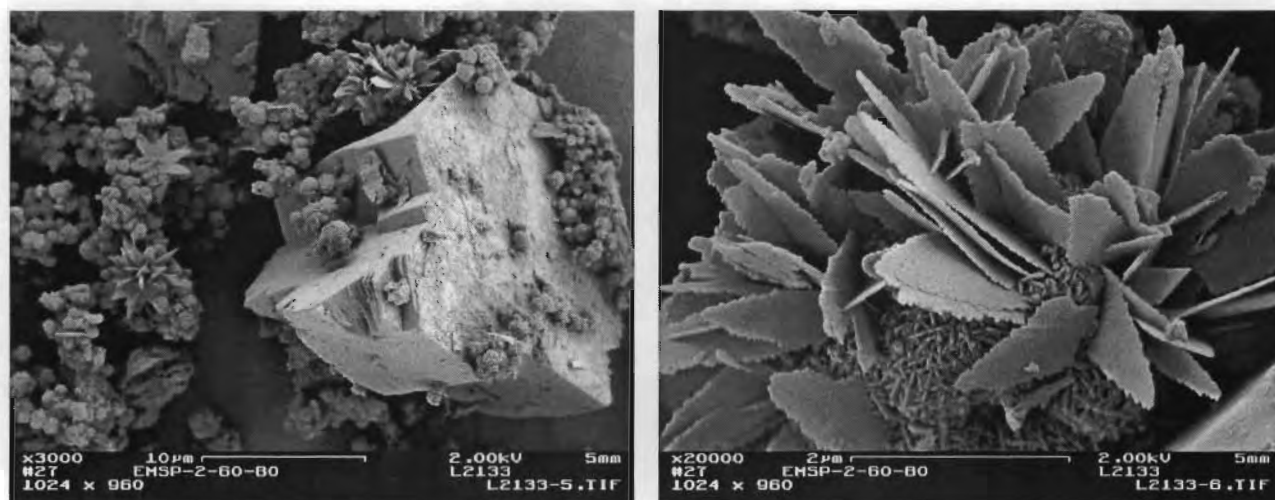
Figure 1. (Left) Massive crystals of gibbsite with minor quantities of bladed nordstrandite and textured spherical cancrinite formed after 60-day reaction period at 80°C from low Si (0.01 M), high Al (0.5 M), and low OH (0.1 M). (Right) A close-up of nordstrandite and cancrinite crystals.
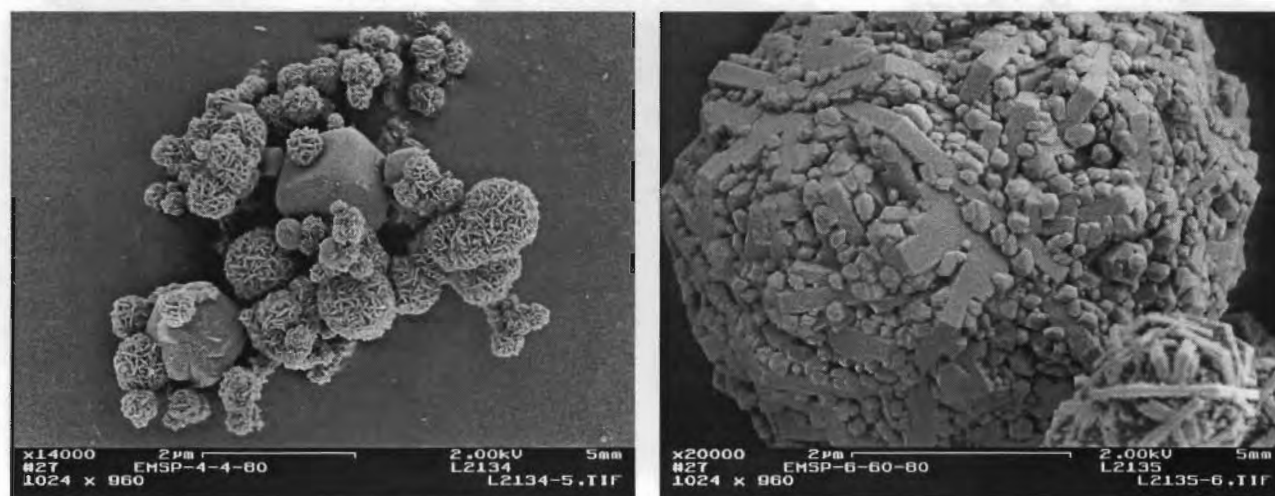
Figure 2. (Left) Aggregates of cubic zeolite A and spherical cancrinite crystals formed after 4-hr reaction period at 80°C from low Si (0.01 M), high Al (0.5 M), and high OH (1.0 M). (Right) A magnified view of well-crystallized cancrinite formed after 60-day reaction period at 80°C from low Si (0.01 M), high Al (0.5 M), and very high OH (4.5 M).

The data we have obtained so far are unique because we have examined aluminosilicate formation under very low silica-high aluminum (Al/Si) mol ratio conditions (20 to 50) and a range of hydroxyl conditions (0.1 to 4 M) that are similar to actual waste processing conditions. Our literature review indicated that all previous studies on aluminosilicate (zeolites) formation were typically conducted at Al/Si mol ratios approaching unity. Therefore, the implications of our study are that during waste concentration in evaporators, hard scale-forming aluminosilicates can form even in the presence of very low concentrations (0.01 M) of silica in the feedstock. More recent testing at the SRS in support of the high-level waste evaporator plugging issue has shown similar trends in the formation of aluminosilicate phases. Comparison of our results with those reported above show very similar trends - that is, initial formation of an amorphous precipitate followed by a zeolite phase that transforms to sodalite, which finally converts to cancrinite. Our results also show the expected trend of an increased rate of transformation of initial precipitates into denser scale-forming aluminosilicate phases (sodalite and cancrinite) at higher temperature. The results of our studies can be used to avoid feedstock compositions that would result in rapid formation of enhanced quantities hard scale-forming aluminosilicate phases such as sodalite and cancrinite. Two manuscripts that describe the studies are being prepared for submission to selected peer-reviewed journals.

The work conducted by our collaborators at the Princeton University focused on understanding the mechanisms by which organics inhibit the nucleation and growth of insoluble aluminum oxyhydroxides, specifically to evaluate the ability of an organic to chelate with the aluminum cation or active sites on the surfaces of complexes and particles. The initial focus has been on the use of simple carboxylic acids, to stabilize colloidal alumina particles in aqueous suspension. Our investigations demonstrated the very complex chemistry that appears to exist within deceptively simple solutions containing only aluminum oxyhydroxides and/or aluminum cations, the organic moiety, NaOH, and water. Nuclear magnetic resonance with ^{27}Al solution on control solutions containing aluminum nitrate in water demonstrated the development of a large aluminum complex $(Al_{13}O_4(OH)_{24}(H_2O)_{12}^{7+}$ polycation, "Al_{13}") at OH/Al molar ratios near 2.46 (Figure 3), assumed to be the precursor to aluminum oxyhydroxide particle formation and precipitation. The effect of citric acid $(HOOCCH_2COH(COOH)CH_2COOH)$, a tricarboxylic acid, is to inhibit particle formation, apparently by preventing the formation of or breaking up the large aluminum complex, directly chelating to and stabilizing the Al^{3+} cation in solution (Figure 4).
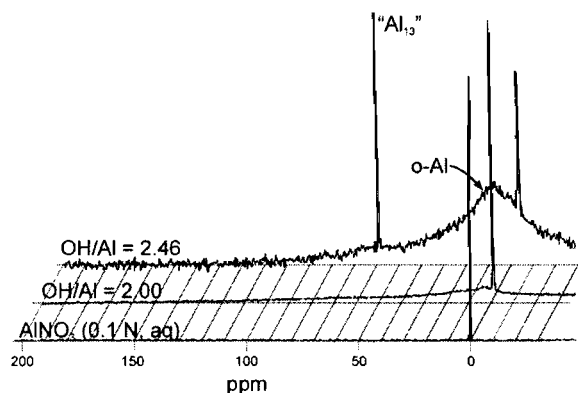

Figure 3. Addition of NaOH to aqueous solutions of aluminum nitrate results in the formation of a soluble 13-Al oxyhydroxide complex ("Al_{13}").

1.18

Although effective at low pH and high reactant concentrations, citric acid is ineffective in high-pH solutions and low reactant concentrations, as shown by quasi-elastic light scattering. Under these conditions, precipitation occurs in spite of the presence of the acid. Other carboxylic acids—tricarballylic acid (TCA) and 2,4-dihydroxy benzoic acid—are effective under these same conditions, although at very high ratios of acid to aluminum (Figure 5). Tricarballylic differs chemically from citric acid in the absence of a hydroxide group on the central carbon ($HOOCCH_2CH(COOH)CH_2COOH$), which appears to improve citric acid solubility in water relative to TCA.
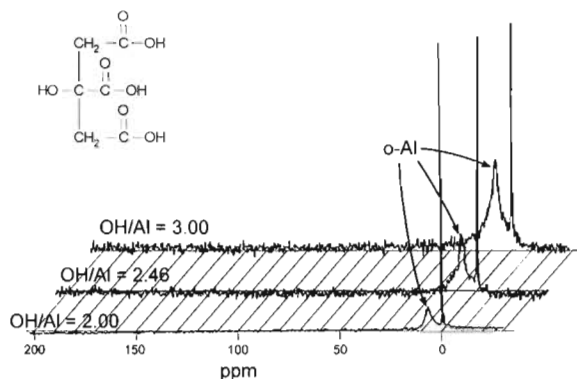
Figure 4. Citric acid (inset structure) prevents precipitation of aluminum-containing materials by inhibiting or decomposing the large soluble complexes believed to provide the seeds for the nucleation and growth of insoluble species.
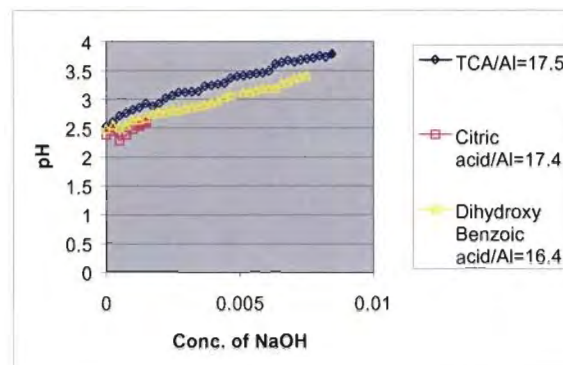
Figure 5. At higher pH and low reactant con-centrations, citric acid fails to prevent precipita-tion of aluminum-containing phases. TCA and 2,4-dihydroxy benzoic acid, although having lower solubility in water, effectively prevent the formation of insoluble species, albeit at very high acid to aluminum ratios (plots truncate at point of precipitation).

Planned Activities

We will be conducting experiments at higher temperatures (120°C and 175°C) to examine the rate of formation and transformation of aluminosilicate phases (to be completed March 2003). We will conduct low angle x-ray scattering studies to understand formation of clusters during the very early stages of the reaction period; these studies are scheduled for completion by June 2003. Following these activities, we plan to initiate solution thermodynamic studies. Our collaborators at Princeton University will be conducting [27]Al nuclear magnetic resonance spectrometry to determine the structure of the stabilized aluminum-containing species in solution in the presence of TCA and 2,4-dihydroxy benzoic acid. Additional studies would include the use of polyelectrolytes such as poly(acrylic acid) to stabilize or dissolve aluminum complexes.

Non-Invasive Diagnostics to Measure Physical Properties in High-Level Wastes

(Project Number: 73827)

Principal Investigator

David M. Pfund
Pacific Northwest National Laboratory
P.O. Box 999, MSIN K7-15
Richland, WA 99352
509-375-3879 (phone)
509-375-2806 (fax)
david.pfund@pnl.gov

Co-Investigator

Robert L. Powell
University of California, Davis
Department of Chemical Engineering and Materials Science
One Shields Avenue
Davis, CA 95616-5294
530-752-8779 (phone)
rlpowell@ucdavis.edu

Graduate Student

Nihan Dogan, Ph.D.

Research Objective

This project addresses the need for a technique that can determine the rheological properties of tank wastes under processing conditions and permit the monitoring and control of slurries during transport. The work consists of applying ultrasonic Doppler velocimetry and using it to measure the viscosity of flowing waste. We will use suspensions that simulate tank waste and will work under realistic flow conditions.

The work will also include a demonstration of a tomographic measurement of solids loading and velocity profiles and an investigation of the utility of this approach in estimating mass flow rate. A tomographic system uses a number of independent line-of-sight measurements to solve the problem of simultaneously measuring the solids loading and velocity profiles within the pipe. Determining mass flow rate and weight percent solids requires knowledge of the speed of sound as a function of loading; questions that will be addressed include effects of the particle size and density distributions.

Finally, this work will investigate the use of ultrasonic techniques to measure sedimentation interface and rate. A tool that could result from successful demonstration could be used to monitor sedimentation progress during in-tank pretreatment and waste processing.

Research Progress and Implications

This report summarizes work after 18 months of a 3-year project.

A new self-contained ultrasonic Doppler velocimeter (UDV) was designed and built during the first year of the project. The new unit closes the gap between a laboratory experiment and a field-deployable unit instrument for measuring velocity profiles, volumetric flow rates, and viscosities. It combines the UDV instrument, acquisition of pressure and temperature measurements, and real-time calculations of viscosity versus shear rate into one package. New capabilities have been added to make it perform without the need for operator intervention or batch laboratory experiments:

- It is a multiple-frequency instrument (1 MHz, 2 MHz and 5 MHz).

- It provides a measure of signal quality at each radial position that is used to improve data analysis.

- It will measure the sound speed of the fluid concurrently with velocity measurement, automatically compensating for temperature and composition variations and eliminating the need for a new calibration when a new fluid is being metered.

1.22

Preliminary tests of the new instrument were performed in fall 2001. The tests revealed the need for modifications to the instrument. The modifications, made during spring 2002, included the following:

- The electronics that drive the ultrasound transducers were improved to increase the signal-to-noise ratio.

- The instrument's computer software was revised to improve the user interface, reduce the amount of post-processing required, and allow the mass production of data.

- The software was tested, errors were corrected, and documentation is being prepared.

The new UDV system will be tested with slurry simulants in our existing flow loop. The loop has been modified to improve operation at higher flow rates with viscous materials. New pressure sensors were purchased and installed for use with the slurries.

A new technique was developed that will allow the construction of fast arrays of ultrasonic transducers for tomography applications. Long-duration pulses are integrated to increase the signal-to-noise ratio. The pulses are encoded with information that allows sharp time resolution and enables many transducers to use the same bandwidth at the same time.

We have met twice with our collaborators from the University of California, Davis. Pacific Northwest National Laboratory personnel visited Davis in January 2002. A graduate student from UC Davis performed experiments in our laboratory during summer 2001.

Planned Activities

- Diagnostic tests of the new UDV system are scheduled for June 2002.

- Tests of the new UDV system with slurry simulants will be done in August 2002.

- Application of the new long-duration pulse technique to the measurement of time-of-flight through slurries is slated for September 2002.

Information Access

Dogan N, RL Powell, MJ McCarthy, R Pappas, DM Pfund, and DM. Sheen. 2002. In-line ultrasonic sensor for characterization of opaque suspensions. Presentation to the ACS National Meeting, Orlando, Florida, April 7-11, 2002(abstract accessible at http://chemistry.org/portal/PersonalScheduler/EventView.jsp?paper_key=204262&session_key= 34673)

Pappas RA, JA Bamberger, LJ Bond, MS Greenwood, PD Panetta, and DM Pfund. 2001. Ultrasonic Methods for Characterization of Liquids and Slurries. In *2001 IEEE Ultrasonics Symposium Proceedings,* Vol. 1, pp. 563-566. Institute of Electrical and Electronics Engineers, Piscataway, New Jersey.

Investigating Ultrasonic Diffraction Grating Spectroscopy and Reflection Techniques for Characterizing Slurry Properties

(Project Number: 81889)

Principal Investigator

Margaret S. Greenwood
Pacific Northwest National Laboratory
P.O. Box 999, MSIN K5-26
Richland, WA 99352
509-375-6801 (phone)
509-375-6736 (fax)
Margaret.greenwood@pnl.gov

Co-Investigators

Leonard J. Bond
Pacific Northwest National Laboratory
P.O. Box 999, MSIN K5-26
Richland, WA 99352
509-375-4486 (phone)
509-372-4583 (fax)
Leonard.bond@pnl.gov

Lloyd Burgess
University of Washington
Seattle, WA 98195
206-543-0579 (phone)
lloyd@cpac.washington.edu

Anatol Brodsky
University of Washington
Seattle, WA 98195
206-543-1676 (phone)
brodsky@cpac.washington.edu

Graduate Student

Mazen Lee Hamad

Research Objectives

The objectives of the project are to investigate the use of 1) ultrasonic diffraction grating spectroscopy (UDGS) for measuring the particle size of a slurry and 2) shear wave reflection techniques to measure the viscosity of a slurry. For the first topic, the basic principle is to extend the methods that have been successful in optics, called grating light reflection spectroscopy (GLRS), to ultrasonics. At the University of Washington, researchers are using GLRS to measure nanometer-sized particles and particles up to two microns in size in slurries. The goal of the research with ultrasonics is to measure particles in the range of a few microns to about 100 microns, which is the range of particle sizes for slurries in the radioactive waste tanks at U.S. Department of Energy (DOE) sites. The collaborators at the University of Washington will provide the theoretical algorithm that extracts particle size information from the experimental measurements of the critical frequency and amplitude. For the second topic, the research will use multiple reflections of ultrasonic shear waves at the interface between a solid and a liquid or slurry. Such reflections are known to provide information about the viscosity, but the goal here is to develop a method to make on-line measurements. This will include using the self-calibrating method, developed by Greenwood, for which a patent application has been submitted. In both phases of the research, collaboration with partners at the University of Washington will provide the theoretical basis for analysis of the experimental data.

Research Progress and Implications

This report summarizes work after one year of a three-year project. In our experiments with UGDS, the diffraction grating consists of equally spaced triangular grooves machined into the face of a stainless steel half-cylinder, as shown in Figure 1. The incident ultrasonic wave travels through the stainless steel and strikes the back of the diffraction grating at an angle θ. This produces diffracted ultrasonic waves traveling in the liquid or slurry in contact with the grating, as well as a reflected wave observed by the receive transducer. In the experiment the ultrasound sweeps through a range of frequencies and at each frequency, the amplitude of the receive signal recorded. As the frequency of the ultrasonic wave decreases, the angle of the m = 1 diffracted wave in the liquid increases. At the critical frequency, this wave reaches 90°. In Figure 2, the location of the m = 1 wave in the liquid is shown as the frequency of the incident wave changes. At 90° it becomes an evanescent wave, which is an exponentially decaying wave

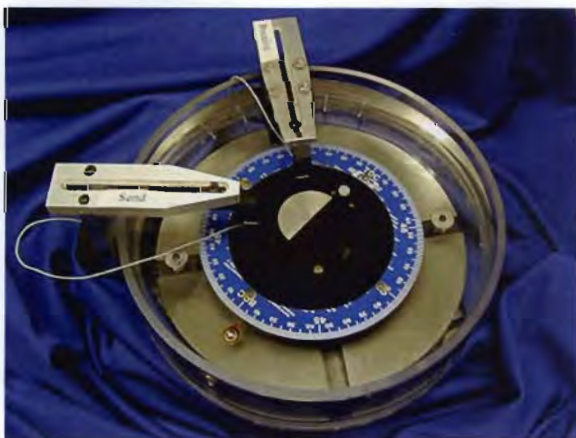**Figure 1**. Experimental apparatus showing the immersion chamber, stainless steel grating, and send and receive transducers

Transmitted Longitudinal Waves in Water
30 deg Incident Angle on 300 micron SS Grating

Figure showing the movement of diffracted waves, with labels:
- Incident Longitudinal Wave
- Grating
- Water
- Diffracted Longitudinal Wave at 5.65 MHz, m = 1, Angle = 90 deg
- at 6 MHz, m = 1
- Diffracted Longitudinal Wave at 7 MHz, m = 1
- Transmitted Longitudinal Wave, m = 0
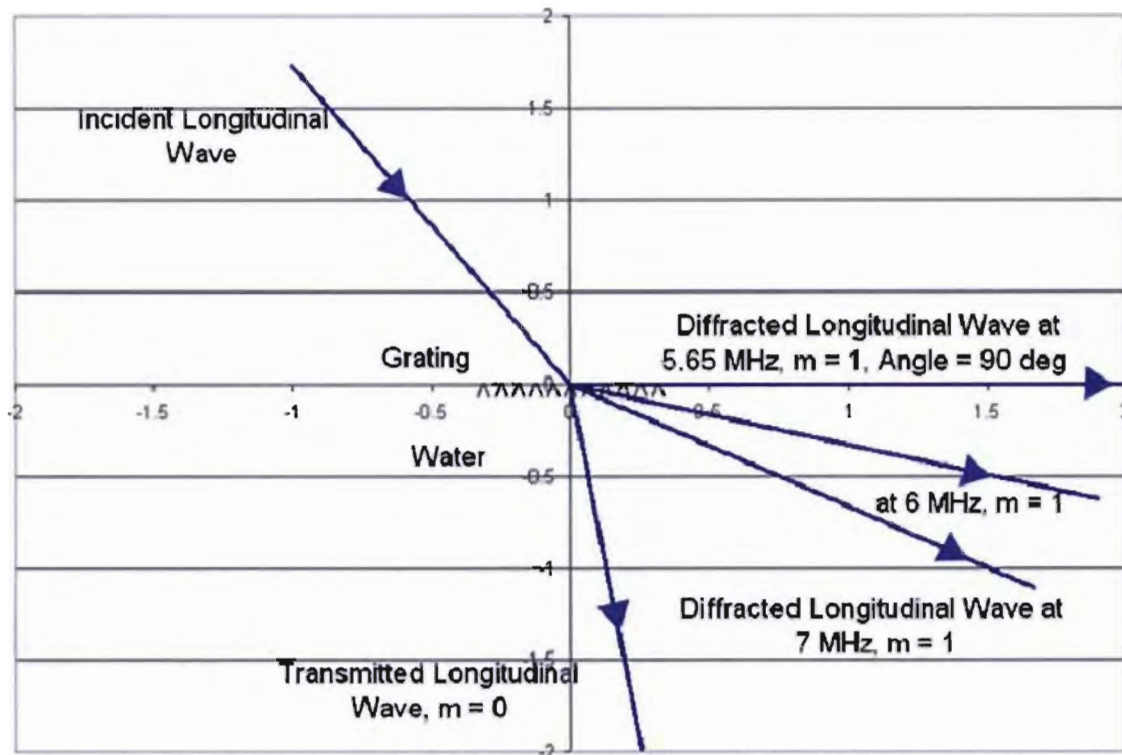
Figure 2. Movement of the m = 1 Wave in the Liquid to a Larger Angle as the Frequency Decreases

in the liquid or slurry. At a frequency below the critical frequency, the evanescent wave disappears and the energy is shared by all other waves. The objective is to observe the increase in signal at the critical frequency. For a slurry, the evanescent wave is attenuated due to Rayleigh scattering, and the amplitude of the receive signal at the critical frequency decreases. Because the attenuation is dependent upon particle size, this is the mechanism to determine particle size.

Because the critical frequency depends upon the grating spacing, the velocity of sound in the liquid, and the incident angle, the experiments were designed to vary all three parameters. The experiments were carried out using water and sugar water solutions, up to 30% by weight to vary the velocity of sound. The diffraction gratings consisted of 1) stainless steel (SS) with a 300-micron grating spacing, 2) SS with a 200-micron grating spacing, and 3) a Rexolite plastic grating with a 406-micron grating spacing.

For each SS grating, data were obtained at incident angles of 20°, 30°, 40°, and 50° for water, 10% sugar water (SW), 20% SW, and 30% SW. Figure 3 shows the data obtained for the
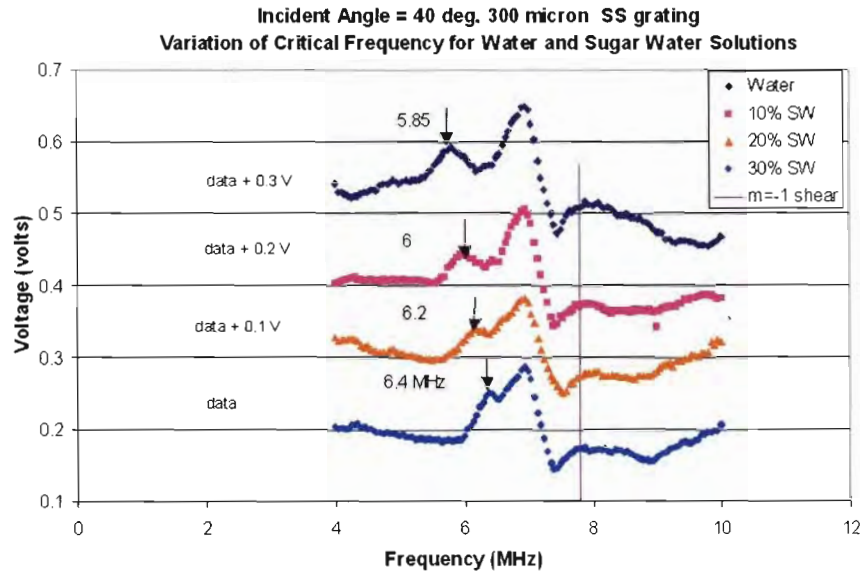
Figure 3. Data Obtained for 300-micron Stainless Steel Grating for an Incident Angle of 40°

300-micron SS grating at an incident angle of 40° and Figure 4, for the 200-micron SS grating at an incident angle of 30°. The experimental data are in *very good agreement* with the theoretical values of the critical frequency, shown by the arrows in Figures 3 and 4. The 32 sets of data for the SS gratings show similar agreement between the experimental and theoretical values of the critical frequency. This is a very important result, for the data show the ability to determine the critical frequency, which will be used in later experiments with slurries for the determination of particle size.

For the Rexolite grating, data were obtained for water at seven incident angles. At an incident angle of 25°, data were obtained for the following weight percentages of sugar water: 1.5%, 3%, 4.5%, 6%, 7.5%, 10%, 15%, 20%, 25%, and 30%. For water, the experimental data show good agreement with the predicted critical frequency. For the sugar water solutions, the critical frequencies cannot be distinguished from those for water. However, a peak in the graph of voltage versus frequency (Figure 5) shows that the height of the peak is very sensitive to the density of the SW solutions. Thus, an unexpected result is that the diffraction grating can act as a density sensor.

The immersion chamber shown in Figure 1 is mounted on a turntable. Within the last 3 months, the immersion chamber was motorized, and the data acquisition system was modified to
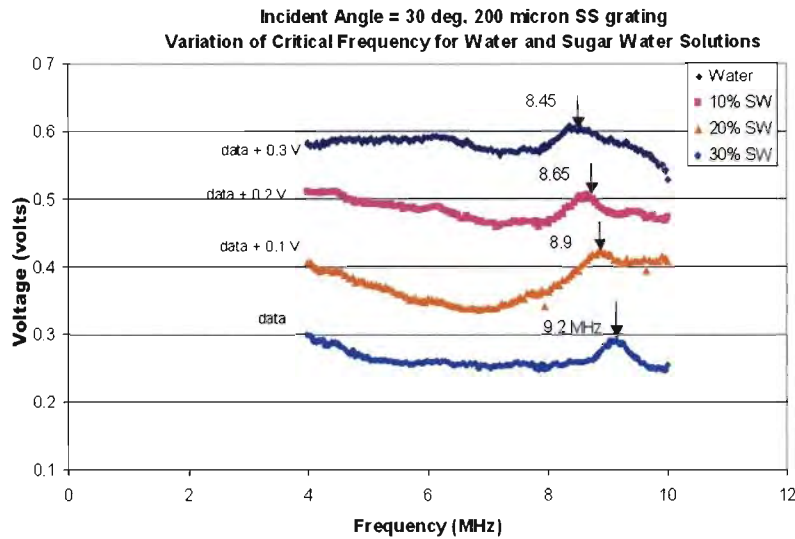
Figure 4. Data Obtained for 200-micron Stainless Steel Grating for an Incident Angle of 30°
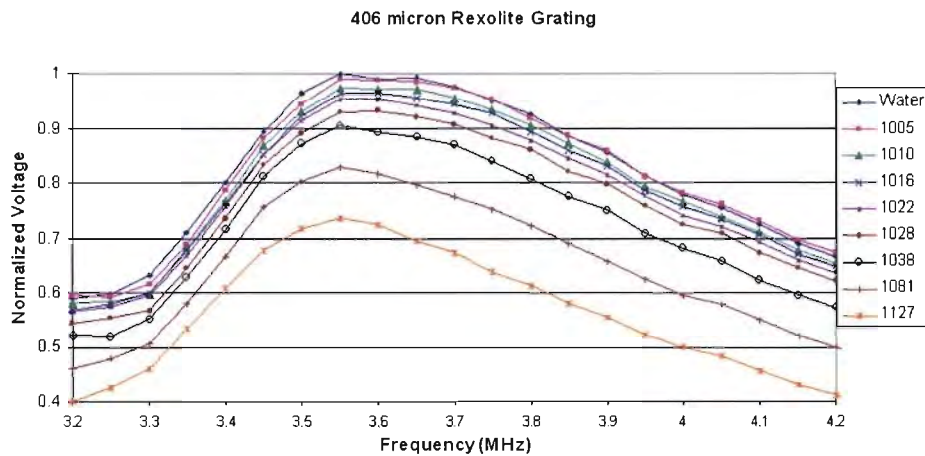
Figure 5. Data Obtained Using Rexolite Grating for Water and Eight Sugar Water Solutions. The legend gives the density of the sugar water solutions in kg/m^3

obtain the spectra of the diffracted waves in the liquid automatically. Thus, the send transducer is fixed at a given incident angle relative to the grating, while the receive transducer moves through a range of angles in order to obtain a spectrum of the diffracted rays in the liquid. This permits observation of the m = 1 diffracted wave in the liquid as it approaches 90° by choosing the appropriate frequency. The results show that the m = 1 peak increases in width as the angle increases. It is quite broad at 78°, and this is related to the width of the peak at the critical frequency, shown in Figures 3 and 4.

Ultrasonic diffraction grating spectroscopy has several advantages over laser technology now being used to monitor particle size in tank waste. First, ultrasound can penetrate farther into the slurry than visible light and will, therefore, give more information about the slurry composition. This is due to the fact that the evanescent wave penetrates into the liquid. Second, the ultrasonic sensor is noninvasive and is part of the pipeline wall. A sensor based upon UDGS would be very small—certainly an important advantage.

The following describes some of the theoretical results obtained by collaborators at the University of Washington. There are two important differences between optics and ultrasonics. The first is that light consists of transverse waves, while an ultrasonic wave can be either a longitudinal wave or a transverse (shear) wave. Second, when a glass optical grating is in contact with a liquid or slurry, the velocity of light in glass is *smaller* than the velocity in the liquid. However, for ultrasonics the velocity in the solid, such as in stainless steel, is *larger* than that in the liquid. These differences have some important consequences when considering the critical frequency at which the m = 1 diffracted wave in the liquid becomes 90° and the wave becomes evanescent. For example, for the ultrasonic data in Figures 3 and 4, small peaks occur at the critical frequency. The derivative of this curve gives positive slope, zero slope at the peak maximum, and then negative slope. A plot of the slope versus the frequency gives an S-shaped curve. In contrast, the optical case gives the reverse effect—a maximum for the derivative and an S-shaped curve for the amplitude versus frequency (or wavelength). This difference between optics and ultrasonics has been explained as a result of differences in the velocity of the two types of waves in solids and liquids, described above.

The shape of the curve at the critical frequency contains a great deal of information about the characteristics of the liquid or slurry. At the critical frequency, an evanescent wave is formed that decays exponentially *in the liquid*. That is, the measurement is a bulk measurement, not a measurement at a surface. At this point, the evanescent wave interacts with the liquid and with particles in the slurry. This interaction will depend upon velocity of sound, the dissipation parameters, and the coherence loss. The phrase *coherent* means that the propagation has the same direction as the original wave and also the same phase as the original wave. When the evanescent wave scatters from the particles in the slurry, loss of coherence results.

The critical frequencies shown in Figure 2 were calculated assuming that the velocity of sound was a real quantity. The velocity of sound can also have an imaginary part, usually considered small. The theoretical analysis shows that the value of the critical frequency depends upon both the real and imaginary parts of the velocity of sound. In future experimental studies, the effect of the imaginary part will be considered to see what role it plays.

1.30

In optics, the Rayleigh-Gans approximation was used to analyze the data and determine particle size. In anticipation of the experimental work soon to be carried out for slurries, an analogous formulation has been derived.

In future work, we will continue both experimental and theoretical studies of information provided by the data at the critical frequency. Information will be obtained from the data as a function of frequency and the derivative of this signal.

Planned Activities

Our planned activities include the following nine tasks:

1. Another stainless steel grating is being fabricated and is designed to enhance the signal at the critical frequency. Analysis of the data will be completed by July 15, 2002.

2. Parts for experiments to measure viscosity have been ordered, and experiments will be under way in July. Analysis of the data will be completed by September 1, 2002.

3. We will confer with collaborators about particle suspensions, i.e., particle size, for initial experiments with particle suspensions by September 1, 2002.

4. Apparatus for measurement with particle suspension will be designed and fabricated by October 2002.

5. We will carry out initial experiments with several particle sizes beginning in January 2003.

6. Data will be compared with theoretical calculations in May 2003.

7. We plan to obtain more experimental data over a large range of particle sizes and, if necessary, the theoretical algorithm for determination of particle size by August 2003.

8. In March 2004, we will refine measurement techniques for particle sizing so that it can be used for process control.

9. By September 2003, we will define the algorithm for particle sizing for use in process control.

Physical Characterization of Solid-Liquid Slurries at High Weight Fractions Using Optical and Ultrasonic Methods

(Project Number: 81964)

Principal Investigator

P. D. Panetta
Pacific Northwest National Laboratory
P.O. Box 999, MSIN K5-26
Richland, WA 99352
509-372-6107 (phone)
509-375-6497 (fax)
Paul.Panetta@pnl.gov

Co-Investigators

R. A. Pappas
Pacific Northwest National Laboratory
P.O. Box 999, MSIN K5-26
Richland, WA 99352
509-375-4546 (phone)
509-375-6736 (fax)
Richard.Pappas@pnl.gov

L. J. Bond
Pacific Northwest National Laboratory
P.O. Box 999, MSIN K5-26
Richland, WA 99352
509-375-4486 (phone)
509-372-4583 (fax)
Leonard.Bond@pnl.gov

J. A. Bamberger
Pacific Northwest National Laboratory
P.O. Box 999, MSIN K7-15
Richland, WA 99352
509-375-3898 (phone)
509-375-3641 (fax)
Judith.Bamberger@pnl.gov

University of Washington Investigators

L. W. Burgess
Center for Process Analytical Chemistry
University of Washington
Seattle, WA 98195-1700
206-543-0579 (phone)
Lloyd@cpac.washington.edu

M. Brodsky
Center for Process Analytical Chemistry
University of Washington
Seattle, WA 98195-1700
206-543-1676 (phone)
Brodsky@cpac.washington.edu

Graduate Student

S. L. Randall, Chemistry

Research Objective

The goal of this research project is to address the need for rapid, on-line methods that can be used to characterize the physical properties of high-level radioactive waste (HLW) slurries during all phases of the remediation process, from in-tank characterization of sediments to monitoring of the concentration, particle size, and degree of agglomeration and gelation of slurries during transport. Both optical and ultrasonic methods are being considered. The project has been divided into three tasks:

1. Develop optical and acoustic measurements to provide the fundamental science needed for successful device development and implementation

2. Develop theories that describe the interrelationship between wave propagation and the physical properties of the slurry

3. Perform inversions of the theories and compare them with the experimental measurements to nonintrusively characterize slurries.

The optical methods are being investigated at the University of Washington, and the acoustic methods are being investigated at Pacific Northwest National Laboratory (PNNL). Similarities between the acoustic and the optical measurements are an ongoing topic of communication between the investigators at the University of Washington and PNNL; however, this report focuses only on PNNL's investigations of acoustic methods.

Research Progress and Implications

During fiscal year 2002, the PNNL research team has focused on developing ultrasonic measurement methods that can be used to characterize solid-liquid suspensions at concentrations up to 40 wt%. Ultrasonic measurements are beneficial because the waves penetrate deep into materials and produce data that describe an average property. We focused our efforts on ultrasonic backscattering measurements, which are best suited for providing quantitative results at the high slurry concentrations expected in the waste remediation process. A schematic of the measurement device and examples of the measurements are provided in Figure 1. Figures 2 through 5 illustrate other ultrasonic measurements made during this reporting period: speed of sound (Figure 2), attenuation (Figure 3), backscattering (Figure 4), and diffuse field (Figures 5a and 5b). The speed of sound and the attenuation were used to characterize the slurries and as inputs for analyzing the backscattering data. Results from measurements made on glass spheres in water indicate that the ultrasonic measurements are very sensitive to both particle size and concentration.
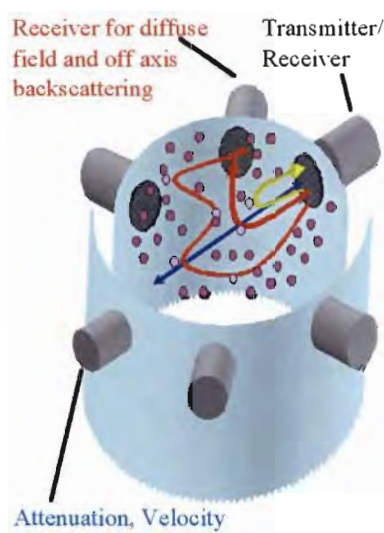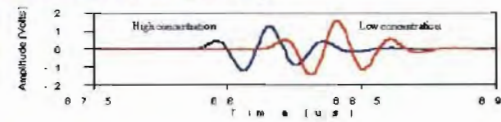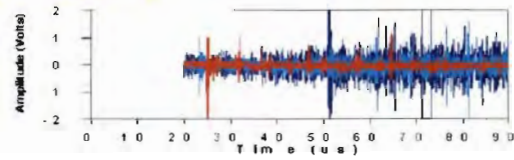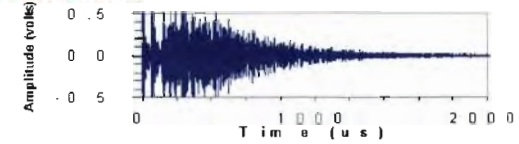
Figure 1. Ultrasonic Measurement Device and Resulting Signals
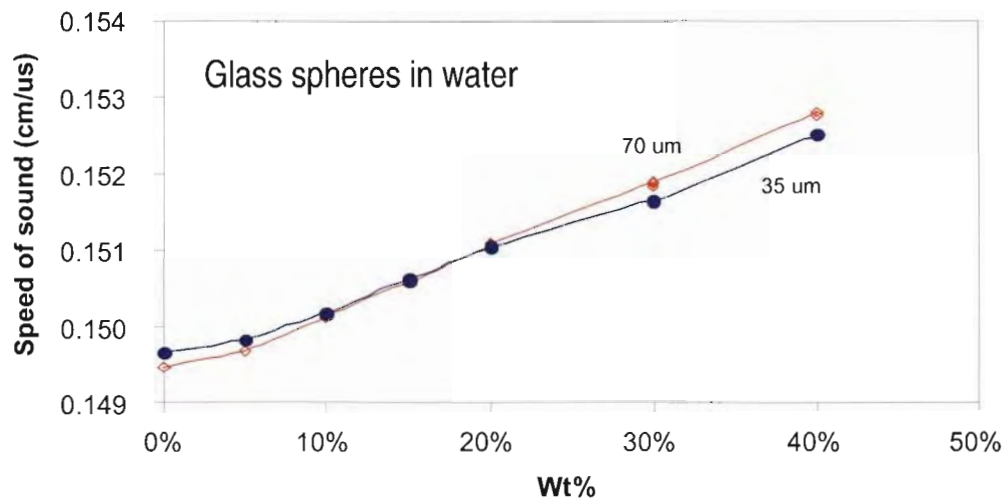
Figure 2. Speed of Sound vs. Concentration

1.35
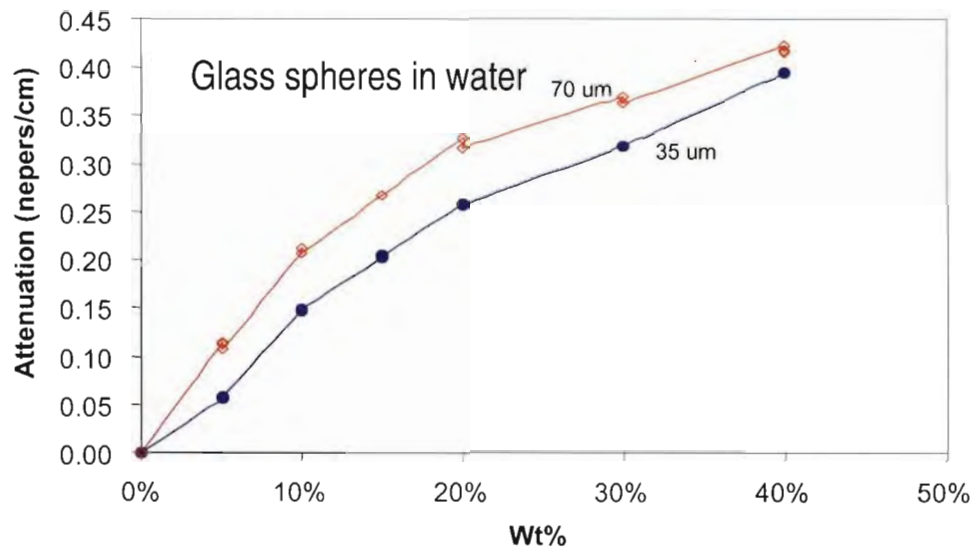
Figure 3. Ultrasonic Attenuation vs. Concentration
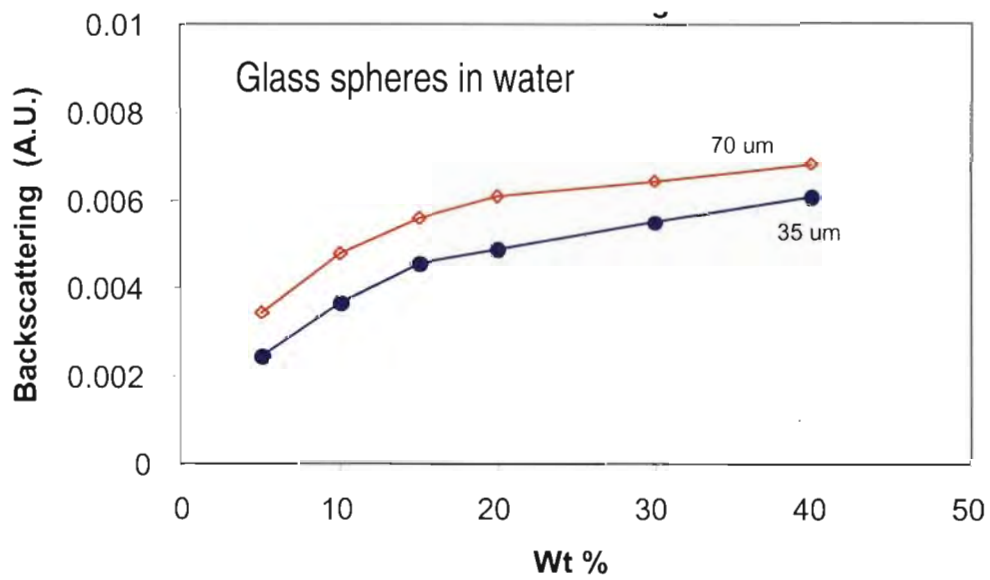
Figure 4. Ultrasonic Backscattering vs. Concentration

1.36
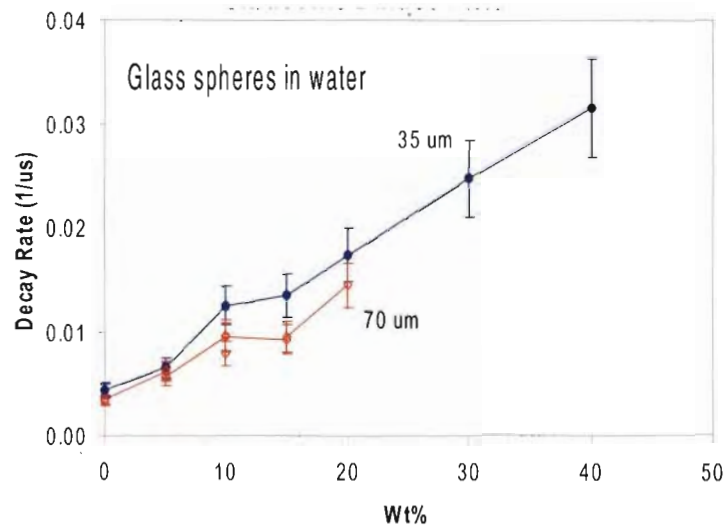
Figure 5a. Diffuse Field Decay Rate vs. Concentration
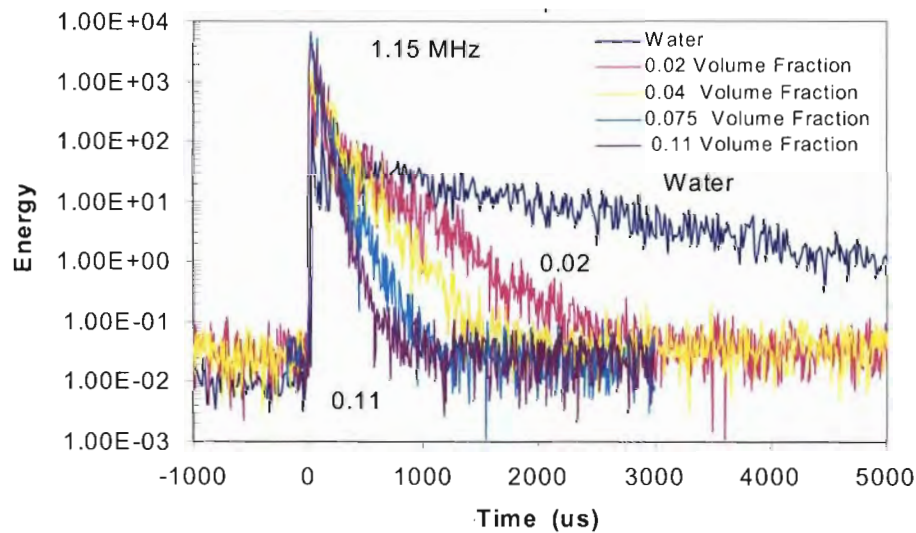
Figure 5b. Diffuse Field as a Function of Particle Concentration

The backscattering and diffuse field measurements are appealing because the theoretical description of the scattering processes is relatively simple. Future plans include extending existing theories to include multiple scattering and particle-particle interactions that occur at high concentrations. It then will be possible to compare results based on the developed acoustic and optical theories with results obtained from experiments. Work has begun on developing a theoretical understanding of the coherence effects in acoustic scattering by nonuniform media. The main goal of this effort is to determine expressions that will allow us to mathematically

1.37

solve the inverse problem—characterization of studied media (including dense slurries) by acoustic scattering data. We have exploited this theoretical approach previously in optics and applied it to the analysis of optical low-coherence reflectometry.

Planned Activities

Upcoming work will include evaluation of polydispersed standard systems for both the optical and acoustic methods. The polydispersed systems will be formulated by mixing several of the previously analyzed monodispersed systems to provide average, and known, particle characteristics. Studies then will be performed on individual slurry surrogate components. Eventually we will use optical and acoustic methods developed in this project to analyze a complex matrix composed of multiple surrogate components.

Speciation, Dissolution, and Redox Reactions of Chromium Relevant to Pretreatment and Separation of High-Level Tank Wastes

(Project Number: 81896)

Principal Investigator

Dhanpat Rai
Pacific Northwest National Laboratory
P.O. Box 999, MSIN P7-50
Richland, WA 99352
509-373-5988 (phone)
509-372-1632(fax)
mailto:dhan.rai@pnl.gov

Co-Investigators

Linfeng Rao
Lawrence Berkeley National Laboratory
1 Cyclotron Road Mailstop 70A-1150
Berkeley, CA 94720
510-486-5427 (phone)
510-486-5596 (fax)
LRao@lbl.gov

Sue B. Clark
Department of Chemistry
Washington State University
Fulmer 317 A
Pullman, WA
s_clark@wsu.edu

Research Objectives

This proposed research builds on the fundamental data developed under former EMSP project (65368) and seeks to develop additional fundamental data for chromium (Cr) reactions that are not currently available but are essential for the processing of high-level waste (HLW). Our objectives are to study 1) the dissolution of several solid phases (e.g., CrOOH, $Cr_2O_3(c)$, and Fe and Cr, binary hydroxides, identified to be important from sludge leaching studies) in highly alkaline solutions and in the presence of other electrolytes (e.g., carbonate, phosphate, sulfate, nitrite), and 2) the effect of the nature of Cr solid phases and aqueous species on their redox reactivity with a variety of potential oxidants (e.g., O_2 and ferrate). This information will provide critical support for developing enhanced pretreatment strategies for removing Cr from HLW and will achieve a major cost reduction in HLW disposal.

Thermodynamic and kinetic data concerning the behavior of Cr in multi-component, highly non-ideal electrolyte systems will be obtained. A model describing such behavior will be developed based on these fundamental data, tested with actual HLW tank sludge washing, and incorporated into the Environmental Simulations Program (ESP) model for use by Hanford, Savannah River, and other U. S. Department of Energy (DOE) site personnel for predicting the efficacy of enhanced pretreatment strategies for the removal of Cr from HLW.

Research Progress and Implications

Prior to the research performed under our current EMSP project, little information was available on the solubility, speciation, or redox reactivity of Cr(III) in tank-like environments. Consequently, the behavior of Cr, including dissolution and redox, in the proposed sludge washing processes (caustic leaching or oxidative leaching) was not understood, nor could it be predicted.

Our research thus far has consisted of three major components: 1) characterization of Cr species in solutions from acidic to highly alkaline, 2) determination and modeling of the solubility of $Cr(OH)_3(s)$ in highly alkaline and concentrated/mixed electrolyte solutions, and 3) study of the oxidation of Cr(III) by H_2O_2 and persulfate in alkaline solutions. To enhance the application of our results to "real-world" problems, we compared and tested our results with those from actual tank sludge washing supported by the Tanks Focus Area (TFA). Accomplishments under this EMSP project have been communicated in detail in the forms of journal articles, national conference presentations, and regular technical progress reports. The following are brief summaries and highlights.

Speciation of Cr(III) in Acidic to Strongly Alkaline Solutions

Chromatographic Separation of Cr(III) Oligomers. Several methods have been developed to isolate macro amounts of Cr(III) oligomers using chromatographic techniques. This allows us to investigate the chemical structures (i.e., speciation) of the separated fractions and to study the oxidation of isolated oligomers. The effect of solution pH was evaluated by conducting the separations with Cr solutions under different conditions. A capillary electrophoresis approach was also developed to separate minor quantities of the oligomers and to verify the resolution and separation of chromatography [Rao et al. 2002; Friese et al. 2002a].

Characterization of Cr(III) species. The separated Cr(III) species were characterized by a variety of methods, including UV-VIS, X-ray absorption spectroscopy (EXAFS), and capillary electrophoresis (CE). Selected results are presented below.

The UV-VIS absorption spectra of the solutions containing the separated Cr(III) species (separated by ion exchange) are shown in Figure 1. The energy shift (toward longer wavelength) and the intensity enhancement of the absorption bands, from the monomer through dimer, trimer, and tetramer, to the aged/unseparated solution are interpreted in the context of the structures of the Cr(III) species and the ligand field theory.
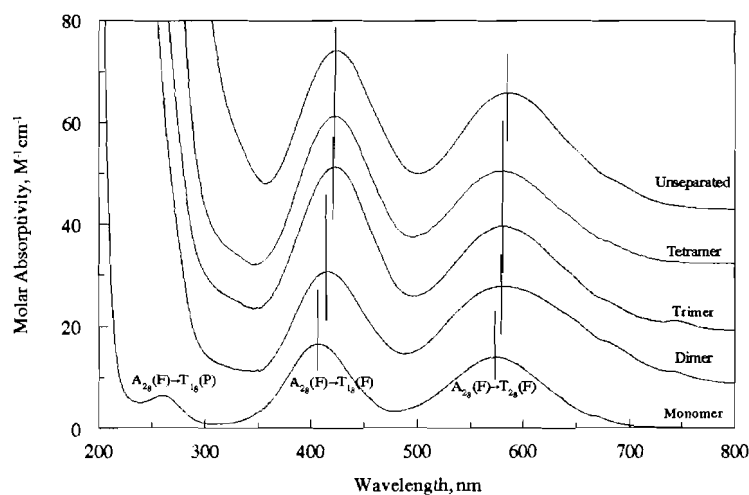
Figure 1. UV/Vis absorption spectra of Cr(III) monomer, dimer, trimer, tetramer and unseparated Cr(III) solutions. The spectra are shifted along y-axis for better viewing.

The UV-VIS absorption bands of the Cr(III) oligomers are quite broad. Consequently, absorption maxima of the separated fractions alone do not guarantee that a single Cr(III) species has been isolated. Yet, isolation of single species is important for resolving EXAFS spectra and for our oxidation studies. Therefore, we have used CE as an additional "quality assurance

1.41

check" and have verified the purity of our isolated fractions of Cr(III) oligomers. Chromatograms of Cr solutions indicate that the charge density of the oligomers increases with the degree of polymerization [Friese et al. 2002a].

Figure 2 shows the Fourier transforms of the EXAFS spectra of a few Cr(III) solution samples. Figure 2a shows the results for the separated monomer in the solution and on the ion exchange resin. The best fit indicates that there are six oxygens around the Cr at 1.97 Å, but no Cr at 3 Å, confirming the monomeric nature of this Cr(III) species. Figure 2b indicates that the separated Cr(III) dimer, both in solution and on the resin, have one Cr at 2.97 Å, confirming the dimeric nature of this species.

Figure 2c shows the effect of alkalinity on the oligomerization of Cr(III) in solutions from acidic to highly alkaline. All of the spectra show an oxygen shell (6 oxygen atoms) at around 1.99 Å. All but the spectra for the solution with pH 2, illustrate the feature (~ 2.99 Å) that results from Cr-Cr scattering. The intensity of the Cr-Cr scattering increases as the alkalinity is increased. This demonstrates that the oligomerization of Cr(III) is facilitated by higher alkalinity. Such effect has significant impact on the solubility of Cr(III) in alkaline solutions, which is described in subsequent discussions on solubility.
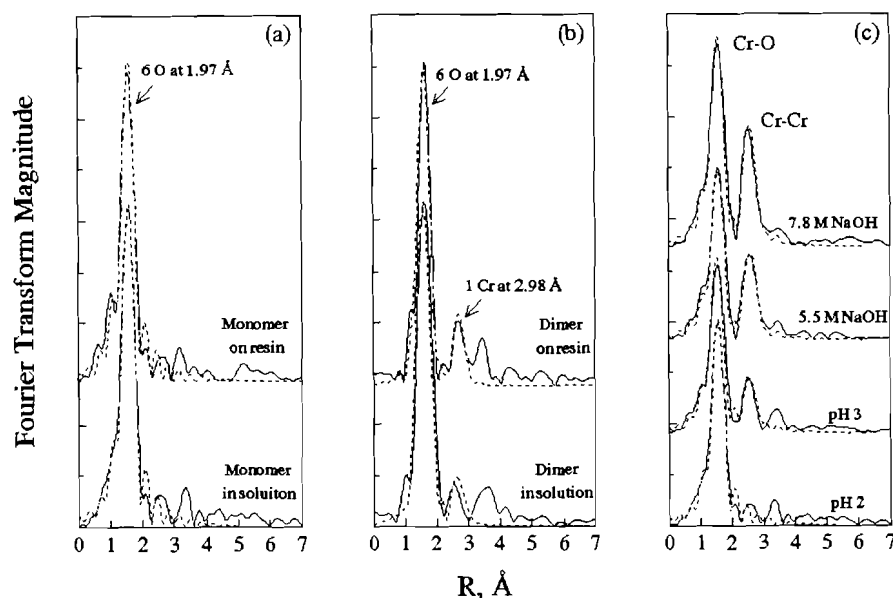
Figure 2. The Fourier transforms of the EXAFS spectra of Cr(III) solutions. Monomer in solution and on resin (a); dimer in solution and on resin (b), and Cr(III) solutions of different alkalinity (c). Solid line: experimental; dashed line: fit.

Impact of Speciation, Ionic Strength, and Mixed Electrolytes on Solubility: Solubility of Cr(OH)₃(am) in Strongly Alkaline Solutions

The solubility of Cr(OH)$_3$(am) was measured in NaOH (0.003 to 10.5 m) and mixed/concentrated NaOH/NaNO$_3$ solutions at 22 ± 2°C [Rai et al. 2002]. A combination of techniques, x-ray absorption spectroscopy (XAS) and stripping analyses, was used to identify aqueous species and to confirm that the soluble Cr was present as Cr(III).

The aqueous Cr concentrations in equilibrium with Cr(OH)$_3$(am) increase dramatically with an increase in NaOH concentrations (Figure 3). Based on the findings in our speciation studies and the thermodynamic analyses of the data, we could model this observed solubility behavior by invoking two dominant Cr(III) species, Cr(OH)$_4^-$ and Cr$_2$O$_2$(OH)$_4^{2-}$, and by including Pitzer ion-interaction parameters for Na$^+$-Cr(OH)$_4^-$ and Na$^+$-Cr$_2$O$_2$(OH)$_4^{2-}$. As shown in Figure 3, the model prediction satisfactorily describes the observed solubility.
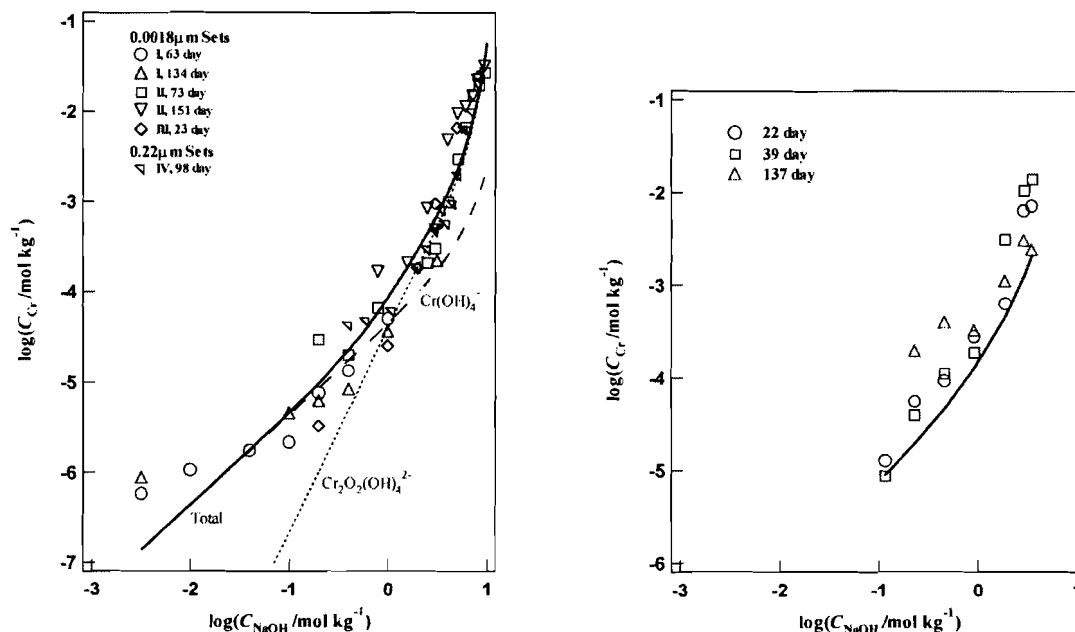
Figure 3. Aqueous chromium concentrations from Cr(OH)$_3$(am) suspensions in NaOH (left) and in 4.6 m NaNO$_3$ containing different concentrations of NaOH (right). Lines represent predicted concentrations using the thermodynamic data reported in Rai et al. [2001]. Solid line represents total chromium concentrations; other lines represent concentrations of different species as marked in the figure.

This model was further tested using the experimental $Cr(OH)_3(am)$ solubility in mixed NaOH and $NaNO_3$ solutions. The Cr concentrations predicted by the model were in reasonably close agreement with the observed concentrations in mixed $NaOH-NaNO_3$ solutions (Figure 3). The thermodynamic parameters for the dissolution of $Cr(OH)_3(am)$ in these systems, along with the ion interaction parameters, are provided in detail in Rai et al. [2002].

Impact of Speciation on Redox: Oxidation of Cr(III) by Peroxide and Persulfate

Two oxidants were studied, peroxide (H_2O_2) and the persulfate anion ($S_2O_8^-$). Peroxide is of interest because of its favorable reduction potential relative to Cr(III) oxidation to chromate, and because its use does not add unwanted components to the already complex waste stream. Persulfate is of interest because of work completed by Russian scientists on its oxidation of Cr(III) in alkaline systems. Krot et al. [1999] indicated that persulfate may be preferred over peroxide and other common oxidants because of its reactivity towards Cr(III) and because it could be applied such that little increase in waste volume occurred. However, for both hydrogen peroxide and persulfate, no mechanistic data were available prior to our work under this EMSP project.

Oxidation of Cr(III) by H_2O_2 in Alkaline Solutions. The oxidation of Cr(III) was followed by monitoring the increase of absorbance of Cr(VI) at 372 nm. The oxidation was found to be the first order with respect to the concentrations of Cr(III) and H_2O_2. As to the dependency on the concentration of OH, there seem to be two reaction pathways: the major one is inversely dependent on [OH], and the other independent of [OH] (insignificant). A general rate equation is written as

$$R = -d[Cr_n(III)]/dt = n\ d[Cr(VI)]/dt = k[Cr_n(III)][\ H_2O_2](1/[OH] + k') \qquad (1)$$
$$= k_{OH}[Cr_n(III)][H_2O_2] \qquad (2)$$
$$= k_{obs}[Cr_n(III)] \qquad (3)$$

where $n = 1, 2$ and 3 for monomer, dimer, and trimer, respectively. Examples of the plots of k_{obs} vs. $[H_2O_2]$ are shown in Figure 4 for the monomer, dimer, and trimer, respectively. It can be seen that, at the same concentrations of H_2O_2 and NaOH, the oxidation rate decreases in the order monomer > dimer > trimer > higher oligomers.

1.44
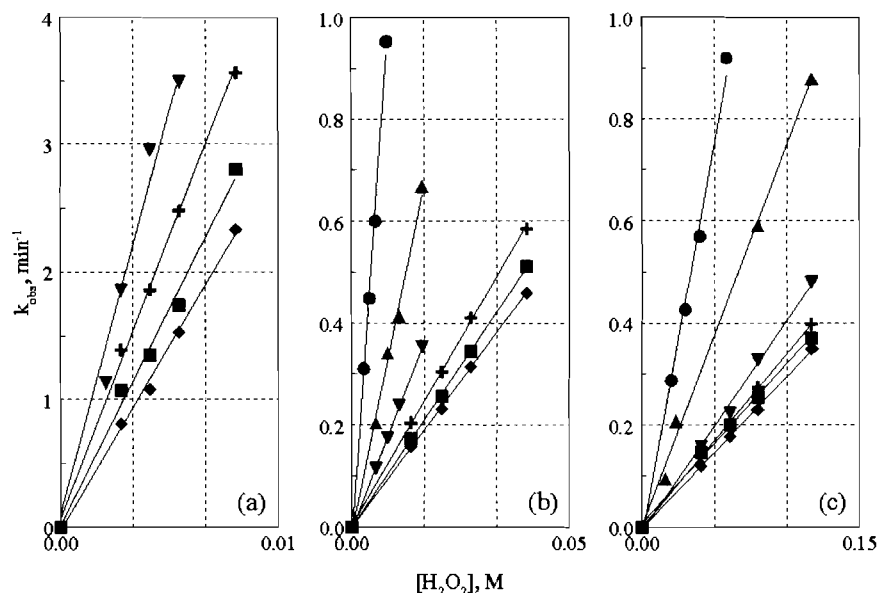
Figure 4. The pseudo first-order rate constant, k_{obs}, as a function of $[H_2O_2]$ at constant $[OH]$.
(a) monomer, (b) dimer, (c) trimer. Symbols: $[OH] = 0.100$ M ($\bullet$), 0.252 M ($\blacktriangle$), 0.504 M
($\blacktriangledown$), 0.756 M (+), 1.00 M ($\blacksquare$), 1.18 M ($\blacklozenge$).

Values of the rate constant k [equation 1], calculated from these plots, are provided in Rao et al. [2002]. These values show that the oxidation rate decreases in the order monomer > dimer > trimer > higher oligomers. If $[H_2O_2] = 0.01$ M and $[NaOH] = 1.0$ M, the time required for 50% oxidation ($t_{1/2}$, in minutes) would be in the order monomer (0.2) < dimer (6) > trimer (22) > unseparated/aged Cr(III) (410). In brief summary, our data indicate that, 1) H_2O_2 can oxidize Cr(III) to Cr(VI) in alkaline solutions; 2) the oxidation probably occurs through a rate-determining step involving the breaking of the bridging bonds in the oligomers and the concomitant release of one hydroxyl group from the Cr(III) moiety upon the attack by H_2O_2; and 3) it is likely that more energy is required to break the bridging bonds in higher oligomers. Consequently, the redox reactivity of the Cr(III) species with H_2O_2 decreases as oligomerization proceeds.

Oxidation of Cr(III) by S_2O_8 in Alkaline Solutions. Oxidation of Cr(III) by persulfate follows a different kinetics mechanism [Friese et al. 2002b). This is most easily demonstrated by comparing Figure 5 with the results of Cr(III) oxidation by peroxide [Figure 4]. When [NaOH] < 1M, the reaction rate is best described by multiple first-order processes. When [NaOH] > 1M, Cr(III) oxidation by persulfate is best described by a single first-order process; note that the linear dependence on oxidant concentration observed with peroxide is only observed with persulfate at very high concentrations of NaOH (e.g., ~ 5M NaOH).

1.45
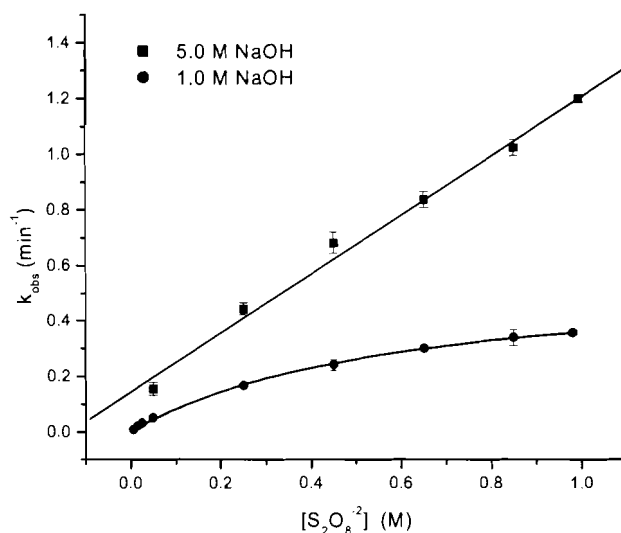
Figure 5. Observed rate constants for the oxidation of Cr(III) by persulfate in NaOH. [Cr(III)] = 1×10^{-4} M, T = 22°C. Note that, unlike oxidation by peroxide, the observed reaction rates are only linear with respect to persulfate concentration when [NaOH] is quite large.

Detailed investigations over wide ranges of conditions (e.g., [NaOH], [persulfate], and temperature) have revealed the following important conclusions: 1) There is a very rapid oxidation step probably involving the sulfate radical (SO_4^-) [Koltoff and Miller 1951]. Conditions that favor oxidation by the persulfate radical include [NaOH] < 1 M and temperatures elevated to at least 30°C. 2) A second process in the oxidation of Cr(III) by persulfate follows Michelis-Menton-type kinetics, suggesting the formation of an intermediate species.

For oxidation with both peroxide and persulfate, there are two implications that are of great significance to the design of oxidative sludge washing to remove Cr: 1) any processes that can break down the oligomers will facilitate the oxidation, thus, the dissolution of Cr; and 2) though the oxidation occurs in alkaline solutions, high concentrations of NaOH will slow the oxidation.

End-User Connection: Tests Against Data on Washed Solids from High-Level Tanks

Ideally, the fundamental data developed under this EMSP project need to be tested with well-designed protocols of actual sludge washing. However, extensive studies with actual sludges are extremely expensive and beyond the scope of this EMSP funding. As a result, we decided to use the data that is available in technical reports from PNNL [Rapko et al. 1995; Lumetta et al. 1996, 1997] on the washing of Hanford tank sludges. Although these data do not cover a sufficiently wide range of hydroxide concentrations or rigidly controlled experimental conditions we desire, they do provide a limited data set to test the applicability of fundamental data developed under the current EMSP.

In the study of the pretreatment of Hanford tank sludges supported by the TFA [Rapko et al. 1995; Lumetta et al. 1996, 1997], three washings were performed on sludges from 14 different Hanford tanks: 1) retrieval and dilute NaOH washes, 2) first caustic leach, and 3) second caustic leach. These sludges are representative of the four major chemical processing operations (REDOX, TBP, $BiPO_4$, and PUREX) used at Hanford.

The comparison of the observed Cr concentrations in the three washes to the predicted Cr concentrations from our thermodynamic model are shown in Figure 6. The predicted concentrations are orders of magnitude lower than the observed for the first wash, fairly close to the observed for the second wash (about one order of magnitude lower for a few sludges), and in excellent agreement with the observed for the third wash. At present, the exact reason for the significant disagreement for the first wash is not known, but we surmise it may result from the presence of Cr(VI), other electrolytes (e.g., carbonate and phosphate) that were not included in the research investigations under the current EMSP project, and probably the leaching protocols. Nonetheless, The excellent agreement for the third wash (and, to less extent, the second) is very encouraging. If the effect of other electrolytes is significant, the extended studies proposed in this renewal will generate an improved thermodynamic model to account for the effects of these electrolytes. If the disagreement is due mainly to the leaching protocols, we will recommend modifications of the leaching protocol to the TFA investigators so that future leaching tests provide more meaningful and informative results. The interim thermodynamic parameters developed under the current program are being included in the TFA's Environmental Simulations Program for use by the site personnel.

← Redox → ←TBP(F)→←BiPO₄→←Purex

Sludges from Tanks containing different Wastes
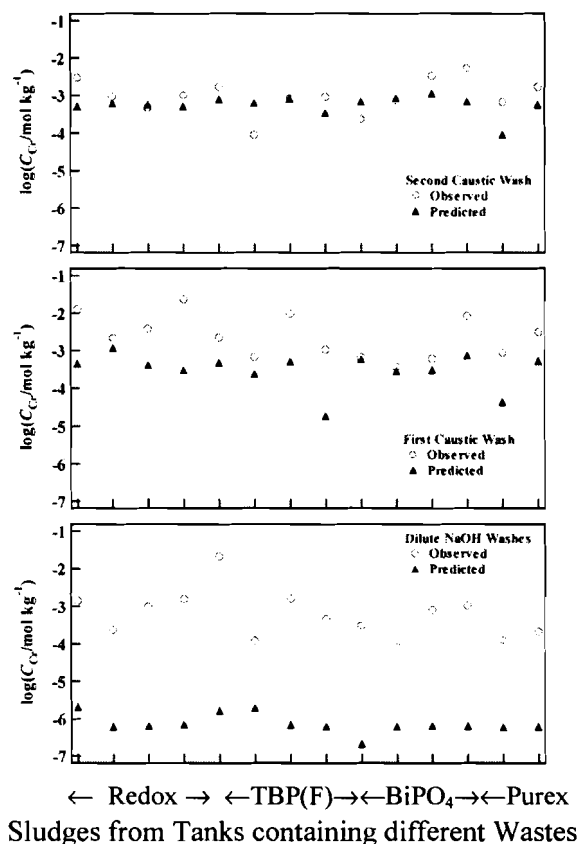
Figure 6. Predicted and observed chromium concentrations in sludge leachates (points on x-axis from left to right represent Hanford tanks S101, S104, S107, S111, BY104, BY108, BY110, T104, C107, BX107, B111, T111, C103, and AN104). Electrolytes in leachates vary from a mixture containing sodium, aluminum, hydroxide, nitrate, nitrite, phosphate, carbonate, and sulfate in various proportions to primarily NaOH (see Rai et al. 2002 for details).

References Cited

Rai D, NJ Hess, L Rao, Z Zhang, AR Felmy, DA Moore, SB Clark, GJ Lumetta. 2002. Thermodynamic Model for the Solubility of Cr(OH)₃(am) in Concentrated NaOH and NaOH-NaNO₃ Solutions. *Journal of Solution Chemistry* 31:343-367.

Rao L, Z Zhang, JI Friese, B Ritherdon, SB Clark, NJ Hess, and D Rai. 2002. Oligomerization of Chromium(III) and its Impact on the Oxidation of Chromium(III) by Hydrogen Peroxide in Alkaline Solutions. J. Chem. Soc., Dalton Trans. 2002(2): 267 – 274.

Friese JI, B Ritherdon, SB Clark, Z Zhang, L Rao, and D Rai. 2002a. Chromatographic Separation and Characterization of Hydrolyzed Cr(III) Species. *Analytical Chemistry* (In press).

Friese JI, B Ritherdon, SB Clark, L Rao, and Z Zhang. 2002b. Oxidation of Cr(III) Oligomers by Persulfate Under Alkaline Conditions. To be submitted to *Inorganic Chemistry*.

Krot NN, FP Shilov, AM Fedoseev, NA Budantseva, MV Nikonov, MAB Yusov, AY Garnov, IA Charushnikova, VP Perminov, LN Astafurova, TS Lapitskaya, VI Makarenkov. 1999. *Development of Alkaline Oxidative Dissolution Methods for Chromium(III) Compounds Present in Hanford Site Tank Sludges*. PNNL-12209, UC-2000.

Koltoff IM and IK Miller. 1951. The Chemistry of Persulfate. I. The Kinetics and Mechanism of the Decomposition of the Persulfate Ion in Aqueous Medium. *J. Am. Chem. Soc.* 73:3055-3059.

Lumetta GJ, BM Rapko, MJ Wagner, J Liu, and YL Chen. 1996. *Washing and Caustic Leaching of Hanford Tank Sludges: results of FY 1996 Studies*. PNNL-11278, Rev. 1. Pacific Northwest National Laboratory, Richland, Washington, USA.

Lumetta GJ, IE Burgeson, MJ Wagner, J Liu, and YL Chen. 1997. *Washing and Caustic Leaching of Hanford Tank Sludge: Results of FY 1997 Studies*. PNNL-11636. Pacific Northwest National Laboratory, Richland, Washington, USA.

Rapko BM, GJ Lumetta, and JJ Wagner. 1995. Washing and Caustic Leaching of Hanford Tank Sludges: Results of FY 1995 Studies. PNNL-10712. Pacific Northwest National Laboratory, Richland, Washington, USA.

Planned Activities

Building on our research accomplishments to date, we are extending our current studies into three important areas: 1) the dissolution/precipitation of other important Cr solid phases, including $CrO(OH)(s)$, and binary Cr/Fe and Cr/Al hydroxide solids; 2) the speciation of Cr(III) in the presence of other ligands (e.g., phosphate, carbonate) and the development of thermodynamic data for important Cr(III) solubility and complexation reactions; 3) the kinetics and mechanisms of the oxidation of Cr(III) by more oxidants, including O_2 and ferrate. The data and model obtained in these studies will be tested with results from actual sludge washing and communicated with the end-users. These data will be incorporated into the Tanks Focus Area ESP model.

Information Access

Journal Articles

Rai D, NJ Hess, L Rao, Z Zhang, AR Felmy, DA Moore, SB Clark, GJ Lumetta. 2002. Thermodynamic Model for the Solubility of $Cr(OH)_3$(am) in Concentrated NaOH and NaOH-$NaNO_3$ Solutions. *Journal of Solution Chemistry* 31: 343-367.

Rao L, Z Zhang, JI Friese, B Ritherdon, SB Clark, NJ Hess, and D Rai. 2002. Oligomerization of Chromium(III) and Its Impact on the Oxidation of Chromium(III) by Hydrogen Peroxide in Alkaline Solutions. J. Chem. Soc., Dalton Trans. 2002(2): 267 – 274.

Friese JI, B Ritherdon, SB Clark, Z Zhang, L Rao, and D Rai. 2002. Chromatographic Separation and Characterization of Hydrolyzed Cr(III) Species. *Analytical Chemistry* (In press).

Friese JI, B Ritherdon, SB Clark, L Rao, and Z Zhang. 2002. Oxidation of Cr(III) Oligomers by Persulfate Under Alkaline Conditions. To be submitted to *Inorganic Chemistry*.

Technical Reports

Rai D, L Rao, SB Clark, NJ Hess, and GJ Lumetta. 1999. Speciation, Dissolution, and Redox Reactions of Chromium Relevant to Pretreatment and Separation of High-Level Tank Wastes. In: *Science to Support DOE Site Cleanup: The Pacific Northwest National Laboratory Science Program Awards*. PNNL- 12208, Pacific Northwest National Laboratory, Richland, WA, pp. 1.61-1.86.

Rai D, L Rao, SB Clark, NJ Hess, and GJ Lumetta. 2000. Speciation, Dissolution, and Redox Reactions of Chromium Relevant to Pretreatment and Separation of High-Level Tank Wastes. In: *Science to Support DOE Site Cleanup: The Pacific Northwest National Laboratory Science Program Awards*. PNNL- 13262, Pacific Northwest National Laboratory, Richland, WA, pp. 1.15-1.17.

Rai D, L Rao, SB Clark, and NJ Hess. March 2000. Speciation, Dissolution, and Redox Reactions of Chromium Relevant to Pretreatment and Separation of High-Level Tank Wastes. Project Summary submitted to EMSP.

Presentations

Rao L, D Rai, SB Clark, AR Felmy, NJ Hess, Z Zhang, and B Ritherdon. 1999. Speciation, Dissolution, and Redox Reactions of Cr(III) in Alkaline Solutions. A presentation at the 218th ACS National Meeting, New Orleans, Louisiana, August 1999.

Rao L, D Rai, SB Clark, Z Zhang, NJ Hess, B Ritherdon, and J Friese. 2000. Dissolution of Cr(OH)$_3$(am)/Cr$_2$O$_3$(c) and Oxidation of Cr(III) in Alkaline Solutions. A presentation at the 219th ACS National Meeting, San Francisco, California, March 2000.

Friese J, B Ritherdon, O Gerasimov, S Lymar, J Hurst, Z Zhang, L Rao, D Rai, and SB Clark. 2000. Oxidation of Trivalent Cr Using Oxidants Relevant to High-Level Radioactive Waste. A presentation at the 219th ACS National Meeting, San Francisco, California, March 2000.

Rai D, L Rao, SB Clark, NJ Hess, and AR Felmy. 2000. Solubility of Cr(III) Compounds and Their Redox Transformation Reactions: Application to Pretreatment of High-Level Waste Sludges. An oral presentation at the EMSP workshop, Atlanta, Georgia, April 2000.

Rai D, L Rao, SB Clark, NJ Hess, and AR Felmy. 2000. Speciation, Dissolution, and Redox Reactions of Chromium Relevant to Pretreatment and Separation of High-Level Tank Wastes. Poster presentation at the EMSP workshop, Atlanta, Georgia, April 2000.

Friese J, B Ritherdon, SB Clark, L Rao, and Z Zhang. 2000. Removing Chromium from High-Level Radioactive Waste Streams: Speciation and Reactivity of Cr(III) Oligomers Under Highly Alkaline Conditions. A presentation at the 221th ACS National Meeting, San Diego, California, April 2001.

New Metal Niobate and Silicotitanate Ion Exchangers: Development and Characterization

(Project Number: 73748)

Principal Investigator

Dr. Yali Su
Pacific Northwest National Laboratory
P.O. Box 999, MSIN K8-93
Richland, WA 99352
509-376-5290 (phone)
509-376-5106 (fax)
ya.su@pnl.gov

Co-Principal Investigators

Dr. Tina M. Nenoff
Sandia National Laboratories
P.O. Box 5800, MS 0710
Albuquerque, NM 87185-0709
505-844-0340 (phone)
505-845-9500 (fax)
tmnenof@sandia.gov

Prof. Alexandra Navrotsky
University of California
Department of Chemical Engineering and Materials Science
One Shields Avenue
Davis, CA 95616-8779
530-752-3292 (phone)
530-752-9307 (fax)
anavrotsky@ucdavis.edu

Contributors

Liyu Li (PNNL)
May Nyman (SNL)
Hongwu Xu (UC Davis)

Research Objective

This project focuses on the synthesis and characterization of silicotitanate- and niobate-based ion exchangers for Cs and Sr removal and their related condensed phases as potential ceramic waste forms, as well as on understanding the structural property relationship and thermodynamic stability of new silicotitanate- and niobate-based ion exchangers and their thermally converted phases. The objective of the project is to provide the U.S. Department of Energy (DOE) alternative materials that can exceed the solvent extraction process for removing Cs and Sr from high-level wastes (HLW) at Hanford and other DOE sites, as well as technical alternatives for disposal of silicotitanate- and niobate-based ion exchange materials.

Research Progress and Implications

This report summarizes progress after 1 year and 8 months of a 3-year project. Work during the first year showed that several new phases include $Na_2Nb_{2-x}Ti_xO_{6-x}(OH)_x \cdot H_2O$ ($x = 0.4$), $CsTi_xAl_{1-x}Si_2O_{6+x/2}$ ($0 = x = 1$), and $Cc\text{-}A_2TiSi_6O_{15}$ (A = K, Rb, Cs) have been synthesized and characterized. Chemical, thermal, and radiation stabilities of CST, thermodynamic stabilities of $Na_5TiNb_4O_{12} \cdot H_2O$ ion exchanger, and Ti-substituted perovskites also have been investigated. This year we have focused on 1) determining the Ba solubility in Cs-containing phase $Cs_2ZrSi_3O_9$ in ceramic waste forms; 2) investigating the structural property relationship of new niobate-based ion exchangers and their related condensed phases (as potential ceramic waste forms); and 3) investigating thermodynamic stabilities of niobate-based ion exchangers and their related compounds by high-temperature oxide melt solution calorimetry.

Ba Solubility in $Cs_2ZrSi_3O_9$

Our previous study at Pacific Northwest National Laboratory (PNNL) indicated that thermal conversion of the Cs-loaded silicotitanates produces a durable waste form. Cesium is trapped in the $Cs_2ZrSi_3O_9$ crystalline phase, whose unique framework structure precludes facile migration of Cs. The stability of Cs-containing compound $Cs_2ZrSi_3O_9$ when it radioactively decays to ^{137}Ba is of concern. To determine whether small amounts of Ba could reside in the $Cs_2ZrSi_3O_9$ structure, two solid substitution series of $Cs_{2(1-x)}Ba_xZrSi_3O_9$ and $Cs_{1-x}Ba_{x)2}ZrSi_3O_{9+x}$ ($x = 0, 0.05, 0.1, 0.15,$ and 0.2) were synthesized and characterized by x-ray diffraction (XRD), thermal gravimetric analyzer/differential thermal analyzer (TGA/DTA), scanning electron microscopy (SEM) and thermal electron microscopy (TEM) techniques. The XRD study shows there is up to 15% substitution of barium for cesium on the $Cs_2ZrSi_3O_9$ lattice. SEM elemental mapping results also indicate up to 15% barium substitution. However, our TEM study surprisingly revealed that there is no measurable substitution of barium for cesium on the $Cs_2ZrSi_3O_9$ lattice. Figure 1 shows the TEM with energy dispersive spectrum (EDS) analysis of $(Cs_{0.9}Ba_{0.1})_2ZrSi_3O_{9.1}$. Region 1 indicates Cs-Zr-Si-O phase with little barium substitution.

1.54
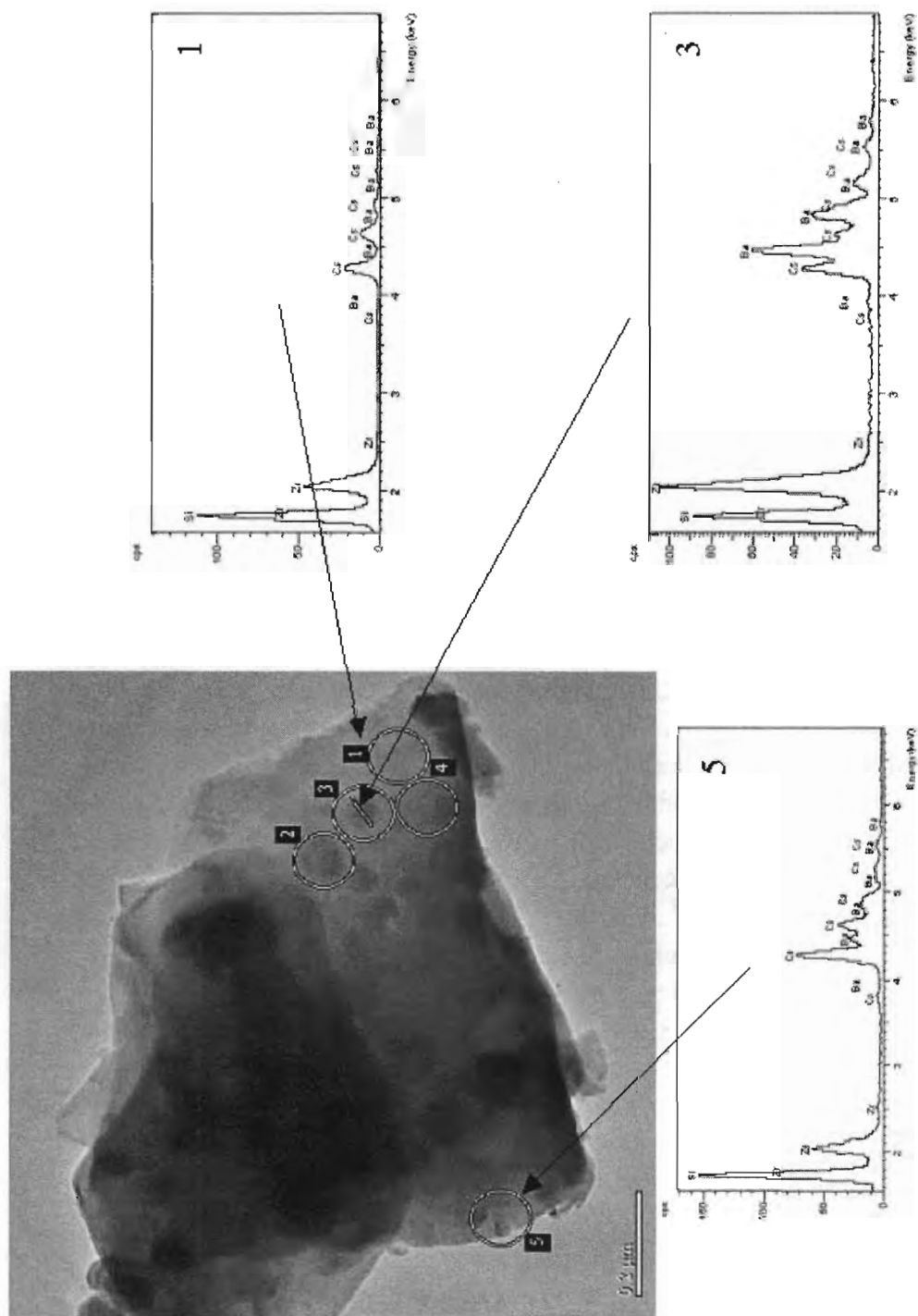
Figure 1. Thermal electron microscopy micrograph of $(Cs_{0.9}Ba_{0.1})_2ZrSi_3O_{9.1}$ with EDS spectra of different region of the sample.

Region 3 shows the Cs-Ba-Zr-Si-O phase with high barium subsitution. Region 5 shows the Cs-Ba-Zr-Si-O phase with low barium substitution. These results, in contrast to results produced by XRD and SEM analyses, indicate that phase separation occurred at the barium-substituted $Cs_2ZrSi_3O_9$ phase. The difference is likely due to the low sensitivity of XRD and SEM techniques. Further, TEM studies show that the Ba-rich phase is a crystalline phase. Therefore, Ba has no solubility in the $Cs_2ZrSi_3O_9$ phase. The Ba-containing phase is currently under investigation at PNNL.

Structural/Property Relationship of Niobate Based Ion Exchangers and their Condensed Phases

$Na_2Nb_{2-x}M^{IV}_xO_{6-x}(OH)_x \cdot H_2O$ (M^{IV} =Ti, Zr; x=0.04~ 0.4)
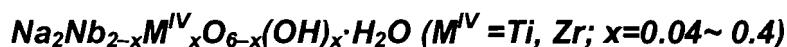
Sandia Octahedral Molecular Sieves (SOMS) is an isostructural, variable composition class of ion exchangers with a general formula of $Na_2Nb_{2-x}M^{IV}_xO_{6-x}(OH)_x \cdot H_2O$ (M^{IV} = Ti, Zr; x = 0.04 – 0.40) where up to 20% of the framework Nb^V can be substituted with Ti^{IV} or Zr^{IV}. This class of molecular sieves is easily converted to perovskite through low-temperature heat treatment (500°C to 600°C). The study reported herein is a thorough investigation of the SOMS materials.

1. Structural and Compositional Characterization of SOMS

The structure of SOMS-1, $Na_2Nb_{1.6}Ti_{0.4}O_{5.6}(OH)_{0.4} \cdot H_2O$, was determined from single-crystal x-ray diffraction data collected at NSLS, BNL. The framework consists of layers of edge-sharing sodium octahedra parallel to the xy plane, interleaved with double chains of edge-sharing, distorted Nb/M^{IV} octahedra running along the b-axis. The two Nb/M^{IV} sites are distorted and completely disordered. Each site has one long (~2.4 Å) and one short (~1.8 Å) axial Nb/M^{IV} -O bond, as well as displacement of Nb/M^{IV} above the equatorial plane. The equatorial Nb/M^{IV} -O bonds are all ~2 Å, but the displacement of above the equatorial plane gives rise to trans O- Nb/M^{IV} –O bond angles as small as 147°. Raman spectroscopy also confirmed these two types of octahedral distortion with peaks at 374, 460, 771 and 884 cm^{-1} for the axial distortion and peaks at 305, 638, and 844 cm^{-1} for the equatorial plane distortion.

Several methods were used to characterize the cation sites in the series of variable composition SOMS materials. Bulk chemical analyses (by Galbraith Laboratories, Inc.) revealed that the sodium content does not increase with increasing M^{IV}. ^{23}Na MAS NMR experiments showed a consistent ratio of octahedral to square planar Na coordination sites of approximately 3:1, as predicted by the structure, for all compositions. Two peaks are apparent: the relatively-narrow octahedral Na peak at –8 ± 1 ppm (Na1[8 per unit cell] plus Na2 [4 per unit cell]) and the significantly-broader square planar Na3 peak at –11 ± 2 ppm (4 per unit cell). Although the ratios of these peaks are the same between minimum (2%) and maximum (20%) titanium

substitution, the spectra of the 2%Ti-SOMS shows better-defined, narrower peaks. This peak-broadening with increased Ti is likely due to the increased disorder on the Nb/Ti1 and Nb/Ti2 framework sites in the second coordination sphere of the Na sites with increasing Ti. Octahedral Na1 bridges Ti/Nb sites through five of its oxygen bonds, octahedral Na2 bridges Ti/Nb sites through all six of its oxygen bonds, and distorted square planar Na3 bridges Ti/Nb sites through two of four of its oxygen bonds. The Na1 is bonded to water through its sixth bond, and Na3 is bonded to water through two of four of its bonds.

A comparison of the ^{1}H MAS NMR spectra of a high (20%) and low (2 %) concentration Ti gave direct evidence for addition of protons on two distinct oxygen sites that accompanies and charge-balances each substitution of a Ti into a framework Nb site. The SOMS has two sites for protons (evidenced by the two hydroxyl peaks in the 20%-Ti SOMS ^{1}H spectrum), and the occupancy of these sites increase with increasing Ti-substitution into the framework.

Infrared spectroscopy also gave evidence for the presence of increasing H-bonded O-H groups within the pores, as well as increased disorder on the Nb/M^{IV} sites with increasing M^{IV} substitution. Mid-IR spectra of 6.7%Ti-SOMS, 10.3%Ti-SOMS and 20%Ti-SOMS were studied for variations. Although all SOMS powders are well crystallized, we see an increased broadening in vibration bands with increasing Ti substitution. The adsorption bands below 1000 cm^{-1} are vibrations of the Na-titanoniobate framework including M-O stretching, M-O-M bending (M = Ti, Nb, Na) and lattice vibrations. These also exhibit broadening with increasing Ti incorporation into the lattice. The broadening of the O-H stretch at 2800 - 3500 cm^{-1} is indicative of hydrogen bonding, which is consistent with the ^{1}H NMR results where we see an increase in acidic protons (made acidic by H-bonding) with increasing M^{IV}. The broadening of the adsorption bands of the lattice vibrations (below 1000 cm^{-1}) with increasing substitution of Ti on the Nb framework sites may be a result of increased disorder, or decreased symmetry of the lattice sites, and the decreased symmetry results in broadening of the adsorption band of each vibrational frequency. The broadening of the IR spectra with increasing Ti-substitution is also consistent with the broadening of the ^{23}Na NMR spectra, as the disorder on the Nb/M^{IV} framework sites increases.

We also carried out Rietveld refinement of the x-ray powder diffraction data for the variable composition Ti- and Zr- SOMS to determine if altering the composition results in a change in the unit cell parameters. These studies showed that for the Ti-SOMS, there is very little change in unit cell parameters with changing Ti concentration. Further, the unit cell changes do not scale with composition. This is likely because: 1) there is only 5% difference between the radii of Ti and Nb (octahedral Ti^{IV} radius = 0.75 Å, octahedral Nb^{V} radius = 0.78 Å) and 2) the framework is flexible enough to accept the increase in protons within the pores with increasing M^{IV} concentration, and therefore only slightly distorts the framework. In contrast, the Zr-SOMS

show a slight increase in unit cell volume, likely because there is a larger size difference between Nb and Zr. However, volume does not scale with increasing Zr^{IV} substituted into the framework (radius of octahedral $Zr^{IV} = 0.86$ Å).

2. Thermal Stability of SOMS

Thermogravimetric analysis-differential thermal analysis (TGA-DTA) of variable composition, Ti- and Zr- SOMS provided information on the thermal stability of SOMS as a function of composition. Figure 2 shows the TGA-DTA spectra of variable composition, Ti-SOMS and Zr-SOMS. All SOMS compositions have two weight loss events upon heating. The weight loss between 150 and 250°C is the loss of framework water and hydroxyls, which varies from 7 – 8.5 wt % for the range of SOMS compositions synthesized. Below 150°C is likely surface water, which may vary in quantity, depending on the method of sample preparation and surface area of the particular sample. There is no further weight loss up to 900°C. Observation of the DTA curve shows both the endothermic loss of water and hydroxyls, and an exothermic event that occurs between 500°C and 600°C. This exotherm corresponds with conversion of the SOMS framework to a perovskite structure. The temperature of perovskite formation varies with SOMS composition; increasing temperature with increasing Ti^{IV} and decreasing temperature with
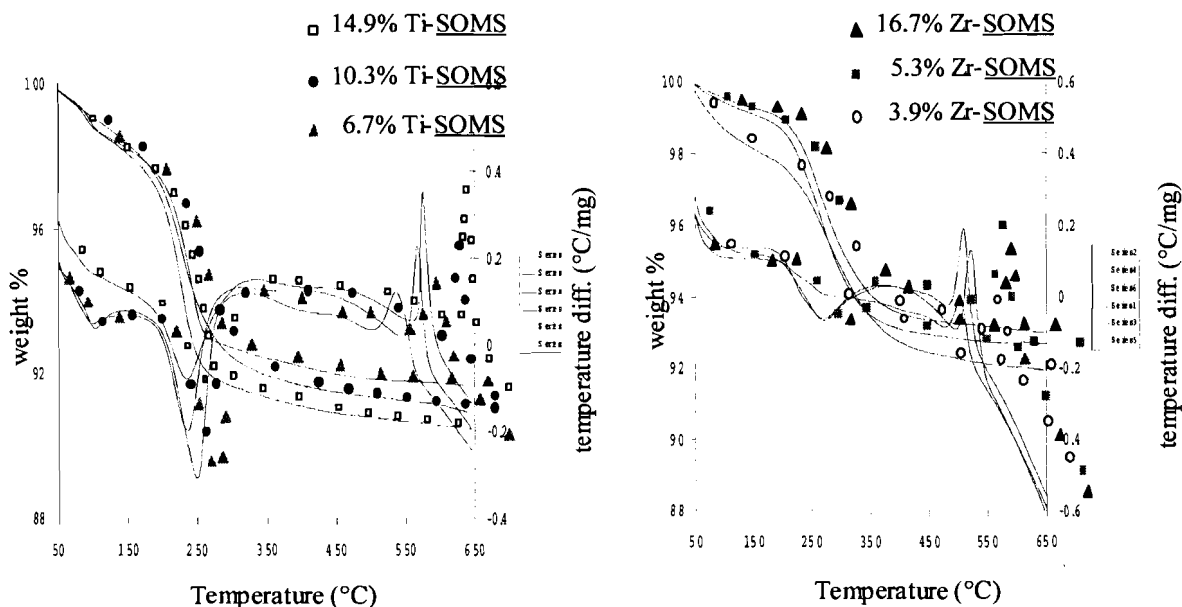
Figure 2. TGA-DTA spectra of 6.7%, 10.3% and 14.9%-Ti SOMS (left) and TGA-DTA spectra of 3.9, 5.3, and 16.7% Zr-SOMS (right). Both show increased weight loss with increasing framework M^{IV}, due to the corresponding increase in charge-balancing protons. The temperature of conversion to perovskite increases with increasing Ti in the framework, and the temperature of conversion to perovskite decreases with increasing Zr in the framework.

1.58

increasing Zr^{IV}. These results suggest that Ti^{IV} stabilizes the SOMS structure, while Zr^{IV} destabilizes the SOMS structure. The "stabilization" of SOMS with increasing Ti^{IV} in the framework (along with corresponding increase in OH content) may be due to the hydrogen bonding within the pores. The Zr-SOMS should also have increased H-bonding with increasing Zr^{IV}, but may be "destabilized" by the size mismatch between Nb^{V} and Zr^{IV}.

3. Sr Selectivity of SOMS

The proton added to the SOMS framework for each Nb^{V}—M^{IV} (M = Ti, Zr) substitution is responsible for the divalent cation selectivity. The charge-balanced ion exchange takes place by

$$Na^+_{SOMS} + H^+_{SOMS} + Sr^{2+}_{solution} \rightarrow Sr^{2+}_{SOMS} + Na^+_{solution} + H^+_{solution}$$

where a divalent Sr in solution exchanges for a proton plus a sodium in the SOMS. We observed in the 20% Ti-SOMS that the maximum exchange capacity for Sr exactly matches that of the Ti concentration, which matches the framework OH concentration.

Further, the proton peaks in the ^1H NMR spectra of Sr-exchanged, 20% Ti-SOMS are much diminished (undetectable). Figure 3 shows Sr selectivity of 20% Ti-SOMS as a function of pH with 0.1 M Na, 0.01 M Na and no Na as a competitive cation. The selectivity decreases with increasing [Na] concentration, and increases with increasing pH. The increase in Sr selectivity with increased pH is consistent with this exchange mechanism. A basic aqueous medium (high pH) removes framework protons more easily than a lower pH solution. Finally, a comparison of the Sr selectivity of 20% Ti-SOMS with 2% Ti-SOMS in a solution of 0.1 M Na and 50 ppm Sr shows that 2% Ti-SOMS has a K_d of 98 ml/g and 20% Ti-SOMS has a K_d of 1723 ml/g.
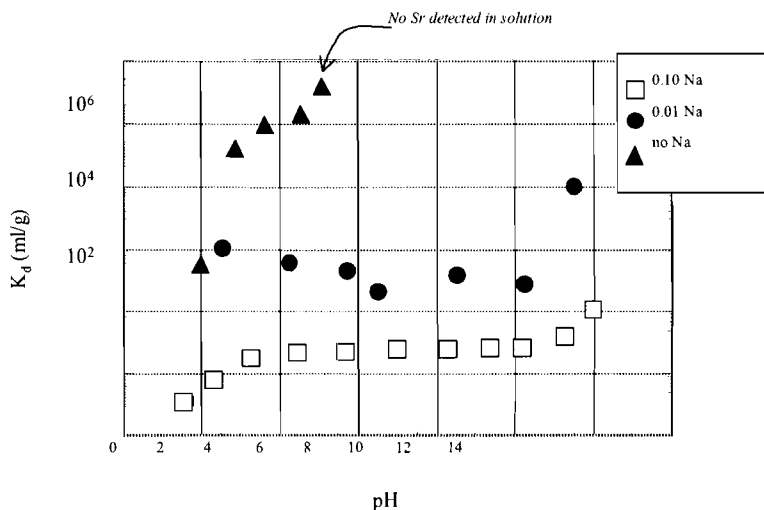
Figure 3. Selectivity (Kd, ml/g) of 20% Ti-SOMS for Sr as a function of pH and concentration of Na as a competing cation.

In summary, SOMS encompassing Ti-SOMS and Zr-SOMS types is a variable-composition class of niobate-based ion exchangers. The framework composition, particularly the Nb:M^{IV} (M = Ti, Zr) ratio, influences the channel composition in two ways. First, we have shown by a variety of

1.59

characterization techniques that the mechanism of charge-balancing the various composition analogs is proton addition. Second, we have shown that ion exchange occurs by exchange of a sodium plus a proton for a divalent cation, such as strontium. From TGA-DTA of the variable composition SOMS materials, we have learned the framework composition also affects the stability of the SOMS, by way of its temperature of thermal conversion to perovskite. Increasing Ti^{IV} concentration in the SOMS framework results in increased temperature of perovskite formation, and increasing Zr^{IV} concentration in the SOMS framework results in decreased temperature of temperature of perovskite formation. This corresponds with **increasing** SOMS stability with increasing Ti concentration, and **decreasing** SOMS stability with increasing Zr concentration. The instability of the Zr-SOMS is tentatively attributed to the larger "misfit" of the Zr^{IV} into the Nb^{V} framework sites, in that Zr^{IV} is considerably larger than Nb^{V}. The Ti^{IV}, however is very similar radius to Nb^{V}, and the stabilization of SOMS by increasing Ti^{IV} may be attributed to increased H-bonding within the pores.

The SOMS materials have provided a unique opportunity to investigate form-function properties of a class of ion exchanger materials. Our investigations have shown that by varying the Nb^{V}/M^{IV} framework composition directly varies the proton population within the channels which in turns controls properties such as ion exchange behavior and thermal stability. Drawing from this knowledge we may further modify this class of materials to develop or enhance other unique properties of the SOMS materials. Furthermore, a full understanding of the SOMS class of materials may also lead to the rational design of other classes of materials that are tailored for a specific property such as ion exchange.

$Na_{2-x}M_xNb_{1.6}Ti_{0.4}O_{5.8+yx}$, (M=Sr, Y, and Zr) series

A suite of perovskite phases with the compositions $Na_{2-x}M_xNb_{1.6}Ti_{0.4}O_{5.8+yx}$, (M=Sr, Y, and Zr), has been investigated at PNNL. In this series, portion of Na^+ is replaced by Sr^{2+}, Y^{3+} or Zr^{4+}, and the charge is balanced by incorporation of additional O^{2-} anions. Our motivation for this study is two-fold. First, $Na_{2-x}Sr_xNb_{1.6}Ti_{0.4}O_{5.8+0.5x}$ phases are the thermally converted ceramic waste forms from Sr loaded SOMS. To assess the feasibility of Sr removal by SOMS, a thorough understanding of the structures and chemical durability for this series of perovskite phases is essential. Second, to understand the stability of Sr-containing compounds that radioactively decay to Y and subsequently to Zr, the solubility studies of Y and Zr in $Na_{2-x}Y_xNb_{1.6}Ti_{0.4}O_{5.8+x}$, and $Na_{2-x}Zr_xNb_{1.6}Ti_{0.4}O_{5.8+1.5x}$ are critical. Figure 4 shows XRD pattern of $Na_{2-x}Sr_xNb_{1.6}Ti_{0.4}O_{5.8+0.5x}$ ($0 \leq x \leq 0.8$). All the XRD patterns can be indexed based on the structural model of $NaNbO_3$. Rietveld analysis of powder XRD data reveals that with increasing Sr content, cell volume increases. This trend is consistent with the replacement of Na^+ by the larger Sr^{2+} and the occurrence of additional O^{2-} in the structure. Synthesis of $Na_{2-x}Y_xNb_{1.6}Ti_{0.4}O_{5.8+x}$, and $Na_{2-x}Zr_xNb_{1.6}Ti_{0.4}O_{5.8+1.5x}$ was also carried out. XRD patterns show that there is up to 10%

substitution of Y for sodium in the $Na_2Nb_{1.6}Ti_{0.4}O_{5.8}$ lattice. However, there is no measurable substitution of zirconium for sodium in the $Na_2Nb_{1.6}Ti_{0.4}O_{5.8}$ lattice in our preliminary studies. Work will continue to evaluate the solubility of Y and Zr and to determine chemical and thermal durabilities of Sr substituted perovskite series.
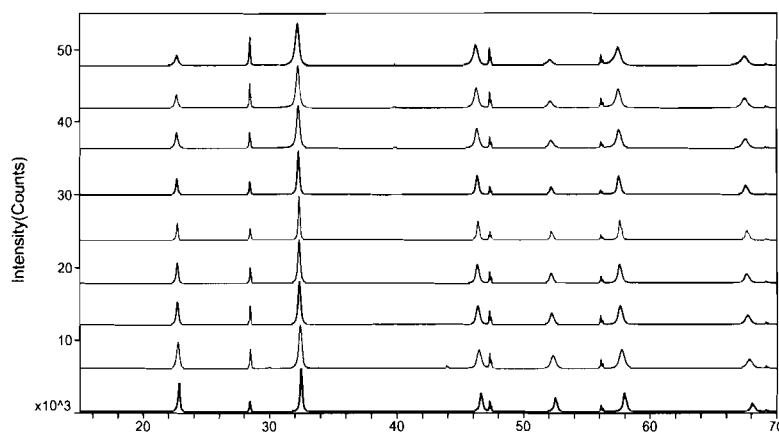
Figure 4. XRD patterns of Na2-xSrxNb1.6Ti0.4O5.8+0.5x perovskites with x = 0, 0.1, 0.2, 0.3, 0.4, 0.5, 0.6, 0.7, and 0.8.

Thermochemistry of $Na_2M_xNb_{2-x}O_{6-x}(OH)_x \cdot H_2O$ (M = Ti, Zr) Ion Exchangers and Their Dehydrated Perovskites

Using the hydrothermal method, researchers at SNL synthesized two series of octahedral molecular sieves, $Na_2Ti_xNb_{2-x}O_{6-x}(OH)_x \cdot H_2O$ and $Na_2Zr_xNb_{2-x}O_{6-x}(OH)_x \cdot H_2O$ ($0 < x \leq 0.4$). These microporous phases exhibit high selectivity for radioactive Sr^{2+} over monovalent cations such as Na^+. Upon heating, they dehydrate and convert to dense perovskite phases. The enthalpies of drop solution of the microporous phases and their corresponding perovskites were measured in molten $3Na_2O \cdot 4MoO_3$ at 974 K using high-temperature reaction calorimetry at UC-Davis. Based on the measured calorimetry data and the reported thermochemical parameters for the related oxides, enthalpies of formation from the oxides and from the elements were calculated via appropriate thermodynamic cycles. As Ti/Zr content increases, the enthalpies of formation of the microporous phases become more exothermic (Figure 5), suggesting a stabilizing effect of the substitution $Ti^{4+} + H^+ \rightarrow Nb^{5+}$ on the framework structure. This trend is
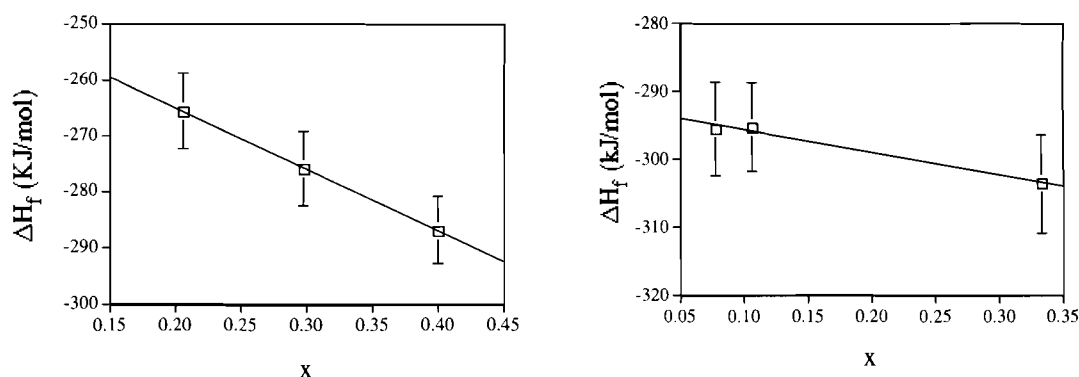
Figure 5. Enthalpies of formation of microporous phases $Na_2Ti_xNb_{2-x}O_{6-x}(OH)_x \cdot H_2O$ (left) and $Na_2Zr_xNb_{2-x}O_{6-x}(OH)_x \cdot H_2O$ (right) from the oxides as a function of composition

consistent with that observed in aluminosilicate zeolites: the higher the degree of hydration the more negative the enthalpy of formation. In contrast, the corresponding perovskites show less exothermic formation enthalpies with increasing Ti/Zr (Figure 6) and are thus less stable with respect to the constituent oxides. This behavior is likely due to the increased amounts of O^{2-} vacancies, required to compensate the charge imbalance between Ti^{4+} and Nb^{5+}, in the structures.

We intend to perform the calorimetric measurements on a series of Sr-exchanged microporous phases. Combined the new data with those for Sr-free samples, the enthalpy of the Na-Sr exchange reaction will be determined. The goal is to gain a fundamental understanding of the Na-Sr exchange energetics and to provide a thermodynamic basis for the development of a potential waste form for ^{90}Sr.
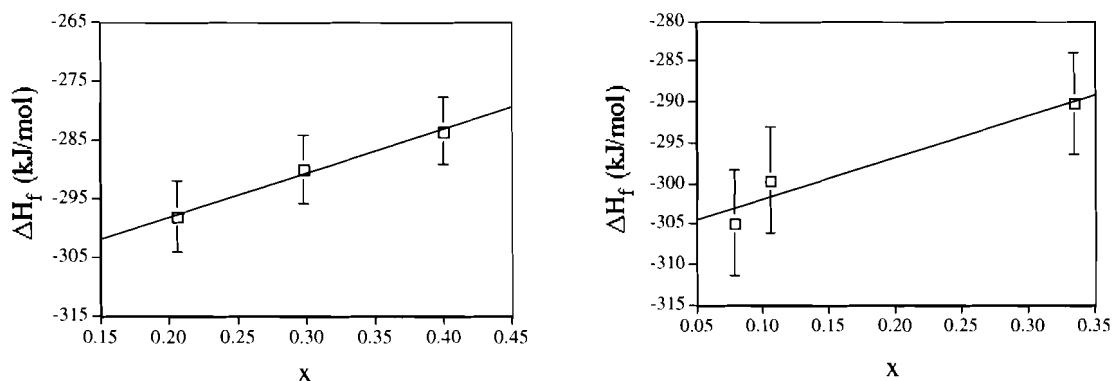
Figure 6. Enthalpies of formation of perovskites $Na_2Ti_xNb_{2-x}O_{6-0.5x}$ (left) and $Na_2Zr_xNb_{2-x}O_{6-0.5x}$ (right) from the oxides as a function of composition

Planned Activities

Future work will concentrate on continuing to develop and characterize new niobate based ion exchanger materials and their related condensed phases and determining their thermodynamic stabilities so that long term predictions of durability can be made. In addition, chemical and thermal durabilities of the niobate based pervoskite waste form will be evaluated.

Information Access

Publications

Nyman M, A Tripathi, JB Parise, RS Maxwell, and TM Nenoff. 2002. Sandia Octahedral Molecular Sieves (SOMS): Structural Effects of Charge-Balancing the Heteroatomic-Substituted Framework. *J. Amer. Chem. Soc.*124(3), 1704-1713.

Nyman M, F Bonhomme, RS Maxwell, and TM Nenoff. 2002. First Rb-silicotitanate phase and its K- Structural Analog: New Members of the SNL-A Family (Cc-$A_2TiSi_6O_{15}$; A=K, Rb, Cs). *Chem. Mater.* 13(12), 4603-4611.

Nenoff TM. 2002. SOMS: Sandia Octahedral Molecular Sieves for Rad Waste Cleanup, *Materials Technology* 17(3), in press.

Xu H, A Navrotsky, ML Balmer, and Y Su. 2002. Crystal chemistry and phase transitions in substituted pollucites along the $CsAlSi_2O_6$-$CsTiSi_2O_{6.5}$ join: A powder synchrotron XRD study. *Journal of the American Ceramic Society* 85:1235-1242.

Xu H, A Navrotsky, ML Balmer, and Y Su. 2002. Thermochemistry of substituted perovskites in the $NaTi_xNb_{1-x}O_{3-0.5x}$ system. In *Perovskite Materials, MRS Symposium Proceedings* (in press).

Hess N, Y Su, and ML Balmer. 2001. Evidence of Edge-Sharing TiO5 Polyhedra in Ti-Substituted Pollucite, $CsTi_xAl_{1-x}Si_2O_{+x/2.}$ *J. Phys. Chem. B* 105:6805-6811.

Balmer ML, Y Su, H Xu , ER Bitten, DE McCready, and A Navrotsky. 2001. Synthesis, Structure Determination, and Aqueous Durability of $Cs_2ZrSi_3O_9$. *J Am. Ceram. Soc.* 84:153-160.

Xu H, A Navrotsky, ML Balmer, Y Su, and ER Bitten. 2001. Energetics of Substituted Pollucites Along the $CsAlSi_2O_6$-$CsTiSi_2O_{6.5}$ Join: A High-Temperature Calorimetric Study. *J. Am. Ceram. Soc.* 84:555-560.

Xu H, Y Zhang, and A Navrotsky. 2001. Enthalpies of formation of microporous titanosilicates ETS-4 and ETS-10. *Microporous and Mesoporous Materials* 47:285-291.

Balmer ML, DE McCready, and Y Su. 2001. Cubic-to-Tetragonal Phase Transition in Ti-Substituted Pollucite. Submitted to *J. Am Ceram. Soc.,* 2001.

Young JS, Y Su, L Li, and M Balmer. 2001. Characterization of Aluminosilicate Formation on the Surface of a Crystalline Silicotitanate Ion Exchanger. *Microscopy and Microanalysis* 7(2): 498.

Nyman M, A Tripathi, JB Parise, RS Maxwell, WTA Harrison, and TM Nenoff. 2001. A new family of Octahedral Molecular Sieves: Sodium Ti/Zr(IV) Niobates. *J. Amer. Chem. Soc.* 123(7):1529-1530.

SuY, L Li, JS Young, and ML Balmer. 2001. *Investigation of Chemical and Thermal Stabilities of Cs Loaded UOP IONSIV IE-911 Ion Exchanger*. PNNL-13392-2, Pacific Northwest National Laboratory, Richland, Washington.

Nyman MD, TM Nenoff, and TJ Headley. 2001. *Characterization of UOP IONSIV IE-911*. SAND2001-0999, Sandia National Laboratories, Albuquerque, New Mexico.

Nyman MD, TM Nenoff, and TJ Headley. 2001. *Interactions of UOP IONSIV IE-911 with pretreatment and simulant solutions (UOP batches 98-5, 99-7, 99-9)*. SAND2001-2266, Sandia National Laboratories, Albuquerque, New Mexico.

Presentations

Xu H, A Navrotsky, MD Nyman, TM Nenoff, ML Balmer, and Y Su. 2002. Thermochemistry of niobate-based microporous phases $Na_2M_xNb_{2-x}O_{6-x}(OH)_x$ H_2O (M = Ti, Zr) and their dehydrated phases. 104th Annual Meeting of the American Ceramic Society, St. Louis, Missouri, April 28-May 1, 2002 (invited).

Xu H, A Navrotsky, ML Balmer, Y Su, MD Nyman, and TM Nenoff. 2002. Synthesis, crystal chemistry and energetics of $NaTi_xNb_{1-x}O_{3-0.5x}$ perovskites. Materials Research Society 2002 Spring Meeting, San Francisco, California, April 1-5, 2002.

Su Y, L Li, JS Young, and ML Balmer. 2001. Investigation of Chemical and Thermal Stabilities of Cs-Loaded Crystalline Silicotitanate, Materials Research Society 2001 Fall meeting, Boston, Massachusetts, November 26-30, 2001.

Xu H, A Navrotsky, MD Nyman, TM Nenoff, Y Su, and ML Balmer. 2001. Synthesis, Crystal Chemistry and Energetics of Microporous Silicotitanates in the (K1-Xcsx)3ti4si3o15(Oh)•Nh2o System", Materials Research Society 2001 Fall meeting, Boston, Massachusetts, November 26-30, 2001.

Nyman M, JL Krumhansl, C Jove-Colon, P Zhang, TM Nenoff, TJ Headley, Y Su, and L Li. 2001. Chemical Interactions of Uop Insiv Ie-911 (Cst) with Srs Waste Simulants, Materials Research Society 2001 Fall meeting, Boston, Massachusetts, November 26-30, 2001.

Nyman MD, TM Nenoff, A Tripathi, J Parise, A Navrotsky, and H Xu. 2001. A/Nb/Ti/Si oxideframework condensed and microporous phases and their application to radionuclide squestration and immobilization. Materials Research Society 2001 Fall meeting, Boston, Massachusetts, November 26-30, 2001.

1.64

Nenoff TM, M Nyman, A Tripathi, JB Parise, WTA Harrison, RS Maxwell, RC Ewing. 2001. SOMS, a new class of molecular sieves with high selectivity for radioactive Sr+. Inorganic Chemistry Gordon Conference, Rhode Island, July 2001 (invited).

Nenoff TM, M Nyman, A Tripathi, JB Parise, WTA Harrison, RS Maxwell. 2001. *SOMS*: Sandia Octahedral Molecular Sieves. A new class of ion exchangers selective for the removal of Sr^{2+} from waste streams. 13th International Zeolite Conference, Montpelier, France, July 2001.

Awards

Sandia National Laboratories Team Employee Recognition (ERA) Award for the Development of Sandia Octahedral Molecular Sieves (SOMS), April 2002.

Development of Fundamental Data on Chemical Speciation and Solubility for Strontium and Americium in High-Level Waste: Predictive Modeling of Phase Partitioning During Tank Processing

(Project Number: 73749)

Principal Investigators

Dr. Andrew R. Felmy
Pacific Northwest National Laboratory
P.O. Box 999, MSIN K8-96
Richland, WA 99352
509-376-4079 (phone)
509-376-3650 (fax)
ar.felmy@pnl.gov

Dr. Gregory Choppin
The Florida State University
Department of Chemistry, B-164
Tallahassee, FL 32606-3006
904-644-3875 (phone)
904-644-8281 (fax)
Choppin@chemmail.chem.fsu.edu

Dr. David A. Dixon
Pacific Northwest National Laboratory
P.O. Box 999, MSIN K1-83
Richland, WA 99352
509-372-4999 (phone)
509-375-6631 (fax)
da.dixon@pnl.gov

Research Objective

In this project, Pacific Northwest National Laboratory (PNNL) and Florida State University (FSU) are investigating the speciation of Sr and Am/Cm in the presence of selected organic chelating agents over ranges of hydroxide, carbonate, ionic strength, and competing metal ion concentrations present in high-level waste (HLW) stored in tanks at Hanford and other U.S. Department of Energy (DOE) sites. The chelating agents that are being studied are EDTA (ethylenediaminetetraacetic acid), HEDTA (N-(2-hydroxyethyl)ethylenediaminetriacetic acid), NTA (nitrilotriacetic acid), IDA (iminodiacetic acid), citrate, and oxalate.

The project comprises integrated research tasks that approach the problem of chemical speciation using macroscopic thermodynamic measurements of metal-ligand competition reactions, molecular modeling studies to identify structures or complexes of unusual stability, and mass spectrometry measurements of complex charge/mass ratio that can be applied to mixed metal-chelate systems. This fundamental information then is used to develop thermodynamic models designed to predict changes in chemical speciation and solubility resulting from various tank-processing conditions. In this way we can develop new approaches that address fundamental problems in aqueous speciation and, at the same time, provide useful and practical information needed for tank waste processing.

Current strategies for reducing the total volume of radioactive tank waste requiring disposal at Hanford and other DOE sites call for the development of methods that can be used to selectively dissolve and remove non-radioactive elements, such as Al, P, and Cr, while retaining or precipitating the radioactive elements, including Sr and the actinide elements, in the tank sludge. This partitioning between solids and precipitates is fundamentally dependent on the chemical speciation of the elements present in the tank processing solutions. Of particular importance is separation of the radioactive and hazardous actinide elements and fission products from the sludge and supernatants, particularly from supernatants containing high concentrations of strong chelating agents that can act to dissolve the actinides and fission products as well as interfere with subsequent metal ion extraction processes. Specifically, the fundamental understanding of chemical speciation reactions gained from these studies will help us identify other potential mechanisms (e.g., competition, displacement, or other reactions) that could be used for removing Sr and Am/Cm from organic chelates present in the HLW.

Research Progress and Implications

In fiscal year 2002, we focused our efforts on the following three areas:

1. finalizing our studies of Cm(III) speciation in the presence of the organic chelates

2. developing an accurate chemical model for the complexation of Sr with EDTA and HEDTA.

3. adding Pitzer's equations to the Environmental Simulation Program (ESP).

Studies of Cm(III) Speciation

In this project area, we performed fluorescence spectroscopic and lifetime measurements for Cm(III) solutions at approximately constant Cm(III) concentration (8.6×10^{-9} M to 8.6×10^{-9} M) over broad concentration ranges of HEDTA (2×10^{-5} M to 1.0×10^{-1} M) and NaOH (1.0×10^{-9} M to 7.5 M). Part of the fluorescence spectra are shown in Figure 1. The spectra clearly indicate
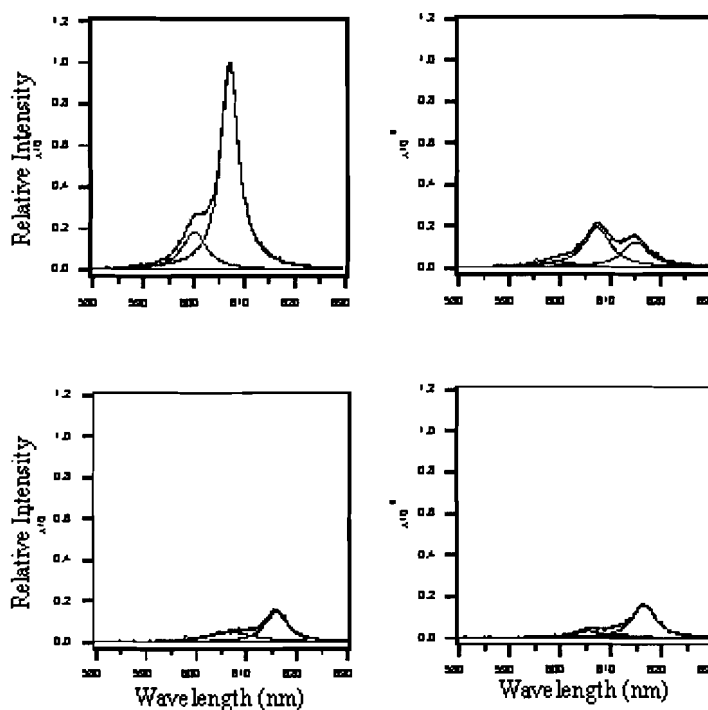
Figure 1. Fluorescence emission spectra of Cm(III) in the presence of HEDTA in different NaOH solutions. [Cm(III)] = 9.6×10^{-9} M; [HEDTA] = 0.01 M; The concentrations of NaOH are 0.01 M (top left); 0.50 M (top right); 3.00 M (bottom left); and 7.5 M (bottom right). λ_{ex} = 375 nm.

three major Cm(III) species with spectral maximums occurring at 600.4 nm, 607.0 nm, and 616.0 nm, respectively, under the test experimental conditions. The red-shift in the fluorescence spectra suggest that all three Cm(III) species involve inner-sphere complexation between Cm(III) and HEDTA. The number of water molecules calculated from the fluorescence decay constants confirm that the spectrum located at 600.4 nm corresponds to the 1:1 Cm-HEDTA complex, CmHEDTA, while the spectrum located at 607.0 nm corresponds to the 1:2 complex, $Cm(HEDTA)_2^{3-}$. For the third species, if a mononuclear species were assumed, there would be seven water molecules in the inner sphere of Cm(III), which is completely contradictory with the largest red-shift of the fluorescence spectra. Therefore, it is plausible to assign this species to a multi-nuclear Cm(III)-HEDTA-oxo (hydroxyl) complex. Energy transfer from excited Cm(III) ions to unexcited ions leads to a large apparent fast fluorescence decay (seemingly from more inner-sphere waters) while the strong inner-sphere complexation between Cm(III) and HEDTA is maintained. The unusually large red-shift may indicate the existence of additional covalent bonding between Cm(III) centers, such as those through μ-oxo or hydroxyl bonding, in the molecule or cluster of molecules.

To further elucidate the nature of the third species, we prepared a series of solid suspensions containing 0.001 M HEDTA and excess solid $Eu(OH)_3$ at different NaOH concentrations. After three days of equilibration under constant agitation, we separated the solids in the suspensions by high-speed centrifugation. After this initial separation step, we then filtered a portion of the supernatant through a filter medium with cutoff molecular weight of 40,000 Daltons. Time-resolved fluorescence spectra were recorded for the solid fraction, the supernatant, and the aqueous filtrate. The resulting spectra (partly shown in Figure 2) indicate that, for the solid fraction, characteristic $Eu(OH)_3$ spectra dominate at short delay times. However, at longer delay times ($\geq$ 700 μs), the fluorescence spectra are typical of inner-sphere Eu(III)-HEDTA type complexes, which suggests that Eu(III)-HEDTA complexation probably occurred at the surface of solid $Eu(OH)_3$. For the supernatant, the fluorescence spectra is again a mixture of the solid $Eu(OH)_3$ and Eu(III)-HEDTA complex, although the relative amount of the solid is apparently much smaller when compared to that of the solid. In the filtered supernatant, the contribution of the solid $Eu(OH)_3$ was negligible. These results demonstrate that in highly basic solutions, because of the extremely small solubility product of $Eu(OH)_3$ and the mono-nuclear type Eu(III)-HEDTA and Eu(III)-HEDTA-OH complexes that are present, surface complexation between HEDTA and $Eu(OH)_3$ colloids and clusters may also contribute to the solubility of Eu(III). The similar spectroscopic characteristics of Eu-HEDTA in excess solid $Eu(OH)_3$ and Cm(III)-HEDTA complexes with much lower metal concentration in concentrated NaOH solutions further suggest that the surface compexation between HEDTA and $Cm/(Eu)(OH)_3$ colloids and clusters may be the dominant factor responsible for their solubility.

1.70
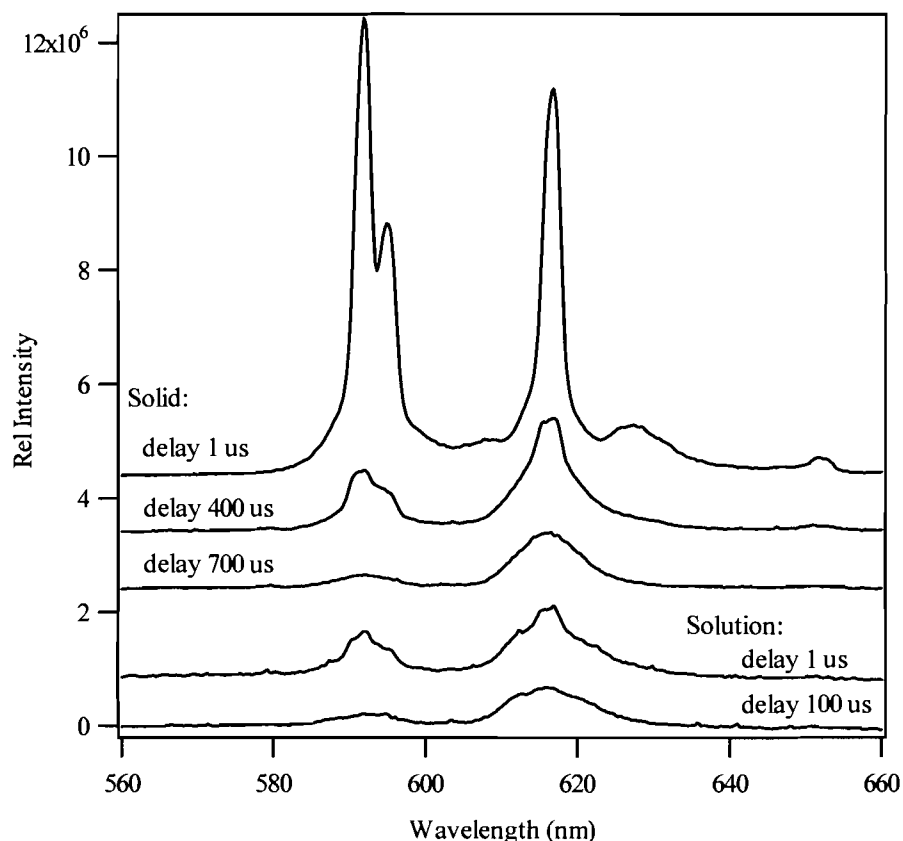
Figure 2. Time-resolved fluorescence emission spectra of Eu(III) in the presence of 0.001 M HEDTA and excess solid Eu(OH)$_3$(s) after equilibration in 7.5 M NaOH for three days. Top three spectra are for the solid and bottom two spectra are for the supernatant after high-speed centrifugation. The spectral traces are offset along the vertical axis for clarity. λ_{ex} = 465 nm.

Studies on Strontium Speciation

During fiscal year 2002, with partial support from the Hanford River Protection Project/Waste Treatment Plant (RPP/WTP), an aqueous thermodynamic model was developed to accurately describe the effects of Na$^+$ complexation, ionic strength, carbonate concentration, and temperature on the complexation of Sr^{2+} by EDTA under basic conditions. The model is based on published data of apparent equilibrium constants, enthalpies, and heat capacities and on the extensive set of solubility data on SrCO$_3$(c) in the presence of EDTA that we have developed during this EMSP project. The solubility data for SrCO$_3$(c) were obtained in solutions with Na$_2$CO$_3$ concentrations ranging from 0.01m to 1.8m and NaNO$_3$ concentrations ranging from 0 to 5m, and at temperatures extending to 75°C. The final aqueous thermodynamic model is based upon the equations of Pitzer, and it requires the inclusion of a NaEDTA^{3-} species as well as mixing terms between the highly charged anions CO$_3{}^{2-}$ and NaEDTA^{3-}. An accurate model for the ionic strength dependence of the ion-interaction coefficients for the SrEDTA^{2-} and

NaEDTA^{3-} aqueous species allows the extrapolation of standard state equilibrium constants for these species, which are significantly different from the 0.1m reference state values available in the literature.

These data already have been used at the Hanford site as part of the RPP/WTP.

Addition of Pitzer's Equations to ESP

During fiscal year 2002, considerable effort has been spent on incorporating new thermodynamic data (developed under EMSP and elsewhere) into the chemical processing models used at Hanford and other DOE sites. This effort resulted in the release of the "beta" version of the ESP, which includes the Pitzer equations, at the Hanford and Savannah River sites. This enhanced capability will allow all of the new thermodynamic data developed under EMSP to be used by the site contractors.

Planned Activities

In fiscal year 2003, we plan to finalize our studies of the effects of base concentration on the organic chelates and strontium species. In addition, we will study the effects of metal ions that can compete with the trivalent actinides and Sr for the chelates. These efforts will focus on Ni, which forms some of the strongest aqueous complexes known with EDTA under highly basic conditions.

Information Access

Publications and Presentations (FY02 only)

Felmy AR, H Cho, GR Choppin, DA Dixon, GT MacLean, JR Rustad, Z Wang, and X Xia. 2001. Development of Accurate Chemical Models for Tank Applications: Coupling Engineering Application with Good Science. Lunch hour presentation as an example of a successful EMSP Program, EMSP Tanks Focus Area (TFA) Workshop, November 7-8, 2001, Richland, Washington.

Felmy AR 2001. Thermodynamic Modeling and Equilibrium Data. Presentation to the RPP-WTP Review Panels, October 31, 2001, Richland, Washington.

Wang Z, X Xia, MJ Mason, and AR Felmy. 2001. Investigations of Cm(III) Speciation in Strongly Basic Solutions by Time Resolved Laser Fluoresence Spectroscopy. 222nd ACS National Meeting, August 26-30, Chicago Illinois.

Sanders S, R Young, and AR Felmy. 2001. Inclusion of Pitzer Equations in the ESP Computer Model (Beta Version). Tanks Focus Area Milestone Report B.3-1 (September 2001).

Felmy AR and GT MacLean. 2001. *Development of an Enhanced Database for the ESP Model: The Fluoride and Phosphate Components*. WTP-RPT-018 Rev. 0. Prepared for Bechtel National Inc. by Pacific Northwest National Laboratory, Richland, Washington.

Felmy AR and P McKenzie. 2002. Incorporation of Pitzer Parameters in ESP. TFA Salt Cake Dissolution and Waste Chemistry Workshop, May 14-16, 2002, Richland, Washington.

Felmy AR 2002. Thermodynamic Modeling and Equilibrium Data. Presentation to the RPP-WTP Review Panels, April 2002, Richland, Washington.

Other Contributions

In addition to the previously described scientific contributions, the principal investigators on this project also worked to enhance the overall success of the EMSP program. Specific examples of these activities are described below.

A.R. Felmy (PNNL) was a co-organizer of the "Accomplishment of the Environmental Management Sciences Program (EMSP) Symposium" at the 222nd ACS National Meeting held in Chicago, Illinois on August 26-30, 2001. The symposium consisted of five different sessions covering the areas of subsurface science, solution and tank chemistry, radionuclide and contaminant separation methods, analytical and sensing techniques, and waste form treatment and development. There were 65 oral or poster presentations in the symposium.

G.R. Choppin (FSU) serves as a member of the EMSP Advisory Committee and the NAS/NRC Board of Radioactive Waste Management.

Computational Design of Metal Ion Sequestering Agents

(Project Number: 73759)

Principal Investigator

Dr. Benjamin P. Hay
Pacific Northwest National Laboratory
P.O. Box 999
Richland, WA 99352
509-372-6239 (phone)
509-375-6631 (fax)
ben.hay@pnl.gov

Co-Principal Investigators

Dr. David A. Dixon
Pacific Northwest National Laboratory
P.O. Box 999
Richland, WA 99352
509-372-4999 (phone)
509-375-6631 (fax)
david.dixon@pnl.gov

Dr. Brian M. Rapko
Pacific Northwest National Laboratory
P.O. Box 999
Richland, WA 99352
509-376-1571 (phone)
509-372-3861 (fax)
brian.rapko@pnl.gov

External Collaborators

Professor Robert T. Paine
Department of Chemistry
University of New Mexico
Albuquerque, NM 87131
505-277-1661 (phone)
505-277-2609 (fax)
rtpaine@unm.edu

Professor Kenneth N. Raymond
Department of Chemistry
University of California, Berkeley
Berkeley, CA 94720
510-642-7219 (phone)
510-486-5283 (fax)
raymond@garnet.berkeley.edu

Dr. Bruce A. Moyer
Oak Ridge National Laboratory
Oak Ridge, TN 37831
423-574-6718 (phone)
423-574-4939 (fax)
moyerba@ornl.gov

Prof. James E. Hutchison
Department of Chemistry
University of Oregon
Eugene, OR 97403
541-346-4228 (phone)
541-0346-0487 (fax)
hutch@oregon.uoregon.edu

Research Objectives

Organic ligands that exhibit a high degree of metal ion recognition are essential precursors for developing separation processes and sensors for metal ions. Since the beginning of the nuclear era, much research has focused on discovering ligands that target specific radionuclides. Members of the Group 1A and 2A cations (e.g., Cs, Sr, Ra) and the f-block metals (actinides and lanthanides) are of primary concern to the U.S. Department of Energy (DOE). Although there has been some success in identifying ligand architectures that exhibit a degree of metal ion recognition, the ability to control binding affinity and selectivity remains a significant challenge. The traditional approach for discovering such ligands has involved lengthy programs of organic synthesis and testing that, in the absence of reliable methods for screening compounds before synthesis, have resulted in much wasted research effort.

This project seeks to enhance and strengthen the traditional approach through computer-aided design of new and improved host molecules. Accurate electronic structure calculations are coupled with experimental data to provide fundamental information about ligand structure and the nature of metal-donor group interactions (design criteria). This fundamental information then is used in a molecular mechanics model (MM3) that helps us rapidly screen proposed ligand architectures and select the best members from a set of potential candidates. By using combinatorial methods, molecule building software has been developed that generates large numbers of candidate architectures for a given set of donor groups. The specific objectives of this project are as follows:

- Further understand the structural and energetic aspects of individual donor group- metal ion interactions and incorporate this information within the framework of MM3.

- Further develop and evaluate approaches for correlating ligand structure with reactivity toward metal ions, in other words, screening capability.

- Use molecule structure building software to generate large numbers of candidate ligand architectures for given sets of donor groups.

- Screen candidates and identify ligand architectures that will exhibit enhanced metal ion recognition.

These new capabilities are being applied to ligand systems identified under other DOE-sponsored projects in which studies have suggested that modifying existing architectures will lead to dramatic enhancements in metal ion binding affinity and selectivity. With this in mind, we are collaborating with researchers at the University of New Mexico, University of California at Berkeley, University of Oregon, and Oak Ridge National Laboratory to obtain experimental

validation of the predicted new ligand structures. Successful completion of this study will yield molecular-level insight into the role that ligand architecture plays in controlling metal ion complexation and will provide a computational approach to ligand design.

Research Progress and Implications

This project is a renewal of EMSP Project No. 54679, "Architectural Design Criteria for f-Block Metal Sequestering Agents," that began in September 1996 and ended in May 2000. Funding for the project was renewed in October 2000, and this report summarizes progress after 1 year and 7 months of a 3-year period. Research has focused on three areas. These are 1) the completion of diamide studies, 2) coupling molecular mechanics screening methods with a *de novo* structure-based design program, HostDesigner, and 3) application of computational methods to ligand design.

Over the past decade, there has been a worldwide effort to develop processes for separating trivalent transuranic elements from nitric acid media based on the use of lipophilic diamide ligands. Because the sequestering agents contain only C, H, O, and N atoms, diamide process solvents are completely incinerable, resulting in less secondary waste than alternative systems that use phosphorous-containing ligands. However, the weak extraction efficiency of conventional diamides necessitates the use of high ligand concentrations, resulting in increased costs as well as difficulties with third-phase formation and hydraulic behavior of process solvents. Using theoretical models developed at the W. R. Wiley Environmental Molecular Sciences Laboratory, we have designed a new class of bicyclic diamide structures that are highly organized for complexation with trivalent f-block elements (see Figure 1). The designer ligands differ from conventional diamides only in the way that the two amide binding sites are connected. Single-crystal x-ray diffraction of their metal complexes verifies that the new diamides bind to f-block metal ions in the expected manner. Liquid-liquid extraction measurements reveal that the computer-designed architecture yields a dramatic performance enhancement, exhibiting a partitioning of Eu(III) to a ligand-containing organic phase that is *10 million times more effective* than that observed for conventional diamides. An invention report on the bicyclic diamide compounds, 3,9-diaza-3,9-dialkylbicyclo[4.4.0]decane-2,10-diones, was filed at Pacific Northwest National Laboratory (PNNL).

To bring the powerful concepts embodied in *de novo* structure-based drug design to the field of coordination chemistry, we have developed a computer program named HostDesigner with support from PNNL Laboratory-Directed Research and Development and Chemical Sciences, Office of Basic Energy Sciences, DOE Office of Science. This software builds millions of potential host structures from molecular fragments, screens the candidate structures with respect to their complementarity for a targeted metal ion guest, and outputs a list of lead candidates for

conventional diamide   computer designed diamide
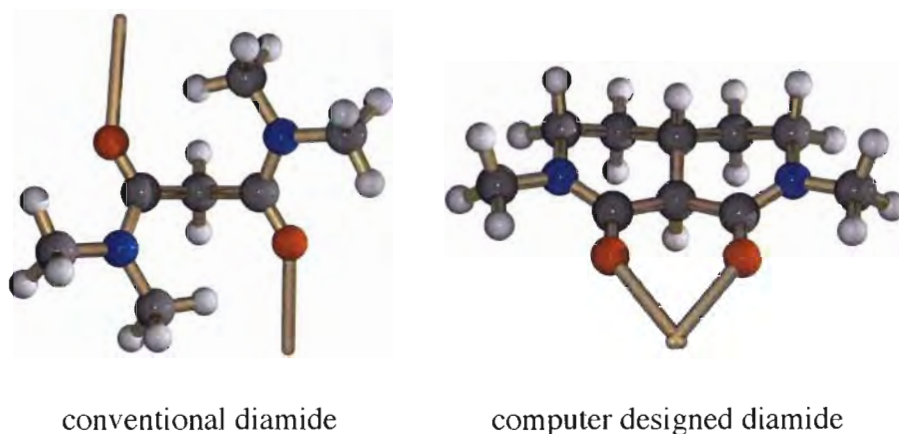
Figure 1. A comparison of the three-dimensional structure of a conventional diamide ligand with that of the new bicyclic diamide. The vectors on each oxygen atom, which indicate the direction required for optimal interaction with a metal ion, diverge in the malonamide structure and converge in the computer-designed structure.

further evaluation. One of the goals of this project was to couple the HostDesigner software with a molecular mechanics program (MM3) to provide a more accurate ranking of structures in terms of their complementarity for the targeted metal ion. This task was successfully completed, and post-processing of the HostDesigner output with MM3 strain energy analyses is now automated, provided the force field parameters for the system under study are available. Because force field parameters for metal complexes are limited, another task within this project is to extend the MM3 model to treat additional donor group-metal ion interactions. Research to extend the MM3 model to amines, carboxylates, and aminocarboxylates, was initiated in the first year of this project.

The computer-aided design technologies being developed in this project are now being applied in collaborations with two research groups. One application, with Oak Ridge National Laboratory, focuses on the design of new calix[4]crown ether architectures that provide more effective and more selective interactions with the cesium cation. The approach involves 1) using HostDesigner to add binding sites to existing scaffolds and/or to add structure to preorganize the host molecule, 2) MM3 analysis of lead structures for complementarity, and 3) conformational analysis of the most complementary structures to evaluate their degree of preorganization. In addition, HostDesigner is being used to identify optimal molecular structure for combining unidentate donor groups, for example ethers and amines, to form multidentate host structures that complement metal ions of different sizes. A second application, with the University of California, Berkeley, uses a similar approach to identify optimal ways to link bidentate chelates, such as catecholamides and hydroxypyridinones, in order to design more efficient receptors for trivalent and tetravalent f-block metal ions.

Planned Activities

- In collaboration with Oak Ridge National Laboratory and the University of California-Berkeley, we will continue application of computer-aided design methods to identify improved host architectures.

- Beginning in November 2002, we will apply computer-aided ligand design methods to phosphine oxide and pyridine-N-oxide based ligands for f-block elements in collaboration with the University of New Mexico.

Information Access

The original project, which combined theoretical and experimental approaches to investigate the interactions of amide ligands with metal ions, resulted in 28 presentations at meetings, workshops, and conferences, and 14 journal articles. Since the renewal of the original project, there have been an additional eight publications and eleven presentations. In addition, abstracts are submitted for six presentations at future conferences.

Publications since May 2000

Vargas R, J Garza, DA Dixon, and BP Hay. 2000. How Strong is the C(alpha)-H•••O=C Hydrogen Bond? *J. Am. Chem. Soc.* 122:4750-4755 and highlighted in a *Chemical and Engineering News* [78(19):15] News of the Week article, Protein Folding. Weak Hydrogen Bonds in Peptide Backbones May Play Significant Role.

Vargas R, J Garza, DA Dixon, and BP Hay. 2000. Conformational Analysis of N,N,N',N'-Tetramethylsuccinamide: Importance of C-H•••O Hydrogen Bonds? *J. Phys. Chem. A* 104:5115-5121.

Rapko BM, BK McNamara, GJ Lumetta, RD Rogers, GA Broker, and BP Hay. 2000. Coordination of Lanthanide Ions Containing Non-Coordinating Counteranions with N,N,N',N'-Tetramethylsuccinamide (TMSA). I. Preparation and Characterization of [(TMSA)$_4$Ln][A]$_3$, A = ClO$_4^-$, CF3SO$_3^-$. *Inorg. Chem.* 39:4858-4867.

Lumetta GJ, BK McNamara, BM Rapko, RL Sell, RD Rogers, GA Broker, and JE Hutchison. 2000. Synthesis and Characterization of Mono- and Bis-(tetraalkyl-malonamide)uranium(VI) Complexes, *Inorganica Chimica Acta* 309:103-108.

Rao L, P Zanonato, P Di Bernardo, and A Bismondo. 2000. Calorimetric and Spectroscopic Studies of Eu(III) Complexation with Tetramethylmalonamide and Tetramethylsuccinamide in Acetonitrile and Dimethylsulfoxide. *Inorg. Chim. Acta* 306:49-64.

Rao L, P Zanonato, P Di Bernardo, and A Bismondo. 2001. Complexation of Eu(III) with Alkyl-Substituted Malonamides in Acetonitrile. *J. Chem. Soc. Dalton Trans.* 1939-1944.

Hay BP and RD Hancock. 2001. The Role of Donor Group Orientation as a Factor in Metal Ion Recognition by Ligands. *Coord. Chem. Rev.* 212:61-78.

Lumetta GJ, BM Rapko, PA Garza, BP Hay, RD Gilbertson, TJR Weakley, and JE Hutchison. 2002. Deliberate Design of Ligand Architecture Yields Dramatic Enhancement of Metal Ion Affinity. *J. Am. Chem. Soc., Comm. Ed.* 124:5644-5645 and highlighted in *Science Magazine* as an Editors' Choice article, "Designer Bindings" (296, 985) and in *Chemical and Engineering News* as a Science Concentrate, "Designed Ligands Boost Metal Binding" [80(20):37].

Presentations since May 2000

Hay BP. 2000. Building a Better Mousetrap: Ligand Design with Molecular Mechanics. American Chemical Society, Pacifichem 2000 Meeting in Honolulu, Hawaii, December 2000.

Hay BP, DA Dixon, and BM Rapko. 2001. Computational Design of Metal Ion Sequestering Agents (EMSP 54679). Tanks Focus Area (TFA) FY 2001 Midyear Review, Salt Lake City, Utah, March 2001.

Gilbertson RD, BM Rapko, BP Hay, JE Hutchison, and TJR. Weakly. 2001. Synthesis of a Conformationally Constrained Malonamide and Its Coordination Chemistry with Uranyl Nitrate. 221st American Chemical Society National Meeting, San Diego, California, April 2001.

Lumetta GJ, BK McNamarra, BM Rapko, RD Rogers, GA Broker, and JE Hutchison. 2001. Extraction of U(VI) with Malonamides: What's Really Going On? 221st American Chemical Society National Meeting, San Diego, California, April 2001.

Hay BP. 2001. HostBuilder: A Combinatorial Structure Generator for Host Discovery, Separations Group Seminar, Oak Ridge National Laboratory, Oak Ridge, Tennessee, June 2001.

Hay BP, DA Dixon, and BM Rapko. 2001. Computational Design of Metal Ion Sequestering Agents. EMSP Symposium, 222nd American Chemical Society National Meeting, Chicago, Illinois, August 2001.

Klinckman TR, DA Dixon, and BP Hay. 2001. An MM3 Force Field for Metal Complexes with Amines, Carboxylates, and Aminocarboxylates. Inorganic Poster Session, 222nd American Chemical Society National Meeting, Chicago, Illinois, August 2001.

Hay BP. 2001. Toward the Computer-Aided Design of Metal Ion Hosts. Departmental Seminar, Georgia Institute of Technology, Atlanta, Georgia, October 2001.

Hay BP. 2001. Toward the Computer-Aided Design of Metal Ion Hosts. Departmental Seminar, University of Memphis, Memphis, Tennessee, October 2001.

Hay BP. 2001. HostBuilder: A Combinatorial Molecular Structure Generator and Its Application to the Design of Metal Sequestering Agents. Raymond Group Seminar, University of California-Berkeley, Berkeley, California, December 2001.

Hay BP. 2002. Computer-Aided Design of Ion Receptors. Chemical and Analytical Division Seminar, Oak Ridge National Laboratory, Oak Ridge, Tennessee, May 2002.

Rapko BM, GJ Lumetta, BP Hay, PA Garza, JE Hutchison, RD Gilbertson, and TR Weakley. 2002. Bicyclic Diamides Exhibit Exceptional Affinity for Europium(III). Abstract submitted to the Actinides Separation Conference to be held in Berkeley, California, June 2002.

Hay BP. 2002. Extending the MM3 Force Field for Application to the Structure-Based Design of Metal Ion Hosts. Abstract submitted to the Symposium on New Developments in Force Fields for Molecular Modeling, Computers in Chemistry Division, 224th American Chemical Society National Meeting to be held in Boston, Mass., August 2002.

Hay BP, GJ Lumetta, BM Rapko, PA Garza, RD Gilbertson, TRJ Weakley, and JE Hutchison. 2002. Deliberate Design of Ligand Architecture Yields Dramatic Enhancement in Metal Ion Affinity. Abstract submitted to the Inorganic Poster Session, 224th American Chemical Society National Meeting to be held in Boston, Mass., August 2002.

Zhang C and BP Hay. 2002. Computer-Aided Design of Cesium Receptors Based on Calix[4]arene Scaffolds. Abstract submitted to the Inorganic Poster Session, 224th American Chemical Society National Meeting to be held in Boston, Mass., August 2002.

Uddin J, TK Firman, and BP Hay. 2002. Computer Aided Design of Complementary Chelate Ring Architecture. Abstract submitted to the Coordination Chemistry Symposium, Inorganic Chemistry Division, 224th American Chemical Society National Meeting to be held in Boston, Mass., August 2002.

Gilbertson RD, JE Hutchison, TJR Weakley, BM Rapko, and BP Hay. 2002. Efficient Synthesis and Coordination Complexes of a New Ligand Architecture with High Affinity for f-Block Elements. Abstract submitted to the Inorganic Poster Session, 224th American Chemical Society National Meeting to be held in Boston, Mass., August 2002.

Technetium Chemistry in HLW: Role of Organic Complexants

(Project Number: 81921)

Principal Investigator

Nancy J. Hess
Pacific Northwest National Laboratory
P.O. Box 999, MSIN P7-50
Richland, WA 99352
509-376-9808 (phone)
509-372-1632 (fax)
nancy.hess@pnl.gov

Co-Principal Investigators

David L. Blanchard, Jr.
Pacific Northwest National Laboratory
P.O. Box 999, MSIN P7-25
Richland, WA 99352
509-372-2248 (phone)
509-372-3861 (fax)
dl.blanchard@pnl.gov

Dhanpat Rai
Pacific Northwest National Laboratory
P.O. Box 999, MSIN P7-50
Richland, WA 99352
509-373-5988 (phone)
509-372-1632 (fax)
dhan.rai@pnl.gov

James A. Campbell
Pacific Northwest National Laboratory
P.O. Box 999, MSIN P8-08
Richland, WA 99352
509-376-0899 (phone)
509-376-2329 (fax)
james.campbell@pnl.gov

Yuanxian Xia
Pacific Northwest National Laboratory
P.O. Box 999, MSIN P7-50
Richland, WA 99352
509-373-5767 (phone)
509-372-1632 (fax)
yuanxian.xia@pnl.gov

Herman M. Cho
Pacific Northwest National Laboratory
P.O. Box 999, MSIN K8-98
Richland, WA 99352
509-376-2685 (phone)
509-376-2303 (fax)
hm.cho@pnl.gov

Steven D. Conradson
Los Alamos National Laboratory
MST-8, MS G755
Los Alamos, NM 87545
505-667-9584 (phone)
505-667-8021 (fax)
conradson@lanl.gov

Research Objective

Technetium complexation with organic compounds in tank waste plays a significant role in the redox chemistry of Tc and the partitioning of Tc between the supernatant and sludge components in waste tanks. These processes need to be understood so that strategies to effectively remove Tc from high-level nuclear waste prior to waste immobilization can be developed and so that long-term consequences of Tc remaining in residual waste after sludge removal can be evaluated. Only limited data on the stability of Tc-organic complexes exists, and even less thermodynamic data on which to develop predictive models of Tc chemical behavior is available. To meet these challenges, we present a research program to study Tc-speciation in actual tank waste using state-of-the-art analytical organic chemistry, separations, and speciation techniques. On the basis of such studies, we will acquire thermodynamic data for the identified Tc-organic complexes over a wide range of chemical conditions in order to develop credible models to predict Tc speciation in tank waste and Tc behavior during waste pretreatment processing and in waste tank residuals.

Research Progress and Implications

This report summarizes work after 9 months of a 3-year study. Hanford waste tanks AN-102 and T-111 have been selected for initial analysis based on the availability of samples and previous analytical results that suggest high concentrations of Tc and organics. Samples from AN-102 will be analyzed using electrospray-mass spectroscopy to identify the Tc-organic complexes. The oxidation state of Tc in samples from T-111 will be analyzed using x-ray absorption spectroscopy (XAS) at the Stanford Synchrotron Radiation Laboratory.

Technetium in T-111 sludge is resistant to removal using leaching and washing techniques that have been successful in removing pertechnetate from high-level waste sludge in other tanks, which suggests that Tc is present in a reduced oxidation state and may be complexed with organics. A previous analysis of the organic fraction of T-111 sludge indicated that a large portion of the organic compounds is unique to this tank. Analysis of the Tc K-edge with XAS will allow determination of the oxidation state of Tc in supernatant and sludge fraction of the waste. If sufficiently high concentrations of Tc are encountered, then the complexation of Tc may be possible as well.

Procedures have been developed for running radioactive tank waste samples on the capillary electrophoresis (electrospray) mass spectrometer (CE/MS). These procedures include contacting AN-102 supernatant with ion exchange resins to remove ^{137}Cs and ^{90}Sr to reduce the radiation dose without affecting the complexation of Tc. An enclosure to contain possible radioactive contamination during analysis also has been designed. We currently are investigating analog Tc-organic compounds to study the fragmentation of these complexes in negative ion mode and

to test the performance of the system. We then will run model Tc-organic compounds prior to analyzing actual tank waste. The application of a CE/MS system to Hanford tank waste will require development of additional methods. Actual tank waste or simulated tank waste is extremely high in salt content. The high salt content tends to suppress the signal during electrospray ionization. Therefore, methods will be evaluated to remove the salts without removing any of the metal-organic complexes prior to analysis using electrospray mass spectrometry.

Planned Activities

Sludge and supernatant samples from T-111 will be analyzed using XAS at the Stanford Synchrotron Radiation Laboratory in June 2002 to determine the Tc oxidation state.

Electroactive Materials for Anion Separation – Technetium from Nitrate

(Project Number: 81912)

Principal Investigator

Timothy L. Hubler
Pacific Northwest National Laboratory
P.O. Box 999, MSIN K8-93
Richland, WA 99352
509-373-0249 (phone)
509-372-2549 (fax)
tim.hubler@pnl.gov

Co-Investigators

James McBreen
Brookhaven National Laboratory
DAS, Bldg. 480
Upton, NY 11973
631-344-4513 (phone)
631-344-4071 (fax)
jmcbreen@bnl.gov

William H. Smyrl
Corrosion Research Center
Department of Chemical Engineering
and Materials Science
University of Minnesota Minneapolis
221 Church Street SE
Minneapolis, MN 55455
612-625-0717 (phone)
612-626-7246 (fax)
smyrl001@maroon.tc.umn.edu

Scot D. Rassat
Pacific Northwest National Laboratory
P.O. Box 999, MSIN K6-28
Richland, WA 99352
509-372-1861 (phone)
509-372-1861 (fax)
scot.rassat@pnl.gov

Michael A. Lilga
Pacific Northwest National Laboratory
P.O. Box 999, MSIN K8-93
Richland, WA 99352
509-375-4354 (phone)
509-372-4732 (fax)
mike.lilga@pnl.gov

Graduate Students
Gregory Anderson
Marcia Toline Giacomini

Research Objective

The general aim of this project is to design and prepare new electroactive ion-exchange (EaIX) materials that can be used to remove the radioactive components from high-level radioactive waste (HLW) at U.S. Department of Energy (DOE) sites nationwide. The specific objective is to develop and investigate redox-active polymers, such as polyvinylferrocene (PVF), that can be used to remove pertechnetate (TcO_4^-) ion from HLW. Electroactive materials are an important class of materials for this application because they can minimize or eliminate secondary waste streams associated with HLW processing, thereby reducing the costs of environmental cleanup.

The technologies currently available for treatment and disposal of approximately 90 million gallons of HLW at the DOE Savannah River Site, Idaho National Engineering and Environmental Laboratory, and Hanford Site are neither cost-effective nor practical. Processes to separate the HLW constituents from the low-level waste (LLW) fraction are required to reduce the volume of waste that must be treated and disposed of and to reduce the cost of treatment and disposal. Use of EaIX materials, conjoined with the use of porous membranes that also are under development, can significantly reduce or eliminate secondary wastes associated with more traditional ion-exchange or solvent extraction technologies and, thus, can help improve the effectiveness and reduce the cost of DOE's waste treatment and disposal efforts.

Beyond its importance as a cost issue, separation of TcO_4^- from HLW also addresses a critical environmental issue. The most common isotope of technetium (^{99}Tc) has an extremely long half-life of 210,000 years. Rapid development of advanced methods to remove and separate this long-lived radioactive isotope is important because most of the technetium in the DOE HLW probably is in the form of TcO_4^-, which is highly mobile in soils and groundwater. This project is focused on anion separation and, in particular, the selective separation of TcO_4^- from a solution containing excess NO_3^-. The results of this research can be used to also design EaIX materials to remove other anions.

Research Progress and Implications

This report summarizes work completed in the first 40 months of a 6-year project. During the first 3 years of the project, we addressed critical issues surrounding the use of PVF as an electroactive material for selective separation of TcO_4^- from HLW. These issues were concerned with primarily 1) the generally lower molecular weight of PVF polymers that were obtained from conventional synthetic methods and 2) the inability of these polymers to withstand alkaline pH conditions.

We have been able to obtain PVF polymers with $\overline{M}_w = 1.1 \times 10^3$ kD, which is significantly higher than the 5.0×10^3 kD weights that can be obtained using conventional syntheses.

Preparation of higher molecular weight polymers is important because our studies showed that these materials would delaminate readily from electrode surfaces, especially when an oxidizing potential was reached. The delamination issue essentially has been eliminated with the new materials.

The other issue we addressed was the stability of these polymers under alkaline conditions. Ferrocene and its derivatives are generally stable in alkaline solutions, but once the metal center is oxidized to give the ferrocenium moiety, the metallocene rapidly decomposes. Metallocenes can be made stable in alkaline solution by dialkylation of the cyclopentadienyl rings so that the alkyl groups do not possess ionizable protons on the carbon directly attached to the metallocene ring. Most of our studies have focused on the preparation of *tert*-butyl derivatives of ferrocene. These functionalized polymers exhibit enhanced resistance to decomposition under alkaline conditions as evidenced in their cyclic voltammograms obtained in 0.5-M NaOH solution. An additional benefit is probably conferred on selectivity of the polymers for TcO_4^- as the greater hydrophobicity around the alkylated ferrocene center favors interaction with anions that have lower hydration energies.

Characterization of the ReO_4^--doped PVF films by x-ray absorption near edge structure (XANES) may indicate that ReO_4^- interacts with the Fe centers in the PVF polymers, as there appears to be perturbation of the ferrocenium molecular orbitals.

Additional studies initiated in the past 12 months have focused on the use of polymers to prepare electroactive membranes and on the preparation of new materials. For ion separation, membrane-based separation processes are more desirable than ion-exchange processes for several reasons: 1) no periodic downtime occurs (e.g., the separation medium need not be regenerated), 2) no cross-contamination occurs (i.e., entrained fluid is always in an ion-exchange bed), and 3) less secondary waste is generated (i.e., no rinsing or elution is required). Currently, however, one typically must rely on ion-exchange processes when high selectivity is required. Efficient separations of ions with the same charge, for example, cannot be achieved using conventional membranes. An electroactive membrane prepared as carbon nanotubes coated with PVF has been demonstrated to selectively transport monovalent anions across the membrane. A solution of $NaNO_3$ and Na_2SO_4 was shown to selectively transport the NO_3^- ion across the electroactive membrane. Preparation of iron phenanthroline complexes that are stable under extreme pH conditions (both acidic and alkaline) has been initiated.

Planned Activities

During summer 2002, we will undertake further x-ray absorption spectroscopy studies at Brookhaven National Laboratory on TcO_4^- doped PVF films to development an improved understanding of the interactions between the polymer and TcO_4^-. Additionally, we will study

the selectivity and uptake of TcO_4^- into these polymers and will undertake further development of the electroactive membrane concept. One primary goal here is to covalently attach the polymers to the carbon nanotubes by November 2002. Also, to speed discovery of a material that is stable under waste tank processing conditions, we will be investigating other electroactive materials, such as the iron phenanthroline complexes.

Information Access

Invited presentations

Hubler TL. 2001. Separating and Sensing the Pertechnetate Ion: Use of Electroactive Vinylferrocene-Based Polymers for Separations and Smart Materials for Spectroelectrochemical Detection of TcO_4^-. 9th International Symposium on Macromolecule Metal Complexes, Brooklyn, New York, August 2001.

Hubler TL. 2001. Separating and Sensing the Pertechnetate Ion: Use of Electroactive Vinylferrocene-Based Polymers and Smart Materials for Spectroelectrochemical Detection of TcO_4^-. 56th Northwest Regional Meeting of the American Chemical Society, Seattle, Washington, June 2001.

Publication

Balasubramanian M, HS Giacomini, HS Lee, J McBreen, and JH Sukamto. 2002. X-Ray Absorption Studies of Poly(vinylferrocene) Polymers for Anion Separation. Accepted for publication, *J. Electrochem. Soc.* 2002.

Millimeter-Wave Measurements of High-Level and Low-Level Activity Glass Melts

(Project Number: 81897)

Principal Investigators

Dr. Paul P. Woskov
Massachusetts Institute of Technology
Plasma Science and Fusion Center
NW16-110
167 Albany Street
Cambridge, MA 02139
617-253-8648 (phone)
617-253-0700 (fax)
ppw@psfc.mit.edu

Dr. S. K. Sundaram
Pacific Northwest National Laboratory
P.O. Box 999, MSIN K6-24
Richland, WA 999352
509-373-6666 (phone)
509-376-3108 (fax)
sk.sundaram@pnl.gov

Dr. William E. Daniel, Jr.
Westinghouse Savannah River Company
Building 999-W
Aiken, SC 29808
803-819-8463 (phone)
803-819-8416 (fax)
gene.daniel@srs.gov

Research Objective

The primary objective of the current research is to develop on-line sensors for characterizing molten glass in high-level and low-activity waste glass melters using millimeter-wave technology. Existing and planned waste glass melters lack sophisticated diagnostics due to the hot, corrosive, and radioactive melter environments. Without process control diagnostics, the Defense Waste Processing Facility (DWPF) and current planned melters (i.e., Hanford) operate by a feed-forward process control scheme that relies on predictive models with large uncertainties. This scheme severely limits production throughput and waste loading. In addition, operations at the DWPF have shown susceptibility to anomalies such as foaming and combustion gas buildup, which can seriously disrupt operations. Future waste chemistries will be even more challenging. The scientific goals of this project are to develop new reliable on-line monitoring capabilities for important glass process parameters such as temperature profiles, emissivity, density, viscosity, and other characteristics using the unique advantages of millimeter-wave electromagnetic radiation. Once successfully developed and implemented significant cost savings would be realized in melter operations by faster production throughput, reduced storage volumes (through higher waste loading), and reduced risks (prevention of anomalies).

Research Progress and Implications

As of the end of the first year of the project renewal period, laboratory experiments and analytical modeling advances have been made in the millimeter-wave on-line monitoring technology. These experiments and modeling include 1) acquisition of additional millimeter-wave viscosity data on two more glasses (TV and E glasses), 2) acquisition of millimeter-wave emissivity data on new refractory materials (K3, CrO_2, AZS), 3) advances in the analysis and modeling of the viscosity data, 4) formalization of the thermal return reflection method for temperature and emissivity measurement, 5) a research paper written on the thermal return refection (TRR) method, 6) initiation of design and fabrication of a new compact millimeter-wave receiver for field tests, and 7) start of planning for a viscosity field test.

The experimental activities were carried out at a wavelength of 2.19 mm (137 GHz) with a heterodyne receiver adapted for both passive and active probing measurements at the Massachusetts Institute of Technology millimeter-wave furnace test stand. A refractory mullite $(3Al_2O_3 \cdot 2SiO_2)$ waveguide was lowered vertically through a hole in the top of the furnace, normal to the monitored surface and into near contact or immersion into the melt. The mullite waveguide diameter was larger (1-5/8 in.) for the emissivity and temperature measurements to lower waveguides transmission losses, with a smaller diameter (1-1/8 in.) for viscosity measurements to reduce the speed of glass flow at viscosities < 100 Poise to be within the response of the electronics data acquisition system. Each sample test requires approximately a

24-hour period to warm up, take the measurements, and then cool down to make changes. Many data files have been acquired and are in the process of being analyzed.

In parallel with the data analysis, the analytical modeling has been advanced to better interpret the results. A significant advance this year has been to formalize the TRR method for emissivity and temperature measurements. The TRR method is implemented by a beamsplitter that divides the thermal signal from the viewed sample into two components, one going to the receiver and the other to a side mirror. The side mirror can be removed or blocked. When the side mirror is blocked, the thermal measurement is like a conventional radiometric measurement. When the side mirror is unblocked, the part of the thermal signal transmitted through the beamsplitter is redirected at the sample. If the sample is not an ideal blackbody, its reflection will cause an increase in the receiver signal that is dependent on the magnitude of the sample reflectivity. This in turn is directly related to the emissivity. The implications of this are very important for non-contact thermal analysis of materials at high temperature. Currently there are no good non-contact methods for such analysis.

Another notable development has been the design of a compact millimeter-wave receiver using a subharmonic mixer. The use of a subharmonic mixer makes the receiver system more compact and reduces millimeter-wave electronics costs. The plan is to make the receiver compact enough so that it can be attached to the end of the waveguide and move with it as the waveguide is inserted or retracted from the melter. In this way, the receiver-to-waveguide alignment would remain ridged without the need for a more complicated optics arrangement. Three millimeter-wave vendors were contacted, and several designs for the new receiver were considered before the decision to go with the subharmonic mixer was made.

Planned Activities

The development of the millimeter-wave on-line glass process monitoring technology will continue. More high-temperature millimeter-wave data of glasses and refractory materials will be acquired and analyzed. In particular, the experiments will be partially focused on preparing for a viscosity monitoring field test. A glass frit representative of the field test material will be first tested in the laboratory to determine optimum instrumentation parameters such as waveguide diameter. The refractory material measurements will also be evaluated toward identifying more corrosion resistant materials for millimeter-wave waveguide fabrication. The analytical model for analysis of the data will also continue to evolve. An experimental determination of the instrumentation optical coupling constants will be developed. The compact millimeter-wave receiver system will also be fabricated to facilitate the field test.

Information Access

Woskov P, JS Machuzak, P Thomas, SK Sundaram, and WE Daniel. 2000. *Millimeter-Wave Monitoring of Nuclear Waste- An Overview*. MIT PSFC Report # JA-02-1, www.psfc.mit.edu/library/02ja/02JA001/02JA00_abs.html, 2002.

Sundaram SK, WE Daniel, P Woskov, and J Machuzak. 2001. Cold Cap Monitoring Using Millimeter-Wave Technology. In *Proceedings of the American Ceramic Society*, April 2001 meeting, Indianapolis, Indiana.

Radiation Effects in Nuclear Waste Materials

(Project Number: 73750)

Principal Investigator

William J. Weber
Pacific Northwest National Laboratory
P.O. Box 999, MSIN K8-93
Richland, WA 99352
509-376-3644 (phone)
509-376-5106 (fax)
bill.weber@pnl.gov

Co-Investigators

Lumin Wang
Nuclear Engineering & Radiological
Sciences
The University of Michigan
2355 Bonisteel Boulevard
Ann Arbor, MI 48109-2104
734-647-8530 (phone)
lmwang@umich.edu

Nancy J. Hess
Pacific Northwest National Laboratory
P.O. Box 999, MSIN P7-50
Richland, WA 99352
509-376-9808 (phone)
509-372-1632 (fax)
nancy.hess@pnl.gov

Jonathan P. Icenhower
Pacific Northwest National Laboratory
P.O. Box 999, MSIN K6-81
Richland, WA 99352
509-372-0078 (phone)
509-376-2210 (fax)
jonathan.icenhower@pnl.gov

Suntharampillai (Theva) Thevuthasan
Pacific Northwest National Laboratory
P.O. Box 999, MSIN K8-93
Richland, WA 99352
509-376-1375 (phone)
509-376-5106 (fax)
theva@pnl.gov

Research Objective

The objective of this project is to develop a fundamental understanding of radiation effects in glasses and ceramics, as well as the influence of solid-state radiation effects on aqueous dissolution kinetics. This study will provide the underpinning science to develop improved glass and ceramic waste forms for the immobilization and disposition of high-level tank waste, excess plutonium, plutonium residues and scrap, other actinides, and other nuclear waste streams. Furthermore, this study will develop predictive models for the performance of nuclear waste forms and stabilized nuclear materials. The research focuses on the effects of alpha and beta decay on defect production, defect interactions, diffusion, solid-state phase transformations, and dissolution kinetics. Plutonium incorporation, ion-beam irradiation, and electron-beam irradiation are used to simulate the effects of alpha decay and beta decay on relevant glasses and ceramics in experimental studies. Computer simulation methods are used to provide an atomic-level interpretation of experimental data and continuum-level modeling.

Research Progress and Implications

This report summarizes progress after 15 months of a 3-year project. The co-investigator at the University of Michigan did not receive funding until September 2001; thus, this report summarizes progress after only 7 months for those activities.

Computer Simulation Efforts

Computer simulation studies of ionization effects in glasses are continuing to wrap up the studies initiated under our previous EMSP project. Computer simulations of radiation damage processes in ceramics are continuing. An initial collaborative study on threshold displacement processes in zircon has been completed. This study has illustrated for the first time the importance of heterogeneous displacement sequences on damage production processes in complex ceramics. This collaborative effort has expanded to include a group of researchers from the French Atomic Energy Commission (Commissariat a l'Energie Atomique, or CEA).

Alpha-Decay Effects in Glasses and Ceramics

Because some dissolution measurements were performed on the Pu-doped glasses immediately after preparation in 1982, the same dissolution measurements are being performed on these glasses in their current radiation-damaged state for comparison. In addition, a comprehensive set of dissolution kinetics experiments is in progress on the ^{239}Pu-doped glass (lightly damaged) and the ^{238}Pu-doped glass (highly damaged) using the single-pass flow-through (SPFT) test method to measure the forward reaction rate of these glasses. All experiments are being run at 90°C in

pH = 2 solutions using the SPFT apparatus developed at Pacific Northwest National Laboratory (PNNL). These tests still are ongoing, and data will not be available until later this year.

Simulation of Radiation Effects Using Ion Beams

Pyrochlores of the type $Gd_2(Ti_{1-x}Zr_x)_2O_7$ exhibit an increase in resistance to radiation-induced amorphization with increasing x (Zr content). Detailed studies of the effects of composition and radiation damage on the dissolution behavior in this pyrochlore system are now in progress. The stability of the $A_2B_2O_7$ pyrochlores is governed by the ionic radii ratio of the A and B site cations (r_A/r_B). In collaboration with other scientists at Lawrence Berkeley National Laboratory (LBNL), a detailed characterization is being performed of $Gd_2(Ti_{1-x}Zr_x)_2O_7$ pyrochlores, with x = 0, 0.25, 0.5, 0.75, and 1.0, whose ionic radii ratios span the complete pyrochlore stability field from r_A/r_B = 1.74 (x = 0) to r_A/r_B = 1.46 (x = 1), by near-edge x-ray absorption fine-structure spectroscopy at the titanium L and oxygen K-edges. The results indicate that Ti is in a distorted octahedral environment (like TiO_2) for x = 0, and the deviation from the regular octahedral symmetry decreases for increasing x. For x ≥ 0.75, the Ti occupies a regular octahedral site, as in $SrTiO_3$. Likewise, the results support that Zr systematically replaces Ti with increasing x and, furthermore, the coordination number of Zr increases with increasing x.

To assess the aqueous dissolution behavior of the $Gd_2(Ti_{1-x}Zr_x)_2O_7$ system, SPFT testing has been conducted on monolithic specimens. As in the case of the Pu-doped glasses, the tests were run at 90°C in pH = 2 solutions using the SPFT apparatus developed at PNNL. In this system, the goal is to quantify the difference in dissolution rate as a function of composition. As noted above, the compositional variation of interest is the exchange of Zr^{4+} for Ti^{4+}, which is known to induce disorder in the materials. At the extreme end of the exchange scale, pure $Gd_2Zr_2O_7$ is manifested as the disordered fluorite structure, rather than the pyrochlore structure, due to the processing procedures, because pyrochlore requires long-term annealing below the order-disorder transformation. Fully ordered samples with the pyrochlore structure across the composition also are being prepared for testing. Preliminary data for the as-processed samples show that, as the extent of Zr^{4+} exchange for Ti^{4+} increases, the dissolution rate decreases. The data indicate that, as x increases from 0 to 0.75, the dissolution rate decreases systematically by a factor of about 30. However, in the case of the end-member $Gd_2Zr_2O_7$ (x = 1.0) that crystallizes into the defect fluorite structure during processing, the dissolution rate is higher than that of the pyrochlore $Gd_2Ti_2O_7$ end-member. These results suggest that the disordered fluorite structure has a higher dissolution rate than the ordered pyrochlore state. Preliminary data for the highly ordered pyrochlore specimens indicate the dissolution rates are substantially lower than their as-prepared counterparts. The results reveal that the dissolution kinetics of these samples depends on both chemical composition and the degree of disorder within the lattice. Although Zr-rich pyrochlore samples are more disordered than their Ti-rich counterparts, addition of Zr clearly decreases the dissolution rates.

In collaboration with researchers at the Australian Nuclear Science and Technology Organization (ANSTO), several complex zirconate and titanate pyroclores were irradiated, using an irradiation protocol developed under this project, to produce a stable radiation damage state that simulates the state expected from alpha decay over long time periods at ambient temperature. Glancing angle x-ray diffraction (XRD) confirms that the zirconate compounds are more radiation-resistant that the titanate compounds, which readily transform to an amorphous state. The samples are undergoing additional testing by the ANSTO collaborators. Additional samples have been prepared for irradiation as part of this collaboration with the ANSTO group.

Using the same irradiation protocol, samples of $Ca_2Nd_8(SiO_4)_6O_2$ (apatite structure) have been irradiated with 2-MeV Au ions to produce a fully amorphous state to a depth of about 600 nm, which has been confirmed by cross-sectional transmission electron microscopy (TEM). These samples are currently undergoing dissolution testing using the SPFT test method as described above, and detailed characterization of the amorphous state is being performed. Additional studies are planned to investigate the temperature dependence. The results of these studies will be compared to previous results due to alpha-decay damage in samples of this material containing ^{244}Cm, which should assist in validation of the irradiation protocol.

Based on the results of systematic experimental studies using short-lived actinides, ion-beam irradiation, and new models of radiation damage processes in ceramics, predictive models of radiation-damage behavior due to alpha decay are emerging. Based on ion-beam data, one of the parameters that can be predicted is the critical temperature, T_c, below which radiation-induced amorphization will occur for any given alpha decay rate (actinide content). This is illustrated in Table 1 for several materials of interest.

Table 1. Critical Temperature, Tc, for Ceramics Under Different Damage Rates

Irradiation Conditions	Dose Rate (dpa/s)	$Gd_2Ti_2O_7$ (K)	$ZrSiO_4$ (K)	$SrTiO_3$ (K)	$CaTiO_3$ (K)
Ion Beam	3.3×10^{-3}	980	975	395	420
10 wt% ^{239}Pu	8.5×10^{-12}	580	578	234	249

Simulation of Radiation Effects Using Electron Beams

We attempted to assess the effects of beta decay using a gamma irradiation facility under our previous project; however, the original 3-year time period proved insufficient to achieve the necessary dose levels. At the end of the project period, sample doses equivalent to only 25 years of storage were achieved in the gamma irradiation facility. Because of the interruption of funding, the irradiation facility no longer is available, and these experiments have been

terminated The only method now available to evaluate the effects of beta decay on the performance of nuclear waste glasses is electron-beam irradiation. This requires establishing a suitable and reliable radiation protocol for glasses, similar to that developed for radiation-induced amorphization in ceramics. The work being carried out at the University of Michigan under this project is focused on understanding radiation-damage processes in complex glasses and developing the necessary protocols to perform accelerated radiation effects testing.

Initial studies at the University of Michigan have focused on a series of Na-borosilicate (NBS) glasses developed under our previous project. The composition of these glasses is given in Table 2.

Table 2. Chemical Composition of NBS Glasses

Oxide	NBS-1 (wt%)	NBS-2 (wt%)	NBS-3 (wt%)
B_2O_3	17.72	17.78	17.86
Fe_2O_3	0	4.99	0
FeO	0	0	4.61
Na_2O	16.67	15.83	15.90
SiO_2	64.61	61.39	61.63

The preliminary results, performed by a new postdoctoral fellow at the University of Michigan, indicate a significant mobility of Na under irradiation with 200-keV electrons at room temperature, which is consistent with many previous observations. There is a rapid decrease in the Na concentration in the area under irradiation, and the addition of the FeO or Fe_2O_3 to the glass appears to hinder the mobility of the Na. Ongoing studies will investigate the effects of dose rate on this behavior and on the oxidation state of the Fe.

Planned Activities

Computer Simulations

The multi-institutional collaborative efforts on damage production processes and stable damage states in complex ceramics will continue, and improved interatomic potentials will be used in molecular dynamic simulations of high-energy collision processes in an effort to understand the nature of radiation resistance in some of these complex ceramics.

The studies of electronic excitations in glasses will be brought to closure.

Alpha-Decay Effects in Glasses and Ceramics

It is critical to determine the local changes in structure of the boron in the three Pu-doped glasses that have been previously studied under this project, as this information may be important to understanding the changes in dissolution kinetics. These measurements will be carried out using LBNL's user facility, the Advanced Light Source. The presence of any molecular oxygen that may have been produced in these glasses because of radiation-induced decomposition will be probed using Raman and infrared photoluminescence.

The dissolution tests on the Pu-doped glasses are expected to be completed by the end of the year. An annealing study of the amorphous ^{238}Pu-zircon will be carried out at 600, 700, and 800°C, and x-ray absorption spectroscopy (XAS) measurements (as used under our previous EMSP project) will be performed to understand the early stages of annealing. This recovery process is important to developing and validating long-term predictive models. In addition, Raman spectroscopy will be used to measure the decrease in width of the antisymmetric stretching vibrational band of the SiO_4 tetrahedra in the Pu-zircons as a function of annealing temperature.

After these tests are completed, this project will cease all work on actinide-containing materials. Project funding will support related waste disposal and laboratory clean-up efforts.

Electron and Ion Irradiation Studies

The University of Michigan will continue to lead studies on using electron beams and light-ion (H^+, He^+) beams to study the effects of ionization (from beta and alpha decay) on the structure and stability of complex glasses. Heavy-ion irradiation also will be used to simulate the radiation effects induced by alpha-recoil particles. In situ TEM study during the ion-beam irradiation will be performed using the IVEM-Tandem facility at Argonne National Laboratory. More detailed analysis on ionizing radiation effects in these glasses will be performed with more advanced TEM techniques including energy dispersive spectrometer (EDS) elemental mapping and electron energy loss spectroscopy (EELS), as well as energy filtered TEM and electron diffraction. The elemental mapping should reveal any radiation-induced chemical segregation, and energy-filtered electron diffraction may reveal any small change in the radial distribution function (local atomic arrangements) in the irradiated area.

Ion-irradiation experiments at PNNL will continue to employ heavy ions in studies of irradiation effects in ceramics to further validate irradiation protocols that simulate alpha-decay behavior in ceramics, such as the continuing work on the apatite and proposed work on zirconolite. In addition, the effects of radiation damage on the dissolution behavior of the $Gd_2(Ti_{1-x}Zr_x)_2O_7$ system will be completed over the next year. Small-angle XRD and cross-sectional TEM will be performed on these samples. These studies will provide important data on ceramics that are

relevant to predicting the performance of ceramics for special waste streams and nuclear materials, such as the pyrochlores and silicotitanates.

Information Access

Weber WJ. 2000. *Radiation Effects in Nuclear Waste Materials*. Final Report, EMSP Project Number 54672, (http://emsp.em.doe.gov/products.htm).

Begg BD, NJ Hess, WJ Weber, R Devanathan, JP Icenhower, S Thevuthasan, and BP McGrail. 2001. Heavy-Ion Irradiation Effects on Structures and Acid Dissolution of Pyrochlores. *Journal of Nuclear Materials* 288(2-3):208-216.

Zhao D, L Li, WJ Weber, and RC Ewing. 2001. Gadolinium Borosilicate Glass-Bonded Gd-Silicate Apatite: A Glass-Ceramic Nuclear Waste Form for Actinides. In *Scientific Basis for Nuclear Waste Management XXIV*, eds. KP Hart and GR Lumpkin, Mater. Res. Soc. Symp. Proc. 663, pp. 199-206. Materials Research Society, Warrendale, Pennsylvania.

Song J, LR Corrales, G Kresse, and H Jónsson. 2001. Migration of Oxygen Vacancies in α–Quartz: The Effects of Excitons and Electron Holes. *Physical Review* B 64:134102.

Park B, WJ Weber, and LR Corrales. 2001. Molecular Dynamics Simulation Study of Threshold Displacements and Defect Formation in Zircon. *Physical Review* B 64:174108, 1-16.

Hess NJ, BD Begg, SD Conradson, DE McCready, PL Gassman, and WJ Weber. 2002. Spectroscopic Investigations of the Structural Phase Transitions in $Gd_2(Ti_{1-y}Zr_y)_2O_7$ Pyrochlores. *J. Phys. Chem.* B 106:4663-4677.

Stewart MWA, BD Begg, ER Vance, K Finnie, H Li, GR Lumpkin, KL Smith, WJ Weber, and S Thevuthasan. 2002. The Replacement of Titanium by Zirconium in Ceramics for Plutonium Immobilization. In *Scientific Basis for Nuclear Waste Management XXV*, eds. BP McGrail and GA Cragnolino, Mater. Res. Soc. Symp. Proc.713, JJ 2.5, pp. 1-8. Materials Research Society, Warrendale, Pennsylvania.

Weber WJ and RC Ewing. 2002. Radiation Effects in Crystalline Oxide Host Phases for the Immobilization of Actinides. In *Scientific Basis for Nuclear Waste Management XXV*, eds. BP McGrail and GA Cragnolino, Mater. Res. Soc. Symp. Proc. 713, JJ3.1, pp. 1-12, Materials Research Society, Warrendale, Pennsylvania.

Icenhower JP, BP McGrail, WJ Weber, BD Begg, NJ Hess, EA Rodriguez, JL Steele, CF Brown, and MJ O'Hara. 2002. Dissolution of $A_2Ti_2O_7$ ($A = Y^{3+}$, Gd^{3+}, or Lu^{3+}) Pyrochlore by Experiment at pH = 2, T = 90°C: Evidence for Solubility Control Using a Linear Free Energy Model. In *Scientific Basis for Nuclear Waste Management XXV*, eds. BP McGrail and GA Cragnolino, Mater. Res. Soc. Symp. Proc. 713, JJ6.2, pp. 1-7. Materials Research Society, Warrendale, Pennsylvania.

William J. Weber (http://emslbios.pnl.gov/id/weber_wj)

2.0 Decontamination and Decommissioning

Microbially Promoted Solubilization of Steel Corrosion Products and Fate of Associated Actinides

(Project Number: 64931)

Principal Investigator

Yuri A. Gorby
Pacific Northwest National Laboratory
P.O. Box 999, MSIN P7-50
Richland, WA 99352
509-373-6177 (phone)
509-376-1321 (fax)
yuri.gorby@pnl.gov

Co-Investigators

Gill G. Geesey
Montana State University
Center for Biofilm Engineering
409 Cobleigh Hall
Bozeman, MT 59717
406-994-4770 (phone)
gill_g@erc.montana.edu

Frank Caccavo, Jr.
Whitworth College
Department of Biology
Mail Stop 3902
300 W. Hawthorne Road
Spokane, WA 99251
509-777-4576 (phone)
fcaccavo@whitworth.edu

James K. Fredrickson
Pacific Northwest National Laboratory
P.O. Box 999, MSIN P7-50
Richland, WA 99352
509-373-6177 (phone)
509-376-1321 (fax)
jim.fredrickson@pnl.gov

Research Objective

The U.S. Department of Energy (DOE) statements of need call for "biological and physical chemical parameters for effective decontamination of metal surfaces using environmentally benign aqueous-based biopolymer solutions and microbial processes with potential for decontaminating corroding metal surfaces." Improved understanding of the fundamental processes of microbial reductive dissolution of iron oxide scale on corroding carbon steel will support assessment and potential application of an environmentally benign and cost-effective strategy for in situ decontamination of structural metal surfaces and piping.

This research is designed to develop a safe and effective biological approach for decontaminating mild and stainless steels that were used in the production, transport, and storage of radioactive materials.

Research Progress and Implications

This report summarizes research progress made during the 3-year tenure for this project. An extension with minimal carryover funds was requested and granted to complete and submit manuscripts for publication. During this research, we have

- Demonstrated that Fe(III)-reducing bacteria reduce Pu(IV) (insoluble) to Pu(III) (soluble).

- Confirmed that the bacteria sorb and accumulate trivalent cations, such as Pu(III).

- Demonstrated that bacteria attached to oxide surfaces are very difficult to remove. Concluded that recovery of bacteria with sorbed Pu(III) would be impractical.

- Demonstrated that Fe(II) and reduced quinone-like compounds, which are both products of anaerobic respiration, can reduce chemically reduce solid Pu(IV) to dissolved Pu(III).

- *Conceptualized a bead-based system that effectively removes Pu from iron oxides and accumulates Pu(III) in beads of sodium alginate that can be easily separated from the bulk aqueous phase.*

Dissimilatory iron-reducing bacteria enzymatically reduce and dissolve iron oxides, which are common components of corrosion films, and release soluble species of plutonium, Pu(III). Consistent with our previous hypothesis, cell surfaces sorb Pu(III) and remove it from the bulk aqueous phase. However, we incorrectly hypothesized that bacteria with sorbed actinides could be easily detached and recovered from the surfaces that they had colonized and enzymatically altered. In fact, we have demonstrated that although cells do naturally detach from oxide surfaces during their growth cycle, they leave behind negatively charged reactive portions of

their outer surface that are strong sorbants for cations. Without a means for recovering both intact bacteria, their subcellular products and associated contaminants, the use of iron-reducing bacteria for decontaminating corroded steel surfaces would not be feasible. Hence, we have targeted an approach that avoids direct contact and attachment of cells to the corrosion films but allows for reduction, dissolution, and sorption of corrosion products and associated actinides.

Description of Bead-Based Treatment

Iron reducing bacteria are encapsulated in small beads of sodium alginate. Encapsulation prevents direct contact between the bacteria and the contaminated oxide surface. Anthraquinone disulfonate (AQDS) is used as a dissolved electron shuttle to carry electrons from the bacteria to Fe(III) and Pu(IV) on the corrosion film. AQDS reduces Fe(III) to Fe(II) and Pu(IV) to Pu(III). The reduced forms of these metals are very soluble and partition to the aqueous phase. The bacterial surface and the sodium alginate sorb and accumulate Fe(II) and Pu(III). The beads, which now contain most of the Pu(III), can be easily separated from the bulk aqueous phase. The benign process requires no hazardous chemicals or extreme pH conditions.
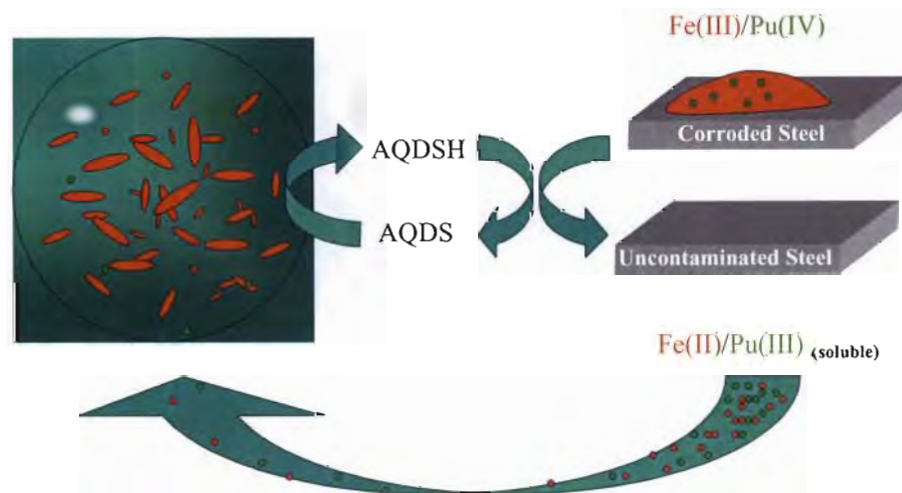
Figure 1. This illustrates a conceptual model of a bead-based system for decontaminating corroded steels. Metal-reducing bacteria are enrobed in porous alginate beads. Oxidized anthraquinone disulfonate, AQDS, which will serve as a dissolved electron shuttle between immobilized cells and elements in the corrosion film, diffuses into the beads and is enzymatically reduced by the bacteria. The reduced AQDSH diffuses out of the bead and chemically reduces and dissolves Fe(III) and Pu(IV) in the corrosion film. Soluble Fe(II) and Pu(III) sorb to cationic exchange sites within the alginate beads. The beads and accumulated actinides can then be easily separated from the bulk aqueous phase and the uncontaminated steel.

2.3

Carryover funds were insufficient to evaluate the bead-based system for removing Pu from contaminated corrosion. However, the system was tested for its ability to remove dissolved radionuclides (uranium and technetium) from aqueous media. Figure 2 illustrates that iron-reducing bacteria embedded in a porous alginate matrix reduce dissolved Tc(VII) (as pertechnetate ion) to poorly soluble TcO$_2$. Vials 1 and 2 contain alginate beads that are blackened by TcO$_2$ precipitates. Vial 3 served as a control and contains beads with no cells. All of the Tc(VII) remained in the aqueous phase. Vials containing dissolved U(VI) in lieu of Tc(VII) yielded similar results. These results clearly demonstrate the potential for removing dissolved radionuclides from solution using an environmentally benign bead-based approach.
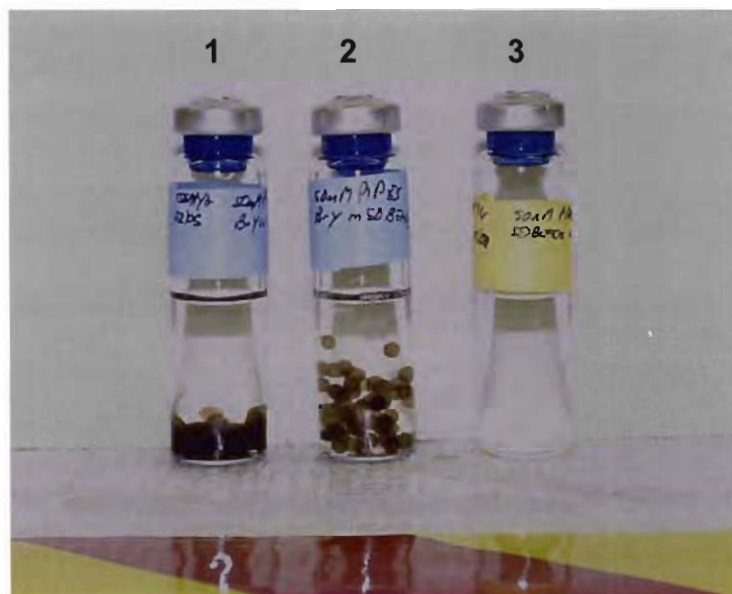
Figure 2.   Vials demonstrating the ability of iron-reducing bacteria in alginate beads to remove dissolved Tc(VII) from solution. 100 μM of Tc(VII) were reduced and precipitated within the beads in vials 1 and 2. Vial 3 served as a negative control and lacked bacterial cells. Beads without bacteria are difficult to see because they contain none of the dark Tc(IV) precipitate.

Information Access

Rai D, YA Gorby, JK Fredrickson, DA Moore, and M Yui. 2002. Reductive Dissolution of PuO$_2$(am): The Effect of Fe(II) and Hydroquinone. *J. Sol. Chem.* (in press).

Gorby YA, J Mclean, A Dohnalkova, A Korenevsky, K Rosso, E Vinogradov, and TJ Beveridge. 2002. Membrane vesicles form the dissimilatory iron reducing bacterium Shewanella putrefaciens strain CN32. *FEMS Microbial. Lett.* (in review).

Das A and F Caccavo, Jr. 2001. Adhesion of the dissimilatory Fe(III) - Reducing bacterium Shewanella alga BrY to crystalline Fe(III) oxides. *Curr. Microbiol.* 42:151-154

Caccavo F and A Das. 2002. Adhesion of Dissimilatory Fe(III)-Reducing Bacteria to Fe(III) Minerals. *Geomicrobiol. J.* 19:161-177.

Das A and F Caccavo, Jr. 2000. Dissimilatory Fe(III) oxide reduction by Shewanella alga BrY requires adhesion. *Curr. Microbiol.* 40:344-347.

Contaminant-Organic Complexes: Their Structure and Energetics in Surface Decontamination Processes

(Project Number: 82773)

Principal Investigator

Calvin C. Ainsworth
Pacific Northwest National Laboratory
P.O. Box 999, MSIN K3-61
Richland, Washington 99352
509-375-2670 (phone)
509-375-6954 (fax)
calvin.ainsworth@pnl.gov

Co-Investigators

Benjamin P. Hay
Pacific Northwest National Laboratory
P.O. Box 999, MSIN K1-83
Richland, Washington 99352
509-372-6239 (phone)
509-375-6631 (fax)
benjamin.hay@pnl.gov

Samuel J. Traina
Ohio State University
School of Natural Resources
2021 Coffey Road
Columbus, OH 43210
614-292-9037 (phone)
traina.1@osu.edu

Satish C. B. Myneni
Princeton University
Department of Geosciences
151 Guyot Hall
Princeton, NJ 08544
609-258-5848 (phone)
smyneni@princeton.edu

Research Objective

The current debate over possible decontamination processes for U.S. Department of Energy (DOE) facilities is centered on disparate decontamination problems, but the key contaminants (uranium [U], plutonium [Pu], and neptunium [Np]) are universally important. There is no single decontamination technique or agent for all metal surfaces and contaminants with which DOE is faced. However, more innovative agents used alone or in conjunction with traditional processes can increase the potential to reclaim for future use some of these valuable resources or, at the least, decontaminate the metal surfaces to allow disposal as nonradioactive, nonhazardous material. This debate underscores several important issues: 1) regardless of the decontamination scenario, metal (Fe, U, Pu, Np) oxide film removal from the surface is central to decontamination; and 2) simultaneous oxide dissolution and sequestration of actinide contaminants against re-adsorption to a clean metal surface will influence the efficacy of a process or agent and its cost.

This renewal project is a logical extension of our previous work and will build strongly upon its findings to address the above issues. Current research will extend the scientific understanding of powerful, microbially produced chelates (siderophores) and newly developed information resulting from a fiscal year 1998 Environmental Management Science Program (EMSP) project by further investigating the use of siderophores and siderophore-like designed chelates as decontamination and sequestering agents. Investigations focus on critical actinide contaminants (i.e., U, Pu, Np), and catecholamide siderophores. Our scientific theme is evaluation of siderophores as complexants for tetravalent actinides sorbed to Fe oxide surfaces and dissolution of actinide solids.

The continued research integrates 1) studies of macroscopic dissolution/desorption of common actinide (IV) (Th, U, Pu, Np) solids and species sorbed to and incorporated into Fe oxides, 2) molecular spectroscopy (Fourier transform infrared [FTIR], Raman, x-ray absorption spectroscopy [XAS]) to probe the structure and bonding of contaminants, siderophores and their functional moieties, and how these change with the chemical environment, and 3) molecular mechanics and electronic structure calculations to design model siderophore compounds to test and extend the MM3 model. Our goals are 1) to develop the fundamental knowledge necessary to relate the energetics of contaminant and Fe oxide dissolution, contaminant desorption and the structure/reactivity of siderophores, and 2) to develop the information necessary to tailor catecholamide-type siderophore structure and properties to DOE's disparate metal surface decontamination needs.

Research progress from all three participating institutions is presented to give a complete overview of ongoing efforts. These are

- Pacific Northwest National Laboratory (PNNL) efforts in the areas of Fe oxide dissolution, desorption of surface sorbed contaminants on Fe oxide surfaces (primarily Th), and MM3 modeling of siderophore structures

- Ohio State University (OSU) work in the area of dissolution of substituted Fe oxides and Cr oxides, and the desorption of Eu from these surfaces

- Princeton University's efforts in spectroscopy of Fe oxide surface sorbed siderophore structure.

Research Progress and Implications

Pacific Northwest National Laboratory

Dissolution studies to date have concentrated on the hydroxamic acid-type ligands with one, two and three hydroxamate functional groups; acetohydroxamate, routotrillic acid, and desferrioxamine B (DFB). Batch-type pH-stat investigations have shown dissolution rates of iron oxides (geothite, hematite, and magnetite) increase by more than an order of magnitude as the number of functional groups per molecule increase (i.e., acetohydroxamate, routotrillic acid, and DFB) even though the total concentration of hydroxamic acid groups remains constant. Unlike oxide dissolution in the presence of ethylenediaminetetraactic acid (EDTA), the Fe oxide dissolution rate appears to decrease linearly as pH is increased from 4.5 to 9.0. This suggests that, unlike EDTA, there is limited binuclear adsorption of the ligand, or readsorption of the dissolved Fe-siderophore at low pH when the surface is positively charged. In addition, these results imply that siderophores, in general, will easily and quickly dissolve Fe oxide mineral surfaces under less harsh conditions and with less waste.

Thorium is a tetravalent ion that is a good analog to the tetravalent actinides U(IV), Pu(IV), or Np(IV); its solubility in 0.1 M $NaNO_3$ is approximately 5 x 10^{-3} M to 5.5 x 10^5 M from pH 3 to 5, respectively. Upon precipitation, it forms an amorphous ThO_2, and at higher temperatures or long aging times, formation of a crystalline ThO_2 is observed. Th(IV) studies were performed at 25°C, Th = [1 x 10^{-5} M], ph 4.0, 1g/L hematite (a major corrosion product). Th(IV) adsorption to hematite, for the conditions utilized, increased rapidly from 0% sorbed to 100% sorbed over the pH range 3 to 4.5. After adsorption, two different hydroxamates (routotrillic acid, and DFB) were utilized to desorb the Th and dissolve hematite. The rates of desorption and dissolution were studied as a function of time, hydroxamates type, and aging of the Th-hematite surface complex. Results to date from theses studies show that sorbed Th is fully solubilized by both siderophores. However, the routotrillic acid exhibits a faster rate of solubilization than the

trihydroxamate, DFB. In addition, it is clear from that the rate of Fe solubilization is slowed by the presence of Th. The Fe and Th release curves show two distinct regions that exhibit different solubilization rates. During the early period of solubilization (about 180 min), Th release is faster than the sorbent Fe but, as time progresses, these two rates become essentially equal. Once most of the Th is desorbed, Fe solubilization continues at a rate comparable to that observed without Th.

Although it is believed that, like other metals, Th sorbs to hematite forming a mononuclear surface complex, it should, at higher surface densities, begin to form polynuclear surface species and surface-bound mixed metal oxides. The above experiments were performed at a Th(IV) concentration that is approximately a factor of ten below its solubility at pH 4.0. Because of this, we are currently assuming its surface species is a mononuclear inner-sphere complex that is homogeneously distributed over the hematite surface (this assumption will be tested by XAS analysis later this year). However, the possibility exists that even at these low concentrations, Th surface speciation is a mix of mononuclear and polynuclear species, which will impact data interpretation. Regardless, the data presented here does show that Th is rapidly removed from the hematite surface and that its latter rate is equal to that of Fe solubilization. Interestingly, the sum of the Th and Fe release rates is about equal to the Fe release rate in the absence of Th. These results are different from that observed for hematite sorbed Eu release (OSU); these differences are currently being explored.

The Th(IV) studies began under the previous project and are currently being completed. Primarily, aging studies of Th on the surface of hematite prior to exposure to a siderophore are ongoing to test the potential for time-dependent polynuclear species formation and its impact on Th solubilization. More data is required before definitive conclusions can be drawn about Th solubilization or a comparison made between the behavior of Th and Eu. We expect to generate that data over the next 6 months, including surface spectroscopy of Th from which a more discriminating picture of Th surface speciation and its mechanism of solubilization will be elucidated.

In the first 3 years of the project, we used molecular modeling methods to investigate a series of tris-catecholate ligands. Structural criteria for the design of multidentate catecholates ligands were derived from 1) an examination of crystal structure data and 2) geometries and potential energy surfaces obtained from electronic structure calculations. These structural criteria were incorporated within a molecular mechanics model. Application of this model yielded the first quantitative structure-stability relationship for Fe(III) complexation by tris-catecholamide ligands. This result establishes a method that can be used to evaluate the metal ion affinity of other possible catecholate ligand architectures. Thus, our previous studies provided criteria to design catecholate-based hosts and methods to evaluate quantitatively the metal ion binding potential of proposed host structures. Building upon this information, we have initiated the

computer-aided design of bis-, tris-, and tetrakis-catecholate ligands that are structurally organized for complexation with tetravalent actinides U(IV), Np(IV), and Pu(IV).

An extended MM3 model has been developed for Fe(III) complexes with catecholamides. Assignment of Fe-O stretch, Fe-O-C bend, and Fe-O-C-C torsion parameters was based on geometries and potential energy surfaces from density functional theory calculations and crystal structure data, and were investigated at the MP2 level of theory. These included rotational potential surfaces for several C-C bond types and hydrogen bonds involving phenol. The resulting model describes empirical relationships between force constants and physical properties. In addition to these metal-dependent interactions, several unknown intra-ligand interactions reproduce crystal structures with the expected level of accuracy. By changing only the M-O stretching parameters, a good agreement between calculation and experiment is obtained for other metal ions. In addition, we have found that this model is applicable to tropolonate complexes. Published barriers to octahedral inversion are reproduced to within ± 2 kcal/mol for [Al(III)(tropolonate)$_3$] and [Ga(III)(cat-echolamide)$_3$]$^{3-}$.

Application of this model has led to the first quantitative structure-activity relationship for catecholamide ligands. Conformational searches yielded the lowest energy forms of the six protonated ligands shown in Figure 1. Conformational searches were also run to identify the lowest energy forms of their Fe(III) complexes. We obtained the difference in steric energy
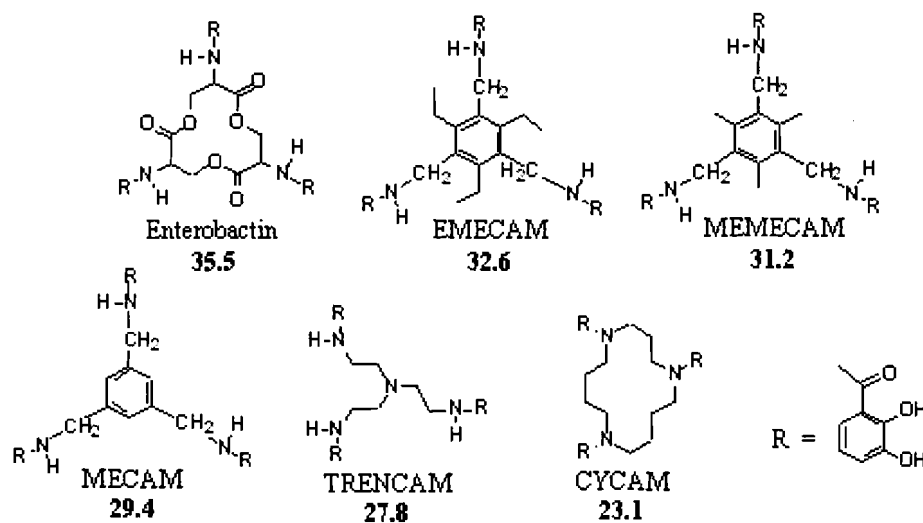

Figure 1. The Six Tris-Catecholamide Siderophore Architectures That Have Been Studied. Relative affinities for Fe(III) are given as pFe values (10 μM ligand, 1 μM Fe(III), and pH 7.4).

between the Fe-L complex and the hexaprotonated ligand. A plot of pFe vs. this energy difference yields the linear correlation. This result suggests that this method can be used to screen other candidate architectures for ligands based on the catecholamide donor group.

PNNL is collaborating with the Department of Chemistry, University of California, Berkeley, providing computer-aided host design to assist with the discovery of improved metal ion sequestering agents. The potential for UC-Berkeley to supply several siderophore-like (Figure 1) compounds is under discussion; the compounds will be used for testing hypotheses regarding actinide (IV) solubilization and sequestration. Current laboratory experiments on solubilization of $Th(IV)O_2$ and desorption of Th(IV) sorbed to oxide surfaces are nearing completion. Results have been submitted or are being submitted to scientific journals.

Ohio State University

Investigations to date have focused on studying the dissolution of oxides and desorption of metals by the siderophore DFB, with different metal ions adsorbed onto the solids. To further understand the effects of sorbed metals on oxide dissolution by DFB, XAS was used to probe the surface structural environment of sorbed metal ions. With the knowledge of the interactions between DFB, oxides, and metal ions, we can have a better understanding of how siderophore reacts with iron oxides in an environment where multiple metals including different lanthanides and actinides are present. Our results indicated that while DFB effectively dissolved iron oxides with different adsorbed metals, this process was affected also by the type of the metal adsorbed.

Two different solids, hematite (α-Fe_2O_3) and 15% Cr-substituted hematite (α-$Fe_{1.69}Cr_{0.31}O_3$), were used as substrates, and different metals including Ga, Zn, Pb, and Eu were chosen as adsorbates representing different types of metals. Macroscopic sorption studies were conducted for metals on these solids with initial metal concentration of 10^{-4}M, solid surface area of 40 m^2/L, and 0.01M $NaNO_3$ as background electrolyte over the pH range between 4 to 9. It was found that the percentage adsorption isotherms of most of these metals was not affected by different substrates under the experimental conditions used in this study, with the exception of Zn, for which the adsorption edge shifted to a lower pH value with Cr-substituted hematite (data not shown).

For the kinetic dissolution experiments, the solid concentrations were adjusted to have 40 m^2/L of initial solid surface areas in each sample. The samples were reacted with different metals at an initial concentration of 10^{-4}M with 0.01M $NaNO_3$ as background electrolyte for 24 hours before adding 10^{-3} M DFB. All dissolution experiments had been conduced at solution pH of pH = 7 ± 0.1 over a 60-hour period after adding DFB at 25°C purged with nitrogen gas. The extent of metal ion desorption by DFB was also measured for all samples as shown on Figure 2 (only Zn and Eu shown here). Metal ion desorption occurred rapidly, and the extent of metal desorption reached a plateau for all metals under investigation within 2 hours of reaction time.

Although DFB has a higher affinity to Fe than to other metals under investigation, metal ions were desorbed from the solid surfaces faster than Fe dissolution at the beginning of the reaction after DFB was added. The extent of metal ion desorption from solid surfaces by DFB varied among different metal ions, probably due to DFB-metal complexation reactions.

Figure 3 shows that Fe release increases with time for all samples, unlike the behavior of metal ion desorption. In general, Cr substitution enhanced Fe release by DFB as much as ten times more than that of pure hematite. No Cr release, however, was observed for all samples during the reaction time in this study. For pure hematite, samples with adsorbed metals had less dissolved Fe by DFB than the one without. Different types of metal ion seemed to have no
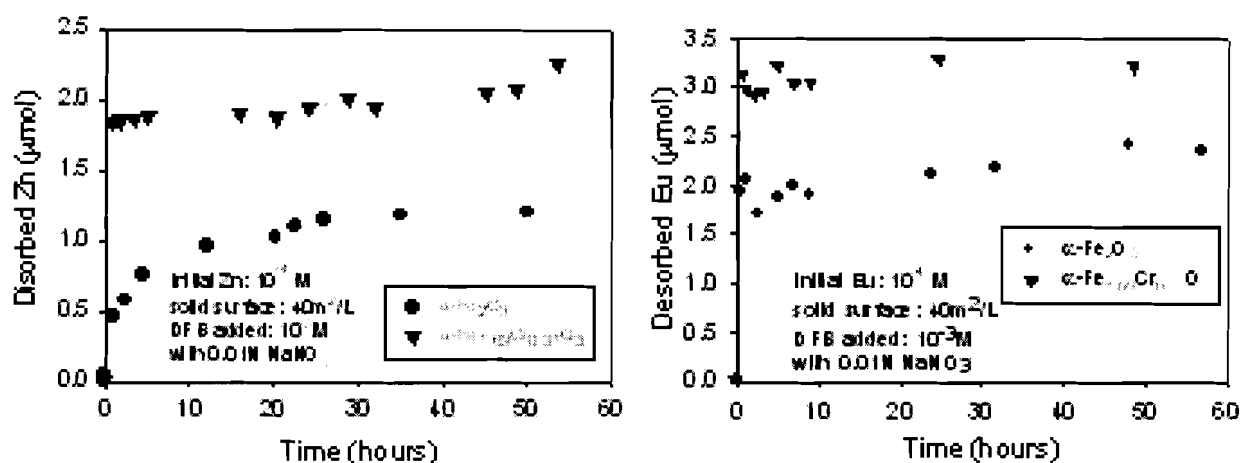
Figure 2. Metal Ion Desorption from Different Solids by DFB

(a) Fe dissolution of hematite
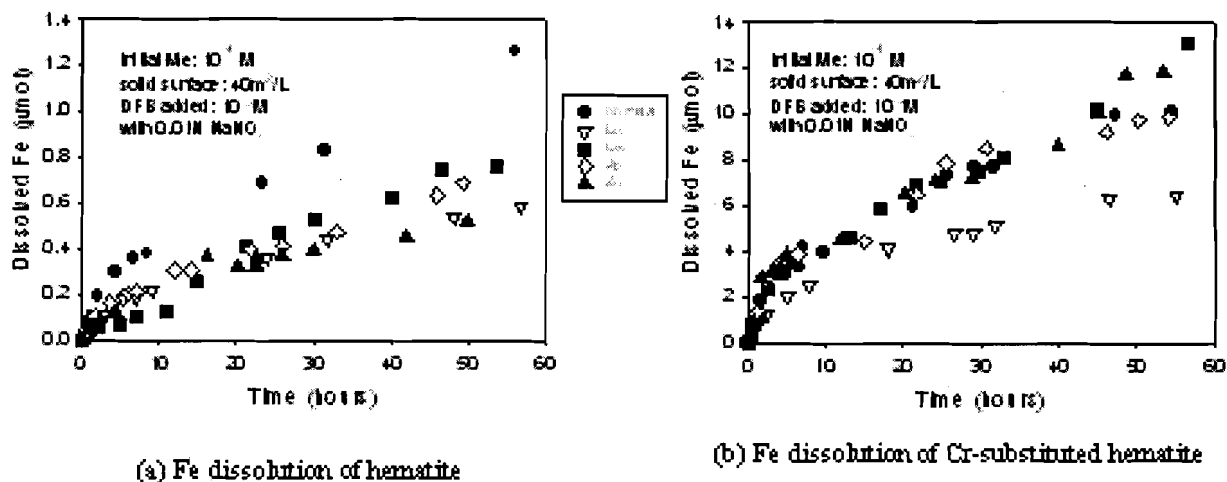
(b) Fe dissolution of Cr-substituted hematite

Figure 3. Fe Dissolution of Hematite and 15% Cr-Substituted Hematite by DFB with Different Adsorbed Metal Ions vs. Reaction Time

2.13

significant effects on Fe dissolution under these experimental conditions. This result suggested that while adsorbed metals blocked available surface sites on hematite surfaces for DFB, causing less Fe release, Fe dissolution by DFB from the well crystalline structure of hematite was not affected by the adsorbed metal ions.

For 15% Cr-substituted hematite, on the other hand, most of the metals had no effect on Fe dissolution by DFB except for Eu, from which less dissolved Fe was observed. Our previous studies also showed that adsorbed Eu retarded Fe release by DFB from iron oxides and Cr-substituted iron oxides with different extent of Cr substitution. It is not clear why the system with Eu behaved differently from systems with other metals by the results from these macro-scopic experiments. One possible explanation is that since Eu can form spinel structure as that of hematite, Eu may be incorporated into the oxide structure or forms stronger bonded complexes on the oxide surfaces comparing to the other metals. While Cr substitution introduces disorder to the oxide structure enhancing the Fe dissolution by DFB, strongly adsorbed Eu still blocks the surface site in the disordered oxide structure and thus reduces Fe dissolution. Our results from XAS study indicated that Eu forms strong surface complexes on solid surfaces. To date, the spectroscopic results from other metals were not conclusive, requiring further investigation.

Princeton University

We have been working on the functional group chemistry of model siderophore molecules, such as acetohydroxamic acid (aHa) and DFB, using vibrational (infrared [IR] and Raman) and XAS (C-, and N-groups in the ligand, and Fe-ligand complexes) in aqueous solutions and at the mineral-water interfaces. These experimental studies are complemented with theoretical calculations (Gaussian - B3LYP/6-31G(d) basis set) to gain insight on the structure and reactivity of model siderophores in aqueous solutions. We focused our preliminary studies on the protonation and deprotonation, and Fe^{3+} complexation of aHa and desB. We conducted a series of studies to understand the variations in the chemical state of siderophore molecule as a function of pH and Fe^{3+} ion concentration. Theoretical calculations were used to verify the vibrational spectra and the band assignments, and in the identification of energetically favored chemical species. To mimic the aqueous conditions in theoretical calculations of aHa, three water molecules were included adjacent to the hydroxamate groups.

The protonation and deprotonation reactions of aHa in aqueous solutions were examined by Holmen et al. (1997), and our experimental spectra agree with their reported values. However, our spectral analysis and interpretation differ from theirs. A series of ATR-FTIR (pH 4.5 to 10) and Raman spectroscopy (pH 6 to 12) studies on aHa solutions showed dramatic changes in the vibrational bands of hydroxamate functional group, and small changes in the alkyl group vibrations with aHa deprotonation and Fe^{3+} complexation (Figure 4). The most noticeable
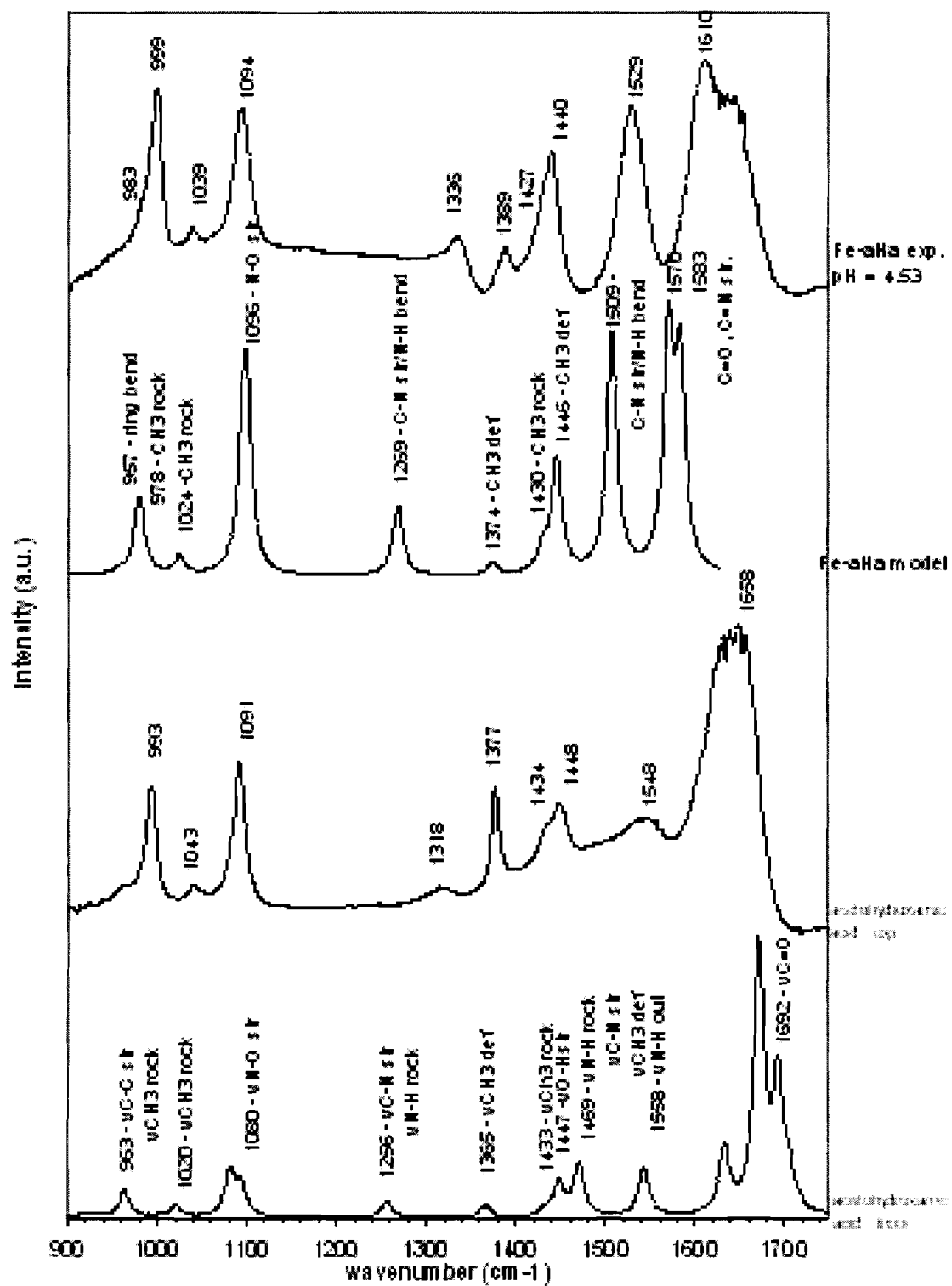
Figure 4. Experimental and Theoretical Vibrational Spectra of aHa in Protonated and its Fe-Complex Forms. The spectral analysis is done based on the theoretical calculations.

changes in the vibrational spectra of aHa (either because of protonation or Fe^{3+} complexation) are as follows: 1) changes in the vibrational bands of C=O, indicating the variations in the double bond character and the C-O bond length, 2) changes in the C-N stretch, which is related to the deprotonation/ protonation of the molecule, and 3) changes in the N-O stretch. Our theoretical and experimental studies give evidence that the proton connected to the oxygen atom leaves during deprotonation rather than the one connected to N.

In the neutral aHa molecule, the carbonyl peak is at 1658 cm^{-1} and shifts to 1610 cm^{-1} upon complexation with Fe^{3+}. This is due to the increasing bond length of C=O as it becomes complexed to iron and also due to the emergence of a C=N stretch character due to the resonance properties of aHa. In addition, the N-O stretch shifts from 1091 cm^{-1} to 1094 cm^{-1} upon complexation. In previous papers, the N-O stretch was assigned to low-energy bands around 900 cm^{-1}, but calculations involving water and deuterated water seem to favor our new assignment. This reassignment of N-O stretch is important to the prediction of metal-hydroxamate complexes, since the N-O group is at the center of Fe-aHa complex. Another shift that directly probes the iron-binding site is the amide II and amide III bands, which are related to a coupling of C-N stretch and N-H bend. The amide II is attributed to mainly N-H bend as well as the NOH bend and amide III is mainly attributed to C-N stretching. From Figure 1, amide II shifts to lower frequencies and amide III goes to higher frequencies. This corresponds to a more constrained N-H bond and shorter C-N bond, which in agreement with both experimental and theoretical data.

Planned Activities

At PNNL, future studies will focus on the catecholamide siderophores. Investigations will continue to focus on the Fe oxides (geothite, hematite, and magnetite). However, studies of UO_2 and PuO_2 dissolutions will begin during the last quarter of fiscal year 2002 and continue into the final year of this project. Modeling efforts will continue to expand to include the hydroxamate siderophores. In the final year of this project, investigations are anticipated with actual contaminated steel coupons from the Hanford Site.

Results of OSU studies indicated that types of metal ions affected Fe dissolution by DFB. This founding is significant because decontaminating processes in DOE facilities encounter different lanthanides and actinides. To have a better understanding of the iron dissolution and metal desorption processes by DFB, we will focus our work on

- dissolution experiments with actinides, thorium, and uranium
- further XAS studies on different metal ion sorption on the oxides
- effects on iron dissolution with different siderophores.

2.16

Princeton's analysis and interpretation of the experimental and theoretical results of aHa will aid in the interpretation of the nature of desB, a bigger molecule but with the same functional moieties as aHa, in aqueous solutions and at the interfaces. X-ray spectroscopic studies on aHa and desB and their Fe^{3+} complexes in aqueous solutions and mineral surfaces will further increase our knowledge on this system. In the coming months, our focus will be on the x-ray spectroscopy evaluation of aHa and desB in aqueous solutions, and the vibrational spectroscopy of these molecules on Fe- and Cr-doped Fe-oxide surfaces.

Cited Reference

Holmen BA, MI Tejedor-Tejedor, and WM Casey. 1997. Hydroxamate Complexes in Solution and at the Goethite-Water Interface: A Cylindrical Internal Reflection Fourier Transform Infrared Spectroscopy Study. *Lang.* 13:2197-2206.

Information Access

Publications (bold signifies output since renewal)

Bluhm M, BP Hay, SK Sanggoo, EA Dertz, and KN Raymond. Corynebactin and a Serine Trilactone Based Analogue - Chirality and Molecular Modeling of Ferric Complexes. *Inorg. Chem.* Submitted.

Beak DG, CC Chen, SJ Traina, and JM Bigham. Synthesis and Characterization of Hematite, Maghemite, and Their Chromium Substituted Analogs. In preparation.

Chen CC and SJ Traina. Macroscopic and Microscopic Investigation of Europium and Neodymium Partitioning at Iron Oxide-Water Interfaces. In preparation.

Chen CC and SJ Traina. Sorption of Strontium, Lead, Zinc, and Europium on Iron Oxides and Cr-Substituted Iron Oxides. In preparation.

Chen CC and SJ Traina. A Kinetic Study of Dissolution of Iron Oxides and Cr-Substituted Iron Oxides with Sorbed Metal Ions by Siderophore. In preparation.

Hay BP and RD Hancock. 2001. The Role of Donor Group Orientation as a Factor in Metal Ion Recognition by Ligands. *Coord. Chem. Rev.* 212:61.

Vargas R, J Garza, DA Dixon, and BP Hay. 2001. $C(sp^2)$-C(aryl) Bond Rotation Barrier in N-Methylbenzamide. *J. Phys. Chem. A.* 105:774-778.

Vargas R, J Garza, DA Dixon, and BP Hay.* 2001. Conformational Analysis of N-Benzylformamide. *J. Mol. Struct. (THEOCHEM)*. In press.

Hay BP, DA Dixon, R Vargas, J Garza, and KN Raymond. Structural Criteria for the Rational Design of Selective Ligands. 3. Quantitative Structure-Stability Relationship for Iron(III) Complexation by Tris-Catecholamide Siderophores. *Inorg. Chem.* Submitted.

Ainsworth CC, K Wagnon, and A Mortimer. Interaction Between Hydroxamic Acid Siderophores and Fe Oxides: Adsorption and Dissolution. In preparation.

Ainsworth CC and K Wagnon. The Effect of Surface Area and Morphology on the Dissolution of Hematite by Desferrioxamine B. In preparation.

Presentations

Uddin J and BP Hay. 2002. Computer-Aided Design of Actinide Receptors Containing Catecholate Chelate Rings. Abstract submitted to the Inorganic Poster Session, 224th American Chemical Society National Meeting in Boston, Mass, August 2002.

Ainsworth CC, B Hay, and S Traina. 2001. Contaminant-Organic Complexes: Their Structure and Energetics in Surface Decontamination Processes. EMSP D&D Kick-Off Meeting, November 27 & 28, 2001, Oak Ridge National Laboratory.

Hay BP. 2000. Ligand Design with Molecular Mechanics. Theory, Modeling, and Simulation Monthly Seminar Series, Richland, WA, March 23, 2000.

Hay BP, R Vargas, J Garza, and DA Dixon. 2000. Metal Ion Complementarity in a Series of Tris-Catecholamides. 219th American Chemical Society Meeting in San Francisco, CA, March 26, 2000.

Hay BP. 2000. Ligand Design with Molecular Mechanics. 219th American Chemical Society Meeting in San Francisco, CA, March 26, 2000.

Hay BP. 2000. Building a Better Mousetrap: Ligand Design with Molecular Mechanics. Invited Speaker, American Chemical Society, Pacifichem 2000 Meeting in Honolulu, HI, December 16, 2000.

Beak DG, CC Chen, JM Bigham, and SJ Traina. 1999. Synthesis and Properties of Hematite, Maghemite, and Their Chromium Substituted Analogs. The Clay Minerals Society, 36th annual meeting, Purdue University, IN, June 1999.

Chen CC and SJ Traina. 2000. Macroscopic and Microscopic Investigation of Lanthanide Ions Partitioning at Oxide/Water Interfaces. EMSP National Workshop, Atlanta, GA, April 2000.

Traina SJ and CC Chen. 2000. XAS Investigation of Lanthanide Ion Sorption on Iron Oxide and Cr-Substituted Iron Oxide Surfaces. Goldschimdt Conference, Oxford, UK, September 2000.

Chen CC and SJ Traina. 2001. Dissolution of Iron Oxides and Cr-Substituted Iron Oxides with Sorbed Europium by the Siderophore Desferrioxamine B. Goldschimdt Conference, Hot Springs, VA, May 2001. To be presented.

Development of Biodegradable Isosaccharinate-Containing Foams for Decontamination of Actinides: Thermodynamic and Kinetic Reactions between Isosaccharinate and Actinides on Metal and Concrete Surfaces

(Project Number: 82715)

Principal Investigator

Dhanpat Rai
P.O. Box 999, MSIN P7-50
Pacific Northwest National Laboratory
Richland, WA 99352
509-373-5988 (phone)
509-372-1632 (fax)
dhan.rai@pnl.gov

Co-Investigators

Robert C. Moore
Sandia National Laboratories
P.O. Box 5800, Mail Stop 0779
Albuquerque, NM 87185-0779
505-844-1281 (phone)
505-844-2348 (fax)
RCMOORE@sandia.gov

Mark D. Tucker
Sandia National Laboratories
P.O. Box 5800, Mail Stop 0734
Albuquerque, NM 87185-0734
505-844-7264 (phone)
505-844-1480 (fax)
MDTUCKE@sandia.gov

Linfeng Rao
Lawrence Berkeley National Laboratory
1 Cyclotron Road Mailstop 70A-1150
Berkeley, CA 94720
510-486-5427 (phone)
510-486-5596 (fax)
LRao@lbl.gov

Research Objective

Actinide contamination of steel and concrete surfaces is a major problem within the U.S. Department of Energy (DOE) complex. For steel surfaces, the primary problem is contamination of sections of nuclear power reactors, weapons production facilities, laboratories, and waste tanks. For concrete, there are an estimated 18,000 acres of concrete contaminated with radioactive materials that need decontamination. Significant efforts have gone into developing decontamination technologies. Almost all current decontamination technologies rely on removal of the contaminated surface layer by mechanical means or by chemical methods using harsh chemicals. Some of the technologies are ineffective. Others are expensive, labor-intensive, and hazardous to workers. Still others create secondary mixed wastes that are not environmentally acceptable.

This project seeks fundamental information that will lead to the development of a new and more environmentally acceptable technology for decontamination of Pu on steel and concrete surfaces. The key component of this technology is isosaccharinate (ISA), a degradation product of cellulose materials that is biodegradable and binds strongly with Pu. Isosaccharinate will be incorporated into foams for use in decontamination of Pu from steel and concrete surfaces. To develop a fundamental basis for this proposed technology, we will 1) study the effect of pH and common ions (Na and Ca) on the speciation and thermodynamic reactions of ISA over wide ranges of pH and concentrations of Na and Ca, 2) develop thermodynamic and kinetic data for ISA reactions with Pu(IV) and Fe(III), and 3) determine the fundamental Pu concentration-controlling reactions involving steel and concrete surfaces and test contaminated surfaces using ISA-containing foams for Pu removal. Our ultimate goal is to develop a technology, based on sound fundamental principles, for decontaminating tetravalent actinides. The proposed research is a multi-laboratory effort that includes fundamental chemistry studies conducted at Pacific Northwest National Laboratory and Lawrence Berkeley National Laboratory, and foam formulation and decontamination research conducted at Sandia National Laboratories.

Research Progress and Implications

This report summarizes the results of the first 6 months of a 3-year project. Progress is described in the following paragraphs.

Isosaccharinate is not commercially available. Therefore, methods were perfected to produce large quantities of solid calcium isosaccharinate. Methods were also developed to change this calcium isosaccharinate to more soluble sodium isosaccharinate for use in studies involving development of equilibrium and kinetic data for important ISA reactions.

Preliminary tests to determine the possible efficacy of isosaccharinate to decontaminate steel and concrete surfaces containing uranium showed that isosaccharinate indeed holds promise as a decontaminating agent.

Experiments were planned to develop extensive thermodynamic data for complexation constants of isosaccharinate with a number of metals including actinides (trivalent, tetravalent, pentavalent and hexavalent) and matrix elements (e.g., Fe(II), Fe(III), and Ca) of contaminated surfaces.

Preliminary ^{13}C- nuclear magnetic resonance studies show that deprotonation of carboxylic acid groups is complete at pH 5 and that no further deprotonation reactions of ISA are apparent in the pH range from 5 to 12, which is contrary to that suggested in the literature.

Studies on the solubility of NpO_2(am) as a function of pH at fixed ISA concentrations, and as a function of ISA and at fixed pH, showed that ISA strongly complexes Np(IV) in a large range of pH values, extending to as high as pH 12. These studies show that similar behavior can be expected with Pu(IV) systems and that ISA holds promise as an effective decontaminating agent for Pu.

Planned Activities

We will develop fundamental data over a wide range in pH values on the types of aqueous complexes and complexation constants of ISA with actinides and with metals such as Fe and Ca that compete with actinides for ISA complexation. Both the equilibrium and kinetic data for these important reactions will be developed.

We will formulate foams containing ISA, then test ISA solutions and ISA-containing foams for their effectiveness to decontaminate actinides from metal surfaces and concrete.

3. Soil and Groundwater Cleanup

Fixation Mechanisms and Desorption Rates of Sorbed Cs in High-Level Waste Contaminated Subsurface Sediments: Implications to Future Behavior and In-Ground Stability

(Project Number: 73758)

Principal Investigator

John M. Zachara
Pacific Northwest National Laboratory
P.O. Box 999, MSIN K8-96
Richland, WA 99352
509-376-3254 (phone)
509-376-3650 (fax)
john.zachara@pnl.gov

Co-Investigators

James P. McKinley
Pacific Northwest National Laboratory
P.O. Box 999, MSIN K3-61
Richland, WA 99352
509-375-6861 (phone)
509- 375-6954 (fax)
james.mckinley@pnl.gov

Calvin C. Ainsworth
Pacific Northwest National Laboratory
P.O. Box 999, MSIN K3-61
Richland, WA 99352
509-375-2670 (phone)
509-375-6954 (fax)
calvin.ainsworth@pnl.gov

R. Jeff Serne
Pacific Northwest National Laboratory
P.O. Box 999, MSIN K6-81
Richland, WA 99352
509-376-8429 (phone)
509-376-5368 (fax)
jeff.serne@pnl.gov

Research Objective

Research is investigating mineralogic and geochemical factors controlling the desorption rate of $^{137}Cs^+$ from subsurface sediments on the Hanford Site contaminated with different types of high-level waste. The project will develop kinetic data and models that describe the release rates of $^{137}Cs^+$ from contaminated sediments over a range of potential geochemical conditions that may evolve during waste retrieval from overlying tanks, or in response to meteoric water infiltration. Scientific understanding and computational techniques will be established to predict the future behavior of sorbed, in-ground $^{137}Cs^+$.

Research Progress and Implications

This project was initiated on October 1, 2000. Since its inception, we have been investigating $^{137}Cs^+$ desorption behavior from contaminated sediments (10^6 to 10^8 pCi/g ^{137}Cs) from Hanford's S-SX tank farms (41-09-39 and SX-108 boreholes). The sediments were contaminated with Cs-containing redox waste fluids in 1970 that were elevated in temperature ($\approx 100°C$) and contained high levels of base (OH^-), salt ($NaNO_3$), and aluminate [$Al(OH)_4^-$]. The highly reactive nature and elevated temperature of the waste fluid induced a complex suite of mineral reactions that decreased in magnitude with increasing distance from leaked tank SX-108. The mineralogic properties of the sediments and the ^{137}Cs-hosting micaceous sorbents in the contaminated sediments were characterized in detail using techniques such as x-ray absorption spectroscopy and transmission electron microscopy.

Desorption kinetic studies were performed in batch mode in Na^+, K^+, and Rb^+ electrolytes and in the presence of a Cs-selective adsorbent. Three separate adsorbed pools of $^{137}Cs^+$ were defined: 1) a rapidly exchangeable pool ($\approx 20\%$ to 25%), 2) a kinetically exchangeable pool ($\approx 15\%$ to 20%), and 3) a poorly exchangeable or fixed pool ($\approx 60\%$). The kinetics of desorption was complex and was influenced by the hydration status of the exchanging cation. Poorly hydrated cations such as Rb^+ and K^+ induce collapse of mica edges, which, in turn, physically prevents $^{137}Cs^+$ desorption. A multisite exchange/slab diffusion model was developed that well described the Cs desorption process in all four sediments studied, as well as the observed experimental results in different electrolytes (see Figure 1 for examples of results and model simulation). The physical model was based on X-ray microprobe measurements of Cs distribution in micaceous particles, where Cs was found to be localized to specific areas on the mica edge and in connected cleavage channels running parallel to the C crystallographic axis.

The results are immediately useful to the Department of Energy (DOE)-Hanford Site. Of major significance, our work has shown that approximately 60% of the in-ground $^{137}Cs^+$ pool in the S-SX tank farm is immobile and is unlikely to desorb from the sediments under any reasonable geochemical scenario. Thus, our research has reduced by more than 50% the effective in-ground
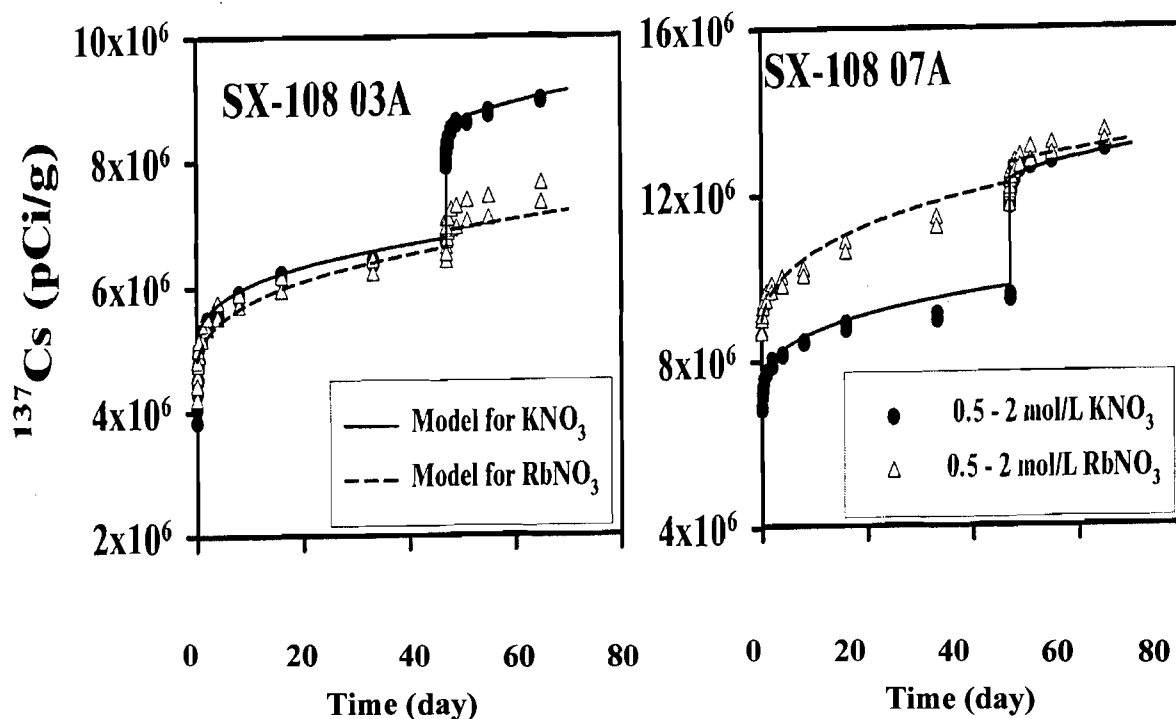
Figure 1. Kinetic desorption data for the release of 137Cs+ from two contaminated sediments collected beneath leaked Hanford tank SX-108. The sediments were first placed in 0.5 mol/L KNO3 or RbNO3, and desorption was followed for approximately 50 d, after which the electrolyte concentration was increased to 2 mol/L by addition of solid electrolyte salt. The increased 137Cs+ desorption resulting from the mass action effect of the electrolyte salt was followed. The solid and dashed lines represent the results of simulations with the slab diffusion model. The two sediments differ in the fraction of 137Cs+ that is desorbed by Rb+, a result of mineral transformation caused by reaction with high base in the REDOX waste supernatant.

inventory of $^{137}Cs^+$ that needs be considered from the risk perspective. Moreover, our model and associated database allow prediction of the rate and amount of the exchangeable $^{137}Cs^+$ fraction that may desorb from contaminated sediments, depending on the composition of the vadose zone porewater (i.e., whether it originates from rainwater infiltration or leakage during single-shell tank waste recovery).

Planned Activities

Research in the remaining 1.5 project years will focus on $^{137}Cs^+$-contaminated sediments from the B-BX-BY and T-TX-TY tank farms that have received bismuth phosphate wastes as well as wastes from B-Plant and the Plutonium-Uranium Extraction (PUREX) facility. The different major-ion chemistries of these three process wastes may have driven different suites of reactions that impact Cs desorption. Such factors will be evaluated through a well formulated set of

desorption kinetic experiments. Over this 1.5-year period, time-of-flight and dynamic secondary ion mass spectroscopy, transmission electron microscopy, and other state-of-the-art science techniques will be applied in efforts to map the depth distribution and structural association of sorbed Cs in mineral particles isolated from the contaminated sediments. These latter measurements will refine our physical model of Cs sorption location in mineral particles, improving our kinetic $^{137}Cs^+$ model.

Information Access

Zachara JM, SC Smith, C Liu, JP McKinley, RJ Serne, and P Gassman. 2002. Sorption of Cs^+ to Micaceous Subsurface Sediments from the Hanford Site, USA. *Geochim. Cosmochim. Acta,* **66**:193-211.

Origins of Deviations from Transition-State Theory: Formulating a New Kinetic Rate Law for Dissolution of Silicates

(Project Number: 81908)

Principal Investigator

Jonathan Icenhower
Pacific Northwest National Laboratory
P.O. Box 999, MSIN K6-81
Richland, WA 99352
509-372-0078 (phone)
509-376-2210 (fax)
jonathan.icenhower@pnl.gov

Co-Investigators

B. P. McGrail
Pacific Northwest National Laboratory
P.O. Box 999, MSIN K6-81
Richland, WA 99352
509-376-9193 (phone)
509-376-2210 (fax)
pete.mcgrail@pnl.gov

A. Luttge
Rice University
Dept. Geology and Geophysics-MS 126
P.O. Box 1892
Houston, TX 77251-1892
713-348-6304 (phone)
aluttge@rice.edu

D. London
University of Oklahoma
Dept. Geology and Geophysics
100 E. Boyd Str.
810 SEC
Norman, OK 73019-0628
405-325-7626 (phone)
dlondon@ou.edu

Research Objective

Present models for dissolution of silicate minerals and glasses, based on transition-state theory (TST), overestimate the reaction rate as solution compositions approach saturation with respect to the rate-governing solid. Therefore, the reactivity of key materials in the environment, such as feldspar, mica, and borosilicate glass, is uncertain, and any prediction of future aqueous durability is suspect. The core objective of this investigation is to determine the origin of these discrepancies and to fashion a quantitative model that reliably predicts the reactivity of silicate materials in realistic environmental conditions. This is being accomplished using newly developed experimental techniques checked against computer simulations based upon first-principle theory.

Research Progress and Implications

Research thus far has focused upon select borosilicate glass compositions and feldspar studies. Dissolution experiments with borosilicate glass compositions along the sodium silicate–reedmergnerite join are aimed at revealing the relationship between melt (glass) structure and durability. Glasses with increasing amounts of sodium silicate contain a larger fraction of non-bridging oxygen (NBO) compared to end-member reedmergnerite (the boron version of albite). We selected this series of glasses because a number of models advocate a relationship between the number of NBOs and durability. Another glass series under investigation is a set of sodium nepheline compositions with variable amounts of Al/B. The glass compositions are designed such that the amount of "excess" sodium (i.e., more sodium than Al+B on a molar basis) is varied. These glass compositions probe the effects of Na–H exchange, identified as a potential factor in the dissolution of certain glass compositions at rates different from those expected from TST models. Another facet of this investigation is to use the data gleaned from the new technique of vertical scanning interferometery (VSI) to quantify the dissolution of glass and feldspar as the solution approaches saturation. These latter data have been used to construct a new rate model for the dissolution kinetics of crystalline solids.

Durability Experiments with Borosilicate Glass

Single-pass flow-through (SPFT) experiments have been used to quantify rates of reaction in the glass specimens. Our investigations have revealed that the forward rate of dissolution is constant with respect to glass chemical composition. This observation is consistent with the notion that glass dissolution is rate-limited by the rupture of the Si–O bond and is insensitive to even gross differences in major and minor element composition. This is a radical departure from the received wisdom of glass dissolution kinetics and must be carefully checked for its veracity. Ion-exchange kinetics appears to decrease in importance as molar Na/(Al+B) approaches unity. Again, this is consistent with our theory and implies that controlling the exchange of Na^+ for H^+

during reaction will strongly ameliorate the matrix dissolution rate. The Na–H exchange leaves behind OH⁻, which raises the local pH in the vicinity of the Si–O bond and catalyses the silanation reaction, and, ultimately, the release of H_4SiO_4 to solution, thereby affecting the matrix dissolution rate.

Vertical Scanning Interferometry Experiments

Dissolution rates of silicate materials also have been quantified using VSI experiments at Rice University. By measuring the absolute height difference between a reacted and a pristine surface, the dissolution rate of a glass monolith or crystal can be determined without relying on solution analyses. This is important because obtaining measurable quantities of elements from a dissolving silicate near saturation, using SPFT techniques, is very difficult. Our experiments have revealed a viable mechanism for the dissolution of silicate crystals based on *step waves* emanating from *etch pits*. Etch pits are the result of dislocations (crystal imperfections) that intersect the mineral surface. The step waves move across the surface of the mineral, producing a relatively flat surface punctuated by the etch pits, as revealed by VSI techniques. We predict that the movement of the step waves will slow when dissolution cavities form as the system nears saturation. This theory also can explain the nonlinearity in the dissolution rates as the system approaches saturation, although more experiments are needed to confirm this.

Synthesis Experiments

Experiments on methods to grow synthetic feldspar and micas are being conducted at the University of Oklahoma. Once the methods are perfected, researchers will work to synthesize crystals doped with isotopic tracers for use in dissolution experiments near saturation.

Planned Activities

We will complete glass-water reaction experiments with borosilicate glass compositions along the feldspar-jadeite-nepheline join. In all of these experiments, substantial amounts of Al will be substituted for boron, making the glass compositions relevant to the needs of the Hanford Site. All of these experiments will be conducted near saturation and will aid us in quantifying the deviation from model expectations.

The dissolution rate of select glass coupons will be determined using VSI techniques. These experiments will be conducted in June 2002 and are the first study of their kind. Because no relevant studies exist to guide us, we are unsure of what surface features may be revealed as dissolution proceeds (although it is likely that etch pits will not be a concern). However, the method will be useful in calibrating the difference, if any, between rates obtained from VSI and SPFT methods.

Dissolution measurements using the VSI methods will be completed on feldspar specimens near saturation. These will be compared against rate measurements obtained from feldspar crystals containing radiotracers.

We will refine the method for synthesizing feldspar crystals. Once completed, the method will be used to grow radiotracer-containing crystals at Pacific Northwest National Laboratory for dissolution work.

Information Access

Icenhower JP, BP McGrail, A Luttge, and D London. Dissolution Behavior of Aluminoborosilicate Glass Near Silica Saturation: Origin of Deviation from TST Expectations. Invited talk for *EMSL 2002, Symposia and User's Meeting*, May 22, 2002, Richland, WA.

Lasaga AC and A Luttge. Mineralogical Approaches to Fundamental Crystal Dissolution Kinetics—I. Submitted to *American Mineralogist*.

Physicochemical Processes Controlling the Source-Term from Tank Residuals

(Project Number: 81893)

Principal Investigator

Dr. B. P. McGrail
Pacific Northwest National Laboratory
P.O. Box 999, MSIN K6-81
Richland, WA 99352
509-376-9193 (phone)
509-376-2210 (fax)
pete.mcgrail@pnl.gov

Contributors and Collaborators

B. K. McNamara
Pacific Northwest National Laboratory
P.O. Box 999, MSIN P7-25
Richland, WA 99352
509-376-1408 (phone)
509-373-9675 (fax)
Bruce.Mcnamara@pnl.gov

S. V. Mattigod
Pacific Northwest National Laboratory
P.O. Box 999, MSIN K6-81
Richland, WA 99352
509-376-4311 (phone)
509-376-5368 (fax)
shas.mattigod@pnl.gov

G. J. Lumetta
Pacific Northwest National Laboratory
P.O. Box 999, MSIN P7-22
Richland, WA 99352
509-376-6911 (phone)
509-373-9675 (fax)
gregg.lumetta@pnl.gov

S. L. Wallen
Department of Chemistry
University of North Carolina at Chapel Hill
Campus Box 3290
Chapel Hill, NC 27599-6011
919-962-2933 (phone)
wallen@email.unc.edu

Research Objective

After remediation and closure of the high-level waste tanks at Hanford (and at other DOE sites), residual radionuclide-bearing solids will remain in the form of sludge and hard heel adhering to the inner surfaces of the tanks. Radionuclide release from these residuals represents a potentially significant source of contaminants migrating in the sediments underlying the tanks. A recent composite analysis for the Hanford Site has shown the radionuclide source term from the residual solids to be one of the most significant long-term dose contributors on site, essentially equivalent in magnitude to a number of well-known discharges from leaking single-shell tanks. However, this assessment was based on a highly conservative release model for the tank residuals. The conservative model is being used in lieu of a true scientific understanding of the processes controlling the release rate from the sludge that is applicable to the Hanford vadose zone environment. Currently, the U.S. Department of Energy (DOE) is planning to spend hundreds of millions of dollars to remove 99% or more of the waste from Hanford high-level waste tanks that may have no real long-term environmental benefit. Through this project, we will significantly improve the fundamental scientific basis for estimating the release rate of ^{99}Tc, the principal long-term dose contributor from tank residual wastes.

We envision an improved conceptual model that considers diffusion of water and oxygen in the sludge under conditions of partial hydraulic saturation, but 100% relative humidity, consistent with the subsurface environment at Hanford. Key chemical processes are also considered, including the oxidation of reduced Tc compounds in the sludge and the chemical changes in sludge phase assemblage that will occur over time. A combination of novel experimental methods is proposed to investigate these processes. This comprehensive study will provide a sound technical basis for DOE and local stakeholders to make more informed cost/benefit/risk decisions regarding closure of Hanford high-level waste tanks.

Research Progress and Implications

This project was initiated in FY02 and is being performed cooperatively between Pacific Northwest National Laboratory (PNNL) and the University of North Carolina at Chapel Hill (UNC-CH). Efforts to date have focused on producing and characterizing tank sludge simulants that will be the focus of studies over the next 2 years. Unexpected difficulties were encountered in retaining Re, a non-radioactive surrogate for ^{99}Tc, during sludge preparation. Incorporation of a reducing agent during the sludge preparation solved this problem.

During preparation of SAPO-34 zeolite to be used in Re adsorption studies, we unexpectedly synthesized a pure sodalite with perrhenate in the beta cage. This compound has never been reported in the literature. Consequently, additional characterization work is underway to define the structure and bonding in this compound.

3.10

Preparation of a Re-Bearing Sludge

A literature study was carried out to investigate tank sludge types that might retain ^{99}Tc. Specifically, the waste type was to be contained in Hanford single shell tanks (SSTs) and originate from the plutonium-uranium extraction (PUREX), oxidation-reduction (redox), or BiPO$_4$ processes. Additionally, this sludge should exhibit sustained levels of ^{99}Tc after waste retrieval operations. Existing analytical data associated with sludge washing and sludge leaching studies, carried out at PNNL and at Los Alamos National Laboratory, indicated that sludge in tank series B-201–204 and T-101–111 should retain ^{99}Tc after sluicing and retrieval operations. Specifically, the data suggested that B-202 and T-111 will retain 98% and 88% ^{99}Tc, respectively, in the remaining sludge solids after waste retrieval operations.

A T-111 sludge simulant was chosen, and preparations began with caustic precipitation of metal nitrate salts and (NH$_4$)$_2$ReCl$_6$ as a technetium mimic. The supernatant was decanted from centrifuged sludge, and the sludge washed in 0.1-$\underline{M}$ hydroxide. This type of preparation apparently promoted oxidation of the precipitated ReO$_2$, and it readily washed from the sludge. A number of alternative preparations were tried with similar results. An alternative, successful small-scale preparation utilized metal chloride salts with thiosulfate as reductant. Reagents were purged under argon, and preparations were carried out in a glove bag under argon. The final sludge product contained 1.28 mg ReO$_2$/g wet sludge as analyzed by inductively coupled plasma mass spectroscopy. Scale-up of this procedure was hampered by various solubility issues and also limited by the time required to prepare multigram quantities of pure (NH$_4$)$_2$ReCl$_6$. The yield of Re was only about 10% from this preparation, and the loss may be due to the relatively high solubility of ReO$_2$ as the hydrous oxide in basic solution. The final wet sludge product, however, has the appearance of the actual, as-received T-111 sludge. It has very high water content and contains about 1.28 mg ReO$_2$/g wet sludge. Approximately 750 grams of the wet sludge have been prepared.

Readsorption on Zeolites

The objective of this task is to synthesize selected zeolite minerals that are present in tank sludge and conduct adsorption experiments to ascertain their ability to retard transport of ^{99}Tc. We developed a synthesis scheme to obtain samples of pure nitrated cancrinite. Additionally, we have synthesized pure samples of SAPO-34 using morpholine templates.

3.11

During these studies, we unexpectedly synthesized samples of pure sodalite with perrhenate substitution in the beta cage, as shown in Figure 1. This compound has never been reported in literature. The significance of this discovery is that perrhenate (and, by analogy, pertechnetate) can also be trapped in the sodalite structure.

Preliminary characterization of this material has been completed and a manuscript is in preparation for publication. Figure 2 shows x-ray powder diffraction data for the sodalite. As shown, the Rietveld refinement of the structure agrees well with the experimental x-ray diffraction (XRD) pattern, indicating that perrhenate ion is entrapped in the beta cage of sodalite.

Figure 1. Crystal Structure of Sodalite (Re), $Na_8(AlSiO_4)_6(ReO_4)_2$ Viewed Along (111)

A Raman spectrum was also collected on the $Na_8(AlSiO_4)_6(ReO_4)_2$ powder. The Raman scattered light was collected at room temperature in 180° mode with a fiber optic probe. Scattered laser light is passed through a holographic notch filter with an optical density of 4 but 80% transmissivity for Raman scattered light. The probe is coupled to a Holospec (Kaiser Optical Systems) spectrograph. The spectrograph features fast f/1.8 optics, HoloPlex™ transmission grating, and back-illuminated charge-coupled device detector. Incident light was provided by a 532-nm diode-pumped ND:YAG laser operated at about 150 mW. Exact assignment of the peaks

Figure 2. Experimental Versus Refined XRPD Data for Sodalite (Re), $Na_8(AlSiO_4)_6(ReO_4)_2$

in Figure 3 is still in progress. However, the peak at 975 cm^{-1} is probably an asymmetric T-O-T stretching vibration (T being the atom at the center of a tetrahedron, e.g., Si or Al) [1,2]. The peak at 923 cm^{-1} may be a ν_3 stretching vibration for ReO$_4$- in tetrahedral coordination [3].

Diffusion in Tank Sludge

The goal of the UNC-CH group in the initial phase of this project is to incorporate luminescent and para-

Figure 3. Raman Spectrum of Na$_8$(AlSiO$_4$)$_6$(ReO$_4$)$_2$

magnetic species into a silica nanoparticle for the development of nuclear magnetic resonance and luminescence measurements of H$_2$O and O$_2$ diffusion coefficients in single-phase sludge-simulant samples. The synthetic procedure is based on a reverse microemulsion process that involves performing a solgel reaction in the interior H$_2$O pool of the microemulsion system. An example of the type of particles typical in this process are shown in Figure 4. The control of the particle morphology and the effect of various solvents on this system are currently being

investigated. The Triton-N101 surfactant used previously in cyclohexane has been determined to have limitations with respect to the size and polydispersion of the nanoparticle reporters. The incorporation of the luminescent Eu^{3+} is being pursued through the processing of Eu(NO$_3$)$_3$ in basic solution to produce a hydrated precipitate that was peptized with acid to produce a sol that was incorporated into the reverse microemulsion sol-gel silica synthesis. Preliminary results indicate incorporation of the luminescent system into the silica particles; however, the particle size and polydispersity have not been evaluated.

Figure 4. Silica Nanoparticles Produced via Microemulsion Technique

Planned Activities

We have successfully prepared a T-111 tank sludge simulant with sufficient Re to support planned measurements of its transport and oxidation behavior. These experiments will begin sometime in early FY03. A manuscript on the newly discovered perrhenate sodalite is in preparation. Future work on pure zeolite phases will focus on the degree of substitutions in

3.13

cancrinite and sodalite structures in mixed oxyanion systems (NO_3/ReO_4). Experiments to understand potential adsorption and desorption mechanisms of TcO_4 on cancrinite, sodalite, and SAPO-34 materials will also begin.

References Cited

Ariai J and SRP Smith. 1981. The Raman Spectrum and Analysis of Phonon Modes in Sodalite. *J. Phys. C: Solid State Phys.* 14:1193-1202.

de Man AJM and RA van Santen. 1992. The Relation Between Zeolite Framework Structure and Vibrational Spectra. *Zeolites* 12:269-279.

Brenchley ME and MT Weller. 1994. Synthesis and Structures of $M_8[AlSiO_4]_6 \cdot (XO_4)_2$, M = Na, Li, K; X = Cl, Mn Sodalites. *Zeolites* 14:1994.

Technetium Attenuation in the Vadose Zone: Role of Mineral Interactions

(Project Number: 70177)

Principal Investigator

Nancy J. Hess
Pacific Northwest National Laboratory
P.O. Box 999, MSIN P7-50
Richland, WA 99352
509-376-9808 (phone)
509-372-1632 (fax)
nancy.hess@pnl.gov

Co-Investigators

Steven D. Conradson
Los Alamos National Laboratory
MST-11, MS D429
Los Alamos, NM 87545
505-667-9584 (phone)
conradson@lanl.gov

James P. McKinley
Pacific Northwest National Laboratory
P.O. Box 999, MSIN K6-81
Richland, WA 99352
509-375-6841 (phone)
james.mckinley@pnl.gov

Kenneth M. Krupka
Pacific Northwest National Laboratory
P.O. Box 999, MSIN K6-81
Richland, WA 99352
509-376-4412 (phone)
ken.krupka@pnl.gov

Dhanpat Rai
Pacific Northwest National Laboratory
P.O. Box 999, MSIN P7-50
Richland, WA 99352
509-373-5988 (phone)
dhan.rai@pnl.gov

Raymond E. Wildung
Pacific Northwest National Laboratory
P.O. Box 999, MSIN P7-54
Richland, WA 99352
509-376-5680 (phone)
r.wildung@pnl.gov

Research Objective

High-level waste (HLW) has leaked into the vadose zone from buried single-shell tanks at the Hanford Site. Contaminant plumes containing radionuclides are slowly migrating toward the groundwater table. The accepted model of contaminant migration places technetium (Tc) at the leading edge of the plume due to the high mobility of the anionic species, TcO_4^-, in its oxidized state. However, recent drilling and sampling programs at the B-BX-BY and S-SX Hanford Site tank farms have revealed that the Tc distribution within the contaminant plume is more complex than anticipated and some Tc may be retained in the vadose zone as insoluble precipitates. This research project investigates possible mechanisms by which Tc associated with HLW leakages can be attenuated in the vadose zone. It **also** will provide fundamental information on surface-mediated reduction/precipitation reactions of Tc on Fe^{II}-containing mineral surfaces and the stability of Tc precipitates under conditions in the vadose zone at the Hanford Site. This information will provide much needed data for the development of models of Tc mobility in the vadose zone following closure of the tank farms. With reliable models, a major cost reduction in remediation efforts may be achieved by selecting sites that present the greatest environmental threat and designing remediation methods with the greatest efficacy.

Research Progress and Implications

This report summarizes work after 2.5 years of a 3-year study. We hypothesized that if Tc was to be retained in the vadose zone it must be present as a reduced precipitate. To test our hypothesis, we undertook three main tasks: 1) to evaluate the reductive capacity of Hanford formation sediments; 2) to determination of Tc speciation in contaminated Hanford formation sediments; and 3) to conduct solubility experiments under reducing conditions at which Tc^{IV} species are stable in solution.

Reductive Capacity

The reductive capacity of Hanford formation sediments has been evaluated by two methods: using sequential chemical extractions to determine the distribution of Fe^{II} and Fe^{III} species on sediments and using one-dimensional flow experiments to test the capacity of Hanford sediments to reduce pertechnetate. Using the methods of Heron et al. (1994), untreated sediments were compared to sediments that had been pretreated with 4 M NaOH for 200 hr and 450 hr. Although little change was observed between untreated and 200 hr pretreated sediments, the total quantity of Fe^{II} and Fe^{III} species more than doubled from 1260 μg/g to 2720 μg/g between the 200 hr and 450 hr pretreatments. The increase was largely due to an increase in availability of Fe^{III} species. The number of Fe^{II} surface sites was largely independent of pretreatment whereas the number of ion-exchangeable Fe^{II} species actually decreased upon pretreatment probably due to the precipitation of $Fe(OH)_2$.

The flow experiments were designed to simulate the geochemical conditions created by the leakage of HLW into the vadose zone and to test the reactions between pertechnetate and the sediments under caustic conditions. Solutions of oxygen-free 4 M NaOH and known concentrations of pertechnetate were injected into the loaded column and the concentration of Tc in the effluent was measured as a function of time. These experiments demonstrated that 1) the amount of Tc retained is independent of the concentration of Tc injected, 2) the lag in Tc retention observed between 1 and 2 pore volumes likely results from the gradual increase in Fe^{II} concentration as Fe bearing mineral phases dissolve in the presence of 4 M NaOH, and 3) the rate of Tc retention was also found to be weakly dependent on the flow rate through the column. Twelve sediment samples were removed from along the length of the column and subjected to various "oxidative conditions" to determine how tightly Tc was retained on the sediments. These conditions included oxygen-saturated water, 5 M HCl, 0.1 M HNO_3, and 1 M HNO_3. Oxygen-saturated water, 0.1 M HNO_3 and 5M HCl were relatively ineffective at oxidizing and remobilizing the Tc. Only 1 M HNO_3 removed all the retained Tc. The failure of mild oxidative treatments to remove more than 25% of the Tc from the column sediments strongly suggests that Tc is present as reduced species that are relatively insoluble and resistant to re-oxidation.

Autoradiography and scanning electron microscopy (SEM) analysis of the caustically treated sediments were conducted to determine whether reduced Tc precipitate was preferentially associated with specific mineral phases, such as Fe-oxides, or whether it was homogeneously distributed over all mineral surfaces. Figure 1 shows an autoradiographic map of the six sediment samples from the column. The dark spots on the autoradiographic map indicate that the Tc is highly localized and associated with mineral grains. The arrow near Sample 10 points to a region that was selected for SEM analysis. Figure 2a is the SEM image of this area, and it shows two grains several hundred microns in diameter. The bright areas in the backscattered electron (BSE) image of this same region, Figure 2b, indicate concentrations of elements with large number of electrons, such as Fe. Figures 2c and 2d are higher resolution BSE images of the grain on the right in Figures 2a and 2b. The white square in Figure 3d shows the area where an energy dispersive
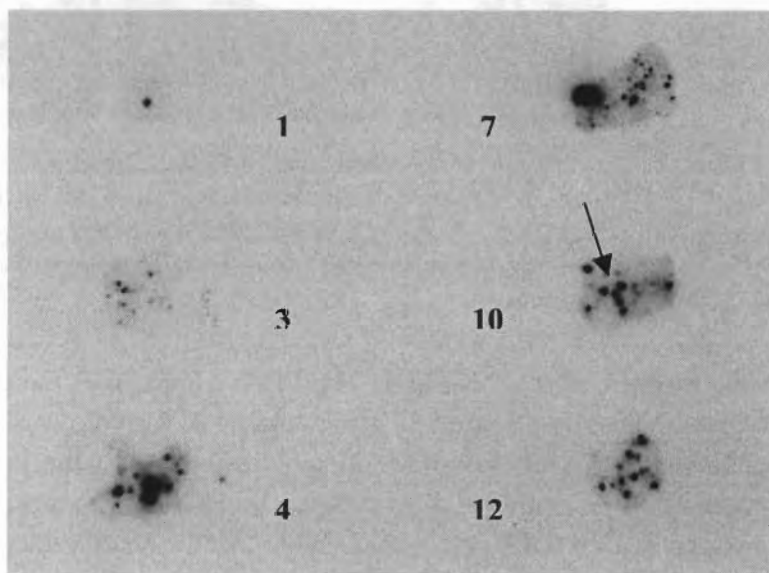
Figure 1. Autoradiographic map of six samples removed from the 1-D column. An arrow shows the location of the SEM studies in Figure 2.
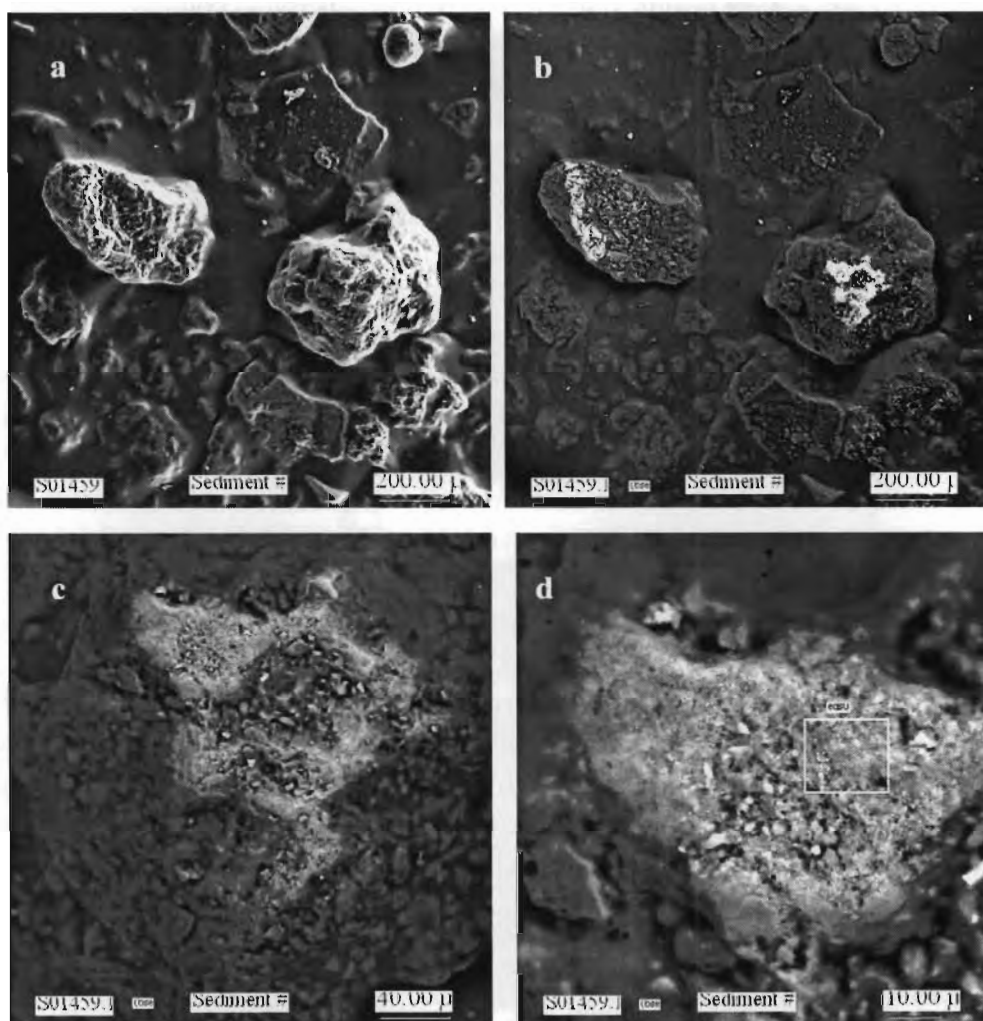
Figure 2. Scanning electron microscope images of Sample 10, Area 3 (indicated by arrow in Figure 1). Figure 2b is the backscattered electron (BSE) image of the region shown in Figure 2a. Figure 2c is a high-resolution BSE image of the grain on the left. Figure 2d, at higher resolution, shows the area where an energy dispersive spectrum, displayed in Figure 3, was aacquired.

spectrum (EDS) was acquired. The EDS, which gives the elemental composition of the scanned region, is shown in Figure 3. The presence of the elements Si, Al, O, Ca, Na, and K reflect the abundant quartz and feldspar minerals that constitute the Hanford formation sediments. The presence of Fe and Ti in this spectrum indicates the presence of minor amounts of Fe-oxides, perhaps Ti-rich magnetite grains. Note that Tc could not be observed in the EDS spectrum because the Tc K emission is at too high an energy, and the Tc L emission intensity is too weak to be detected at the Tc concentrations present in the sample. However, there is a direct correlation between the dark spots on the autoradiographic map, which indicate the presence of Tc, and high concentrations of Fe in the EDS of the SEM images.
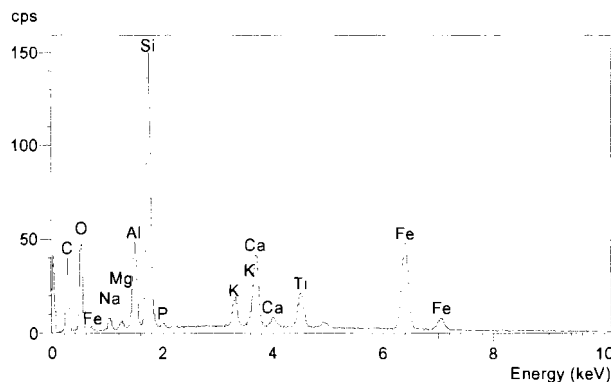
Figure 3. Energy dispersive spectrum of region indicated by the white box in Fig 2d. The intensity of Fe Kα and Kβ peaks indicate the presence of Fe-rich mineral phases.

The experimental results obtained under this task were critical in directing the research focus of the renewal proposal. We have demonstrated that the reductive capacity of Hanford sediments increases under basic conditions. In addition, we have found a set of experimental conditions that are relevant to the leakages of HLW from waste tanks at the Hanford Site under which pertechnetate is reduced by Hanford formation sediments. Furthermore, we observed evidence of the association of Tc with Fe-oxides that suggests surface-mediated reduction of pertechnetate is the operable mechanism.

Speciation of Hanford Formation Sediments

To determine the speciation of the Tc in the vadose zone, and especially whether Tc is associated with Fe-oxides, Tc-contaminated samples were obtained from three boreholes drilled in the SX tank farm in the 200 West Area at the Hanford Site. The horizons were selected for either autoradiography or x-ray absorption spectroscopy (XAS) analysis. Samples from five horizons from the 299-W23-19 borehole (B8809) adjacent to Tank SX-115 were selected for autoradiography experiments because the radioactivity was exclusively due to ^{99}Tc, and therefore, there would be no interference from other radionuclides such as ^{137}Cs. Only one horizon, which consisted of a very fine sand, showed evidence of nonuniform Tc distribution, suggesting an association of Tc with a particular mineral phase. Unfortunately, efforts to isolate and identify the composition of these sediment grains using scanning electron microscopy were unsuccessful due to the small size of the soil particles.

Since the oxidation state of Tc is the dominant factor in predicting the mobility of Tc in the vadose zone, samples with high Tc concentrations were selected from two boreholes adjacent to tank SX-108 for Tc K-edge XAS studies on beamline 11-2 at the Stanford Synchrotron Radiation Laboratory. Through analysis of the x-ray absorption near edge structure (XANES) portion of the XAS spectrum, the oxidation state of Tc in the samples can readily be determined. The selected samples contained significant Tc contamination in both the water and acid extracts suggesting that Tc was predominantly present as pertechnetate. The samples were analyzed both "as-received" and "water-washed." Ideally, the as-received samples should contain Tc as pertechnetate whereas the water-washed treatment would remove the highly soluble pertechnetate, leaving any insoluble reduced Tc^{IV} species behind. Unfortunately, even sample 4A/B/C, the horizon with the highest Tc contamination, contained insufficient Tc for bulk XAS

analysis. Therefore, a fraction of this sample and sample 15A from the slant borehole were prepared for micro x-ray fluorescence mapping on the PNC-CAT beamline at the Advanced Photon Source.

The micro x-ray fluorescence technique uses an x-ray beam a few microns in diameter that is rastered over the surface area of the sample. The energy of the x-ray beam is sufficient to excite x-ray fluorescence from elements of interest in the sample. The fluorescence spectrum is collected as a function of x-y position providing an elemental map of the sample. Comparison of the Tc distribution to other elements may reveal associations between Tc and other mineral phases; for example, Fe-oxides. The results of micro x-ray fluorescence mapping for samples 15A and 4A/B/C are shown in Figure 4. The elemental maps for Fe, Mn, and Ti are strongly correlated in both samples whereas the elemental maps for Fe and Ca are inversely correlated.
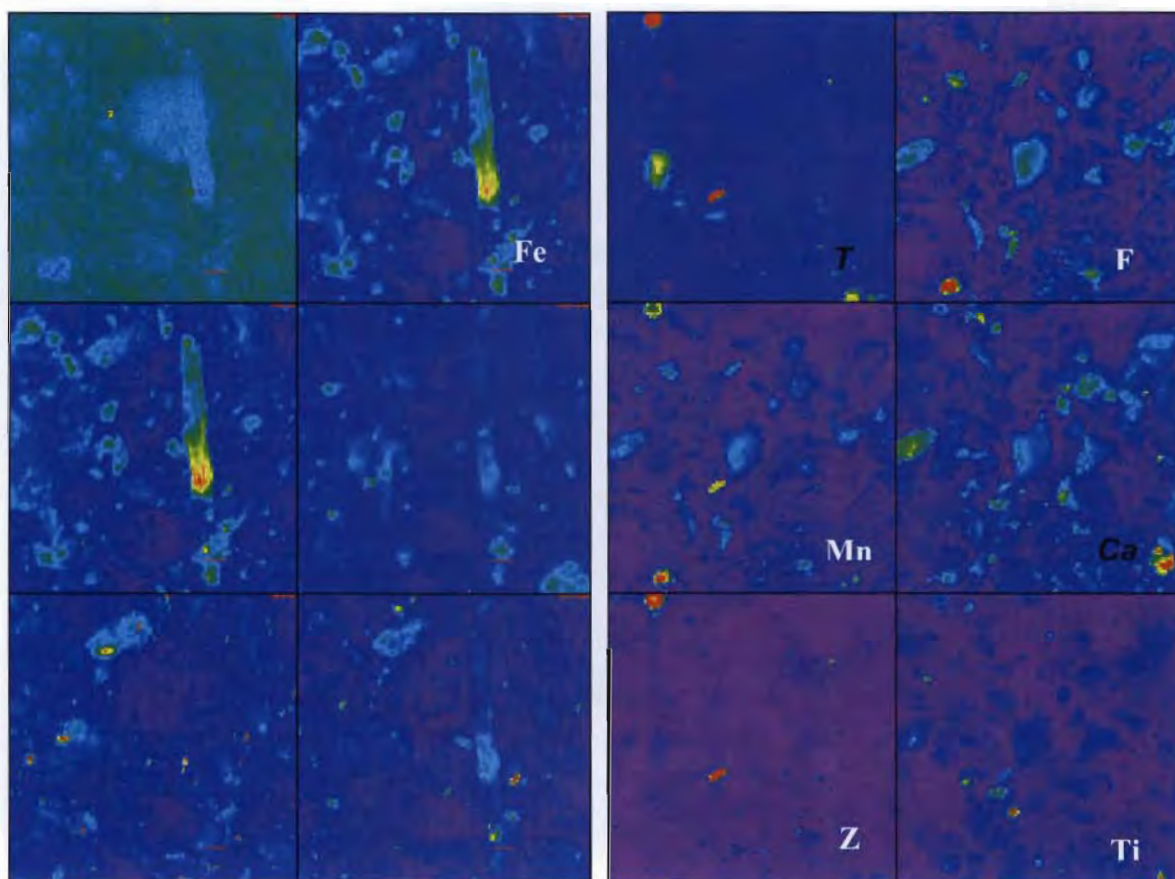
Figure 4. X-ray microprobe elemental maps for samples 15A , left, and 4A/B/C, right. Warm tones indicate high concentrations of the element indicated. The apparent Tc concentrations in sample 4A/B/C are actually due to interference from Zr.

The Fe-Mn-Ti correlation is likely due to the presence of titanomagnetite and Fe-Mn oxide grains. The inverse correlation with Ca probably reflects the presence of feldspars and calcite grains. A detailed analysis of the Tc "hot spots" in sample 4A/B/C using micro-XANES indicated that the apparent Tc signal was due to interference from Zr; the Tc K-edge at 21044 eV and the Zr L_{III}-edge at 22230 eV are too close in energy to be completely resolved.

Efforts to characterize the Tc in contaminated Hanford formation sediments from the tank farm drilling program have been unsuccessful although the reported Tc concentrations should have been sufficient for the experimental techniques we are using. We are currently reviewing the sampling protocols at the drill site and our sample preparation methods to determine if either, or both, of these processes are removing Tc from the samples before analysis. We are hopeful that the drill cores from the B-BX tank farm will provide sediment samples that will permit direct determination of the Tc speciation.

Solubility of Reduced Tc Species

The solubility of reduced Tc species was determined under a wide range of pH conditions and in the presence of high concentrations of chloride and bicarbonate/carbonate. We conducted solubility studies of TcO_2(am) as a function of pH from 6 M HCl to pH5 and as function of chloride concentration from 0.001 to 5 M NaCl. In addition, we have conducted these experiments under carefully controlled reducing conditions such that the preponderance of Tc is present in solution in the reduced Tc^{IV} oxidation state. The oxidation state determination based on solvent extraction techniques has been verified by analysis of the XANES portion of the x-ray absorption spectra and UV-Vis spectroscopy, where the solution concentrations are high enough. Powder x-ray diffraction and analysis of the EXAFS portion of the x-ray absorption spectra were used to characterize the solid phase in equilibrium with the solution phase.

Our solubility measurements are in good agreement with those reported in the literature in the pH range from 1 to 5 as shown in Figure 5. At acidities less than pH = 1, there is increasing discrepancy. At a given pH, increased solubility is observed with increased chloride concentration. Models of Tc solubility based on the existing thermodynamic data are in good agreement at low chloride concentrations and at pH greater than 1 but fail to predict the observed Tc solubility at high chloride concentration. EXAFS analysis of the solution species indicates that $TcCl_6$ species dominate at pH less than or equal to zero. Unfortunately, the concentration of Tc species is not sufficient for EXAFS analysis at higher pH, where mixed hydroxychloride Tc complexes and Tc hydrolysis products are thought to exist. Characterization of the solid phase by EXAFS analysis across the pH range indicates the stability of TcO_2(am) as the solubility
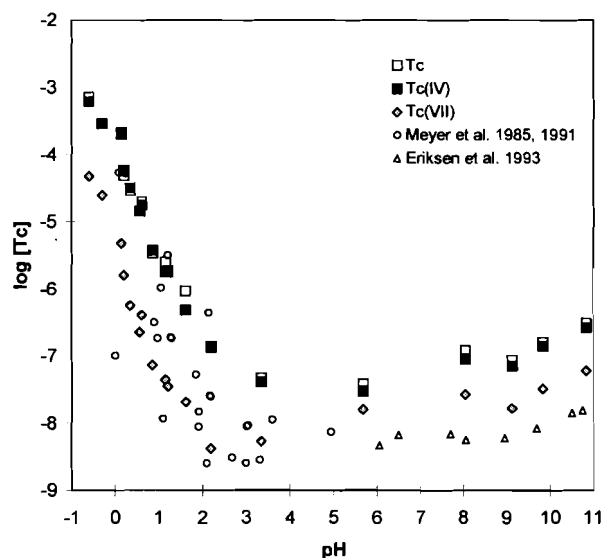
Figure 5a. Measured total Tc, Tc^{IV}, and Tc^{VII} in solution in contact with $TcO_2(am)$. The reported Tc^{IV} data of Meyer and Eriksen are shown for comparison.
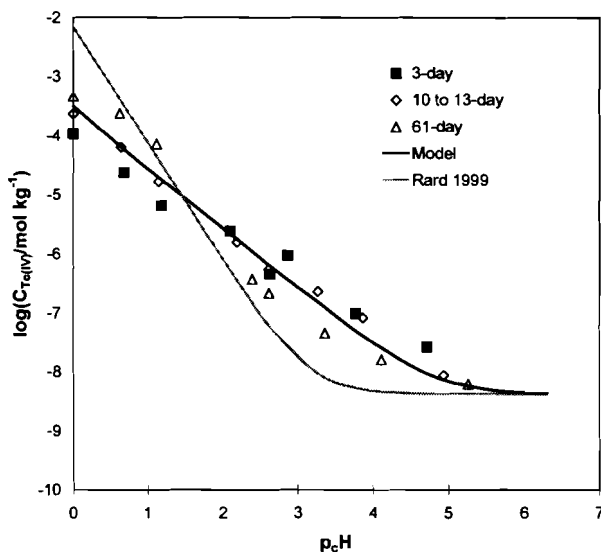
Figure 5b. Aqueous Tc^{IV} concentrations in contact with $TcO_2(am)$ in 2.5 M NaCl solution. The dashed line represents the predicted Tc concentration based on the existing thermodynamic data (Rard 1999). The solid line represents our improved model.

limiting phase. Analysis of the powder x-ray diffraction data from the solid sample indicates that solid phase is amorphous across the pH range. Solubility studies under alkaline conditions and in the presence of carbonate have just been initiated.

Planned Activities

Future experimental work includes batch experiments of Tc(VII) sorption/reduction on hematite, magnetite, biotite, and hornblende; micro-XANES analysis of sediments from column experiments; and solubility experiments in the presence of carbonate at constant ionic strength. Future data analyses include thermodynamic modeling of the solubility data and interpretation of the column studies, which then will be incorporated into journal publications.

Information Access

Journal Articles

Hess NJ, Y Xia, DA Moore, and D Rai. 2002. Thermodynamic model for the solubility of $TcO_2 \cdot nH_2O$ in acidic solutions and high NaCl concentrations. To be submitted to *Journal of Solution Chemistry*.

Szecsody JE, JP McKinley, and NJ Hess. 2002. The effect of hyperalkaline high level waste simulants on the retention of Tc in Hanford Formation sediments. To be submitted to *Environmental Science and Technology*.

Presentations

Hess NJ, K Krupka, J McKinley, D Rai, R Wildung, and S Conradson. 1999. Technetium Attenuation in the Vadose Zone: Role of Mineral Interactions, EMSP Kickoff Workshop, November 1999, Richland, Washington.

Hess NJ, Y Xia, D Rai, K Krupka, J McKinley, R Wildung, and S Conradson. 2000. Technetium Attenuation in the Vadose Zone: Role of Mineral Interactions, National DOE/EMSP Workshop, April 2000, Atlanta, Georgia.

Hess NJ, D Rai, J McKinley, K Krupka, R Wildung, and S Conradson. 2000. Technetium Attenuation in the Vadose Zone: Role of Mineral Interactions, FY2001 Vadose Zone Principal Investigator Workshop, November 2000, Richland, Washington.

Hess NJ, J Szecsody, J McKinley, D Rai, K Krupka, R Wildung, and S Conradson. 2001. Technetium Attenuation in the Vadose Zone: Role of Mineral Interactions, FY2002 Vadose Zone Principal Investigator Workshop, November 2001, Richland, Washington.

Web addresses

1999-2000 Progress Report. http://www.osti.gov/em52/2000projsum/70177.pdf

Poster Board EMSP Workshop, April 2000.
http://www.osti.gov/em52/NWS2000_Posters/id70177.pdf

The Influence of Calcium Carbonate Grain Coatings on Contaminant Reactivity in Vadose Zone Sediments

(Project Number: 70121)

Principal Investigator

John M. Zachara
Pacific Northwest National Laboratory
P.O. Box 999, MSIN K8-96
Richland, WA 99352
509-376-3254 (phone)
509-376-3650 (fax)
mailto:john.zachara@pnl.gov

Co-Investigators

Scott Chambers
Pacific Northwest National Laboratory
P. O. Box 999, MSIN K8-93
Richland, WA 99352
509-376-1766 (phone)
509-376-5106 (fax)
sa.chambers@pnl.gov

Gordon E. Brown, Jr.
Stanford University
Stanford, CA 94305
650-723-9168 (phone)
650-725-2199 (fax)
gordon@pangea.stanford.edu

Carrick M. Eggleston
University of Wyoming
P.O. Box 3006
Laramie, WY 82071
307-766-6769 (phone)
307-766-6679 (fax)
mailto:carrick@uwyo.edu

Research Objective

The primary objective of this project is to investigate the role of calcium carbonate grain coatings on adsorption and heterogeneous reduction reactions of key chemical and radioactive contaminants in sediments on the Hanford Site. Research will ascertain whether these coatings promote or discourage contaminant reaction with sediment mineral particles, and whether calcium carbonate phases resulting from waste-sediment reaction sequester contaminants through coprecipitation. The research will provide new conceptual models of contaminant reaction/retardation processes in Hanford sediments (for $^{90}Sr^{2+}$ and $Cr(VI)O_4^{2-}$ primarily) and improved geochemical models to forecast the future behavior of in-ground contaminants.

Research Progress and Implications

This project was initiated in fiscal year 1999 and is in its final year. Two primary research activities have been undertaken: 1) Characterization of $^{90}Sr^{2+}$ adsorption and exchange in pristine and contaminated calcareous Hanford sediments and 2) investigation of the role of calcium carbonate grain coatings on the heterogeneous reduction of $Cr(VI)O_4^{2-}$ by magnetite in model and sediment systems.

Characterization of Strontium Adsorption and Exchange

The ion exchange behavior of Sr^{2+} was studied in pristine, calcareous sediments in both Na and Ca electrolytes. The sediment samples were drawn from Hanford's B-BX-BY and T-TX-TY tank farms. Strontium adsorption in both systems displayed strong dependence on electrolyte concentration, consistent with an ion exchange process. The sand-textured sediments exhibit a small cation exchange capacity (approximately 10^{-5} eq/g) resulting from the presence of detrital layer silicates. A multicomponent cation exchange model (Na-Ca-Sr) was developed for the entire data set that includes three ion exchange selectivity coefficients K_{Na-Sr}, K_{Ca-Sr}, and K_{Na-Ca} (where K = the Vanselow selectivity coefficient) and the measured cation exchange capacities. Because the Hanford sediments contain appreciable ion-exchangeable $^{86/87}Sr^{2+}$, the adsorption process of contaminant $^{90}Sr^{2+}$ (which is typically present at 3 to 4 orders of magnitude lower concentration than indigenous $^{86/87}Sr^{2+}$) is one of isotopic exchange with the native Sr pool. The $^{90}Sr^{2+}$-K_d is therefore controlled by the K_d of the indigenous Sr pool, which, in turn, is predictable from our developed multicomponent cation exchange model. Adsorption experiments with $^{86/87/90}Sr^{2+}$ are currently being performed to document the predictability of these relationships with water compositions characteristic of different Hanford waste-release scenarios.

In other experiments, we have studied the mineralogic association of sorbed $^{90}Sr^{2+}$ and its desorption kinetics from contaminated sediments collected beneath leaked tank B-110 in Hanford's B tank farm complex. The waste stream leaked to these sediments was from the

Sr-recovery process. We have succeeded in isolating $^{90}Sr^{2+}$-containing particles from the sediments (Figure 1) and now are characterizing these in detail using various forms of electron microscopy. We have contacted one sediment sample from the B-110 borehole that contained approximately 10,000 pCi/g of sorbed $^{90}Sr^{2+}$ with various electrolytes intended to desorb

- ion-exchanged $^{90}Sr^{2+}$ (0.01, 1, and 5 mol/L $NaNO_3$; 0.05 mol/L $Ca(NO_3)_2$)
- coprecipitated $^{90}Sr^{2+}$ (1 mol/L NaOAc at pH 5; 0.5 mol/L HCl) (Figure 2).

Figure 1. Samples of B-110 sediment were mounted on TEM stubs and imaged by phosphor-luminescence. The dark areas are mineral grains or aggregate containing ^{90}Sr. These grains were imaged by scanning electron microscopy and then were selectively removed for detailed mineralogic characterization and spatial Sr analysis.
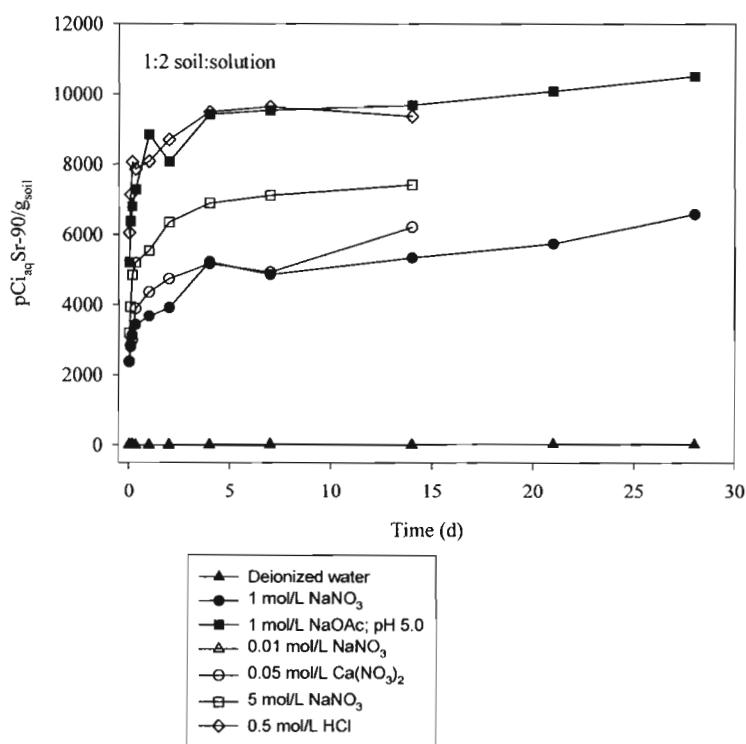
Figure 2. Time-dependent desorption of ^{90}Sr from contaminated B-110 sediment. ^{90}Sr was released to the sediment over 30 years ago in the form of a Sr recovery waste containing Na-HCO_3 and complexants. Extraction with 0.01, 1, and 5 mol/L Na and 0.05 mol/L $(Ca(NO_3)_2$ removes inexchangeable ^{90}Sr, while NaOAc at pH 5 and 0.5 mol/L HCl dissolve host carbonate phases as well.

3.27

The experiments have demonstrated that approximately 75% of the sorbed $^{90}Sr^{2+}$ is associated with the exchange complex, and 25% is associated with carbonate grain coatings that have resulted from waste-sediment reaction. These data now are being modeled with our multicomponent exchange model linked with a precipitation model. Collectively, these results provide a basis for predicting the geochemical behavior of $^{90}Sr^{2+}$ in various waste streams and subsurface sediments at the Hanford site.

Investigation of Calcium Carbonate Grain Coatings

The growth of complete calcium carbonate overlayers on synthetic magnetite (001) surfaces was accomplished by a biomineralization approach termed the polymer-induced liquid precursor (PILP) method. During this solution-based approach, poly-aspartate coats the magnetite surface and acts as a surfactant upon which primarily vaterite nucleates as a continuous film. An atomic force microscopy micrograph taken during early growth stages displayed a beta-sheet-like layer, reminiscent of poly-aspartate, with a carbonate overlayer nucleating atop. These calcium carbonate overlayers of vaterite crystal structure interfere with the reduction of $Cr(VI)O_4^{2-}$ at the magnetite-water interface. Films as thin as 20 to 25 angstroms inhibit the reduction of aqueous chromate throughout the pH range of 6 to 8 for exposures less than one hour (Figure 3). Depending upon the carbonate film thickness, however, $Cr(VI)O_4^{2-}$ reduction did occur after
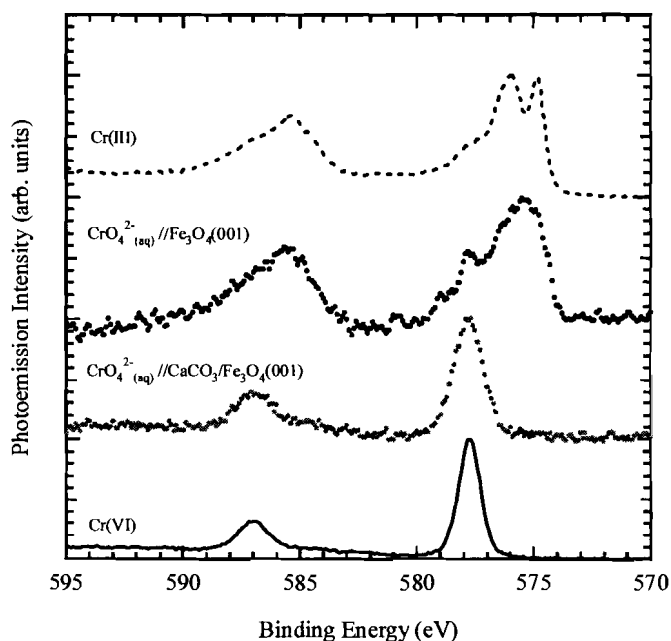
Figure 3. High-energy resolution Cr 2p core-level spectra for synthetic magnetite(001) covered with calcium carbonate (gray) and not covered (black). Reference spectra for Cr(VI) and Cr(III) also are shown.

extended reaction times due to dissolution of the calcium carbonate coatings. Surprisingly, however, secondary ion mass spectrometry (SIMS) analysis of samples from extended reaction showed that Cr was concentrated on the magnetite surface in areas of high carbon and less so in areas of high Fe content. This was puzzling until the experiment was performed in which the $Cr(VI)O_4^{2-}$ solution was also saturated with calcium carbonate. Expecting a lower dissolution rate of the coating due to a saturated solution and less $Cr(VI)O_4^{2-}$ reduction, we found, in contrast, that there was a significant Cr(III) photoemission signature. This was due to photoreduction of Cr(VI) to Cr(III) in the presence of adventitious carbon during analysis in the x-ray photoemission chamber.

These findings provide a clear explanation for why Cr(VI) and Tc(VII) are stable valence states in the Hanford subsurface, in spite of the presence of significant magnetite and ilmenite in the sediments. Calcium carbonate grain coatings prevent heterogeneous reduction.

Planned Activities

Being well on in the last funded year of the project, most of our remaining activity is focused on publication of results. Some lingering experimentation with the $^{90}Sr^{2+}$-containing B-110 sediments and magnetite isolated from the Hanford sediment will continue to completion in the remaining months of fiscal year 2002. Some of our research results from the B-110 sediments will be incorporated into a Corrective Action Assessment Report for the B-BX-BY Tank Farms in July, thereby providing key scientific support for an important decision milestone at the Hanford Site.

Information Access

Droubay T and SA Chambers. 2001. Surface-sensitive Fe 2p photoemission spectra for alpha-Fe_2O_3(0001): The influence of symmetry and crystal-field strength - Art. No. 205414. *Physical Review* B 6420(20):5414-+.

Droubay T and SA Chambers. 2002. Influence of Calcium Carbonate Coatings on Aqueous Hexavalent Chromium Reduction by Fe_3O_4(001). *Surface Science*. Submitted.

Zachara JM, P Lichtner, and SC Smith. 2002. Ion exchange of Sr^{2+} in calcareous subsurface sediment and isotopic exchange of $^{90}Sr^{2+}$ as a retardation mechanism. *Geochimica et Cosmochimica Acta*. Submitted.

Zachara JM, P Lichtner, and SC Smith. 2002. Mineralogic residence and desorption kinetics $^{90}Sr^{2+}$ from contaminated subsurface sediments. *Environmental Science and Technology*. Submitted.

The Aqueous Thermodynamics and Complexation Reactions of Anionic Silica Species to High Concentration: Effects on Neutralization of Leaked Tank Wastes and Migration of Radionuclides in the Subsurface

(Project Number: 70163)

Principal Investigators

Dr. Andrew R. Felmy
Pacific Northwest National Laboratory
P.O. Box 999, MSIN K8-96
Richland, WA 99352
509-376-4079 (phone)
509-376-3650 (fax)
ar.felmy@pnl.gov

Dr. Gregory Choppin
The Florida State University
Department of Chemistry, B-164
Tallahassee, FL 32606-3006
904-644-3875 (phone)
904-644-8281 (fax)
Choppin@chemmail.chem.fsu.edu

Dr. David A. Dixon
Pacific Northwest National Laboratory
P.O. Box 999, MSIN K1-83
Richland, WA 99352
509-372-4999 (phone)
509-375-6631 (fax)
da.dixon@pnl.gov

Research Objective

Highly basic tank wastes contain several important radionuclides, including ^{90}Sr, ^{99}Tc, and ^{60}Co, as well as actinide elements (i.e., isotopes of U, Pu, and Am). These highly basic tank wastes are known to have leaked into the vadose zone at the Hanford Site. Upon entering the sediments in the vadose zone, the highly basic solutions dissolve large concentrations of silica from the silica and aluminosilicate minerals present in the subsurface. These dissolution reactions alter the chemical composition of the leaking solutions, transforming them from a highly basic (as high as 2M NaOH) solution into a pore solution with a very high concentration of dissolved silica and a significantly reduced pH. This moderately basic (pH 9 to 11), high-silica solution has the potential to complex radionuclides and move through the subsurface. Such strong radionuclide complexation is a currently unconsidered transport vector that has the potential to expedite radionuclide transport through the vadose zone. These strong complexation effects have the ability to significantly alter current conceptual models of contaminant migration beneath leaking tanks.

In this project, we are determining the aqueous thermodynamics and speciation of dissolved silica and silica-radionuclide complexes to high silica concentration using a combination of

1. studies of chemical species structure and composition [via nuclear magnetic resonance (NMR) and, where applicable, laser-induced fluorescence spectroscopy and x-ray absorption spectroscopy]

2. molecular simulations to help identify key species structures and assist in interpreting experimental measurements

3. fundamental physical chemistry measurements, including solubility, electromotive force, and isopiestic measurements, to obtain the necessary thermodynamic data for predicting contaminant complexation and waste neutralization reactions.

The radioactive elements we are studying include Sr, Co, Cs, Am(III), and U(VI).

Research Progress and Implications

This report covers the first 2 years of this 3-year project . Our research efforts have been focused in three principal areas: silica speciation studies, complexation studies, and reactive transport modeling.

3.32

Silica Speciation Studies

Speciation and Aqueous Thermodynamics

In aqueous solutions containing moderate concentrations of dissolved silica (i.e., ~ 0.01 M) and high pH (>10), a wide range of silica species can be simultaneously present in solution. These species can include monomers, dimers, trimers, tetramers, and hexamers. The final result was an accurate aqueous thermodynamic model for silica species valid to high ionic strengths and high dissolved silica concentrations

Molecular Simulations

A molecular modeling capability also was developed to help identify structural reasons for observed polysilicate stability, the tendency of the polysilicates to protonate or react with counter ions, and the stability of the polysilicate-metal complexes. Unfortunately, existing molecular modeling capabilities cannot simulate the full range of interactions including fully solvated complexes; dissociating water molecules (which allows protonation); and inclusion of counter ions (i.e., Na^+). Fortunately, extensive crystallographic investigations of the structures of $NaOH \cdot nH_2O$ provide valuable information on the sodium-water and hydroxide-water interaction in well-defined structures. Therefore, we began the development of our modeling capability by conducting computational investigations on the five major NaOH hydrates whose proton positions have been determined: $NaOH \cdot (1, 3.5, 4\alpha, 4\beta, 7)H_2O$. The structural uncertainties associated with the hydrated crystals are much more controlled than in the case of aqueous species; hence, the structural analysis can proceed with less ambiguity. As a first step, we used plane wave pseudopotential density functional methods invoking the Perdew-Burke-Ernzerhof exchange-correlation functional to investigate theoretically the structures of five NaOH hydrates through optimization of lattice parameters and atomic coordinates. This task resulted in the final molecular model used to identify the effects of counter-ion binding and protonation of the aqueous silica complexes.

Kinetics of Polymerization

In addition to the equilibrium thermodynamics of the silicate species, the polymerization kinetics of the aqueous silicate species was studied in a companion effort at Florida State University. Information on the kinetics of polymerization is needed not only to assist in determining the expected equilibration times for the equilibrium speciation studies but also for interpreting the kinetic data for mineral dissolution reactions. In the latter case, polymerization of polysilicate species can be a rate-limiting step in silicate mineral dissolution because monomeric units are believed to control the rate of dissolution. To investigate these issues, the kinetics of the silica

polymerization reactions was investigated by monitoring the concentration of monomeric ortho-silicate using the silica molybdate absorbance method. In this way, the fraction of ortho-silicate was determined over broad ranges of total silica concentration, pH, ionic strength, and aging time.

These studies provided detailed information on the kinetics of polymerization of ortho-silicates. In general, the silicate polymerization rate occurred on the order of minutes to hours, depending upon the specific ionic strength, pH, and total silica concentration studied. The initial rate of polymerization was quite rapid, but a slower rate of polymerization subsequently was observed, due presumably to the formation of higher-order polysilicates. The final equilibrium data also were compared satisfactorily to the aqueous thermodynamic model for polysilicates described above.

Identification of Enantomers

In addition to these thermodynamic results, our NMR analysis also was able to identify previously unknown enantomeric forms of the polysilicate species and thereby explain many previously unidentified peaks in the NMR spectra.

To date, 16 different silicate polymers in concentrated aqueous solutions have been identified conclusively (see Figure 1), with the largest of these containing eight silicon atoms. Essentially all of the found polymers beyond the monomer and dimer were identified solely through the use of solution state ^{29}Si NMR measurements. However, despite the success of past workers in identifying the highest concentration polymers, numerous features in the ^{29}Si NMR spectra of silicate solutions cannot be explained in terms of the 16 known species. This is clearly illustrated in the ^{29}Si NMR spectrum shown in Figure 2. The spectrum is a superposition of spectra from different polymers, and the complicated appearance reflects the numerous distinct molecules that must be present in the solution. Sixty-six resolved lines can be counted in this spectrum, although many more have undoubtedly been missed due to spectral overlap and/or weak signal intensity. Of the 66 lines, the 16 known polymers account for only 32.

The one-dimensional NMR techniques used in previous studies have largely been ineffective in deducing silicate structures from the remaining unassigned NMR peak information. Alternative methods that avoid these difficulties in obtaining the desired correlation information have been introduced in the time since the one-dimensional silicate work was originally reported. These alternative techniques are based on two-dimensional homonuclear correlation spectroscopy (COSY) experiments of ^{29}Si-enriched silicate solutions. With the new data contained in recently acquired two-dimensional spectra, we have renewed the search for silicate polymers that have eluded previous investigators.
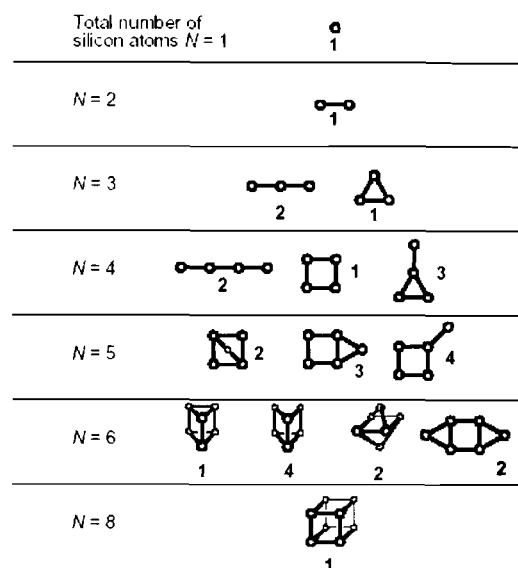
Figure 1. Silicate polymers previously found by ^{29}Si NMR spectroscopy to exist in aqueous solution. The circles represent Si atoms and the sticks symbolize bridging O atoms. The number of ^{29}Si NMR lines associated with each structure is shown next to the molecule. The hexamer in the shaded box has been identified in both cis and trans isomeric forms.
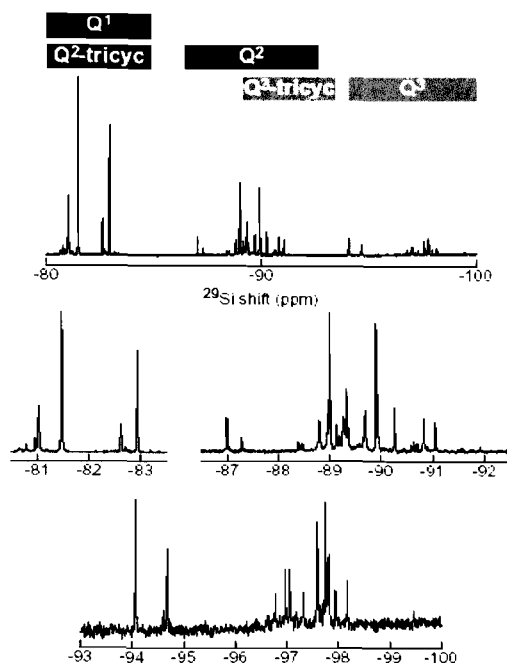
Figure 2. Natural abundance (4.7%) ^{29}Si NMR spectrum of 0.30 molal SiO$_2$ in 0.20 molal NaOH(aq), acquired at a ^{29}Si frequency of 99.30 MHz. The sample temperature was 15°C. The Q^0 region (>-80 ppm) and Q^4 region (<-95 ppm) of the spectrum have been truncated; no Q^4 lines were observed.

3.35

By analogy with tetravalent carbon, a tetravalent silicon atom under certain circumstances will not be superimposable on its mirror image. Any silicate species containing such a site therefore potentially has a structurally distinguishable isomeric counterpart with a different set of NMR lines. The rendering of such sites is problematic in a two-dimensional illustration, and representations such as those in Figure 1, which are common in the scientific literature on solution-state silicate structures, can conceal a multiplicity of distinct molecules that satisfy a given bonding network. Eight examples of silicate polymers containing chiral sites, which are highlighted, are depicted in Figure 3. In at least three of these polymers (C, D, and E), one of the isomers formed by reflecting the chiral site appears not to be a realistic structure. For the other molecules, there is strong evidence indicating the existence of multiple isomeric forms. A manuscript describing the identification of these new species is in preparation.
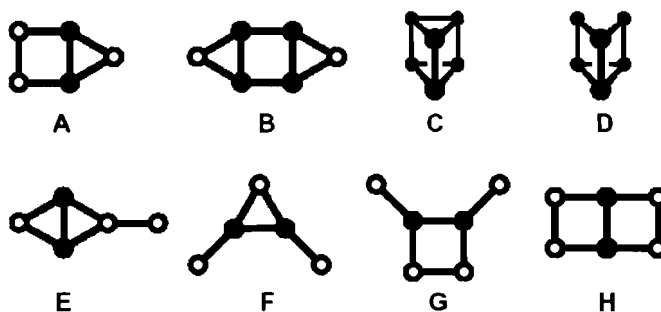
Figure 3. Silicate polymers containing chiral silicon atoms. The chiral sites are symbolized by filled circles. The top four polymers have previously been reported, while the bottom four polymers are proposed for the first time based on new two-dimensional NMR results.

Summary of Silica Speciation Studies

In summary, for the silica speciation studies, we have completed our aqueous thermodynamic model at 25°C, developed a molecular model for polysilicates in solution, studied the kinetics of polmerization, and identified new enantomeric forms of the polysilicates. This effort has resulted in three manuscripts published or in review and one manuscript in preparation.

Complexation Studies

Once an accurate model of the aqueous silica reactions was established, the studies were focused on the radionuclide complexation reactions, specifically with Sr, Co(II), Eu(III)/Am(III), and U(VI). These elements were selected because of their potential importance in the Hanford vadose zone and/or their relevance as analogs for other actinide oxidation states [i.e., Eu(III) as an analog for trivalent actinides and U(VI) as an analog for Pu(VI)]. Cobalt was selected for study even though the half-life of the dominant radioactive isotope ^{60}Co is only 5.26 years. Such a short half-life means that ^{60}Co probably will not represent a significant hazard to groundwater

outside the immediate vicinity of a tank leak. Nevertheless, ^{60}Co is a significant contributor to the gamma logs used to assess the extent of radioactive material contamination in the vadose zone, so its movement and potential complexation with the dominant ligands present still must be assessed, at least in the immediate vicinity of a tank leak.

Studies were initiated at both Pacific Northwest National Laboratory (PNNL) and Florida State University (FSU). The studies at FSU focused on monomeric complexation and were investigated primarily by solvent extraction techniques. The studies at PNNL focused on polysilicate interactions and were conducted at higher base and dissolved silica concentrations. The results of these investigations are reported below.

Strontium Studies

Our current knowledge about the aqueous speciation and solubility of Sr in these basic silica solutions is almost completely absent. No definitive stability constants had yet been published for aqueous strontium silicate species, and only a very limited number of strontium silicate solids (i.e., $SrSiO_3$, Sr_2SiO_4, $Na_4SrSi_3O_9$, $SrSiO_3$, ...) had been identified and characterized . With these factors in mind, the purposes of this study were 1) to determine if highly basic silica-containing solutions result in the formation of soluble strontium-silicate complexes or result in the precipitation of insoluble strontium silicate solids, and 2) to identify, if possible, the phases or solution species that form and their solubility products or aqueous complexation constants. To achieve these objectives, we conducted solubility studies of strontium silicate solutions over a range of dissolved silica, strontium, and hydroxide concentrations extending to long equilibration times (286 days). The solid phases formed in the system were analyzed by a variety of techniques including total chemical analysis, x-ray diffraction (XRD), scanning electron microscopy (SEM), and thermogravimetric analysis (TGA).

The results showed that amorphous strontium silicate precipitates can form from aqueous solution beginning at approximately pH 10 and become quasi-crystalline at higher pH (11.5 to 12). The quasi-crystalline precipitates have a chemical formula of $Sr_5Si_6O_{16}(OH)_2 \cdot 5H_2O$, a structure similar to tobermorite, and a solubility product of log K = -38.0 ± 0.7 for the overall reaction, $5H_2O + Sr_5Si_6O_{16}(OH)_2 \cdot 5H_2O = 5Sr^{2+} + 6H_3SiO_4^- + 4OH^-$. The $Sr_5Si_6O_{16}(OH)_2 \cdot 5H_2O$ phase has not been previously reported. Scanning electron microscopy analysis of the alcohol-washed precipitates showed a fine granular structure similar to calcium silicate hydrates. De-ionized water-washing of the precipitates resulted in dissolution and growth of surface phases with the classical "sheaf of wheat" nucleation structure previously identified only for calcium silicate hydrates. No evidence for Sr^{2+} complexation with polysilicate species was observed. An association constant for the monomeric species $SrH_2SiO_4(aq)$ of log K = 2.86 was estimated, but such a species never accounted for more than 50% of the total dissolved Sr concentration. This conclusion was extensively tested in solutions of variable Si/Sr ratio, pH, ionic strength, and

other characteristics. All of these data indicate that the Sr(II)-anionic silica interactions are not as strong as the corresponding solid phase formation reactions. Therefore, it is unlikely that dissolved silica species can be a significant transport vector for Sr in these basic, high-silica solutions. These studies have been completed and the results submitted and accepted for publication.

Solvent Extraction Studies of Monomeric Silica Complexation

The interactions of UO_2^{2+}, Eu^{3+}, Am^{3+}, Co^{2+}, and Ni^{2+} with monosilicic acid were studied by solvent extraction methods at FSU. Ni^{2+} was included with the other metal ions principally to provide a check on the results for Co^{2+} as described below. The final results are reported in Table 1.

Table 1. Stability Constants for Metal – o-Siliciate Complexes

Metal Ion	Log β_1	Log β_2	I, M
UO_2^{2+}	6.79±0.25	12.85±0.28	0.20
Am^{3+}	7.46±0.22		0.20
Eu^{3+}	7.04±0.15	11.7	0.20
Co^{2+}	4.85±0.25		0.20
Ni^{2+}	5.41±0.23		0.20

The stability constants for UO_2(II), Eu(III), and Am(III) complexes agree fairly well with the corresponding literature values even though the *ortho*-silicate concentration was determined using the new model developed in this project. The value for Am(III) is also greater than for Eu(III) in a consistent fashion for what is expected from carbonate and hydroxide complexes. The value for Co(II) is also slightly less than the value for Ni(II) consistent with complexation strength of these two cations for other ligands. The results for Co(II) are particularly interesting as even the stability constant for the monosilicic acid complex ($CoH_3SiO_4^+$) has an equilibrium constant approximately 1.5 log units greater than the corresponding carbonate complex. Thermodynamic calculations using these data and our new data on silicate species formation, along with the hydrolysis constants for Co(II), indicate that the Co(II) silicate complex will predominate over all other solution species from pH 8 to approximately 11.5 and to high carbonate concentration [saturation with respect to $CoCO_3$(c)]. Therefore, even in the absence of polysilicate complexation, Co(II) transport will be significantly facilitated by the presence of dissolved silica over the typical range of pH values found in the vadose zone. A manuscript on these results is being prepared for publication.

These results for the monomeric complexes also are needed to help unambiguously interpret experiments at higher dissolved silica concentration where a variety of polysilicate-metal complexes can be present.

Anion and Cs⁺ interactions

Anion and Cs$^+$ interactions

In addition to the metal silicate complexation reactions that have been studied, selected experiments were conducted with anions (SO_4^{2-}, F$^-$, and PO_4^{3-}) to determine if any significant silicate-anion interactions occurred in solution. Such interactions have been clearly identified in more acidic solutions, but no clear information existed under basic conditions. Therefore, screening-level studies were conducted. The studies provided measurements of the NMR spectra of identical solutions in which a small fraction of the background electrolyte, $NaNO_3$, was replaced by the corresponding anionic salt (e.g., NaF, Na_2SO_4, ...). In all cases examined, the NMR spectra were identical, indicating a lack of strong complexation effects of these anions at high pH.

Interestingly, when the $NaNO_3$ electrolyte was replaced by $CsNO_3$, new previously unidentified peaks appeared at ^{29}Si chemical shifts values typical of polysilicate complexes. We are preparing different solutions at variable $CsNO_3$ concentration and silicate concentration in an attempt to identify the new species that formed. At this time, our best estimate is that they represent previously unidentified Cs-polysilicate species. Although such species represent only a small fraction of the total Cs in solution (the vast majority is free Cs$^+$), identification of such species and determining the range of their stability may help shed light onto more complex and important Cs-silicate interactions. Such Cs-silicate interactions, specifically Cs uptake at frayed edge sites on aluminosilicates, are believed to be the dominant mechanism of Cs attenuation in the Hanford vadose zone.

Development of Reactive Transport Models

Development of Reactive Transport Models

To help ensure that the thermodynamic data gathered as part of this study were applied to actual vadose zone issues at Hanford and other DOE sites, we collaborated with several investigators on the Hanford Vadose Zone Science and Technology (HVZS&T) program. As part of this collaboration, we have supplied the necessary computer code to implement the Pitzer thermodynamic model in the subsurface reactive transport models being used to model reactive chemical transport in the vadose zone. The most recent thermodynamic database, developed as part of this and other projects, was also supplied and updated during this study.

Information Access

Publications and Presentations

Felmy AR, HM Cho, JR Rustad, DA Dixon, and GR Choppin. 2000. The Aqueous Thermodynamics and Complexation Reactions of Anionic Silica Species to High Concentration. EMSP Vadose Zone Workshop Presentation, November 28, Richland, WA.

Felmy AR, HM Cho, JR Rustad, and MJ Mason. 2001. An Aqueous Thermodynamic Model for Polymerized Silica Species to High Ionic Strength. *J. of Solution Chemistry* **30**:509-525.

Felmy AR, MJ Mason, PL Gassman, and DE McCready. The Formation of Strontium Silicates at Low Temperature and the Solubility Product of Tobermorite Like $Sr_5Si_6O_{16}(OH)_2 \cdot 5H_2O$. *American Mineralogist*. Accepted.

Felmy AR, HM Cho, GR Choppin, DA Dixon, JR Rustad, and Z Wang. 2001. The Aqueous Thermodynamics and Complexation Reactions of Anionic Silica Species to High Concentration. EMSP Vadose Zone Workshop Presentation, November 4-6, Richland, WA.

Krejzler J and GR Choppin. Factors Affecting Free o-Silicate Concentration in Aqueous Solution. *Talanta*. In review.

Krejzler J and GR Choppin. 2001. Complexation of Metal Cations by o-silicates. Presented at the 222nd ACS National Meeting, August 26-30, Chicago, IL.

Lichtner PC and AR Felmy. Estimation of Hanford SX Tank Waste Compositions from Historically Derived Inventories. *Computers & Geosciences*. Special issue on Reactive Transport Modeling in the Geosciences. Accepted.

Rustad JR, AR Felmy, KM Rosso, and EJ Bylaska. Ab initio investigation of the structures of NaOH hydrates and their Na^+ and OH^- coordination polyhedra. *American Mineralogist*. In review.

Wang Z, X Xia, MJ Mason, and AR Felmy. 2001. Investigations of Cm(III) Speciation in Strongly Basic Solutions by Time Resolved Laser Fluorescence Spectroscopy. Presented at the 222nd ACS National Meeting, August 26-30, Chicago, IL.

Other Contributions

In addition to the previously described scientific contributions, the principal investigators on this project also worked to enhance the overall success of the EMSP program. Specifically,

- Andrew Felmy (PNNL) was a co-organizer of the Accomplishment of the Environmental Management Sciences Program (EMSP) Symposium at the 222nd ACS National Meeting held in Chicago, Illinois, on August 26-30, 2001. The symposium consisted of five different sessions covering the areas of subsurface science, solution and tank chemistry, radionuclide and contaminant separation methods, analytical and sensing techniques, and waste form treatment and development. There were 65 oral or poster presentations in the symposium.

- Greg Choppin (FSU) serves as a member of the EMSP Advisory Committee and of the NAS/NRC Board of Radioactive Waste Management.

In addition to other technical presentations, the principal investigators on this project gave two presentations at EMSP/HVZGWP coordination meetings held in Richland, Washington.

Influence of Clastic Dikes on Vertical Migration of Contaminants in the Vadose Zone at Hanford

(Project Number: 70193)

Principal Investigator

Christopher J. Murray
Pacific Northwest National Laboratory
P.O. Box 999, MSIN K6-81
Richland, WA 99352
509-376-5848 (phone)
509-376-5368 (fax)
Chris.Murray@pnl.gov

Co-Investigator

John L. Wilson
Department of Earth and Environmental Science
New Mexico Institute of Mining and Technology
Socorro, NM 87801
505-835-5308 (phone)
970-245-1442 (fax)
jwilson@nmt.edu

Graduate Students

Benjamin Lechler, M.S.
Zachary Brown, M.S.

Research Objective

This research project addresses the effect of clastic dikes on contaminant transport in the vadose zone. Clastic dikes are vertically oriented subsurface heterogeneities common at the Hanford Site, including within the subsurface sediments below the tank farms in the 200 West Area. Previous studies have suggested that clastic dikes may provide a fast path for transport of leaking fluid from the tanks through the vadose zone.

This research is testing the hypothesis that clastic dikes at the Hanford Site provide preferential pathways that enhance the vertical movement of moisture and contaminants through the vadose zone. Current flow and transport models of the vadose zone at the 200 Areas are based on relatively simple hydrogeologic models that assume horizontally layered sediments with no preferential vertical flow paths. To address those scientific needs, our research includes field and modeling studies of the spatial distribution of clastic dikes, the hydrologic properties within dikes, and the potential effect of clastic injection dikes on fluid flow through the vadose zone. The data and models of the clastic dike networks produced for this project should be directly applicable to fate and transport studies conducted at the 200 West Hanford tank farms.

Research Progress and Implications

This report summarizes progress after the first 32 months of a 3-year project. In 2001, the project extended its study of the small-scale hydrogeologic properties of clastic dikes. The main focus of the project was on study of a site near Army Loop Road that had initially been surveyed using ground-penetrating radar in 2000. The ground-penetrating radar survey and the air photo and field mapping were used to select a site to trench across a clastic dike. In June 2001, a clastic dike at the Army Loop Road site was trenched with a backhoe to a depth of ~3.5 m (Figure 1). The exposed clastic dike is in the sand-dominated facies of the Hanford formation. The dike excavated at the Army Loop Road site was much thicker than the dike excavated in 2000 at the S-16 Pond site (2 m vs. 0.7 m).

The dike was excavated in three different levels, each approximately a meter high. After the excavation of each level, the slopes surrounding the excavation were pushed back and the excavation was taken down another level. In this way, we were able to image and measure the properties of cross sections of the dike and matrix at three different levels that were approximately one on top of the other, without creating a safety hazard in the unstable sediment. The face exposed at each level was mapped, and sediment samples were taken for laboratory analysis. We imaged the face using an infrared (IR) camera and a digital 35-mm camera, then made a large number of air permeability measurements.

Figure 1. Clastic Dike Excavation on the Hanford Site

During the last fiscal year, members of the project team at New Mexico Tech made substantial improvements to the air minipermeameter system. The LSAMP II air minipermeameter developed by New Mexico Tech that was employed in the previous fieldwork had a practical range of ~ 9.7x10-04 to 4.9x10-06 m/sec, corresponding to fine to medium sand. However, there are numerous silt bands in the dikes as well, but it was not practical to make measurements in the finer-grained units because the measurements took too long to make. This year, investigators from New Mexico Tech attempted to modify the system so that it could be used to make measurements in some of the finer-grained sediments. The factor that controls the time that it takes to make a measurement (and therefore the lower end of the practical range of the instrument) is the inner tip seal pressure (P_i). Because $P_i = (mg)/A$, where m and A are the mass and area of the piston, respectively, and g is the acceleration due to gravity, in order to increase the tip seal pressure, it is necessary to add mass to the piston because the area of the piston remains the same. However, the calibration of the permeameter assumes that the piston reaches terminal velocity before it reaches the upper photo sensor, and that puts an upper limit to how much mass can be added to the system. The investigators at New Mexico Tech performed a series of calibrations in the laboratory and determined that the mass of the piston could be increased by loading up to an order of magnitude additional mass on the top of the piston with only a 2% error in the measured air permeability values. The increase in mass of the piston extended the range of the air minipermeameter on the lower end by a full order of magnitude.

We employed two air minipermeameters during the fieldwork at the Army Loop Road site—a standard instrument and one with the extended range. This allowed us to make substantially more measurements in 2001 than during the previous year. We took a total of about 450 measurements on the three tiers, one-third in the dike and two thirds in the matrix. The results

indicate the median air permeability of the dike is about one order of magnitude lower than the permeability in the matrix, and that is similar to the results obtained last year. The variability of the data from the dike is much higher than that of the matrix, with a coefficient of variation (i.e., ratio of standard deviation to the mean) of 1.2 in the dike vs. 0.6 in the matrix. The overall variability of air permeability in the dike-matrix system is about four orders of magnitude. This is an important observation, because some methods used for upscaling permeability data assume the variability in the system is low, about an order of magnitude, which means it would be questionable to apply those methods to the clastic dike and its surrounding sediments.

In addition to making a number of measurements of air permeability, we also imaged each face in the excavation using a high-resolution IR camera. Figure 2 shows two composite images of the middle level in the trench. The lower image was made with an ordinary digital camera and the upper image was made using the IR camera. The contrast in the IR imagery is due to variation in the moisture content of the sediment; darker colors indicate more moisture and tend to be associated with finer-grained units with lower air permeability. The dike can be seen as the banded interval that takes up the middle third of the image, and is about 2 m wide.

We found that the IR data and the air permeability moisture data collected from the dike and surrounding matrix are positively correlated with one another, with a linear correlation coefficient of 0.73. Variogram analysis of the two data sets indicated that the spatial continuity of the air permeability and IR data were very similar. Based on the relationship between the two
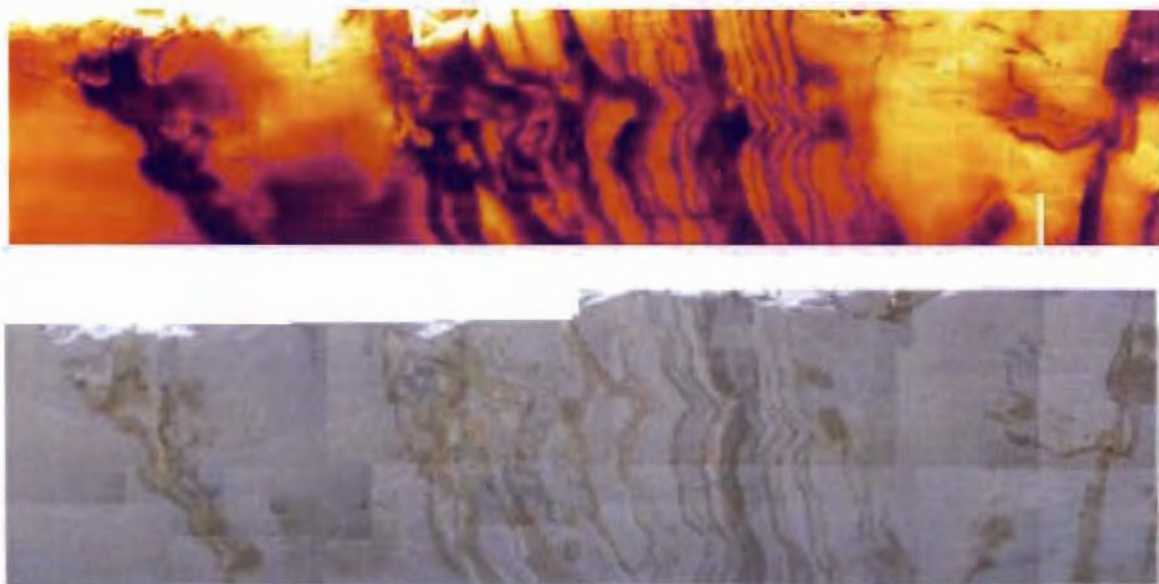

Figure 2. Composite Images of Middle Tier, Clastic Dike Excavation Site. Top shows infrared camera image; bottom displays image made using digital camera.

variables, we used sequential Gaussian simulation to generate simulated estimates of the air permeability in two dimensions over the entire exposure of the dike and matrix with very high resolution (centimeter-scale). The number of simulated air permeability measurements for the entire exposure was approximately 10.5 million, which would be impractical to achieve by taking direct measurements with the air-minipermeameter. The simulations of the air permeability honored the 450 air permeability measurements as well as the IR image through the collocated cokriging algorithm. The high-resolution map of the estimated hydraulic conductivity will be used for input to flow and transport modeling and as the basis for studies of the scaling properties of the system.

One feature noted during our previous excavations of clastic dikes is that there often appears to be a zone of lower permeability in the matrix near the clastic dike. To test that hypothesis, we took several horizontal transects in the matrix on either side of the dike on several different levels. Several of these transects did in fact show a decrease in permeability near the dike. There is no obvious change in grain size near the dike, but we will be performing grain size analysis to verify that. We will also examine the matrix sediment to see if there is an appreciable increase in cementation near the dike.

We made an effort this year to measure the continuity of the vertical bands seen within the clastic dike. A transect was laid out on the floor of the middle layer of the excavation on a horizontal exposure of the dike. Each band encountered in the transect was then traced up and down the excavation to see if it was continuous. The measured continuity is the total trace of one band along each vertical face and across the horizontal exposures (the "floors" of the excavation) linking the vertical faces. So the measured continuity is a combination of both vertical and horizontal continuity within the 2.5-dimensional excavation. The vertical bands that were measured did not include the very thin and very fine-grained clay and silt skins (usually less than 1 cm thick) associated with the major bands. The clastic dike bands that were characterized had a median thickness of 5 cm and ranged from 2.5 to 14 cm. In most cases, the bands could be traced for about 1.6 m before they pinched out or were obstructed by a clay/silt skin cutting across the band. The range of continuity observed was from 0.2 to 7.7 m, with all but one of the bands having an apparent continuity of less than about 2.5 m. This degree of continuity will affect transport through the clastic dike and will be used to guide construction of models of the properties within the dike.

A large-scale infiltration experiment was conducted at the Army Loop Road site in 2001. A drip irrigation system was used to apply the specified fluxes. The application area was centered on the dike and aligned with the longer axis perpendicular to the dike. Three fluxes of water were applied to the clastic dike and surrounding matrix, and the progress of the infiltrating water was monitored for each flux rate. Water content, matric potential, and electrical conductivity were measured throughout the tests using a neutron probe, cross-borehole radar, tensiometers, and

time domain reflectometry (TDR) probes. Eight boreholes were emplaced to a depth of about 7 m and used for the neutron probe and cross-borehole radar measurements. This depth will provide significant information because there are no reports of observations of flow within dikes at this large a scale. For example, in all of the tests reported by Fecht et al. (1998), the maximum depth of observation was < 1.0 m. The measurement frequency during the infiltration test varied depending on the experimental conditions. The TDR probes and tensiometers were installed to a depth of 0.5 m on a transect oriented perpendicular to the dike.

The three fluxes applied were 0.1, 0.01, and 0.001K_s, in that order. For typical soils, this translates roughly into flux values of 10^{-3}, 10^{-4}, and 10^{-5} cm/s. Total flux applied was approximately 15,000 l. Similar fluxes have been used in previous field tests of surface soils at the Hanford Site (see Khaleel 1999, Appendix C). Higher fluxes are difficult to maintain because of the water supply; they also are prone to generate ponding and runoff, which degrade the value of the infiltration test. Lower irrigation fluxes more nearly approximate natural fluxes but they pose problems because of the time required to achieve steady-state conditions. Relating each flux to the resulting equilibrium water content will provide a measure of the unsaturated conductivity function (Youngs 1964). The water content and matric potential data provide a direct measure of in situ water retention.

Once steady state was achieved with the third (and lowest) flux rate, the irrigation supply tank was switched to a solution of KBr and the dye known as Brilliant Blue FCF. The presence of the KBr will significantly affect the TDR signals and make it easier to detect the wetting front in the subsurface. The flux was continued until the KBr moved below the TDR sensing zone (about 0.5 m). Further movement of the water was monitored with neutron probe and cross-borehole radar measurements.

The excavation began after the application of the tracer in the infiltration area. The main excavation face was approximately 8 to 10 m from the edge of the infiltration zone, so that the moisture would not affect the air permeability measurements or IR imaging. However, after construction of the main excavation area was complete, an additional face was cut at the edge of the infiltration area so that the distribution of the tracers could be examined. The upper portion of Figure 3 shows a composite color photographic image of what we termed the "dye" face, with the lower portion of the figure being a map of the moisture distribution in the face. The photographic image shows the very heterogeneous distribution of the blue dye. The dike is in the center-right area of the image, from 3 to 5 m, and tends to transmit less dye. However, some of the deepest penetrations of the dye occur in restricted bands within the dike (Figure 3). The map of the moisture distribution in the lower portion of Figure 3 was made using TDR probe measurements on a 15-cm by 15-cm grid across the entire face. Although the moisture map captures the main features seen in the photographic image, it is obvious that important heterogeneity in the distribution of dye and moisture is not captured in the map, even with the
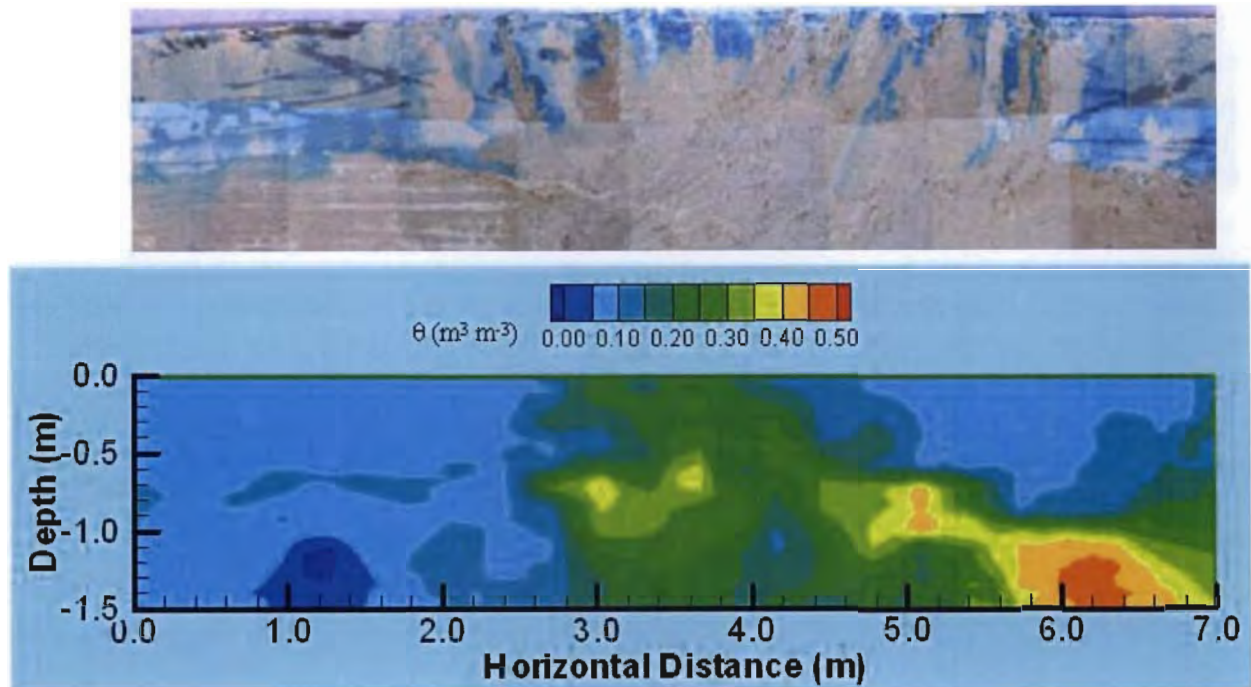
Figure 3. Images of Excavated Portion of Infiltration Experiment. Top: composite image of dye penetration. Bottom: contour map of clastic dike water content. measurements for surface shown in upper image.

relatively dense grid of TDR measurements. Figure 3 shows the vertically integrated moisture distribution every 15 cm and indicates quite clearly that much greater levels of moisture are stored within the clastic dike.

We used tomographic ground-penetrating radar to map the distribution of moisture between pairs of boreholes as the infiltration experiment progressed. Horizontal and vertical resolution of the data is 0.1 m. We took measurements immediately prior to the start of the infiltration experiment near the end of May; immediately after the infiltration had ceased in mid-June; and several months afterward to image the redistribution of the moisture with time. The radar tomography successfully imaged the changing moisture distribution for pairs of boreholes that were on the same side of the clastic dike, but was unable to image the dike itself when the dike was located between the pair of boreholes. This may be due to the near-vertical orientation of the dike and the high rader attenuation potential of the material within the dike.

One important feature noted in the excavation and infiltration experiment was a clastic sill that emanates from one side of the dike. This sill was detected prior to the excavation, when the access boreholes for geophysical monitoring of the infiltration experiment were being emplaced with a cone penetrometer (CPT). Moisture data from the CPT probe, which were recorded prior to any activities at the site, indicated the presence of a high-moisture zone at a depth of about 5 ft

that was present only on the west side of the dike and not the east side. Based on previous experience at the S-16 Pond excavation in 2000, we suspected that the high moisture zone on the west side of the dike was a clastic sill. Subsequently, we found that the sill exerted a major influence on the movement of moisture during the infiltration experiment. Where there is no sill, the moisture appears to have migrated uniformly downward through the sediment. On the western side of the dike, however, moisture penetrates below the sill only at later time periods. When the sill was exposed during the excavation, we found that moisture had migrated several meters laterally within the sill, carrying moisture well outside the infiltration zone. This suggests that clastic sills are important controls on vadose zone transport, at least at local scales. The results also indicate that even though the air permeability and saturated hydraulic conductivity within the dike and sill are very low, clastic dikes may still be fast transport paths under unsaturated conditions in the vadose zone.

Planned Activities

During the remainder of FY 2002, we will complete analysis of the data gathered during the infiltration experiment and the excavation. The data collected from this experiment will be used to derive flow and transport parameters for the dike and surrounding matrix, as well as provide field data with which to perform geostatistical and hydraulic flow modeling. We will continue to apply geostatistical methods to produce numerical two- and three-dimensional grids of the infiltration site for flow and transport modeling of the vadose zone. Flow and transport modeling will be performed in late FY 2002, and the resulting transport models will be compared with observations made during the transport experiments.

References Cited

Fecht KR, KA Lindsey, BN Bjornstad, DG Horton, GV Last, and SP Reidel. 1998. *Clastic Injection Dikes of the Pasco Basin and Vicinity.* BHI-01003, Bechtel Hanford Inc., Richland, Washington.

Khaleel R. 1999. *Far-Field Hydrology Data Package for Immobilized Low-Activity Tank Waste Performance Assessment.* HNF-4769 Rev. 1, Fluor Federal Services, Richland, Washington.

Youngs EG. 1964. An infiltration method for measuring the hydraulic conductivity of unsaturated porous materials. *Soil Sci.* 91:307-311.

Quantifying Vadose Zone Flow and Transport Uncertainties Using a Unified, Hierarchical Approach

(Project Number: 70187)

Principal Investigator

Philip D. Meyer
Pacific Northwest National Laboratory
P.O. Box 999, MSIN BPO
Richland, WA 99352
503-417-7552 (phone)
503-417-2175 (fax)
philip.meyer@pnl.gov

Co-Investigators

Christopher J. Murray
Pacific Northwest National Laboratory
P.O. Box 999, MSIN K6-81
Richland, WA 99352
509-376-5848 (phone)
509-376-5368 (fax)
chris.murray@pnl.gov

Mark L. Rockhold
Pacific Northwest National Laboratory
P.O. Box 999, MSIN K9-36
Richland, WA 99352
509-375-2516 (phone)
509-375-6089 (fax)
mark.rockhold@pnl.gov

Marcel Schaap
George E. Brown, Jr. Salinity Laboratory
450 Big Springs Road
Riverside, CA 92507-4617
909-369-4844 (phone)
909-342-4964 (fax)
mschaap@ussl.ars.usda.gov

Research Objective

The objective of this research is to develop and demonstrate a general approach for modeling flow and transport in the heterogeneous vadose zone. The approach uses similar media scaling, geostatistics, and conditional simulation methods to estimate soil hydraulic parameters at unsampled locations from field-measured water content data and scale-mean hydraulic parameters determined from available site characterization data. Neural network methods are being developed to estimate soil hydraulic parameters from more easily measured physical property data such as bulk density, organic matter content, and percentages of sand, silt, and clay (or particle-size distributions). Field water content distributions are being estimated using various geophysical methods including neutron moderation, ground-penetrating radar, and electrical resistance tomography. One of the primary goals of this research is to determine relationships between the type of data used in model parameterization, the quantity of data available, the scale of the measurement, and the uncertainty in predictions of flow and transport using these methods. Evaluation of the relationships between available data, scale, and uncertainty are using data from a large-scale, controlled field experiment.

Research Progress and Implications

This report summarizes work completed after 2.5 years of a 3-year project. A large-scale injection experiment was conducted in summer 2000 as part of the Hanford Science and Technology (S&T) program at a location on the Hanford Site where a previous injection experiment had been conducted in 1982. The site was instrumented in 1982 with thirty-two, 18-m-deep wells arranged radially around a central injection well. Additional instruments installed as part of the S&T project included polyvinyl chloride access tubes to provide access for cross-borehole ground-penetrating radar and electrical resistance tomography. Five injections of water were made during the S&T experiment over the course of a month with periodic monitoring via the boreholes.

Core samples were collected from three additional boreholes at the site as part of this EMSP project. Approximately 56 of these cores were subsampled for measurements of bulk density, porosity, particle-size distribution, water retention, and hydraulic conductivity. Hydraulic property model parameters have been estimated from the core data. Neural network analysis has been used with the core data to develop pedotransfer functions for the site that relate the more easily determined physical property data to the measured hydraulic properties at the site. Scaling analysis also has been carried out on the core data to estimate scale-mean hydraulic parameters, which are being used to estimate model parameter values at unmeasured locations.

Geostatistical analysis of the site has been carried out using wet bulk density data collected in 1995 at 2.5-cm depth intervals in all of the boreholes and neutron probe data collected in 2000 at

30-cm depth intervals. In this analysis, the wet bulk density distribution was simulated first at 2.5-cm resolution using sequential indicator simulation. These results then were used as soft data to constrain the sequential gaussian simulations of water content, with the neutron probe moisture data spaced at 30 cm used as the hard data. Porosity was calculated from the wet bulk density and the water content using an average particle density. The geostatistical analysis revealed vertical and horizontal anisotropy in the water content and wet bulk density data. The anisotropy in the horizontal directions is mostly due to non-stationarity of the data, with the correlograms suggesting the presence of a trend. The apparent trend appears to be due to greater variability in the sediment layers in the direction parallel to NNW-SSE than there is in the perpendicular direction, i.e., some of the layers appear to pinch out more rapidly in that direction. This causes an increase in the difference in moisture or bulk density values as separation increases along the NNW-SSE axis.

The generated parameter fields span a domain 20 m wide on each side and 12 m deep. Parameters have been generated on this domain at a resolution of 25 cm horizontally and 2.5 cm vertically (approximately 3 million nodes). The parameterization routines, including an upscaling procedure based on volumetric averaging, have been generalized for easy application to other sites. Currently, we are running simulations at a resolution of 50 cm horizontally and 2.5 cm vertically (approximately 1 million nodes). E-type averages of porosity and water content were used to generate the parameters for this simulation.

Planned Activities

The high-resolution model results will be used as a reference for comparison with results obtained using upscaled model parameters and alternative parameterizations based on the neural network analyses and geophysical data. Uncertainties will be evaluated by comparing simulations using different input data and by simulating on different parameter sets generated from alternative geostatistical realizations.

Information Access

Details regarding the field experiment and geophysical data used for model parameterization and testing can be found at http://vadose.pnl.gov/. The hydraulic property data gathered by this project are available from the principal investigator.

Radionuclide Sensors for Water Monitoring

(Project Number: 70179)

Principal Investigator

Jay W. Grate
Pacific N orthwest National Laboratory
P.O. Box 999, MSIN K8-93
Richland, WA 99352
509-376-4242 (phone)
509-376-5106 (fax)
jwgrate@pnl.gov

Co-Investigators

Oleg B. Egorov
Pacific Northwest National Laboratory
P.O. Box 999, MSIN P7-22
Richland, WA 99352
509-376-3485 (phone)
509-372-2156 (fax)
oleg.egorov@pnl.gov

Timothy A. DeVol
Environmental Engineering & Science
Clemson University
Clemson, SC 29634-0919
864-656-1014 (phone)
tim.devol@ces.clemson.edu

Number of Graduate Students Actively Involved in the Project: 2
Number of Undergraduate Students Involved (part-time) in the Project: 1
Number of Post-Doctoral Scholars involved (part-time) in the Project: 1

Number of Ph.D. degrees granted involved in the Project: 1
Number of M.S. degrees granted involved in the Project: 1

Research Objective

Radionuclide contamination in the soil and groundwater at U.S. Department of Energy (DOE) sites is a severe problem requiring monitoring and remediation. Radionuclide measurement techniques are needed to monitor surface waters, groundwater, and process waters. Typically, water samples are collected and transported to the analytical laboratory where costly radiochemical analyses are performed. To date, there has been very little development of selective radionuclide sensors for alpha- and beta-emitting radionuclides such as ^{90}Sr, ^{99}Tc, and various actinides of interest.

The objective of this project is to investigate novel sensor concepts and materials for sensitive and selective determination of beta- and alpha-emitting radionuclide contaminants in water. To meet the requirements for low-level, isotope-specific detection, the proposed sensors are based on radiometric detection. As a means to address the fundamental challenge of short ranges of beta and alpha particles in water, our overall approach is based on localization of preconcentration/separation chemistries directly on or within the active area of a radioactivity detector using automated microfluidics for sample manipulation and sensor regeneration or renewal.

The outcome of these investigations will be the knowledge necessary to choose appropriate chemistries for selective preconcentration of radionuclides from environmental samples, new materials that combine chemical selectivity with scintillating properties, new materials that add chemical selectivity to solid-state diode detectors, new preconcentrating column sensors, and improved instrumentation and signal processing for selective radionuclide sensors. New knowledge will provide the basis for designing effective probes and instrumentation for field analytical chemistry.

Research Progress and Implications

This report summarizes work as of 2 years and 8 months of a 3-year program. The ongoing effort is directed at the investigation of the preconcentration column sensor concepts, development and characterization of the selective scintillating microspheres (SSMs), development and characterization of the chemically selective diode detectors, and development/modeling of the new scintillation detection systems.

The preconcentrating minicolumn radionuclide sensor is based on the use of dual-functionality bead materials. These materials are designed to incorporate both selective separation chemistry for analyte preconcentration and localization within the detector, and scintillating properties, so that radioactivity of retained species can be converted to a measurable light output. To date, we have achieved progress in SSM materials prepared by co-immobilization of selective organic

extractants and scintillating fluors within inert macroporous polymeric beads, immobilization of selective organic extractants on scintillating glass, and by physically mixing sorbent and scintillating bead materials to yield a mixed-bed, composite sensor column. Various scintillating sensor materials selective for Tc, Sr, and actinides were prepared and evaluated during the course of this work.

Using pertechnetate-selective scintillating beads prepared by co-immobilization of selective extractants and scintillating fluors, we have demonstrated the application of SSM resins for the on-line characterization of $^{99}TcO_4^-$ (pertechnetate) in acidified groundwater. For on-line measurements, the resin is used in conjunction with an on-line flow-cell scintillation detector and an automated fluid handling system. The results of these tests clearly indicate that pertechnetate can be readily detected in acidified groundwater samples below the U.S. Safe Drinking Water Act maximum concentration level of 900 pCi/L. Nevertheless, these studies indicated that long-term material stability and analysis of the unacidified groundwater are still problematic when using sensor materials prepared by co-immobilization of scintillator dies and organic extractants within the polymeric bead.

To address sensor stability challenges, we have been investigating more robust sensor designs based on a composite or mixed-bed sensor column configuration. In this configuration, sensor column is comprises a heterogeneous mixture of scintillating and selective sorbent sub-materials that have stability in solution media. We determined that composite bed sensor configuration is efficient for capture and on-column detection of beta emitters such as ^{90}Sr and ^{99}Tc. For example, for the ^{99}Tc sensing, absolute detection efficiency that can be obtained using a composite bed column can be as high as 30%, and the chemical stability is much improved.

Progress has been made in the area of reagentless, equilibrium-sensing approaches. The reagentless sensing approach is particularly well suited for the development of field-deployable, long-term monitoring probes. Using a composite bed sensor with anion exchange sorbent functionality, we have demonstrated the feasibility of reagentless equilibrium ^{99}Tc sensing. As expected from the theoretical model, equilibrium sensor responses were proportional to the sample activity, and the magnitude of the signal was dependent on the sorbent uptake affinity. Reagentless sensing in chemically untreated Hanford groundwater at or below regulatory drinking water levels was possible. The issue of sensor fouling over long periods of operation in chemically untreated groundwater was identified and is being investigated. Presumably, it is due to the fouling of the anion exchange materials with natural organic acids.

Research has commenced on radionuclide sensors based on chemically modified diode detectors. We were successful in developing packaging approaches that resulted in minimal noise in the alpha region and reliable diode operation in solution. Diode leakage current and alpha noise are not significantly affected upon surface modification and packaging for use in solution. Selective

films of reproducible and controlled thickness can be deposited on the surface of diode detectors using a spray coating technique. We obtained actinide-selective thin films by modifying PVC polymer with actinide-selective organic extractants (HDEHP and DIPEX). Uptake characteristics of the thin films as a function of solution composition are being investigated in detail. Initial results indicate that selective thin films exhibit high distribution coefficients for the uptake of actinides from groundwater matrixes acidified to pH 2. For example, Am and U distribution coefficient values exceed 10^6 in Hanford groundwater at pH 2. Initial batch contact results indicate that good energy resolution ($\leq$100 keV FWHM) can be obtained for <0.5-μm-thick films. However, energy resolution is degraded significantly for > 2- μm-thick films. Nevertheless, alpha particle energy resolution for 3 to 5-μm-thick films exceeds practical energy resolution capabilities of scintillation detection. In addition, noise (alpha background) of the diode detectors is much superior to that of scintillation detection.

Research has commenced on the development of modeling approaches for the preconcentrating column sensors. Specifically, we conducted Monte-Carlo computer modeling of the light collection efficiency as well as the beta-particle charge deposition in a heterogeneous scintillation flow-cell. From the charged-particle interaction model, the percentage of electron energy deposited in the scintillator as a function of electron energy was determined. The energy deposited in the scintillator varies with scintillator granule size, packing geometry (porosity), the scintillator material, and the initial location of radioactivity within the flow-cell. The simulation results of electron interactions showed higher packing density and smaller scintillator spheres would result in greater energy deposition in the scintillator, but the absolute effects also depend on the energy and location of electrons within the flow-cell at the time of the decay. This energy deposited in the scintillator has a strong dependence on the initial energy if it is below ~200 keV. The spatial energy distribution for electron interactions provided insight into determining the appropriate size of flow-cell tubing for a given energy. The simulated geometrical detection efficiency was shown to be comparable to the experimental absolute detection efficiency. It was concluded that the charged particle interaction process has greater effect on overall detection efficiency than the photon transport process within the constraints of this study. The light collection efficiency modeling needs further work. The light collection efficiency is shown to be affected more by optical properties including the indices of refraction of scintillator, aqueous phase, and the Teflon tubing; the reflection coefficients of the internal surfaces of the flow-cell holder; and the surface treatment of scintillator granules than by geometrical properties such as the scintillator granule size, the flow-cell volume, and the packing geometry (porosity). Reduced light collection efficiency was observed for scintillator spheres with polished surfaces compared to spheres with ground (rough) surfaces due to losses from total internal reflection. There is currently an inconsistency between the model and the experiments in light collection efficiency as the number of spheres in the flow-cell increase. This discrepancy is due to the discrepancy in

the absorption coefficient of the scintillator used in the model. We plan to conduct specific experiments to elucidate the effects of light collection efficiency as a means of refining the model.

We continued further development of the dual functionality sensing media, with particular emphasis on detection of uranium and actinides. Resins were investigated with bis(2-ethylhexyl)methane-diphosphonic acid ($H_2DEH[MDP]$, Dipex®) extractant, which has a strong affinity for tri-, tetra-, and hexavalent actinides in dilute acids. Extractive scintillating resins were manifested 1) as a mixed bed of scintillating resin and extraction chromatographic resin and 2) by diffusing the organic fluor 2-(1-naphtyl)-5-phenyloxazole (αNPO) into macroporous polystyrene chromatographic resin, then coating with $H_2DEH[MDP]$ or by coating $H_2DEH[MDP]$ on scintillating polyvinyltoluene (PVT) beads. The average detection efficiencies were 51.7 ± 2.6 % and 65.8 ± 10.1 % for natural uranium and [241]Am, respectively, for the extractant-coated scintillator. The resin was stable for solution flow of up to 1000 mL resulting in rapid real-time screening of alpha radiation in natural groundwaters at or below the alpha concentration set forth in the U.S. Safe Drinking Water Act.

Manganese dioxide-coated plastic PVT scintillator and Aliquat 336-based extractive scintillator (ES) resins were prepared and applied toward environmental screening of [99]TcO_4^- and uranium in groundwater, respectively. Off-line screening using a commercially available liquid scintillation counter (LSC), and on-line screening using a modified hand-held survey meter, were evaluated in the laboratory for quantification of [99]TcO_4^- and uranium in groundwater. The detection efficiencies for uranium with the MnO_2-coated PVT resin were determined to be from 17% to 37 % and from 7% to 27 % for the LSC and survey instrument, respectively. The loading efficiency of the uranium out of groundwater ranged from 16% to 26 %. In contrast, the detection efficiencies for ^{99}Tc with the ES resin were determined to be from 2% to 14% and from 2% to 3% for LSC and the hand-held survey meter, respectively, while the loading efficiency of the [99]TcO_4^- in groundwater acidified to pH 2 was nearly 100%. It was shown in this work that it is possible to use MnO_2-coated PVT scintillator resin (MnO_2-PVT) and ES resin with a hand-held survey meter to simultaneously separate and quantify radioactivity in aqueous solutions. This hand-held survey meter can be applied toward environmental screening applications in the field.

Planned Activities

During the remainder of the third year, our activities will be directed at completing experimental work directed at the initial feasibility of ^{99}Tc reagentless sensing in groundwater and developing and testing the chemically modified diode detectors. We plan to complete initial demonstration of the hand-held field survey equipment for detection of U and ^{99}Tc in groundwater. In addition,

we are beginning to work with the DOE Nevada office and Bechtel Nevada on the development of the prototype ^{99}Tc sensor probe suitable for long term/in-situ monitoring.

Information Access

Tan H and TA DeVol. 2002. Development of a Flow-Cell Alpha Detector Utilizing Microencapsulated CsI:Tl Granules and Silicon PIN-Photodiodes. Accepted for publication in *IEEE Tran. Nuc. Sci.*).

Roane JE and TA DeVol. 2002. Evaluation of an Extractive Scintillation Medium for the Detection and Separation of Actinides in Acidic Solutions. Submitted for publication in *Analytical Chemistry*).

Bredt PR, FJ Brockman, DM Camaioni, AR Felmy, JW Grate, BP Hay, NJ Hess, PD Meyer, CJ Murray, DM Pfund, Y Su, EC Thornton, WJ Weber, and JM Zachara. 2001. *Science to Support DOE Site Cleanup: The Pacific Northwest National Laboratory Environmental Management Science Program Awards*. PNNL-13564, Pacific Northwest National Laboratory, Richland, Washington.

Grate JW and OB Egorov. 2001. Automated radiochemical separation, analysis, and sensing. Abstracts of Papers, 222nd ACS National Meeting, Chicago, Illinois, August 26-30, 2001. Invited.

Grate JW and OB Egorov. 2001. Advances in radioanalytical chemistry using automated sequential injection analysis. Abstracts of Papers, 222nd ACS National Meeting, Chicago, Illinois, August 26-30, 2001. Invited.

Egorov O, T DeVol, and J Grate. 2001. Advances in automated radioanalytical chemistry: From groundwater monitoring to nuclear waste analysis. Abstracts of Papers, 222nd ACS National Meeting, Chicago, Illinois, August 26-30, 2001.

DeVol TA, JE Roane, and JD Leyba. 2001. Application of Extractive Scintillator Resins to Quantification of Beta-Emitting Radionuclides in Aqueous Solutions. Presented at LCS 2001, Karlsruhe, Germany, May 7-11, 2001.

Roane JE and TA DeVol. 2001. Scintillating Extraction Chromatography Coupled with Pulse Height Spectrum Analysis for Actinide Separation and Analysis. Presented at the 2001 American Radiation Safety Conference & Exposition, Cleveland, Ohio, June 10-14, 2001.

Drumm L and TA DeVol. 2001. Gross Alpha Radiation Monitoring in Natural Waters. Presented at LCS 2001, Karlsruhe, Germany, May 7-11, 2001.

DeVol TA, OB Egorov, JE Roane, A Paulenova, and JW Grate. 2001. Extractive Scintillating Resin for ^{99}Tc Quantification in Aqueous Solutions, *Journal of Radioanalytical and Nuclear Chemistry*, 249, No. 1 (2001) 181-189.

DeVol TA, JM Duffey, and A Paulenova. 2001. Combined Extraction Chromatography and Scintillation Detection for Off-Line and On-Line Monitoring of Strontium in Aqueous Solutions, *Journal of Radioanalytical and Nuclear Chemistry*, 249, No. 2 (2001) 295-301.

Tan H, RA Fjeld, and TA DeVol. 2000. Digital Alpha/Beta Pulse Shape Discrimination of CsI:Tl for On-Line Measurement of Aqueous Radioactivity, IEEE Trans. *Nuc. Sci.*, 47(4):1516-1521 (2000).

DeVol TA. 2000. Chromatographic Separation and Measurement of Charged-Particle Emitting Radionuclides, Eichrom Technologies, Inc. Eastern Users' Group Workshop, Augusta, Georgia, May 16, 2000.

DeVol TA, JM Duffey, and A Paulenova. 2000. Combination Extraction Chromatography and Scintillation Detection Resin for Quantification of Strontium in Aqueous Solutions, presented at Spectrum 2000, Chattanooga, Tennessee. September 24-28, 2000.

DeVol TA, OB Egorov, JE Roane, A Paulenova, and JW Grate. 2000. Extractive Scintillating Microspheres for ^{89,90}Sr Quantification in Aqueous Solutions, presented at Gordon Conference on Nuclear Waste and Energy, New London, New Hampshire, July 16-21, 2000.

DeVol TA, JE Roane, JM Williamson, JM Duffey, and JT Harvey. 2000. Development of Scintillating Extraction Media for Separation and Measurement of Charged-Particle Emitting Radionuclides in Aqueous Solutions, *Radioactivity and Radiochemistry*, 11, (1) 34-46(2000).

DeVol TA, JM Duffey, and A Paulenova. 2001. Combined Extraction Chromatography and Scintillation Detection for On-line and Off-line Monitoring of Strontium in Aqueous Solutions, presented at the Fifth International Conference on Methods and Application of Radioanalytical Chemistry, Kailua-Kona, Hawaii, April 9-14, 2000.

DeVol TA, OB Egorov, JE Roane, A Paulenova, and JW Grate. 2001. Extractive Scintillating Microspheres for ^{99}Tc Quantification in Aqueous Solutions, presented at the Fifth International Conference on Methods and Application of Radioanalytical Chemistry, Kailua-Kona, Hawaii, April 9-14, 2000.

DeVol TA, JE Roane, and JD Leyba. 2001. Application of Extractive Scintillator Resins to Quantification of Beta-Emitting Radionuclides in Aqueous Solutions, presented at LCS 2001, Karlsruhe, Germany, May 7-11, 2001.

Drumm L and TA DeVol. 2001. Gross Alpha Radiation Monitoring in Natural Waters, Presented at LCS 2001, Karlsruhe, Germany, May 7-11, 2001.

Egorov OB, SK Fiskum, MJ O'Hara, and JW Grate. 1999. Radionuclide Sensors Based on Chemically Selective Scintillating Microspheres: Renewable Column Sensor for Analysis of 99Tc in *Water, Anal. Chem.* 71, 5420-5429(1999).

Egorov OB and JW Grate. 2000. Automating Analytical Separations in Radiochemistry, presented at the Gordon Conference on Nuclear Waste and Energy, New London, New Hampshire, July 16-21.

Egorov OB and JW Grate. 2000. Automated Radionuclide Separations, Analysis and Sensing, presented at the 46th Annual Conference on Bioassay, Analytical, and Environmental Radiochemistry, November 12-17, 2000, Seattle, Washington.

Roane JE and TA DeVol. 2001. Scintillating Extraction Chromatography Coupled with Pulse Height Spectrum Analysis for Actinide Separation and Analysis, presented at the 2001 American Radiation Safety Conference & Exposition, Cleveland, Ohio, June 10-14, 2001.

Tan H and TA DeVol. 2000. Development of a Digital Alpha/Beta Pulse Shape Discriminating System Utilizing CsI(Tl)/Photodiode, Presented at the 44th annual meeting of the Health Physics Society, Denver, Colorado, June 24-29, 2000.

Tan H, RA Fjeld, and TA DeVol. 2000. Digital Alpha/Beta Pulse Shape Discrimination of CsI:Tl for On-Line Measurement of Aqueous Radioactivity. *IEEE Trans. Nuc. Sci.*, 47(4):1516-1521.

Integrated Field, Laboratory, and Modeling Studies to Determine the Effects of Linked Microbial and Physical Spatial Heterogeneity on Engineered Vadose Zone Bioremediation

(Project Number: 70165)

Principal Investigator

Fred Brockman
Pacific Northwest National Laboratory
P.O. Box 999, MSIN P7-50
Richland, WA 99352
509-376-1252 (phone)
509-376-9650 (fax)
fred.brockman@pnl.gov

Co-Investigator

John Selker
Oregon State University
Gilman Hall 240
Corvallis, OR 97330
541-737-6304 (phone)
selkerj@engr.osu.edu

Graduate Students and Research Assistants

Steven Bradley, post-doctoral
Mark Rockhold, post-doctoral
Rockie Yarwood, post-doctoral
Tina Spadoni, B.S., research assistant
Michael Niemet, M.S., research assistant
Thomas Perry, post-B.S. appointment
Nisha Kapadia, post-B.S. appointment
Ginny Williams, post-B.S. appointment

Research Objective

In situ bioremediation of contaminants can offer advantages in cost, speed, public acceptance, and final cleanup levels achieved relative to physical removal methods. However, microbial populations in the unsaturated zone are spatially discontinuous and sparse, especially in deep vadose zones and in arid climates with very low moisture and nutrient flux. In addition, there is a lack of knowledge on 1) the ability of microbes to colonize "empty" regions of the vadose zone in response to nutrient delivery and 2) how microbial colonization is controlled by hydrologic and physical features. These issues raise questions about the feasibility of deep vadose zone bioremediation and the accuracy of flow and transport models for vadose zone bioremediation.

The goal of this research is to provide DOE with an increased understanding of the effect of interacting hydrologic and microbiological processes that control the feasibility of engineered bioremediation of chlorinated compounds in heterogeneous, microbially sparse deep vadose zones. The specific objectives are

- to conduct laboratory research on vadose zone microbial colonization processes as a function of hydrologic and physical features, and use the information to develop an improved vadose zone reactive transport model

- to evaluate a gas-phase nutrient delivery approach for enhancing removal of carbon tetrachloride from the vadose zone.

Research Progress and Implications

This report summarizes the progress achieved during 2.5 years of a 3-year project. Research tasks under way at Pacific Northwest National Laboratory are addressing the ability of microbes to colonize uninhabited porous media under static unsaturated conditions. At Oregon State University, researchers are examining the dynamics of microbial metabolic and colonization processes under flowing unsaturated conditions. Both efforts involve understanding how microbial colonization is controlled by porous media water content and particle size.

Static Unsaturated Conditions

Microbial motility—the ability of microorganisms to swim through water or move over surfaces—has been largely discounted as unimportant in microbial colonization of the subsurface. However, no specific studies of microbial motility under vadose zone conditions are reported in the literature. Our results with a carbon-tetrachloride-degrading bacterium and sorted sand of 0.2 to 0.7 mm in diameter show motility-promoted colonization rates of about 2 cm/day under unsaturated conditions in which the calculated average water film thickness is

>20 micrometers. This adds to the existing base of scientific knowledge on phenomena under unsaturated conditions and challenges conventional scientific wisdom. The significance of these results is that nutrient delivery to coarse-grained regions of the unsaturated subsurface could promote colonization by motile bacteria. If the motile bacteria were able to degrade contaminants, colonization of previously "empty" regions would dramatically increase the rate and efficiency of biodegradation.

In the absence of acetate in the columns, there was substantial movement of bacteria via a physical process during the first 10 minutes after bacterial inoculation. This movement was shown to be an artifact (due to pore-scale water redistribution) because bromide tracer, bacteria, and 1-micrometer yellow-green (negatively charged) and bright-blue (neutral charge) microspheres all traveled similar distances in the first 10 minutes. There was little to no additional bacterial movement due to "random motility (i.e., non-chemotactic exploratory motility) in the subsequent 24 hours. In the presence of acetate in the columns, at a given volumetric water content, bacteria generally traveled farther with increasing sand size (0.71-mm-diameter > 0.53 mm > 0.36 mm > 0.21 mm). Bacterial movement was not detected at 5% volumetric water content in the two smallest sands, which had calculated average water film thicknesses of 3 and 6 micrometers. Colonization in the presence of acetate was also not detected in much longer 12-day experiments with 0.10-diameter sand (4-micrometer calculated average water film thickness) at 1.3% volumetric water content. In the presence of acetate in the columns, at a given sand size, bacteria traveled farther with increasing volumetric water content (20% > 15% > 10% > 5%). After 24 hours, bacteria were present at high density throughout the 4-cm-long column at the higher volumetric water contents and larger sand sizes. We are beginning to model bacterial movement in these unsaturated sorted sands using equations that account for the tortuosity of diffusion paths in partially saturated porous media.

Unsaturated Flow Conditions

The ability of microbes to colonize unsaturated porous media in the presence of flow and soluble nutrients was studied in a two-dimensional chamber, 40 cm wide by 60 cm high by 1 cm thick, instrumented to allow periodic visualization of water distribution, nutrient delivery, and microbial activity. Water distribution is visualized by light transmission, nutrient delivery by use of a dye, and microbial activity by periodic addition of salicylate, which causes the genetically engineered bacterium *Pseudomonas fluorescens* HK44 to produce light in the presence of oxygen. A charge-coupled device camera records data at high resolution (1 mm/pixel) and quantifies, in situ, the temporal and spatial interactions between water content, solute transport, and microbial processes. Experiments were conducted with homogenous porous media and with heterogeneous porous media consisting of a wedge of coarse sand within a matrix of finer sand. Homogeneous porous media experiments were funded largely by a previous National Science Foundation project, with EMSP funds used for final analyses and numerical modeling. EMSP

funds also served to extend the homogeneous systems to heterogeneous layered systems, which are more typical of Hanford sediments. Our results show that microbial growth causes dynamic changes in flow paths and hydraulic properties in unsaturated systems. They also indicate that physical heterogeneity strongly controls microbial activity and colonization in the unsaturated zone. Results from these experiments are being used as input to parameterization and testing of a two-dimensional finite-difference numerical model for predicting contaminant fate and transport in the vadose zone. This model accounts for water flow, transport of solutes and bacteria, microbial growth and degradation kinetics, gas diffusion, and interphase exchange. The model captures new information on interactions between microbial dynamics and vadose zone processes that can be applied in conjunction with experimental studies to gain insights into, and greater understanding of, these processes and phenomena.

We also have developed a colorimetric readout method for real-time monitoring of gas movement through unsaturated two-dimensional chambers. This work is being extended to track movement of gaseous microbial nutrients in the two-dimensional chambers to investigate relationships between hydraulic processes, gaseous nutrient delivery to microorganisms, and microbiological growth.

Field Studies

Field sampling of the contaminated 216-Z-9 trench on the Hanford Site was conducted in June 2001. Contaminants include carbon tetrachloride and transuranic radionuclides. Twenty-four core samples ranging in depth from 102 to 187 ft below ground surface were collected from two boreholes and analyzed. The field sampling was performed to determine 1) the existence of potential microbial activity throughout the depth profile, 2) the ability of indigenous microorganisms to grow using gaseous sources of nitrogen, phosphorus, and carbon, and 3) the ability of indigenous microorganisms to degrade carbon tetrachloride. Potential activity was detected in 87% of the samples, and facultative anaerobic (denitrifying) bacteria were present in 71% of the samples. Gaseous nutrient injection is a means to stimulate unsaturated zone populations without water addition, thereby reducing the likelihood of transporting contaminants to underlying aquifers. Approximately 75% of the samples removed >10% of one or more gaseous carbon sources, with butane most commonly used (30% of samples), followed by propylene (25%), propane (14%), ethane (8%), and methane (3%). Gaseous nitrogen and phosphorus did not stimulate or inhibit removal of gaseous carbon sources compared to no addition of gaseous nitrogen and phosphorus, indicating these sediments contain adequate levels of nitrogen and phosphorus for substantial microbial growth.

We also have collaborated with the U.S. Geological Survey on its Toxic Substances Hydrology Program in the analysis of samples from the Amargosa Desert Research Site (ADRS) in Beattie, Nevada, to determine if far-field migration of ^{14}C-CO_2 may be attributable to microbial activity.

3.66

Land disposal of low-level mixed organic-radioactive waste occurred at both the ADRS and the Hanford Site, and the ADRS serves as an analog for understanding processes occurring at Hanford. The data showed that microbial populations and activity were very low away from the burial trenches and the capillary fringe and would not be generating measurable ^{14}C-CO_2. The results indicate that microorganisms in and immediately adjacent to the buried waste are generating the ^{14}C-CO_2 and that physical transport processes controlled by the site geology are causing far-field migration.

Planned Activities

Microbial Colonization in Static Unsaturated Columns

- Conduct 30-cm-long column experiments at the higher volumetric water contents and larger sand sizes to determine if rates of colonization are maintained over time.

- Conduct experiments with mixtures of sorted sand grain sizes and also with unsorted unsaturated zone sands to determine how much colonization rates are attenuated in porous media that are more geologically common and realistic.

Unsaturated Flow Chambers

- Continue investigation of the spatial and temporal dynamics of microbial processes using gaseous sources of carbon, nitrogen, and phosphorus.

Hanford 216-Z-9 Trench Samples

- Carbon tetrachloride will be spiked into the samples that removed gaseous carbon sources to determine the potential of the hydrocarbon-degraders to remove carbon tetrachloride under unsaturated conditions.

Information Access

Ainsworth CC, FJ Brockman, and PM Jardine. 2000. Biogeochemical considerations and complexities. In *Vadose Zone Science and Technology Solutions*, eds. BB Looney and RW Falta, pp. 829-923. Battelle Press, Columbus, Ohio.

Niemet MR and JS Selker. 2000. A new method for quantification of liquid saturation in 2D translucent porous media systems using light transmission. *Adv. Water Res.* 24:651-666.

Kieft TL and FJ Brockman. 2001. Vadose zone microbiology. In *Subsurface Microbial Ecology and Biogeochemistry*, eds. JK Fredrickson and M Fletcher, pp. 141-169.

Brockman FJ, SN Bradley, and TL Kieft. 2002. Vadose zone microbiology. In *Encyclopedia of Environmental Microbiology*, Vol. 6, pp. 3236-3246. John Wiley & Sons, New York.

Rockhold ML, RR Yarwood, MR Niemet, PJ Bottomley, and JS Selker. 2002. Considerations for modeling bacterial-induced changes in hydraulic properties of variably saturated porous media. *Adv. Water Res.* In press.

Rockhold ML, RR Yarwood, and JS Selker. Interactions between microbial dynamics and transport processes in variably saturated porous media, 1. Model development. Submitted.

Rockhold ML, RR Yarwood, MR Niemet, PJ Bottomley, and JS Selker. Interactions between microbial dynamics and transport processes in variably saturated porous media, 2. Observed and simulated results. Submitted.

Yarwood RR, ML Rockhold, MR Niemet, JS Selker, and PJ Bottomley. A novel experimental system for nondestructive monitoring of interactions between microbial growth, water flow, and solute transport in unsaturated porous media. Submitted.

Yarwood RR, ML Rockhold, MR Niemet, JS Selker, and PJ Bottomley. Bioluminescence as a nondestructive measure of microbial cell density and distribution in unsaturated porous media. Submitted.

Yarwood RR, ML Rockhold, MR Niemet, JS Selker, and PJ Bottomley. Impact of microbial growth on water flow and solute transport in unsaturated porous media. Submitted.

Distribution

OFFSITE

J. R. Beall
Office of Energy Research
U.S. Department of Energy (ER-72)
19901 Germantown Road
Germantown, MD 20874-1290

Gerald G. Boyd
U.S. Department of Energy (EM-90)
Oak Ridge Operations Office
200 Administration Road
Oak Ridge, TN 37831

Michelle Broido
U.S. Department of Energy
19901 Germantown Road, MSIN F-240
Germantown, MD 20874-1290

Julie Conner
U.S. Department of Energy
Idaho Operations Office
785 DOE Place
Idaho Falls, ID 83402

P. M. Davidson
Office of Energy Research
U.S. Department of Energy
19901 Germantown Road (ER-15)
Germantown, MD 20874-1290

S. L. Domoter
Office of Environmental Management
U.S. Department of Energy
19901 Germantown Road (EH-412)
Germantown, MD 20874-1290

Teresa Fryberger
Office of Science
U.S. Department of Energy (SC-75)
19901 Germantown Road
Germantown, MD 20874-1290

David Geiser
U.S. Department of Energy EM-52.1
19901 Germantown Road
1183 Cloverleaf Bldg.
Germantown, MD 20874-1290

Kurt D. Gerdes
Office of Science & Technology
U.S. Department of Energy (EM-541)
19901 Germantown Road
1186 Cloverleaf Bldg.
Germantown, MD 20874-1290

Mark Gilbertson
U.S. Department of Energy (EM-52)
19901 Germantown Road
5A-031/FORS
Germantown, MD 20874-1290

Roland Hirsch
U.S. Department of Energy
Medical Applications and
 Biophysical Research Division
19001 Germantown Road (ER-73)
Germantown, MD 20874-1290

Paul Lurk
U.S. Department of Energy (EM-542)
19901 Germantown Road
1168/Cloverleaf Bldg.
Germantown, MD 20874-1290

No. of
Copies

R. N. Massey
Office of Environmental
  Management
U.S. Department of Energy
19901 Germantown Road (EM-64)
Germantown, MD 20874-1290

W. S. Millman
Office of Energy Research
U.S. Department of Energy
19901 Germantown Road (ER-14)
Germantown, MD 20874-1290

Ken Osborne
DOE Idaho Operations Office
785 DOE Drive
Idaho Falls, ID 83401

J. M. Owendoff
Office of the Deputy Assistant Secretary,
Science and Technology
U.S. Department of Energy
1000 Independence Avenue SW
Washington, DC 20585

A. A. Patrinos
Office of Energy Research
U.S. Department of Energy
19901 Germantown Road (ER-70)
Germantown, MD 20874-1290

Michael R. Pfister
U.S. Department of Energy, EM-1
Environmental Management Advisory
  Board
1000 Independence Ave., SW, Rm. 5B-171
Washington, DC 20585

Ken Picha
U.S. Department of Energy (EM-32)
Office of Eastern Operations
19901 Germantown Road 343/TREV
Germantown, MD 20874-1290

No. of
Copies

Gary D. Roberson
DOE Albuquerque Operations
  Office
Pennsylvania and H St
Kirtland Air Force Base
Albuquerque, NM 87116

Dave Robertson
DOE Idaho Operations Office
785 DOE Drive
Idaho Falls, ID 83401

William L. Scott
DOE Idaho Operations Office
785 DOE Drive
Idaho Falls, ID 83401

Thomas Williams
DOE Idaho Operations Office
785 DOE Drive
Idaho Falls, ID 83401

Jim Wright
U.S. Department of Energy
Savannah River Operations Office
P.O. Box A
Aiken, SC 29802

Lin Yarborough
U.S. Department of Energy
Albuquerque Operations Office
P.O. Box 5400
Albuquerque, NM 87185-5400

John Ahearne
Sigma Xi
99 Alexander Drive
Research Triangle Park, NC 27709

Mansoor Alam
Department of Materials
New Mexico Tech
Socorro, NM 87801

No. of
Copies

No. of
Copies

Richard Begley
101 Red Oak Lane
Aiken, SC 29803

Jimmy Bell
Bell Consultants, Inc.
137 Bowsprit Lane
Kingston, TN 37763

Edgar Berkey
Concurrent Technologies Corporation
320 William Pitt Way
Pittsburgh, PA 15238

Paul Bertsch
University of Georgia
Savannah River Ecology Laboratory
P.O. Drawer E/Bldg 737 A
Aiken, SC 29801

Robert C. Birtcher
Argonne National Laboratory
Building 212
9700 South Cass Avenue
Argonne, IL 60439

David R. Boone
Portland State University
Biology Department
P.O. Box 751
Portland, OR 97207-0751

Anatol M. Brodsky
Center for Process Analytical
 Chemistry
University of Washington
P. O. Box 352700
Seattle, WA 98195

George E. Brown, Jr., Salinity Laboratory
450 West Big Springs Road
Riverside, CA 92507

Gordon E. Brown, Jr.
Stanford University
Stanford, CA 94305

L.W. Burgess
Center for Process Analytical Chemistry
University of Washington
P. O. Box 352700
Seattle, WA 98195

Barry Burks
Oak Ridge National Laboratory
P.O. Box 2008, Bldg. 7601, MSIN-6304
Oak Ridge, TN 37831-6304

Frank Caccavo, Jr.
Department of Biology
Whitworth College Mail Stop 3902
300 W. Hawthorne Road
Spokane, WA 99251

B. Calloway
Westinghouse Savannah River Company
Savannah River Technology Center
Building 773-A/Rm A-229
Mail Stop 28
Aiken, SC 29802

P. M. Castle
Lockheed Martin Idaho Technologies
 Company
P.O. Box 1625, MSIN 5205
Idaho Falls, ID 83415

Gregory Choppin
Florida State University
Department of Chemistry (B-164)
600 W. College Ave.
Tallahassee, FL 32606-3006

No. of
Copies

No. of
Copies

Sue B. Clark
Washington State University
Chemistry Department
1 S.E. Stadium Way
Pullman, WA 99164

Paul Clayton
Vice President for Academic Affairs
 and Provost
Oregon Graduate Institute
P.O. Box 91000
Portland, OR 97291-1000

Larry James
Washington State University at Tri-Cities
100 Sprout Road
Richland, WA 99352-1643

Roger G. Collis
Environmental Technology Partnership
Washington Dept of Community, Trade,
 and Economic Development
2001 Sixth Avenue, Suite 2700
Seattle, WA 98121

L. Coleman
Washington State Department of Ecology
1315 W. 4th
Kennewick, WA 99336

Steven D Conradson
Los Alamos National Laboratory
P. O. Box 1663
Los Alamos, NM 87545

Allen Croff
Martin Marietta Energy Systems, Inc.
Oak Ridge National Laboratory
P.O. Box 2008
Oak Ridge, TN 37831-6178

Rico Cruz
Nez Perce Indian Nation
P.O. Box 365
Lapwai, ID 83450

Daniel M. Dabbs
Princeton University
Princeton, NJ 08544

William E. Daniel, Jr.
Westinghouse Savannah River
 Company
Building 999-W
Aiken, SC 29808

Timothy A. DeVol
Environmental Engineering &
 Science
Clemson University
Clemson, SC 29634-0919

Carrick M. Eggleston
University of Wyoming
Laramie, WY 82071

Gary Eller
Los Alamos National Laboratory
MSIN E5-10
Nuclear Material Technology Division
Los Alamos, NM 87544

Tom Engel
University of Washington
Department of Chemistry
Bagley Hall Room 109
Seattle, WA 98195-1700

Dennis Faulk
U.S. Environmental Protection
 Agency
MAF Plaza
712 Swift, Suite 5 (B5-01)
Richland, WA 99352

No. of
Copies

Tom French
Westinghouse Savannah River Company
Bldg 773-A, A209
P.O. Box 616
Aiken, SC 29802

Gill G. Geesey
Montana State University
Center for Biofilm Engineering
409 Cobleigh Hall
Bozeman MT 59717

Joe Gentilucci
JAG Technical Services, Inc.
127 Savannah Drive
Aiken, SC 29803

T. R. Ginn
172 Everson Hall
Department of Civil and Environmental
 Engineering
University of California, Davis
Davis, CA 95616-5294

Dib Goswami
Washington State Department of Ecology
1315 W. 4th
Kennewick, WA 99336

Paul Hart
Morgantown Energy Technology Center
3610 Collins Ferry Road
Morgantown, WV 26507-0880

Thomas Hirons
Los Alamos National Laboratory
P.O. Box 1663, MSIN J591
Los Alamos, NM 87545

David T. Hobbs
Savannah River Technology Center
Westinghouse Savannah River Company
Aiken, SC 29808

Earl Holtzscheiter
Westinghouse Savannah River Company
Building 773-A/Rm A-229
Mail Stop 28
Aiken, SC 29802

Ken Hubbard
Asst Asso. Provost for Research
 and Economic Development
Dean of Graduate School
University of Montana
University Hall 118
Missoula, MT 59812-1329

Prof. James E. Hutchison
Department of Chemistry
University of Oregon
Eugene, OR 97403

Tom Isaacs
Lawrence Livermore National Laboratory
P.O. Box 808, MS/L-19
Livermore, CA 94551

Art Janata
School of Chemistry and Biochemistry
Georgia Institute of Technology
Atlanta, GA 30332-0400

Arvid Jensen
Lockheed Martin Idaho Technologies
 Company
P.O. Box 1625
Idaho Falls, ID 83415-3204

James R. Karr
Department of Fisheries and Zoology
104 Fisheries Center
University of Washington
Seattle, WA 98195

No. of
Copies

Ken Kemner
Argonne National Laboratory
ER203 C-129
9700 S. Cass Ave.
Argonne, IL 60439

Roy Koch
Vice Provost for Research
Dean of Graduate Studies
Portland State University
P.O. Box 751
Portland, OR 97207-0751

Bruce Kowalski
Chemistry Department (BG-10)
University of Washington
Seattle, WA 98195

Alvin Kwiram
Vice Provost for Research
University of Washington
312 Gerberding Hall
P.O. Box 351237
Seattle, WA 98195-1237

Brenda Lewis
Westinghouse Savannah River Company
P.O. Box 616
Aiken, SC 29802

D. London
University of Oklahoma
Dept. Geology and Geophysics
100 E. Boyd Str., 810 SEC
Norman OK 73019-0628

A. Luttge
Rice University
Dept. Geology and Geophysics-MS 126,
Houston, TX 77251-1892

No. of
Copies

M. R. Martin
Lockheed Martin Idaho Technologies
  Company
P.O. Box 1625, MSIN 2424
Idaho Falls, ID 83415

Todd Martin
Hanford Advisory Board
West 1408 Broadway
Spokane, WA 99201

James McBreen
Brookhaven National Laboratory
DAS, Bldg. 480
Upton, NY 11973

C. Phil McGinnis
Martin Marietta Energy Systems, Inc.
Oak Ridge National Laboratory
P.O. Box 2008
Oak Ridge, TN 37821-6273

M. E. McIlwain
Lockheed Martin Idaho Technologies
  Company
P.O. Box 1625, MSIN 2210
Idaho Falls, ID 83415

D. Meisel
Radiation Laboratory
University of Notre Dame
Notre Dame, IN 46556

W. D. St. Michel
Lockheed Martin Idaho Technologies
  Company
P.O. Box 1625, MSIN 1061
Idaho Falls, ID 83415

No. of
Copies

D. L. Miller
Lockheed Martin Idaho Technologies
 Company
P.O. Box 1625, MSIN 2208
Idaho Falls, ID 83415

Robert C. Moore
Sandia National Laboratories - Albuquerque
P.O. Box 5800
Albuquerque, NM 87185

Jerry Morin
Westinghouse Savannah River Company
Savannah River Technology Center
P.O. Box 616
Aiken, SC 29802

Bruce A. Moyer
Oak Ridge National Laboratory
Bethel Valley Road
Oak Ridge, TN 37831

Satish C. B. Myneni
Princeton University
Department of Geosciences
151 Guyot Hall
Princeton, NJ 08544

Alexandra Navrotsky
Department of Chemical Engineering
 and Material Science
University of California-Davis
One Shields Avenue
Davis, CA 95616-8779

Tina M. Nenoff
Sandia National Laboratories
P.O. Box 5800, MS 0710
Albuquerque, NM 87185-0709

No. of
Copies

Robert T. Paine
Department of Chemistry
University of New Mexico
Albuquerque, NM 87131

Frank Parker
Vanderbilt University
400 24th Avenue South
New Engineering Building
Room 108C
Nashville, TN 37235

Robert L. Powell
University of California Davis
Department of Chemical Engineering and
 Materials Science
One Shields Avenue
Davis, CA 95616-5294

Linfeng Rao
Lawrence Berkeley National Laboratory
MS 70A-1150
1 Cyclotron Road
Berkeley, CA 94720

Kenneth N. Raymond
Department of Chemistry
University of California at Berkeley
531 Latimer
Berkeley, CA 94720-1460

Doug Riggs
Legislative Director
Office of Congressman Doc Hastings,
 4th District, Washington
1323 Longworth Building
Washington, DC 20515

D. Max Roundhill
Department of Chemistry
Texas Tech University
Lubbock, TX 79409-1061

No. of
Copies

No. of
Copies

Richard Scanlan
Dean of Research
Oregon State University
Administration Services Bldg A312
Corvallis, OR 97331

Marcel Schaap
Salinity Laboratory
450 West Big Springs Road
Riverside, CA 92507

Wally Schulz
5314 Arbustos Court, NE
Albuquerque, NM 87111

John Selker
Bioengineering Department
Oregon State University
240 Gilmore Hall
Corvallis, OR 97331- 3906

Jean'ne Shreeve
Vice President for Research and
 Graduate Studies
Professor of Chemistry
University of Idaho
Moscow, ID 83843-4199

Leon T. Silver
Div. of Geological and Planetary Sciences
California Institute of Technology, 170-25
1200 East California Street
Pasadena, CA 91125

Robert Smith
Vice Provost for Research
Dean of Graduate School
Washington State University
Pullman, WA 99164-1030

William H. Smyrl
Corrosion Research Center
Department of Chemical Engineering and
 Materials Science
University of Minnesota, Minneapolis
221 Church Street SE
Minneapolis, MN 55455

R. N. Snelling
Lockheed Martin Idaho Tech Co
P.O. Box 1625, MSIN 2213
Idaho Falls, ID 83415

Joseph D. Spencer
SCUREF
Strom Thurmond Institute
Clemson, SC 29634-5701

Peter Spencer
Center for Research on Occupational and
 Environmental Toxicology L606
Oregon Health Sciences University
3181 SW Sam Jackson Park Road
Portland, OR 97202-3098

Ellen Stallings
Los Alamos National Laboratory
SM #30 Bikini Road
Los Alamos, NM 87545

Alex Stone
Washington State Department of Ecology
1315 W. 4th
Kennewick, WA 99336

Harold Sullivan
Los Alamos National Laboratory
P.O. Box 1663
Los Alamos, NM 87545

No. of
Copies

No. of
Copies

John Swanson
1318 Cottonwood
Richland, WA 99352

Robert Swenson
Vice President for Research
Montana State University
Montana Hall 207
Bozeman, MT 59717

Larry Tavlarides
Syracuse University
334 Hinds Hall
Syracuse, NY 13244

Tom Thomas
Lockheed Martin Idaho Technologies
  Company
P.O. Box 1625, MSIN 3458
Idaho Falls, ID 83415-3423

Major Thompson Steadman Upham
Vice Provost/Dean of Graduate School
University of Oregon
112 Johnson Hall
Eugene, OR 97403-1226

Samuel J. Traina
Ohio State University
School of Natural Resources
2021 Coffey Road
Columbus, OH 43210

Mark D. Tucker
Sandia National Laboratories
1515 Eubank Blvd., S.E.
Albuquerque, NM 87123

Scott W. Tyler
Desert Research Institute
7010 Dandini Blvd.
Reno, NV 89512

Nancy Uziemblo
Washington State Department of Ecology
1315 W. 4th
Kennewick, WA 99336

George Vandegrift
Argonne National Laboratory
Building 205
9700 South Cass Avenue
Argonne, IL 60439

John Veldman
Westinghouse Savannah River Company
Bldg 773-A, A-210
P.O. Box 616
Aiken, SC 29802

S. L. Wallen
Department of Chemistry
University of North Carolina at Chapel Hill
Campus Box 3290
Chapel Hill, NC 27599-6011

Lumin Wang
Nuclear Engineering & Radiological
Sciences
The University of Michigan
2355 Bonisteel Boulevard
Ann Arbor, MI 48109-2104

Jack Watson
Oak Ridge National Laboratory
P.O. Box 2008
Bldg 4500N, MS-6178
Oak Ridge, TN 37831-6178

No. of
Copies

No. of
Copies

E. Thomas Weber
6622 West Victoria Avenue
Kennewick, WA 99336

John L. Wilson
New Mexico Institute of Mining &
  Technology
801 Leroy Place
Socorro, NM 87801

Tom Winston
Ohio Environmental Protection Agency
401 East 5th Street
Dayton, OH 45402

Dr. Paul P. Woskov
Massachusetts Institute of Technology
Plasma Science and Fusion Center
NW16-110
167 Albany Street
Cambridge, MA 02139

ONSITE

16	**U.S. Department of Energy Richland Operations Office**	
	B. Bilson	A3-04
	J. W. Day	K8-50
	J. K. Erickson	K8-50
	J. E. Frey	K8-50
	M. J. Glasper	K8-50
	J. P. Hanson	K8-50
	R. A. Holten	A5-16
	P. W. Kruger	K8-50
	L. S. Mamiya	K8-50
	B. M. Mauss	H6-60
	T. P. Pietrok	K8-50
	L. L. Piper	A6-37
	R. M. Rosselli	A7-50
	F. R. Serier	A5-16
	D. E. Trader	K8-50
	J. J. Waring	T5-54

11	**Hanford Contractors**	
	J. N. Appel	R2-12
	J. G. April	L6-06
	W. B. Barton	R2-11
	R. E. Bauer	S7-65
	R. J. Cash	R2-37
	K. A. Gasper	L4-07
	P. W. Gibbons	K9-91
	J. O. Honeyman	H6-18
	M. N. Jaraysii	H0-19
	K. J. Koegler	H0-23
	J. D. White	H0-23

140	**Pacific Northwest National Laboratory**	
	J. F. Adams	K9-64
	R. C. Adams	K9-32
	C. C. Ainsworth	K3-61
	S. T. Autrey	K2-57
	J. F. Bagley	K1-71
	S. A. Bailey	K5-08
	E. G. Baker	K2-12
	J. A. Bamberger	K7-15
	W. R. Barchet	K9-30
	L. J. Bond	K5-26
	W. F. Bonner	K9-14
	D. M. Boyd	K1-46
	P. R. Bredt (5)	P7-25
	F. J. Brockman	P7-50
	J. W. Brothers	K7-15
	T. M. Brouns	K9-69
	S. A. Bryan	P7-25
	J. L. Buelt	K9-09
	D. M. Camaioni	K2-57
	J. A. Campbell	P8-08
	S. A. Chambers, Sr.	K8-93
	S. D. Colson	K8-88
	L. R. Corrales	K8-91
	J. L. Daschbach	K8-88
	J. L. Devary	K6-96
	D. A. Dixon	K1-83
	T. J. Doherty	K8-21

No. of Copies		No. of Copies	
D. D. Doneen	K8-21	G. L. McVay	K2-50
M. Dupuis	K8-91	B. J. Merrill	K8-15
R. M. Ecker	SEQUIM/L5/312	F. B. Metting	K9-76
O. B. Egorov	P7-22	P. D. Meyer	BPO
P. D. Ellis	K8-98	E. M. Murphy (10)	K9-76
G. J. Exarhos	K2-44	C. J. Murray	K6-81
L. L. Fassbender	K6-05	J. L. Olson	BSRC/S128
A. R. Felmy	K8-96	N. J. Olson	K6-04
J. K. Fredrickson	P7-50	T. L. Page	K9-18
M. D. Freshley	H0-21	R. A. Pappas	K5-26
J. L. Fuller	K8-02	P. D. Panetta	K5-26
P. A. Gauglitz	K6-28	C.H.F. Peden	K8-93
R. E. Gephart	K8-88	L. R. Pederson	K2-50
Y. R. Gorby	P7-50	W. T. Pennell	K9-34
J. W. Grate	K8-93	D. M. Pfund	K7-15
M. S. Greenwood	K5-26	L. M. Peurrung	K6-24
R. L. Gruel	K8-60	L. R. Pond	K8-23
M. S. Hanson	K9-02	L. J. Powell	K1-46
J. S. Hartman	K5-25	B. A. Pulsipher	K5-12
B. P. Hay	K1-83	M. J. Quadrel	K1-50
S. W. Heaberlin	K8-31	R. K. Quinn	K2-20
H. L. Heinisch	P8-15	D. Rai	P7-50
N. J. Hess	P7-50	B. M. Rapko	P7-25
T. L. Hubler	K8-93	S. D. Rassat	K6-28
J. P. Icenhower	K6-81	M. L. Rockhold	K9-36
L. D. Kannberg	K5-02	J. W. Rogers	K9-95
J. M. Kelley	P7-07	B. F. Saffell, Jr.	K2-44
D. E. Knutson	P7-25	J. D. Saffer	K7-40
D. W. Koppenaal	K8-98	R. J. Serne	P8-37
K. M Krupka	K6-81	S. N. Schlahta	K9-14
W. L. Kuhn	K7-15	P. A. Scott	K9-46
J. P. LaFemina	K9-01	L. J. Sealock, Jr.	K5-02
M. A. Lilga	K2-12	W. J. Shaw	K2-57
P. E. Long	K9-33	S. C. Slate	K1-50
G. J. Lumetta	P7-22	K. L. Soldat	K3-53
J. A. Mahaffey	K9-32	S. L. Stein	BSRC/S171
W. J. Martin	K6-81	T. L. Stewart	K9-32
L. M. Martucci	K7-10	Y. Su	K8-93
S. V. Mattigod	K6-81	S. K. Sundaram	K6-24
B. P. McGrail	K6-81	G. Terrones	K7-15
J. P. McKinley	K8-96	S. Thevuthasan	K8-93
B. K. McNamara	P7-25	J. J. Thomas	K7-10
G. W. McNair	K7-97	J. W. Virden	K2-44
		J. F. Wacker	P7-07

No. of
Copies

No. of
Copies

R. A. Walters	K9-15
T. L. Walton	K9-46
T. J. Weber	P7-56
W. J. Weber	K8-93
W. C. Weimer	K9-09
R. E. Wildung	P7-50

R. E. Williford	K2-44
J. M. Zachara	K8-96
T. S. Zemanian	P8-50
TFA Library (2)	K9-69
Hanford Technical Library (2)	P8-55